



# **Compilation of SHRIMP U–Pb geochronological data, Yilgarn Craton, Western Australia, 2000–2001**

*Geoscience Australia  
Record 2001/47*

I.R. Fletcher<sup>1</sup>, J.M. Dunphy<sup>1</sup>, K.F. Cassidy<sup>2</sup> and D.C. Champion<sup>2</sup>

<sup>1</sup> Centre of Excellence in Mass Spectrometry, School of Applied Physics, Curtin University of Technology, GPO Box U1987, Perth WA 6845

<sup>2</sup> Geoscience Australia, GPO Box 378, Canberra ACT 2601

## **Geoscience Australia**

Chief Executive Officer: Neil Williams

## **Department of Industry, Tourism and Resources**

Minister for Industry, Tourism and Resources: The Hon. Ian Macfarlane, MP

Parliamentary Secretary: The Hon. Warren Entsch, MP

© Commonwealth of Australia 2001

This work is copyright. Apart from any fair dealings for the purposes of study, research, criticism or review, as permitted under the Copyright Act, no part may be reproduced by any process without written permission. Inquiries should be directed to the Communications Unit, Geoscience Australia, GPO Box 378, Canberra ACT 2601.

**ISSN: 1039 0073**

**ISBN: 0 6424 6728 5**

***Bibliographic reference:*** Fletcher, I.R. et al., 2001. Compilation of SHRIMP U–Pb geochronological data, Yilgarn Craton, Western Australia, 2000–2001. Geoscience Australia, Record 2001/47.

Geoscience Australia has tried to make the information in this product as accurate as possible. However, it does not guarantee that the information is totally accurate or complete. THEREFORE, YOU SHOULD NOT RELY SOLELY ON THIS INFORMATION WHEN MAKING A COMMERCIAL

# Contents

List of Figures	ii
List of Tables	iv
Introduction	1
Analytical Procedures	3
Data compilation for the QGNG standard	5
9596 9764B: titanite-biotite granodiorite, Breakaway Well	10
9596 9787: biotite granite dyke, Kaluweerie Hill	14
9696 9055: hornblende plagiogranite, Hootanui Well	19
9996 6016A: biotite monzogranite, Tower Hill mine	23
9996 7007A: banded biotite granitic gneiss, Surprise Rocks	27
9996 7007B: biotite monzogranite dyke, Surprise Rocks	31
9996 9014: Alicia Granite	35
200096 7002B: amphibole-biotite tonalite, Mick Adam mine	39
200096 7004: Williamstown peridotite	44
200096 7006D: feldspar-amphibole porphyry clast in volcanoclastic conglomerate, Parkeston	48
200096 7007: feldspar-amphibole-phyric quartz diorite dyke, Tarmoola mine	52
200096 7011D: feldspar porphyry, Centurian mine	57
200096 7013: meta-feldspathic greywacke, Navajo mine	61
200096 9003: Maori Queen Tonalite	66
200096 9004: Danjo Monzogranite	70
200096 9005: biotite monzogranite dyke, Marloo Well	74
200096 9006: Pindinnis Granite	79
200096 9007: Ellington Granite	84
200196 9007A: Monument Monzogranite	88
200196 9019A: biotite granodiorite, Ironstone Point	92
200196 9019B: allanite-fluorite-biotite syenogranite dyke, Ironstone Point	96
200196 9020: Isolated Hill Granodiorite	100
200196 9021: biotite monzogranite dyke, Isolated Hill	105
Acknowledgements	110
References	111

## List of Figures

Figure 1. Approximate locations of samples presented in this Record. The geology, towns and coastline are derived from Geoscience Australia's national geoscience dataset.	2
Figure 2. Data for QGNG, treated as independent data sets.	6
Figure 3. Data for QGNG that were rejected during initial (SQUID) data reduction.	6
Figure 4. Gaussian-summation plot of $^{207}\text{Pb}/^{206}\text{Pb}$ data for QGNG after initial data reduction.	7
Figure 5. Data for QGNG, re-processed using the criteria in text.	8
Figure 6. Representative SEM images for sample 9596 9764B: titanite-biotite granodiorite, Breakaway Well.	11
Figure 7. Concordia plot for zircon data from sample 9596 9764B: titanite-biotite granodiorite, Breakaway Well.	13
Figure 8. Enlargement of main group of zircon analyses for sample 9596 9764B: titanite-biotite granodiorite, Breakaway Well.	13
Figure 9. Representative SEM images for sample 9596 9787: biotite granite dyke, Kaluweerie Hill.	15
Figure 10. Concordia plot for zircon data from sample 9596 9787: biotite granite dyke, Kaluweerie Hill.	16
Figure 11. Enlargement of main group of zircon analyses for sample 9596 9787: biotite granite dyke, Kaluweerie Hill.	17
Figure 12. Representative SEM images for sample 9696 9055: hornblende plagiogranite, Hootanui Well.	20
Figure 13. Concordia plot for zircon data from sample 9696 9055: hornblende plagiogranite, Hootanui Well.	21
Figure 14. Representative SEM images for sample 9996 6016A: biotite monzogranite, Tower Hill.	24
Figure 15. Concordia plot for zircon data from sample 9996 6016A: biotite monzogranite, Tower Hill mine.	25
Figure 16. Representative SEM images for sample 9996 7007A: banded granitic gneiss, Surprise Rocks.	28
Figure 17. Concordia plot for zircon data from sample 9996 7007A: banded biotite granitic gneiss, Surprise Rocks.	30
Figure 18. Gaussian-summation plot for zircon data from sample 9996 7007A: banded biotite granitic gneiss, Surprise Rocks.	30
Figure 19. Representative SEM images for sample 9996-7007B: biotite monzogranite dyke, Surprise Rocks.	32
Figure 20. Concordia plot for zircon data from sample 9996-7007B: biotite monzogranite dyke, Surprise Rocks.	33
Figure 21. Representative SEM images for sample 9996 9014: Alicia Granite.	36
Figure 22. Concordia plot for zircon data from sample 9996 9014: Alicia Granite.	37
Figure 23. Representative SEM images for sample 200096 7002B: amphibole-biotite tonalite, Mick Adam mine.	40
Figure 24. Concordia plot for zircon data from sample 200096 7002B: amphibole-biotite tonalite, Mick Adam mine.	41
Figure 25. Enlargement of main group of zircon analyses for sample 200096 7002B: amphibole-biotite tonalite, Mick Adam mine.	42
Figure 26. Gaussian-summation plot for zircon data from sample 200096 7002B: amphibole-biotite tonalite, Mick Adam mine.	42
Figure 27. Representative SEM CL image for sample 200096 7004: Williamstown peridotite.	45
Figure 28. Concordia plot for sample 200096 7004: Williamstown peridotite.	46
Figure 29. Representative SEM images for sample 200096 7006D: feldspar-amphibole porphyry clast in volcanoclastic conglomerate, Parkeston.	49
Figure 30. Concordia plot for zircon data from sample 200096 7006D: feldspar-amphibole porphyry clast in volcanoclastic conglomerate, Parkeston.	50
Figure 31. Representative SEM images for sample 200096 7007: feldspar-amphibole-phyric quartz diorite dyke, Tarmoola mine.	53

Figure 32. Concordia plot for zircon data from sample 200096 7007: feldspar-amphibole-phyric quartz diorite dyke, Tarmoola mine.	54
Figure 33. Enlargement of main group of zircon analyses for sample 200096 7007: feldspar-amphibole-phyric quartz diorite dyke, Tarmoola mine.	55
Figure 34. Representative SEM images for sample 200096 7011D: feldspar porphyry, Centurian mine.	58
Figure 35. Concordia plot for zircon data from sample 200096 7011D: feldspar porphyry, Centurian mine.	59
Figure 36. Representative SEM images for sample 200096 7013: meta-feldspathic greywacke, Navajo mine.	62
Figure 37. Gaussian-summation plot for zircon age data from sample 200096 7013: meta-feldspathic greywacke, Navajo mine.	63
Figure 38. Concordia plot for zircon data from sample 200096 7013: meta-feldspathic greywacke, Navajo mine.	64
Figure 39. Probability diagram for zircon age data from sample 200096 7013: meta-feldspathic greywacke, Navajo mine.	64
Figure 40. Representative SEM images for sample 200096 9003: Maori Queen Tonalite.	67
Figure 41. Concordia plot for zircon data from sample 200096 9003: Maori Queen Tonalite.	68
Figure 42. Representative SEM images for sample 200096 9004: Danjo Monzogranite.	71
Figure 43. Concordia plot for zircon data from sample 200096 9004: Danjo Monzogranite.	72
Figure 44. Representative SEM images for sample 200096 9005: biotite monzogranite dyke, Marloo Well.	75
Figure 45. Concordia plot for zircon data from sample 200096 9005: biotite monzogranite dyke, Marloo Well.	76
Figure 46. Gaussian-summation plot for zircon age data from sample 200096 9005: biotite monzogranite dyke, Marloo Well.	77
Figure 47. Representative SEM images for sample 200096 9006: Pindinnis Granite.	80
Figure 48. Concordia plot for zircon data from sample 200096 9006: Pindinnis Granite.	81
Figure 49. Gaussian-summation plot for sample 200096 9006: Pindinnis Granite.	82
Figure 50. Representative SEM images for sample 200096 9007: Ellington Granite.	85
Figure 51. Concordia plot for zircon data from sample 200096 9007: Ellington Granite.	86
Figure 52. Representative SEM images for sample 200196 9007A: Monument Monzogranite.	89
Figure 53. Concordia plot for zircon data from sample 200196 9007A: Monument Monzogranite.	90
Figure 54. Representative SEM images for sample 200196 9019A: biotite granodiorite, Ironstone Point.	93
Figure 55. Concordia plot for zircon data from sample 200196 9019A: biotite granodiorite, Ironstone Point.	94
Figure 56. Representative SEM images for sample 200196 9019B: allanite-fluorite-biotite syenogranite dyke, Ironstone Point.	97
Figure 57. Concordia plot for zircon data from sample 200196 9019B: allanite-fluorite-biotite syenogranite dyke, Ironstone Point.	98
Figure 58. Representative SEM images for sample 200196 9020: Isolated Hill Granodiorite.	101
Figure 59. Concordia plot for zircon data from sample 200196 9020: Isolated Hill Granodiorite.	102
Figure 60. Enlargement of main group of zircon analyses for sample 200196 9020: Isolated Hill Granodiorite.	103
Figure 61. Representative SEM images for sample 900196 9021: biotite monzogranite dyke, Isolated Hill.	106
Figure 62. Concordia plot for zircon data from sample 900196 9021: biotite monzogranite dyke, Isolated Hill.	107
Figure 63. Enlargement of main group of zircon analyses for sample 900196 9021: biotite monzogranite dyke, Isolated Hill.	108

## List of Tables

Table 1.	Standard run table for SHRIMP analyses for this project.	4
Table 2.	Data for QGNG, treated as independent data sets.	5
Table 3.	Data for QGNG, re-processed using the criteria in text.	8
Table 4.	SHRIMP analytical results for zircon from sample 9596 9764B: titanite-biotite granodiorite, Breakaway Well.	12
Table 5.	SHRIMP analytical results for zircon from sample 9596 9787: biotite granite dyke, Kaluweerie Hill.	18
Table 6.	SHRIMP analytical results for zircon from sample 9696 9055: plagiogranite, Hootanui Well.	22
Table 7.	SHRIMP analytical results for zircon from sample 9996 6016A: biotite monzogranite, Tower Hill mine.	26
Table 8.	SHRIMP analytical results for zircon from sample 9996 7007A: banded biotite granitic gneiss, Surprise Rocks.	29
Table 9.	SHRIMP analytical results for zircon from sample 9996-7007B: biotite monzogranite dyke, Surprise Rocks.	34
Table 10.	SHRIMP analytical results for zircon from sample 9996 9014: Alicia Granite.	38
Table 11.	SHRIMP analytical results for zircon from sample 200096 7002B: amphibole-biotite tonalite, Mick Adam mine.	43
Table 12.	SHRIMP analytical results for sample 200096 7004: Williamstown peridotite.	47
Table 13.	SHRIMP analytical results for zircon from sample 200096 7006D: feldspar-amphibole porphyry clast in volcanoclastic conglomerate, Parkeston.	51
Table 14.	SHRIMP analytical results for zircon from sample 200096 7007: feldspar-amphibole-phyric quartz diorite dyke, Tarmoola mine.	56
Table 15.	SHRIMP analytical results for zircon from sample 200096 7011D: feldspar porphyry, Centurian mine.	60
Table 16.	SHRIMP analytical results for zircon from sample 200096 7013: meta-feldspathic greywacke, Navajo mine.	65
Table 17.	SHRIMP analytical results for zircon from sample 200096 9003: Maori Queen Tonalite.	69
Table 18.	SHRIMP analytical results for zircon from sample 200096 9004: Danjo Monzogranite.	73
Table 19.	SHRIMP analytical results for sample 200096 9005: biotite monzogranite dyke, Marloo Well.	78
Table 20.	SHRIMP analytical results for zircon from sample 200096 9006: Pindinnis Granite.	83
Table 21.	SHRIMP analytical results for sample 200096 9007: Ellington Granite.	87
Table 22.	SHRIMP analytical results for sample 200196 9007A: Monument Monzogranite.	91
Table 23.	SHRIMP analytical results for sample 201096 9019A: biotite granodiorite, Ironstone Point.	95
Table 24.	SHRIMP analytical results for sample 200196 9019B: allanite-fluorite-biotite syenogranite dyke, Ironstone Point.	99
Table 25.	SHRIMP analytical results for sample 200196 9020: Isolated Hill Granodiorite.	104
Table 26.	SHRIMP analytical results for sample 900196 9021: biotite monzogranite dyke, Isolated Hill.	109

## Introduction

This Record contains zircon U–Pb geochronological data obtained between September 2000 and August 2001 on rocks from the Yilgarn Craton, Western Australia. Approximate positions of sampling localities are shown in Figure 1.

The data were collected as part of the Norseman-Wiluna Synthesis project, a National Geoscience Accord project that operates in collaboration with the Geological Survey of Western Australia. They are helping to meet the objective of providing an improved geological and metallogenic framework for the Norseman-Wiluna region of the eastern Yilgarn Craton, and help provide geochronological constraints on geodynamic and tectonic models for the region. The data were acquired through a collaborative research agreement between Curtin University of Technology, Bentley, Western Australia and Geoscience Australia.

This Record describes the samples analysed and the analytical results obtained, and provides a brief discussion of their geochronological interpretation. The broader geological implications of the data will be published elsewhere. The complete data files, including data for QGNG standards and cathodoluminescence (CL) images showing SHRIMP spot locations, are stored in the Geoscience Australia database, OZCHRON.

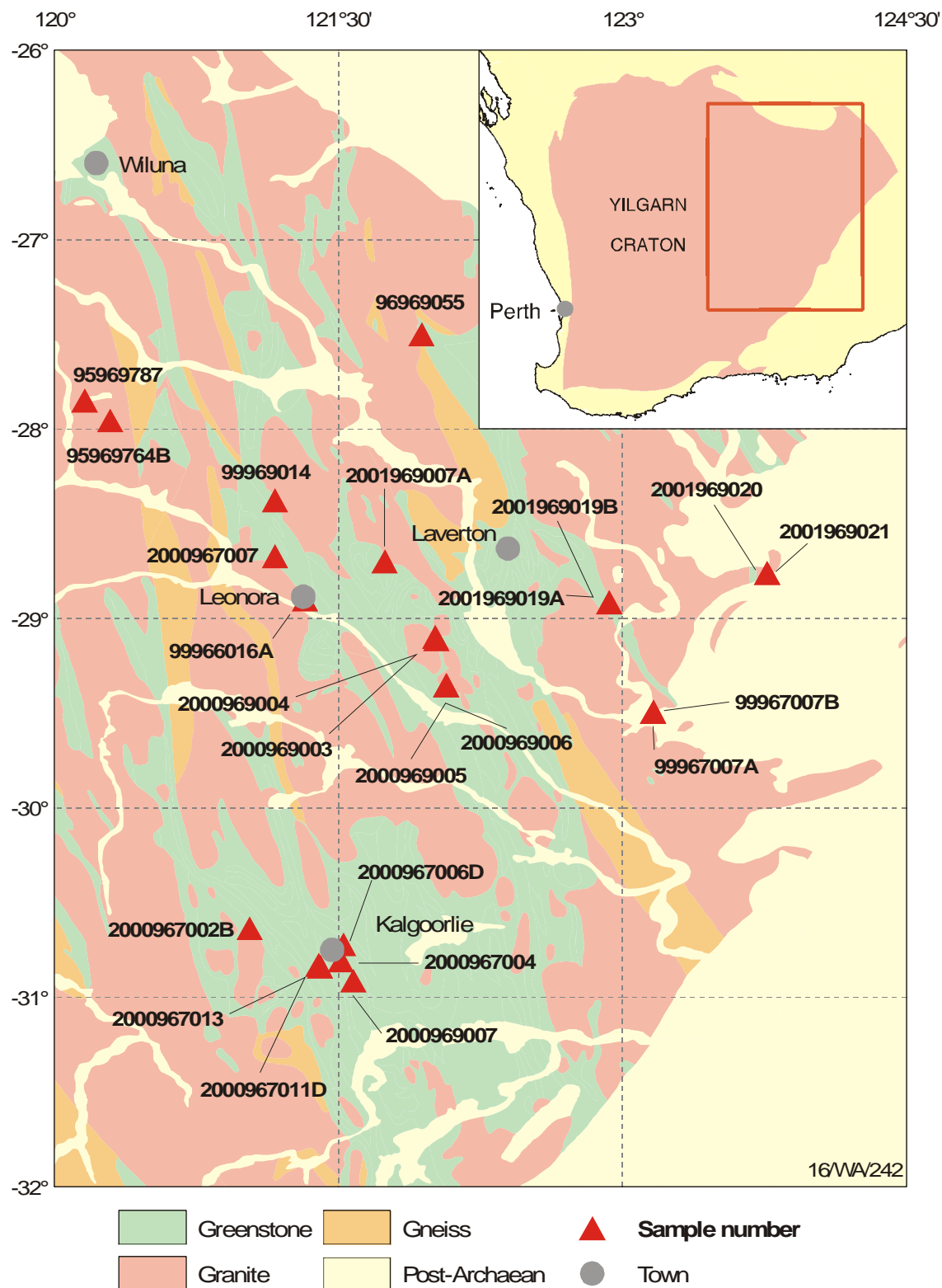


Figure 1. Approximate locations of samples presented in this Record. The geology, towns and coastline are derived from Geoscience Australia's national geoscience dataset.



## Analytical Procedures

### Sample processing

The freshest possible rock was selected at the field site. This usually involved the splitting of boulders to access fresh rock, although blasting of solid outcrop was required for some samples. Some samples were obtained from drillcore in collaboration with company geologists. The locations of field samples ( $\pm 50$  m) were determined using a hand-held GPS; drillcore collar locations were obtained from company data. Grid references in this Record refer to the Geocentric Datum of Australia 1994 (GDA94). Locations mentioned in the text are referenced using Map Grid Australia (MGA) coordinates, Zone 51.

At the field site, the rock was broken into fist-size fragments, having regard to cleanliness at all times to avoid contamination of the sample. Typically, the sample weighed between 10 kg and 20 kg, sometimes more if a low zircon yield was suspected, but less if only drillcore was available. Each rock was inspected and cleaned in the mineral separation lab at Geoscience Australia. Rock was broken down to 2–5 cm pieces using a pre-cleaned hydraulic splitter. The pieces were ultrasonically washed in water, and dried under heat lamps. The first crush used a jaw crusher, or Rocklabs Boyd crusher. Milling used a rotary disc mill or a Rocklabs Continuous Ring Mill.

For samples for which the main geochronological question is their magmatic age, zircon selection was biased towards the least magnetic, clearest grains, without discrimination between grain morphologies. The initial density separation was undertaken using a Wilfley table. This reduced the sample to about 5% of its original weight, and also washed away the fine dust. The highly magnetic grains were then removed using a hand magnet. The second density separation stage used Tetrabromoethane (2.96 g/ml), followed by magnetic separation using a Frantz isodynamic separator. The non-magnetic fraction then went to a third density separation in Methylene Iodide (3.3 g/ml) and additional Frantz separation. Approximately 100–150 zircon grains per sample were selected for mounting by handpicking using a binocular microscope. For the one metasedimentary sample, where zircon provenance is the main factor, zircons were hand-picked without discrimination from the heavy mineral concentrate.

The zircon grains were encapsulated in epoxy, together with similar quantities of the in-house Geoscience Australia multi-grain standard QGNG (Daly et al., 1998) and a small quantity of the Perth standard CZ3 (Pidgeon et al., 1994). The mounts were polished to expose grains in section, and all grains were photographed in transmitted and reflected light, and imaged by CL on a Hitachi S2250 NSEM located in the Electron Microscopy Unit at the Australian National University. After analysis, backscattered electron (BSE) and additional CL images of typical grains of each sample were obtained at the Centre for Microscopy and Microanalysis (CMM) at The University of Western Australia for inclusion in this report. Analysis locations are shown on these images, but in most cases the pits are not visible, as they have been polished away.

All SHRIMP mounts were ultrasonically cleaned in petroleum spirit and a 10% Extran solution, triple rinsed in quartz-distilled water, and dried overnight in a 30°C oven prior to gold-coating with high-purity gold at the CMM.

### Data acquisition

SHRIMP analyses were undertaken on the SHRIMP II located at Curtin University of Technology, Perth, Western Australia, using procedures from Compston et al. (1984) and Smith et al. (1998). In general, attempts were made to analyse examples of all identified grain types. A raster (surface-cleaning) time of 3 minutes was used, and data were acquired over 7 scans through the mass sequence, which is listed in Table 1. The primary  $O_2^-$  beam was typically ~3 nA but up to 5.5 nA, and produced an approximately 20–30  $\mu$ m elliptical spot. The mass resolution at 1%

peak height was 4,500–5,100 with secondary ion sensitivity on CZ3 > 15 cps/ppm Pb/nA. For the one sample of detrital zircons extracted from a sedimentary rock, data acquisition was reduced to five scans of the mass spectrum. No other changes were made.

Most analytical sessions involved analyses of two samples over a continuous 48-hour period, with re-tuning of the instrument after 24 hours. One session was interrupted by a cooling water failure and one was a single day (24 hours). Each mount typically contains four samples, hence two analytical sessions were required for each mount.

Table 1. Standard run table for SHRIMP analyses for this project.

Nominal Mass	Species	Count time (s)
196	ZrO <sub>2</sub>	2
204	Pb	10
204.045	background	10
206	Pb	10
207	Pb	40
208	Pb	10
238	U	5
248	ThO	5
254	UO	2

## Data reduction

QGNG was used for calibration of U/Pb, and CZ3 for U content (550 ppm U; Nelson, 1997). The reference <sup>206</sup>Pb/<sup>238</sup>U age for QGNG, determined by replicate analyses using TIMS, is 1843.1 Ma (L.P. Black, pers. comm., 2001).

Data reduction was undertaken using SQUID 1.02c (Ludwig, 2001). This version of SQUID varies from some others in that it permits operator-specified variations in the exponent used in the Pb/U calibration (equivalent to varying the slope of the conventional ln[Pb/U]:ln[UO/U] calibration line). For most analytical sessions, these parameters were sufficiently well defined and different from the nominal value (2.0) to justify using the values determined from the data.

Corrections for common Pb were based on measured <sup>204</sup>Pb and the isotopic composition of Broken Hill galena. Use of a single common Pb composition for all data is justified because data are only used for age determinations if the common-Pb component is sufficiently small that corrections for its effect on radiogenic <sup>207</sup>Pb/<sup>206</sup>Pb data are so small that they are insensitive to the choice of composition used in making the corrections (over a wide range of Proterozoic–Archaean common-Pb compositions). Data requiring larger corrections commonly give discordant data and are presumed to have experienced some open-system disturbance. The origin and age (and hence composition) or their common Pb component are unknown. These data are not used for age determinations.

## Data presentation

All data from individual analyses are tabulated, and shown in concordia plots, with 1σ precisions. The tabulated data are all common-Pb corrected. Abbreviations used in table headings are

4f206: the proportion of total <sup>206</sup>Pb calculated to be common Pb,

conc.: concordance, defined as  $100 \cdot t[^{206}\text{Pb}/^{238}\text{U}] / t[^{207}\text{Pb}/^{206}\text{Pb}]$ .

The weighted mean <sup>207</sup>Pb/<sup>206</sup>Pb ages determined from grouped data are given in text with 95% confidence limits. The values stated for these ages are rounded off to integers and the corresponding uncertainties are rounded up to cover the range that is required by additional decimal places (e.g.  $2660.2 \pm 5.2$  rounds to  $2660 \pm 6$  Ma).

## Data compilation for the QGNG standard

### Introduction

The QGNG standard zircon was used for Pb/U calibration and as a monitor of  $^{207}\text{Pb}/^{206}\text{Pb}$  reproducibility and accuracy. In total, 365 QGNG analyses were obtained from 12 analytical sessions (eleven 2-day and one 1-day sessions). These analyses were interspersed with sample analyses, and were collected under the same standardised conditions. Data for sessions involving only detrital samples, which recorded only five scans, are not included in this summary.

### Data processing

Data were processed using SQUID 1.02c (Ludwig, 2001), in conjunction with sample data for each session. Common-Pb corrections were calculated using measured  $^{204}\text{Pb}$  and Broken Hill galena composition. The  $^{206}\text{Pb}/^{238}\text{U}$  data are self-calibrated within each analytical session, and are reported in later chapters with the corresponding sample data.

### Data

As is common practice, the QGNG data were assessed session-by-session, generally treating them as independent data sets but to varying degrees applying inferences from the corresponding sample data. Initially, the main consideration is the  $^{206}\text{Pb}/^{238}\text{U}$  calibration, and at this stage it is not uncommon to reject some data. In the present case, almost all such rejections were due to low  $^{206}\text{Pb}/^{238}\text{U}$ . Consideration then moves to  $^{207}\text{Pb}/^{206}\text{Pb}$ , and the data are treated much as those for a sample. The notes on QGNG data that accompany each of the sample reports follow this sequence.

After this initial assessment and culling, the majority of QGNG data sets have  $\text{MSWD} > 1.0$ , with half of them in the range 1.2–1.5 (Table 2). When the data are compiled (Fig. 2) the session-to-session scatter also gives  $\text{MSWD} > 1.0$ . This suggests that either (1) there are systematic errors not properly accounted for in assigning uncertainties to individual analyses, (2, possibly interrelated with 1) the data selection criteria are inadequate, or (3) QGNG is not homogeneous in  $^{207}\text{Pb}/^{206}\text{Pb}$ . In addition, the average  $^{207}\text{Pb}/^{206}\text{Pb}$  age of  $1848.1 \pm 1.1$  Ma is significantly below the TIMS reference value of  $1851.8 \pm 0.6$  Ma ( $2\sigma$ ; L.P. Black, pers. comm., 2001).

Table 2. Data for QGNG, treated as independent data sets.

Session	Date	t[207/206]	+/- 95%	MSWD	n-used	n-total
Z3623i	03/11/00	1845.4	3.1	1.50	28	30
Z3623j	11/11/00	1850.1	4.3	1.30	30	32
Z3624i	29/09/00	1848.5	2.7	0.75	28	29
Z3672i	19/03/01	1847.8	4.1	1.20	29	29
Z3672j	06/04/01	1849.0	3.4	1.06	25	27
Z3679i	05/06/01	1845.2	3.5	1.20	31	36
Z3679j	02/07/01	1848.3	2.6	1.20	31	35
Z3730i	18/06/01	1848.9	2.6	1.19	35	35
Z3730j	22/06/01	1849.0	3.0	0.71	23	23
Z3734i	08/08/01	1845.1	2.9	1.20	29	36
Z3734j	13/08/01	1850.2	2.7	0.78	16	19
Z3734k	25/08/01	1848.5	2.7	0.89	30	34

t[207/206] is the weighted mean  $^{207}\text{Pb}/^{206}\text{Pb}$  age.

n-used is the number of analyses in the calibration data subset, averaged to give t[207/206].

n-total is the number of analyses recorded for the session.

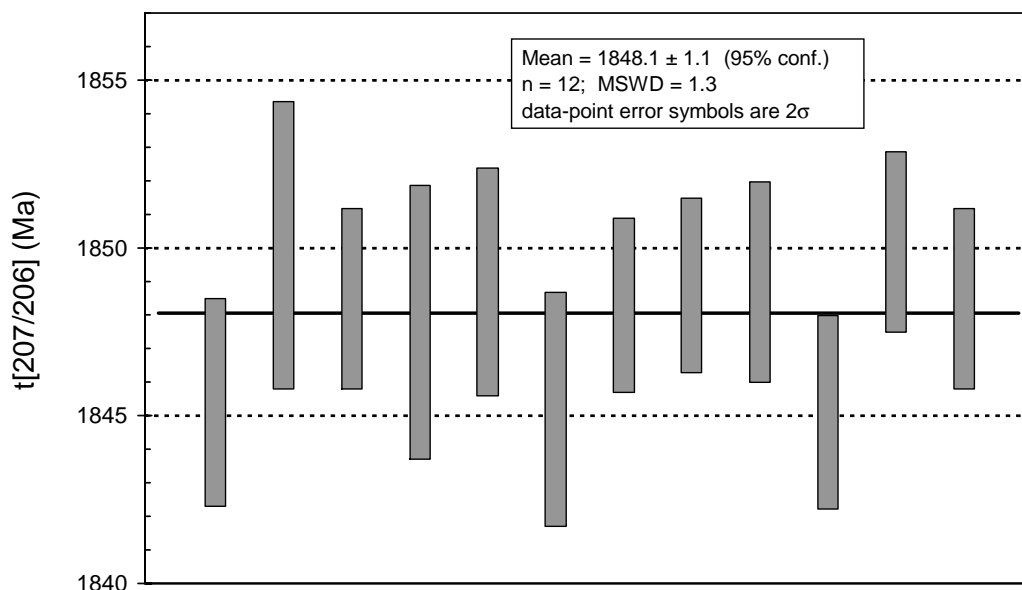


Figure 2. Data for QGNG, treated as independent data sets. Data, in sequence, from Table 2.

### An alternative assessment

Both the age “error” and the apparent excess scatter in  $^{207}\text{Pb}/^{206}\text{Pb}$  suggest that a more detailed assessment is required. In determining an approach to this, there are two additional observations to consider:

- Amongst the QGNG data rejected in the initial assessments, a majority are low in both  $^{207}\text{Pb}/^{206}\text{Pb}$  and  $^{206}\text{Pb}/^{238}\text{U}$  (Fig. 3);
- In the data retained after the initial  $^{206}\text{Pb}/^{238}\text{U}$  assessment, there is a mild skew of  $^{207}\text{Pb}/^{206}\text{Pb}$  to low values (Fig. 4).

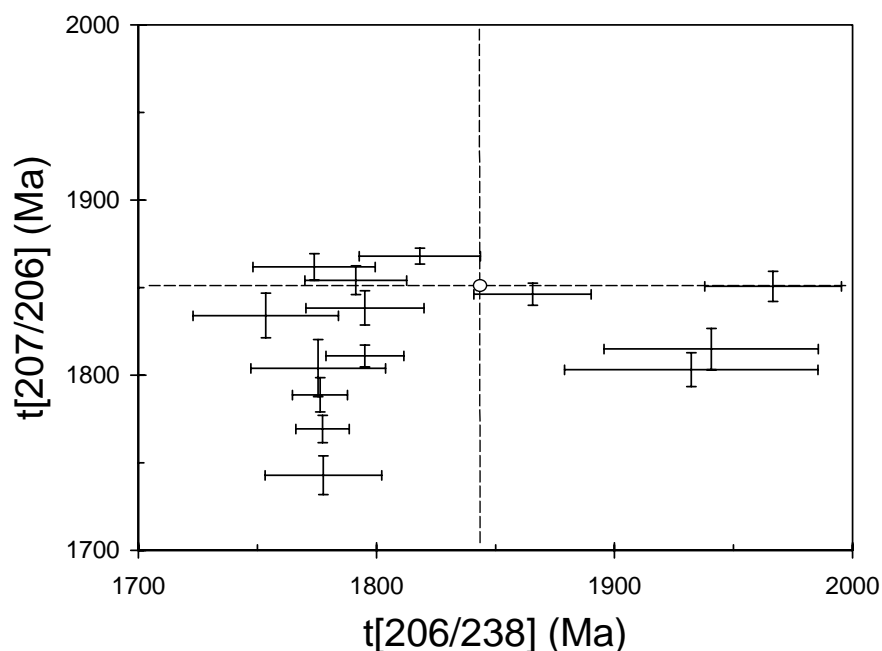


Figure 3. Data for QGNG that were rejected during initial (SQUID) data reduction. Error bars are  $1\sigma$ . Dashed lines are TIMS reference ages.

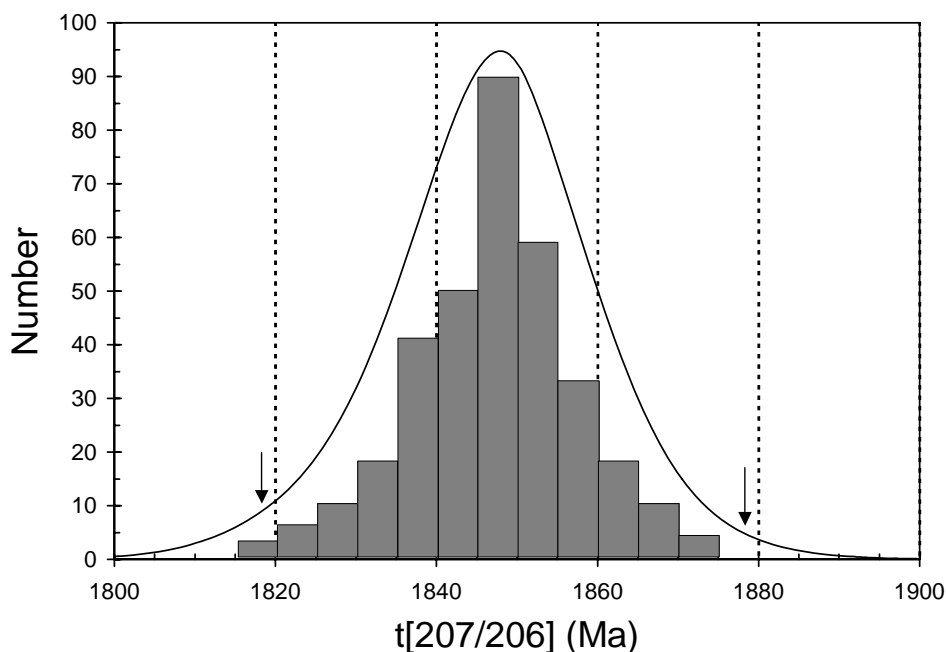


Figure 4. Gaussian-summation plot of  $^{207}\text{Pb}/^{206}\text{Pb}$  data for QGNG after initial data reduction (see Fig. 3), omitting data with  $1\sigma$  precision  $>15$  Ma (10 omissions). Arrows are symmetric about the peak of the curve.

All of these observations suggest that there is real age heterogeneity in QGNG, but it is also possible that b, and to a lesser extent a, are due to systematic factors. It seems to be impossible to differentiate between these two possibilities, and we therefore consider a purely pragmatic alternative approach. This is influenced by the approach commonly adopted for Archaean sample data, in which  $^{207}\text{Pb}/^{206}\text{Pb}$  data in a mildly scattered population are culled from the low-age side, on the presumption that the data scatter is due to early Pb loss. We suggest that it is reasonable to treat these QGNG data in the same way. There are two arguments for this:

1. If there is real skew to low  $^{207}\text{Pb}/^{206}\text{Pb}$  in both QGNG and the corresponding samples, it is appropriate to eliminate the scatter in the same way for both of them;
2. If the scatter in QGNG is due to systematic limitations, the same limitations apply to samples analysed concurrently, and again it is appropriate to use the same data selection procedure.

The QGNG datasets have therefore been re-processed in the following way:

1. SQUID data reduction;
2. Deletion of outliers in  $^{206}\text{Pb}/^{238}\text{U}$ , as outlined above (essentially as identified by SQUID);
3. Deletion of 'abnormal' data ( $>5\%$  discordance [one case, reversely discordant];  $>1000$  ppm U [three cases]; low-precision, possibly due to primary beam instability [one case]);
4. Deletion of any  $>3\sigma$   $^{207}\text{Pb}/^{206}\text{Pb}$  outliers (one high case, low values included in step 5.);
5. Progressive deletion of data from the low  $^{207}\text{Pb}/^{206}\text{Pb}$  side, until MSWD is the smallest possible value  $>1.0$ . (Note that in two sessions MSWD  $< 1.0$  without culling.) Although such severe culling is not justified for single data sets in isolation, for a collection of data sets it forces the mean of the resulting MSWD values close to the ideal value of 1.00.

The re-worked results (Table 3, Fig. 5) show much reduced between-session scatter (MSWD = 0.78) and, due to the low-side culling, an average  $^{207}\text{Pb}/^{206}\text{Pb}$  age closer to the reference value.

Table 3. Data for QGNG, re-processed using the criteria in text.

Session	t[207/206]	+/- 95%	MSWD	n-used	n-total
Z3623i	1846.9	2.8	1.00	21	30
Z3623j	1852.0	3.5	1.01	27	32
Z3624i	1848.5	2.7	0.75	28	29
Z3672i	1848.6	3.6	1.07	26	29
Z3672j	1849.7	3.5	1.01	23	27
Z3679i	1847.1	3.2	1.00	27	36
Z3679j	1849.9	2.5	1.02	26	35
Z3730i	1849.3	2.3	1.02	33	35
Z3730j	1849.0	3.0	0.71	23	23
Z3734i	1850.0	3.0	1.01	20	36
Z3734j	1849.1	3.8	1.30*	16	19
Z3734k	1847.9	2.7	1.09	31	34

\* Session 3734j is a difficult case. MSWD is substantially greater than 1.00, but making one additional data deletion (an outlier at almost  $3\sigma$ ) would take it significantly below (0.83). Other footnotes as in Table 2.

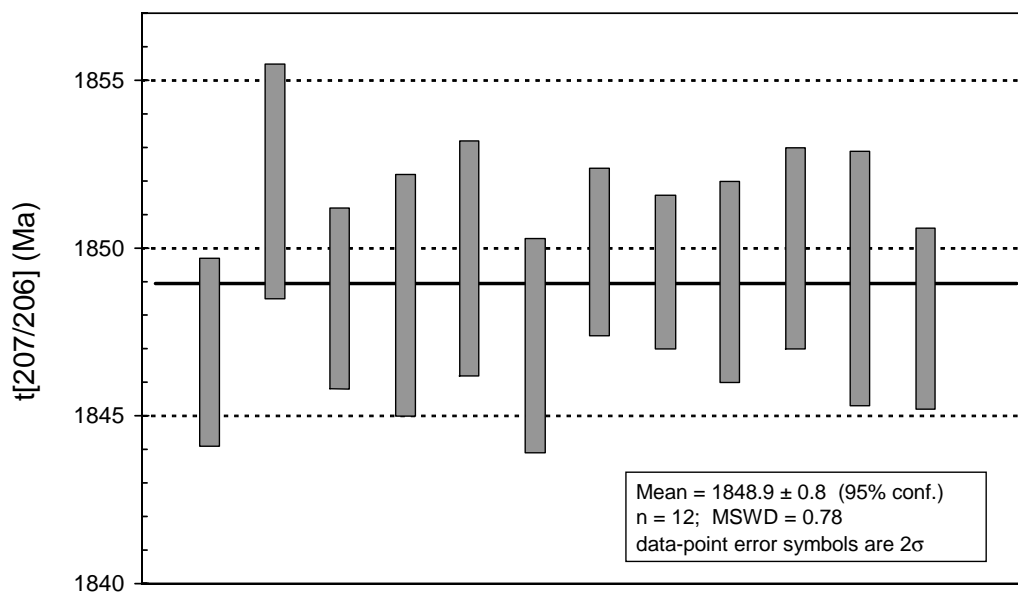


Figure 5. Data for QGNG, re-processed using the criteria in text. Data, in sequence, from Table 3.

## Conclusion

On the basis of this assessment, we conclude that there are no significant between-session variations in  $^{207}\text{Pb}/^{206}\text{Pb}$  data for QGNG, and therefore that there are no significant between-session variations in the sample data recorded in the following chapters. However, there is a -2.9 Ma offset of the weighted mean  $^{207}\text{Pb}/^{206}\text{Pb}$  age for QGNG which, if treated as an error in the  $^{207}\text{Pb}/^{206}\text{Pb}$  ratio, corresponds to a ~3 Ma error in the sample data presented below. The reasons for this offset are unknown, but it is consistent with expectations, both in direction and size, for mass fractionation during ionisation (Williams, 1998, and references therein). The

apparent fractionation is  $-0.16\% \pm 0.06\%/amu$ .

No re-normalisation has been applied to the sample data presented below. If the ~3 Ma apparent defect in  $^{207}Pb/^{206}Pb$  ages is due to mass fractionation it is likely to be a feature of all SHRIMP data, and thus these data are directly comparable with other SHRIMP data. However, in making comparisons with other Pb/Pb dates (e.g. from TIMS), the difference could be significant, and as a rule-of-thumb we consider that no Archaean SHRIMP  $^{207}Pb/^{206}Pb$  dates can be considered as absolute ages to better than ~5 Ma (including a ~2 Ma practical limit for internal precision), in addition to the ~5 Ma uncertainty that derives from the U decay constants. However, data are reported in following chapters without any augmentation of internally-derived uncertainties.

The data assessment procedure described above is believed to provide a more robust measure of between-session reproducibility than treating each session's data as from an independent sample. It also appears to give a better monitor of  $^{207}Pb/^{206}Pb$  data accuracy.



## 9596 9764B: titanite-biotite granodiorite, Breakaway Well

<b>1:250,000 sheet:</b>	Sir Samuel (SG5113)
<b>1:100,000 sheet:</b>	Depot Springs (2942)
<b>MGA:</b>	233860mE                      69047889mN
<b>Location:</b>	The sample was taken from a boulder approximately 2 km north-northeast of Breakaway Well.
<b>Description:</b>	<p>This sample is from a grey fine- to medium-grained equigranular to seriate titanite-biotite granodiorite enclave (&lt;10 m) in a moderately feldspar-porphyritic medium-grained biotite monzogranite. The host granitoid belongs to the Low-Ca grouping of Champion &amp; Sheraton (1997) and the geochemistry of the enclave suggests that it may represent a protolith for Low-Ca granitoids.</p> <p>The unit has a granular texture. Principal minerals are plagioclase (25–30%), K-feldspar (~30%), quartz (30–35%) and biotite (7–9%). Plagioclase is commonly unzoned to weakly zoned. Quartz is present as weakly undulose anhedral grains. Biotite occurs as elongate rectangular to irregular grains that are often aligned. Accessory phases include common subhedral to anhedral titanite (2–3%, to ~2 mm) and subhedral to anhedral Fe-oxides (1–2%), as well as zircon and apatite. Secondary minerals include white mica, epidote, clinozoisite and chlorite.</p>
<b>Mount, pop:</b>	Z3623D

### Description of zircons

Zircon is present mainly as subhedral to euhedral crystals and fragments which generally range in length from about 100  $\mu\text{m}$  to 200  $\mu\text{m}$  (aspect ratio 2:1 to 5:1), but a few larger grains are present (one fragment is >400  $\mu\text{m}$  long). Many of the crystal faces are somewhat rounded although some grains do preserve sharp prismatic terminations. The grains are colourless to pale brown and are generally clear, but small inclusions are present in many grains. Most grains display some form of zoning in the CL images, either euhedral, concentric zoning typical of igneous crystallisation, or a more complex and irregular zoning pattern which can indicate secondary processes such as resorption and recrystallisation (Fig. 6). About one quarter of the grains contain structurally distinct cores.

### Concurrent standard data

There is one clearly anomalous (low  $^{207}\text{Pb}/^{206}\text{Pb}$  and low  $^{206}\text{Pb}/^{238}\text{U}$ ) QGNG analysis (23-1). This was omitted from the calibration. A second analysis (2-1), which was noted to have a brief offset in the secondary beam profiles due to primary beam instability, is an outlier on the  $\ln:\ln$  calibration plot even though its internal calibration factor and the returned  $^{206}\text{Pb}/^{238}\text{U}$  and  $^{207}\text{Pb}/^{206}\text{Pb}$  are normal. This point was omitted, although the internal data rejection procedures seem to have worked appropriately and this omission has no effect on the calibration.

The floating calibration exponent is 2.34, well above the default, and both of the concurrent sample data sets suggest even higher values (>2.5). A value of 2.3 has been used in data reduction. The reproducibility of  $^{206}\text{Pb}/^{238}\text{U}$  for QGNG is 1.40% ( $1\sigma$ ,  $n = 28$  of 30). The corresponding  $^{207}\text{Pb}/^{206}\text{Pb}$  age is  $1845.4 \pm 3.1$  Ma (MSWD = 1.5), but using a standardised set of criteria for assessment of the data (see “Data compilation for the QGNG standard”) gives a  $^{207}\text{Pb}/^{206}\text{Pb}$  age of  $1846.9 \pm 2.8$  Ma (MSWD = 1.0).

Element abundance calibration was based on CZ3 ( $n = 4$ ).

### Sample data

Twenty-nine analyses were completed on 29 grains. Analytical data are presented in Table 4.



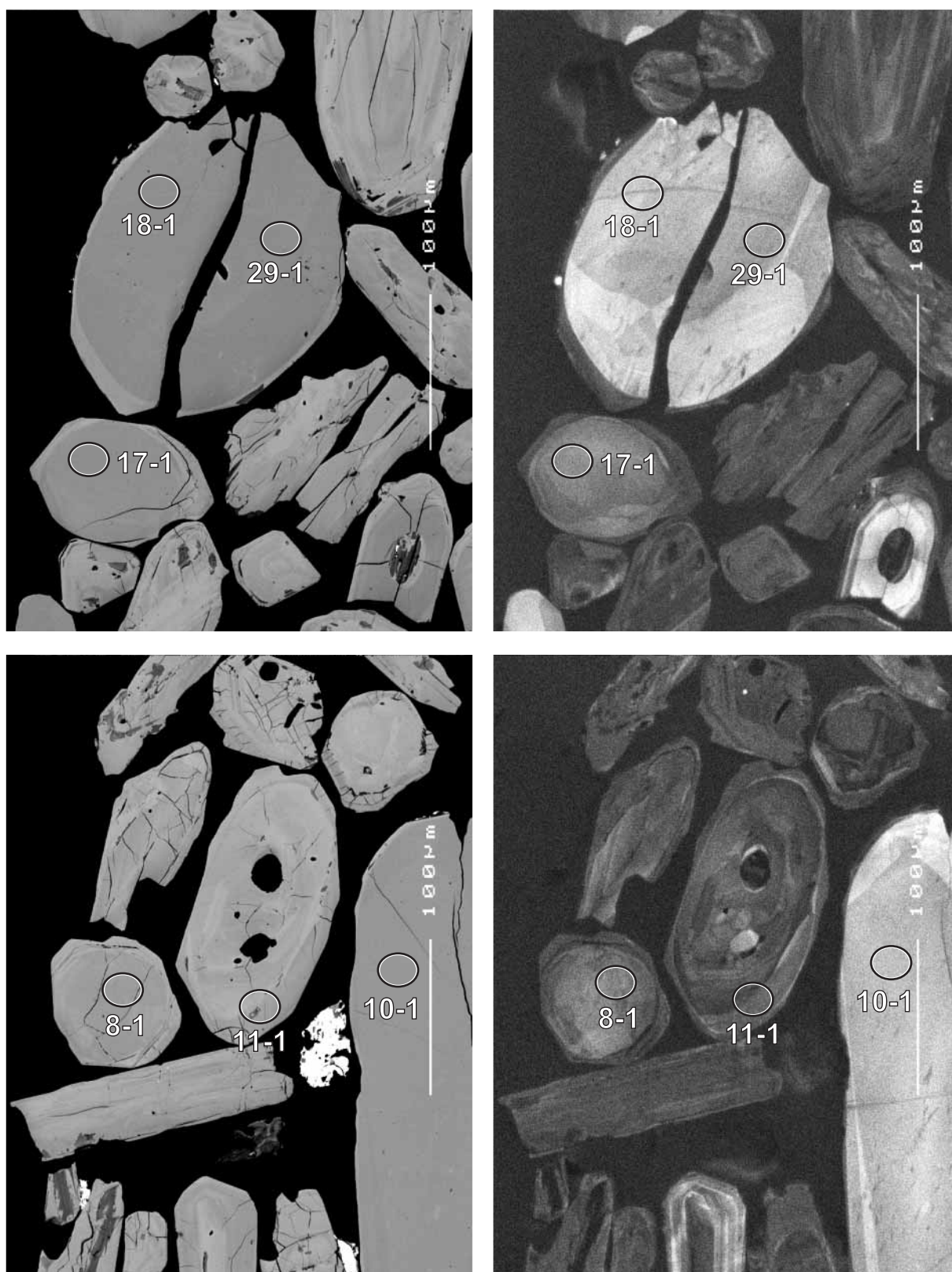


Figure 6. Representative SEM images (BSE on left, CL on right) for sample 9596 9764B: titanite-biotite granodiorite, Breakaway Well. SHRIMP analysis spots are labelled. Scale bar is 100  $\mu\text{m}$ .

Five points are >5% discordant (2-1, 4-1, 11-1, 26-1, 28-1; Fig. 7). These, and one other with >1% common  $^{206}\text{Pb}$  (3-1) are excluded from detailed age considerations.

There is one obviously inherited grain (spot 6-1; ~2850 Ma). The remaining 22 points fall in a single cluster, but there is considerable excess scatter in  $^{207}\text{Pb}/^{206}\text{Pb}$  (Fig. 8). Given the existence of one inherited grain and a skewed distribution tailing to higher dates, the spread is attributed to inheritance. Analyses 10-1 and 29-1 are outliers and 7-1 a possible outlier. Omitting these leaves a population of 19 analyses with a weighted average  $^{207}\text{Pb}/^{206}\text{Pb}$  age of  $2655.1 \pm 3.7$  Ma (MSWD = 1.7). Only a few of the grains with potential cores produced older ages; some gave discordant data and others fall within the main data group. Not all the older dates recorded came from discernable “cores”.

## Geochronological interpretation

The age of  $2655 \pm 4$  Ma is considered to be the magmatic age of the granodiorite.

Table 4. SHRIMP analytical results for zircon from sample 9596 9764B: titanite-biotite granodiorite, Breakaway Well.

grain-spot	U (ppm)	Th (ppm)	4f206 (%)	$^{207}\text{Pb}/^{206}\text{Pb}$	$\pm$	$^{206}\text{Pb}/^{238}\text{U}$	$\pm$	$^{207}\text{Pb}/^{235}\text{U}$	$\pm$	$^{208}\text{Pb}/^{232}\text{Th}$	conc. (%)	$^{207}\text{Pb}/^{206}\text{Pb}$ Age (Ma)	$\pm$
Main Group													
D.1-1	362	23	0.007	0.1795	0.0003	0.506	0.007	12.53	0.18	0.139	100	2648	3
D.5-1	66	63	0.117	0.1813	0.0010	0.509	0.009	12.73	0.23	0.142	100	2665	9
D.8-1	82	40	-0.093	0.1812	0.0009	0.502	0.008	12.55	0.21	0.147	98	2664	8
D.9-1	64	43	0.028	0.1811	0.0010	0.524	0.009	13.09	0.24	0.142	102	2663	9
D.12-1	139	33	0.036	0.1809	0.0006	0.505	0.008	12.60	0.20	0.134	99	2661	6
D.13-1	242	105	0.005	0.1803	0.0005	0.517	0.008	12.84	0.20	0.144	101	2656	4
D.14-1	139	60	0.010	0.1795	0.0006	0.499	0.008	12.36	0.20	0.140	99	2648	6
D.15-1	51	27	0.022	0.1821	0.0010	0.516	0.009	12.94	0.25	0.143	100	2672	9
D.16-1	62	37	0.027	0.1796	0.0009	0.511	0.009	12.66	0.23	0.144	100	2649	9
D.17-1	72	25	0.052	0.1823	0.0012	0.497	0.008	12.49	0.23	0.140	97	2674	11
D.18-1	32	53	-0.086	0.1821	0.0019	0.519	0.010	13.03	0.30	0.142	101	2672	18
D.19-1	60	86	0.087	0.1810	0.0010	0.503	0.009	12.56	0.23	0.142	99	2662	9
D.20-1	243	99	0.147	0.1812	0.0005	0.493	0.008	12.31	0.20	0.124	97	2664	5
D.21-1	185	218	0.004	0.1811	0.0005	0.497	0.008	12.41	0.20	0.139	98	2663	5
D.22-1	113	62	0.048	0.1802	0.0008	0.493	0.008	12.25	0.20	0.132	97	2655	7
D.23-1	237	357	0.061	0.1792	0.0005	0.484	0.008	11.96	0.21	0.135	96	2645	5
D.24-1	105	104	-0.047	0.1803	0.0008	0.520	0.008	12.93	0.22	0.145	102	2655	8
D.25-1	400	111	0.124	0.1796	0.0004	0.497	0.008	12.30	0.19	0.129	98	2649	4
D.27-1	107	80	-0.001	0.1811	0.0012	0.507	0.008	12.66	0.22	0.139	99	2663	11
Discordant and/or high common Pb													
D.2-1	777	488	0.438	0.1575	0.0011	0.371	0.005	8.05	0.13	0.102	84	2429	12
D.3-1	120	52	1.343	0.1841	0.0085	0.510	0.009	12.94	0.64	0.144	99	2690	77
D.4-1	390	352	0.910	0.1825	0.0017	0.422	0.006	10.63	0.19	0.070	85	2675	16
D.11-1	216	116	1.007	0.1899	0.0013	0.426	0.006	11.15	0.18	0.100	83	2742	12
D.26-1	92	31	-0.129	0.1557	0.0048	0.171	0.003	3.68	0.13	0.056	42	2410	53
D.28-1	108	13	0.006	0.1862	0.0039	0.439	0.028	11.26	0.75	0.123	87	2709	34
Inherited or possibly inherited													
D.6-1	143	67	0.049	0.2029	0.0006	0.541	0.008	15.13	0.24	0.151	98	2850	5
D.7-1	13	10	0.358	0.1839	0.0026	0.506	0.013	12.84	0.39	0.137	98	2688	23
D.10-1	33	60	-0.244	0.1862	0.0013	0.541	0.011	13.90	0.29	0.150	103	2708	11
D.29-1	40	77	0.000	0.1844	0.0011	0.510	0.010	12.96	0.26	0.141	99	2692	10

Data are at  $1\sigma$  precision. All Pb data are common-Pb corrected (based on  $^{204}\text{Pb}$  and Broken Hill Pb composition). Analysis date: 03/11/2000; session Z3623i.

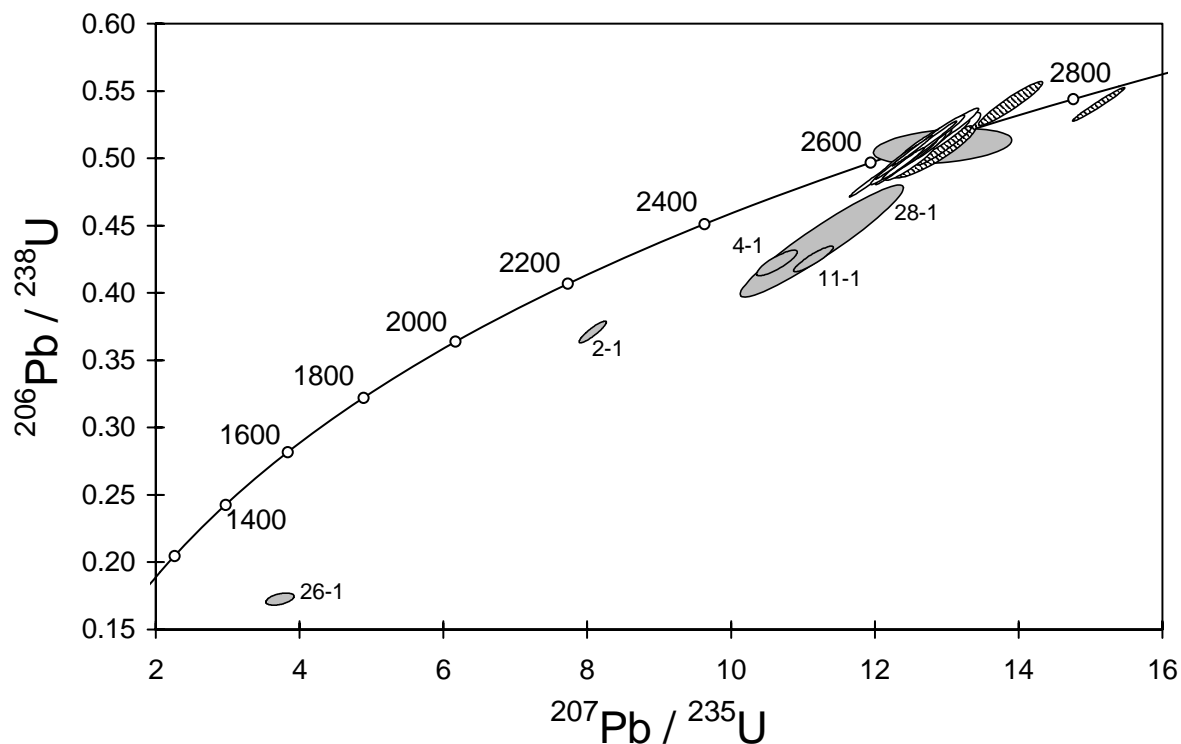


Figure 7. Concordia plot for zircon data from sample 9596 9764B: titanite-biotite granodiorite, Breakaway Well. White filled symbols are used to define the age of the sample; inherited grains have diagonal shading; discordant and/or high common Pb analyses are grey.

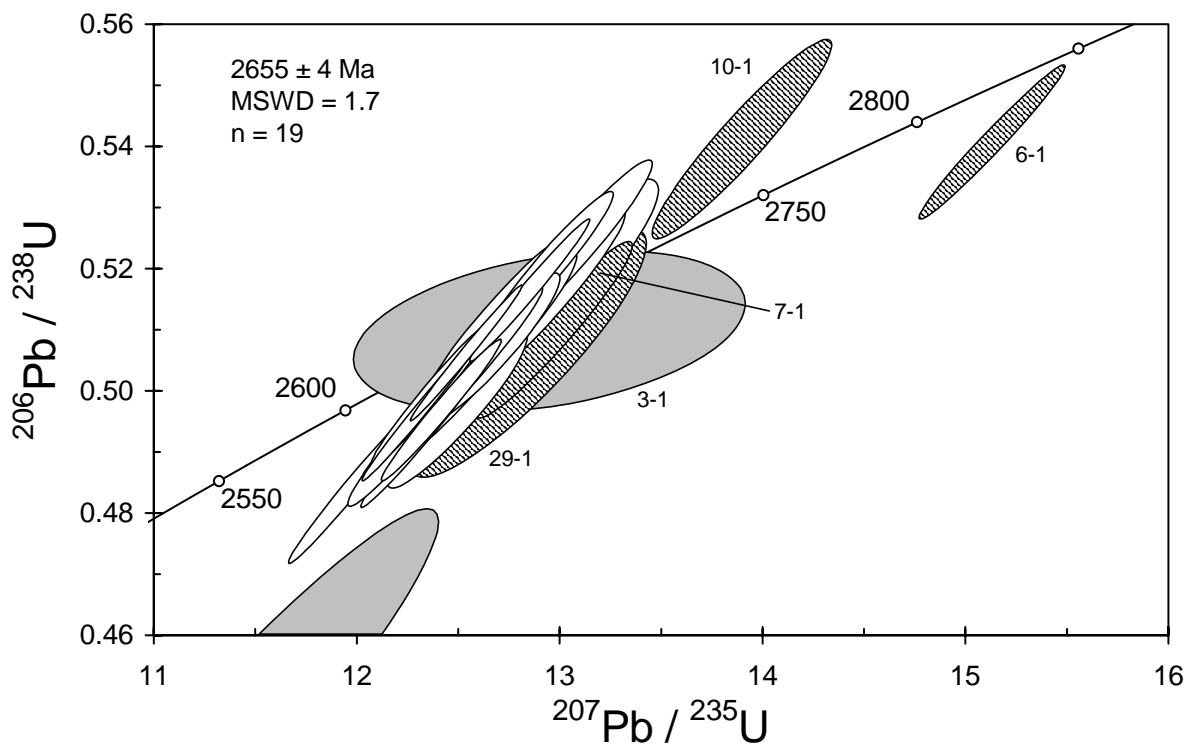


Figure 8. Enlargement of main group of zircon analyses for sample 9596 9764B: titanite-biotite granodiorite, Breakaway Well. Symbol shading as in Figure 7.

## 9596 9787: biotite granite dyke, Kaluweerie Hill

**1:250,000 sheet:** Sir Samuel (SG5113)

**1:100,000 sheet:** Depot Springs (2942)

**MGA:** 220185mE 6916259mN

**Location:** The sample was taken from a boulder forming part of a continuous east-west outcrop, 1 km south of Kaluweerie Hill.

**Description:** This sample is from a blue-grey fine- to very fine-grained equigranular biotite granite dyke. The dyke is one of a series of laterally continuous thin (<20 m) east-west dykes that intrude a grey-white medium-grained biotite monzogranite. The form and orientation of the dykes is similar to Proterozoic dykes in the area. The geochemistry of the dyke, however, indicates that it belongs to the Low-Ca grouping of Champion & Sheraton (1997) and is probably Archaean.

The unit has a granular to strongly granophyric/graphic intergrown texture. Principal minerals are plagioclase, K-feldspar, quartz (present in approximately equal amounts), and biotite (8–10%). Plagioclase is commonly unzoned to weakly zoned, while K-feldspar is variably perthitic. Both feldspars commonly have margins intergrown with quartz, i.e., marginal granophyric or graphic textures. Quartz is present as weakly undulose anhedral grains. Biotite occurs as fine- to very fine-grained rectangular to irregular grains. Accessory phases include common subhedral to anhedral Fe-oxides (1–2%), and anhedral titanite (<2%), as well as zircon and apatite. Secondary minerals include white mica, epidote, clinozoisite, chlorite and rutile.

**Mount, pop:** Z3623B

### Description of zircons

This sample contains euhedral to subhedral zircon grains that are predominantly small- to medium-sized (~70 µm to 150 µm long, aspect ratio 1:1 to 3:1) crystals and fragments, as well as a few larger (250 µm long, 100 µm wide) grains. Most grains are colourless and clear, although some are pale brown and slightly turbid. Acicular inclusions are pervasive in the grains. A strong CL response is obtained from most grains, with pronounced concentric and euhedral zoning (Fig. 9). A lesser number of grains have irregular zoning patterns and/or weak CL. Some structurally discontinuous zones are noted, with obvious core-rim relationships in some grains. The zoning and cores are also visible in some grains as seen in transmitted light photographs.

### Concurrent standard data

There is one clearly anomalous (low  $^{207}\text{Pb}/^{206}\text{Pb}$  and low  $^{206}\text{Pb}/^{238}\text{U}$ ) QGNG analysis (23-1). This was omitted from the calibration. A second analysis (2-1), which was noted to have a brief offset in the secondary beam profiles due to primary beam instability, is an outlier on the  $\ln:\ln$  calibration plot even though its internal calibration factor and the returned  $^{206}\text{Pb}/^{238}\text{U}$  and  $^{207}\text{Pb}/^{206}\text{Pb}$  are normal. This point was omitted, although the internal data rejection procedures seem to have worked appropriately and this omission has no effect on the calibration.

The floating calibration exponent is 2.34, well above the default, and both of the concurrent sample data sets suggest even higher values (>2.5). A value of 2.3 has been used in data reduction. The reproducibility of  $^{206}\text{Pb}/^{238}\text{U}$  for QGNG is 1.40% (1 $\sigma$ , n = 28 of 30). The corresponding  $^{207}\text{Pb}/^{206}\text{Pb}$  age is  $1845.4 \pm 3.1$  Ma (MSWD = 1.5), but using a standardised set of criteria for assessment of the data (see “Data compilation for the QGNG standard”) gives a  $^{207}\text{Pb}/^{206}\text{Pb}$  age of  $1846.9 \pm 2.8$  Ma (MSWD = 1.0).

Element abundance calibration was based on CZ3 (n = 4).



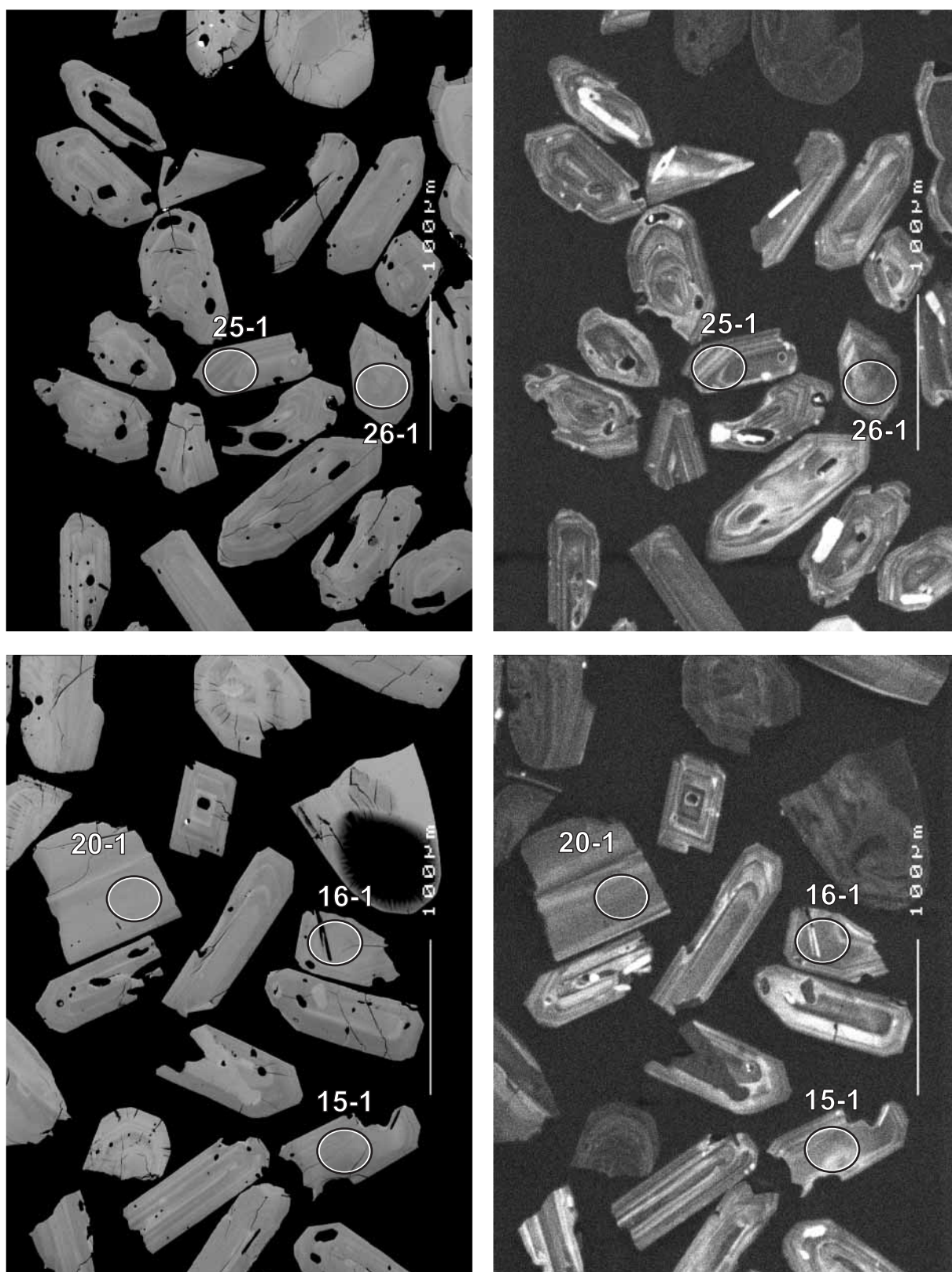


Figure 9. Representative SEM images (BSE on left, CL on right) for sample 9596 9787: biotite granite dyke, Kaluweerie Hill. SHRIMP analysis spots are labelled. Scale bar is 100  $\mu\text{m}$ .

## Sample data

Thirty analyses on 30 grains were undertaken (Fig. 10, Table 5). Five spots are >5% discordant (4-1, 6-1, 8-1, 15-1, 28-1) and are excluded from detailed age considerations, although some of them are consistent with the main group identified below. There are three obviously inherited grains (11-1, 19-1 and 20-1; up to 3266 Ma), and one of the discordant analyses (6-1) also indicates inheritance. There are two analyses (7-1 and 12-1) that are clearly younger than the bulk of the remainder. There is no correlation between zoning patterns and age groupings.

The remaining 20 points show considerable excess scatter (Fig. 11). Much of this is attributable to four high-U analyses (1-1, 5-1, 9-1, 23-1) that have higher ages than the others and might represent a distinct source of inherited grains. Omitting these four, and two marginal (low-precision) young outliers (27-1 and 29-1) leaves a population of 14 points with weighted mean  $^{207}\text{Pb}/^{206}\text{Pb}$  age of  $2625.7 \pm 3.8$  Ma (MSWD = 1.07).

## Geochronological interpretation

The age of  $2626 \pm 4$  Ma is considered to be the intrusion age of the dyke.

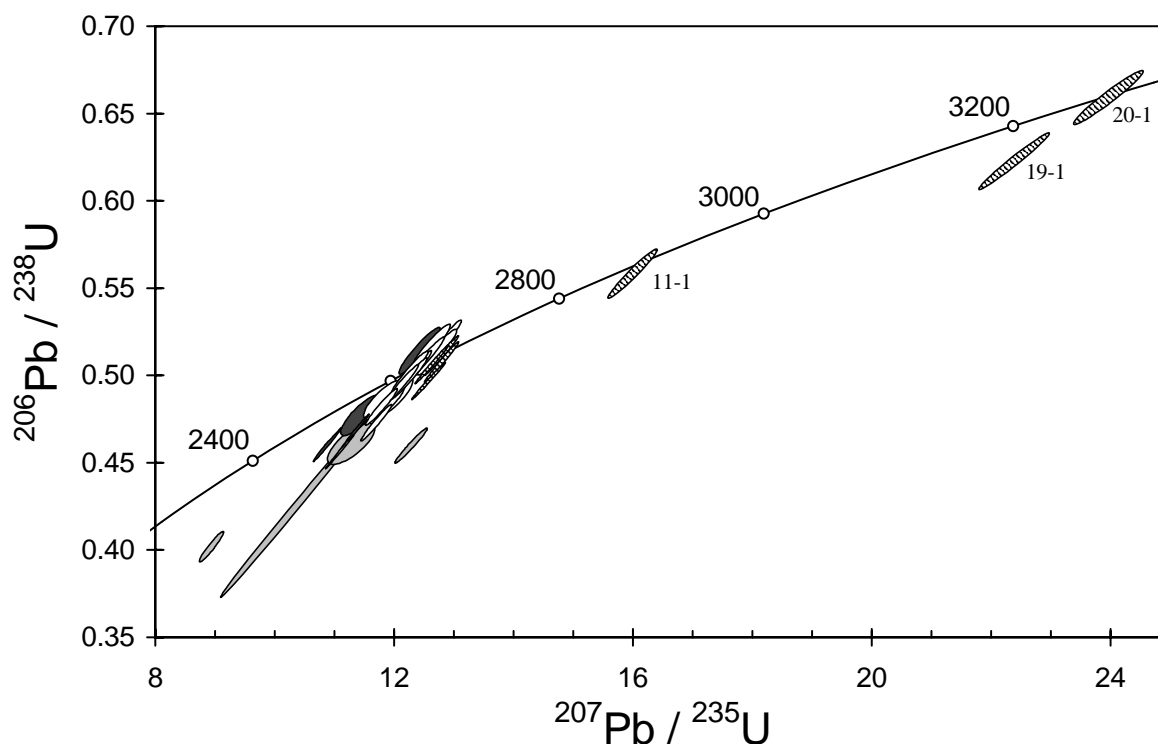


Figure 10. Concordia plot for zircon data from sample 9596 9787: biotite granite dyke, Kaluweerie Hill. White filled symbols are used to define the age of the sample; inherited grains have diagonal shading; discordant analyses are light grey; younger outliers are dark grey.

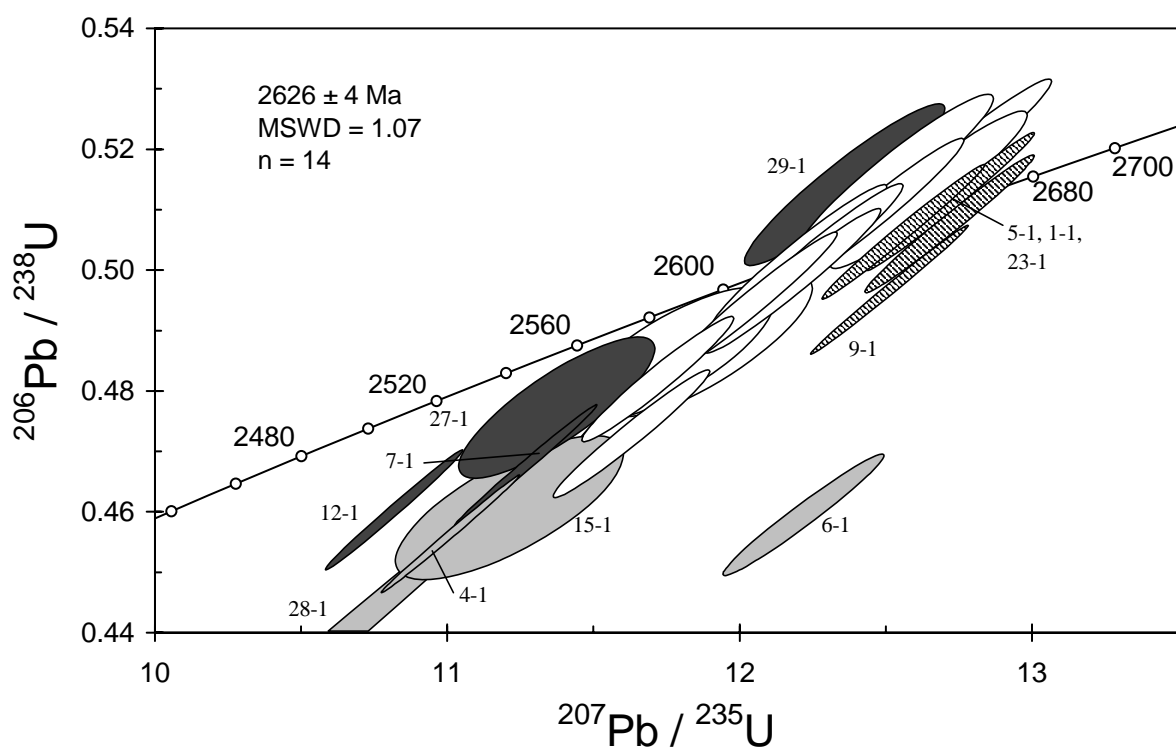


Figure 11. Enlargement of main group of zircon analyses for sample 9596 9787: biotite granite dyke, Kaluweerie Hill. Symbol shading as in Figure 10.

Table 5. SHRIMP analytical results for zircon from sample 9596 9787: biotite granite dyke, Kaluweerie Hill.

grain-spot	U (ppm)	Th (ppm)	4f206 (%)	$\frac{^{207}\text{Pb}}{^{206}\text{Pb}}$	$\pm$	$\frac{^{206}\text{Pb}}{^{238}\text{U}}$	$\pm$	$\frac{^{207}\text{Pb}}{^{235}\text{U}}$	$\pm$	$\frac{^{208}\text{Pb}}{^{232}\text{Th}}$	conc. (%)	$\frac{^{207}\text{Pb}}{^{206}\text{Pb}}$ Age (Ma)	$\pm$
Main Group													
B.2-1	108	206	0.054	0.1762	0.0007	0.502	0.008	12.20	0.20	0.142	100	2618	7
B.3-1	802	641	0.007	0.1763	0.0006	0.482	0.007	11.71	0.17	0.136	97	2618	6
B.10-1	269	1007	0.582	0.1783	0.0006	0.473	0.007	11.62	0.18	0.133	95	2637	6
B.13-1	145	207	-0.004	0.1765	0.0006	0.495	0.008	12.04	0.19	0.135	99	2621	6
B.14-1	89	152	-0.037	0.1767	0.0009	0.501	0.008	12.21	0.21	0.141	100	2622	8
B.16-1	174	300	0.062	0.1755	0.0022	0.486	0.007	11.76	0.23	0.136	98	2611	21
B.17-1	121	246	0.080	0.1773	0.0007	0.498	0.008	12.18	0.20	0.142	99	2627	6
B.18-1	129	240	0.273	0.1781	0.0008	0.516	0.010	12.67	0.26	0.143	102	2635	7
B.21-1	79	130	0.155	0.1768	0.0009	0.482	0.009	11.75	0.23	0.132	97	2623	8
B.22-1	124	270	0.536	0.1770	0.0020	0.487	0.008	11.89	0.23	0.122	98	2625	19
B.24-1	73	133	0.062	0.1786	0.0010	0.513	0.009	12.65	0.22	0.143	101	2640	9
B.25-1	100	132	0.003	0.1773	0.0007	0.510	0.008	12.45	0.21	0.139	101	2627	7
B.26-1	80	122	0.052	0.1761	0.0010	0.516	0.009	12.54	0.22	0.141	103	2616	10
B.30-1	119	222	0.035	0.1769	0.0007	0.502	0.008	12.25	0.20	0.140	100	2624	7
Discordant													
B.4-1	1057	1012	0.035	0.1749	0.0002	0.456	0.006	11.00	0.16	0.125	93	2605	2
B.6-1	1612	89	0.047	0.1929	0.0006	0.459	0.007	12.21	0.18	0.136	88	2767	5
B.8-1	693	477	0.382	0.1598	0.0007	0.401	0.006	8.85	0.13	0.105	89	2454	8
B.15-1	77	170	1.275	0.1764	0.0027	0.461	0.008	11.20	0.26	0.108	93	2620	26
B.28-1	86	164	0.027	0.1756	0.0008	0.422	0.033	10.20	0.79	0.117	87	2611	8
Inherited													
B.11-1	87	214	0.059	0.2069	0.0009	0.559	0.009	15.94	0.27	0.164	99	2881	7
B.19-1	119	269	0.030	0.2603	0.0009	0.623	0.011	22.38	0.39	0.172	96	3249	5
B.20-1	139	50	0.019	0.2632	0.0011	0.660	0.010	23.96	0.39	0.175	100	3266	6
Probably inherited													
B.1-1	215	159	0.033	0.1816	0.0005	0.508	0.008	12.72	0.19	0.140	99	2668	4
B.5-1	392	415	0.006	0.1798	0.0004	0.506	0.007	12.56	0.18	0.139	100	2651	3
B.9-1	806	742	0.038	0.1826	0.0003	0.497	0.007	12.51	0.18	0.138	97	2677	2
B23-1	302	42	-0.002	0.1804	0.0004	0.511	0.008	12.72	0.19	0.141	100	2656	4
Young outliers													
B.7-1	863	66	0.064	0.1746	0.0003	0.468	0.007	11.26	0.16	0.133	95	2603	3
B.12-1	739	308	0.102	0.1703	0.0003	0.460	0.007	10.81	0.16	0.127	95	2561	3
B.27-1	103	236	0.511	0.1728	0.0019	0.477	0.008	11.37	0.22	0.122	97	2585	18
B.29-1	64	67	0.166	0.1743	0.0011	0.514	0.009	12.36	0.23	0.140	103	2599	11

Data are at 1 $\sigma$  precision. All Pb data are common-Pb corrected (based on  $^{204}\text{Pb}$  and Broken Hill Pb composition). Analysis date: 03/11/2000; session Z3623i.



## 9696 9055: hornblende plagiogranite, Hootanui Well

**1:250,000 sheet:** Duketon (GS5114)

**1:100,000 sheet:** Tate (3243)

**MGA:** 395142mE 6957915mN

**Location:** The sample was taken from a small boulder on a ridge of good outcrop, just north of the creek, approximately 2.5 km north of Hootanui Well.

**Description:** This sample is from a metamorphosed grey and white medium- to coarse-grained hornblende plagiogranite. This distinctive unit, with large amphibole clusters (to 5 cm) and very strong magnetic geophysical signature, crops out as an elongate north-south ridge and is interpreted to represent the fractionated felsic component of a layered gabbro that intruded the greenstone sequence.

The sample has a granoblastic and locally granophyric texture. The principal minerals are plagioclase (50–60%), quartz (30–40%) and amphibole (7–15%). Plagioclase occurs as unzoned laths, often with very fine-grained amphibole and quartz inclusions. Plagioclase is also locally coarsely intergrown with quartz, forming a granophyric texture, and more rarely irregularly intergrown with other plagioclase. Quartz is mostly present as recrystallised to variably undulose, elongate grains, but also occurs as small grains within amphibole aggregates. Amphibole occurs as fine- to very fine-grained aggregates, clearly pseudomorphing an originally much larger phase (to >1 cm), probably pyroxene which has broken down to amphibole and quartz during metamorphism. All main minerals also occur as very fine-grained interstitial granular material. Accessory minerals include moderate amounts of titanite, and also zircon and Fe-oxides. Secondary minerals comprise minor to moderate epidote, carbonate and white mica.

**Mount, pop:** Z3623A

### Description of zircons

Most zircon grains are colourless to pale grey-brown, angular, subhedral to anhedral fragments. Rare whole zircon grains with discernable crystal faces are also present. The largest grains and fragments are up to 300 µm in length, but most are about 100 µm to 200 µm. The grains generally contain abundant inclusions, and display unusual interior features in the CL images, some having undulating zone boundaries that give a semblance to “agate” texture (Fig. 12). They are variably embayed and pitted. Faint concentric or parallel zoning is visible in some fragments, although most also display the irregular and complex zoning. A few rare grains are homogeneous, having no visible zoning.

### Concurrent standard data

The first QGNG analysis is an outlier in Pb/U and UO/U, possibly because of poor beam centering following a break in magnet cycling. It has been omitted from the calibration. The CZ3 analysis that follows is normal in UO/U and consistent with later CZ3 analyses in Pb/U, so sample analyses before the second QGNG were retained. Analysis 6-1 has extreme U (>1000 ppm) and has been omitted, even though it appears normal in other respects.

The floating point calibration exponent is 2.38. Although this is not precise enough to distinguish it from the default value of 2.0, data for sample 9696 9055 indicate a similar value. A value of 2.3 has been used for data reduction. The  $^{206}\text{Pb}/^{238}\text{U}$  reproducibility for QGNG is 1.53% ( $1\sigma$ ,  $n = 30$  of 32). The  $^{207}\text{Pb}/^{206}\text{Pb}$  age for the same analyses is  $1850.1 \pm 4.3$  Ma (MSWD = 1.3), but using a standardised set of criteria for assessment of the data (see “Data compilation for the QGNG standard”) gives a  $^{207}\text{Pb}/^{206}\text{Pb}$  age of  $1852.0 \pm 3.5$  Ma (MSWD = 1.01).

Element abundance calibration was based on CZ3 ( $n = 4$ ).

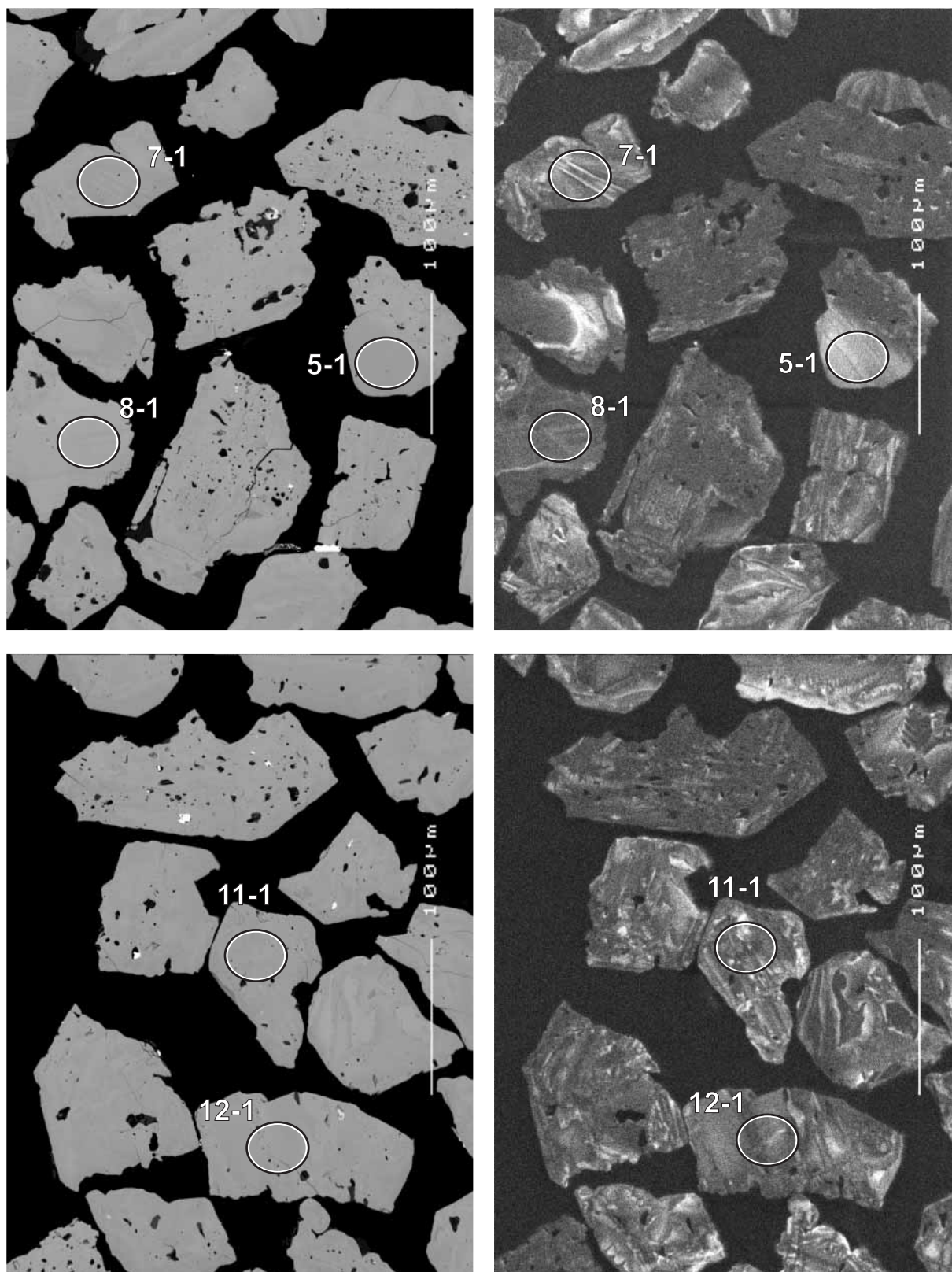


Figure 12. Representative SEM images (BSE on left, CL on right) for sample 9696 9055: hornblende plagiogranite, Hootanui Well. SHRIMP analysis spots are labelled. Scale bar is 100  $\mu\text{m}$ .

## Sample data

Thirty one analyses were performed, on separate grains (Fig. 13, Table 6). Several primary beam irregularities noted during analyses appear to have had no affect on final data. Two analyses (4-1 and 11-1) are discordant; 11-1 also has the highest  $^{204}\text{Pb}$  for this data set. These points are excluded from age considerations. Analysis 19-1 is a distinct young outlier from the remainder of analyses, although this grain is not visibly different from others. With these three omissions, the weighted mean  $^{207}\text{Pb}/^{206}\text{Pb}$  age is  $2756.0 \pm 4.2$  Ma (MSWD = 1.7;  $n = 28$ ). Amongst the remaining data, analysis 20-1 is an old outlier, though not an extreme one. With this additional deletion, the age is  $2754.9 \pm 3.6$  Ma (MSWD = 1.19). Since the deletion of 20-1 is questionable, we use a conservative (though still ~95% confidence) uncertainty of  $\pm 5$  Ma that covers the span of both calculations.

## Geochronological interpretation

The  $^{207}\text{Pb}/^{206}\text{Pb}$  age of  $2755 \pm 5$  Ma is possibly the intrusive age of the plagiogranite. However, the unusual patchy internal textures might be secondary, in which case the date could record an unknown (probably later) event.

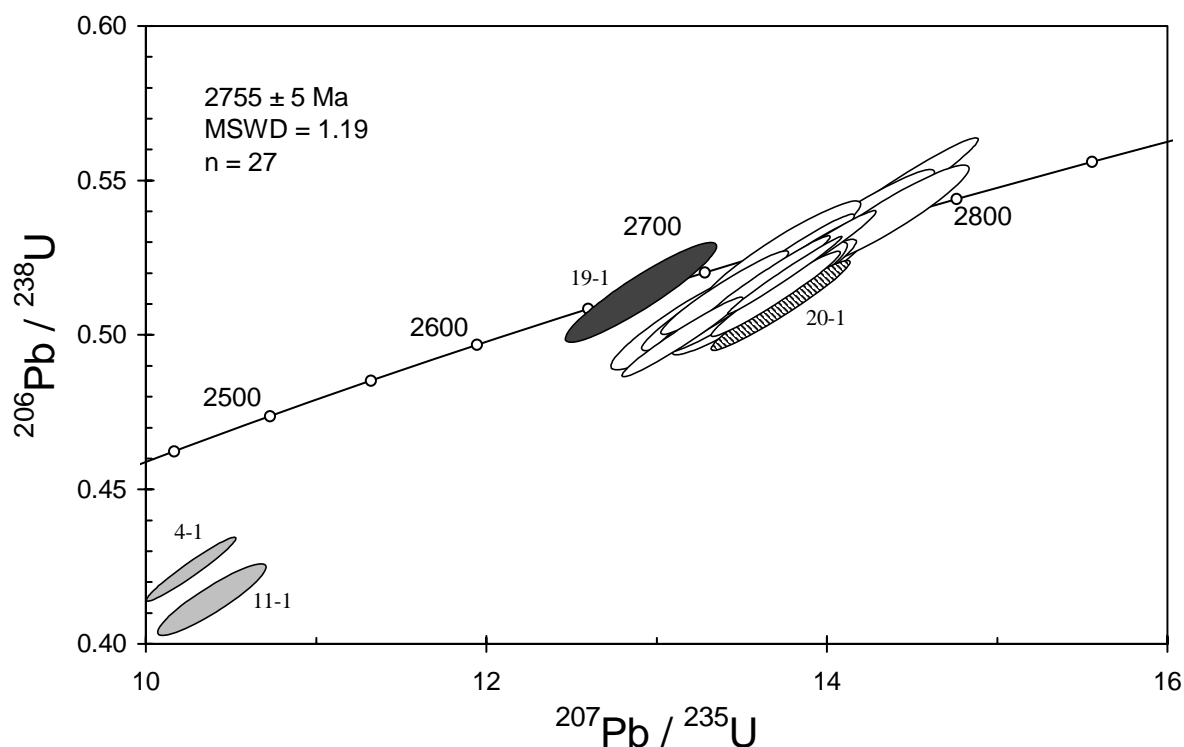


Figure 13. Concordia plot for zircon data from sample 9696 9055: hornblende plagiogranite, Hootanui Well. White filled symbols are used to define the age of the sample; inherited grains have diagonal shading; discordant analyses are light grey; young outlier is dark grey.

Table 6. SHRIMP analytical results for zircon from sample 9696 9055: plagiogranite, Hootanui Well.

grain-spot	U (ppm)	Th (ppm)	4f206 (%)	$\frac{^{207}\text{Pb}}{^{206}\text{Pb}}$	$\pm$	$\frac{^{206}\text{Pb}}{^{238}\text{U}}$	$\pm$	$\frac{^{207}\text{Pb}}{^{235}\text{U}}$	$\pm$	$\frac{^{208}\text{Pb}}{^{232}\text{Th}}$	conc. (%)	$\frac{^{207}\text{Pb}}{^{206}\text{Pb}}$ Age (Ma)	$\pm$
Main group													
A.1-1	72	90	0.068	0.1934	0.0015	0.539	0.011	14.37	0.31	0.152	100	2771	13
A.2-1	186	170	0.053	0.1917	0.0008	0.526	0.009	13.91	0.25	0.135	99	2757	7
A.3-1	176	137	0.069	0.1908	0.0008	0.516	0.010	13.58	0.27	0.140	98	2749	7
A.5-1	50	23	0.302	0.1895	0.0017	0.505	0.011	13.20	0.32	0.134	96	2738	15
A.6-1	73	33	-0.063	0.1933	0.0013	0.515	0.010	13.73	0.29	0.143	97	2771	11
A.7-1	119	59	0.095	0.1909	0.0010	0.507	0.009	13.35	0.26	0.140	96	2750	9
A.8-1	211	190	0.029	0.1909	0.0007	0.518	0.009	13.65	0.24	0.142	98	2750	6
A.9-1	127	84	0.031	0.1927	0.0016	0.516	0.009	13.70	0.28	0.140	97	2765	14
A.10-1	188	103	0.056	0.1910	0.0008	0.499	0.009	13.14	0.23	0.137	95	2751	7
A.12-1	123	43	0.115	0.1896	0.0012	0.509	0.009	13.29	0.26	0.138	97	2739	10
A.13-1	204	176	0.081	0.1912	0.0007	0.515	0.009	13.59	0.24	0.138	97	2752	6
A.14-1	312	134	0.038	0.1916	0.0013	0.508	0.009	13.41	0.26	0.134	96	2756	11
A.15-1	103	67	0.272	0.1912	0.0011	0.507	0.010	13.35	0.27	0.138	96	2753	10
A.16-1	97	82	-0.030	0.1916	0.0010	0.509	0.010	13.44	0.27	0.240	96	2756	9
A.17-1	59	27	0.121	0.1935	0.0014	0.516	0.011	13.76	0.31	0.130	97	2772	12
A.18-1	95	52	-0.021	0.1928	0.0014	0.508	0.010	13.50	0.28	0.136	96	2766	12
A.21-1	127	68	-0.088	0.1904	0.0009	0.524	0.010	13.77	0.26	0.150	99	2745	8
A.22-1	95	80	-0.050	0.1913	0.0011	0.544	0.013	14.36	0.35	0.151	102	2753	9
A.23-1	69	34	0.292	0.1890	0.0015	0.527	0.011	13.74	0.30	0.135	100	2734	13
A.24-1	123	43	0.071	0.1914	0.0010	0.520	0.010	13.71	0.26	0.143	98	2755	9
A.25-1	578	579	0.050	0.1920	0.0005	0.519	0.008	13.75	0.22	0.140	98	2760	4
A.26-1	179	110	0.072	0.1915	0.0009	0.523	0.009	13.82	0.25	0.139	99	2755	7
A.27-1	171	107	0.178	0.1892	0.0010	0.513	0.009	13.39	0.25	0.127	98	2735	9
A.28-1	71	26	0.049	0.1913	0.0014	0.537	0.011	14.17	0.31	0.138	101	2754	12
A.29-1	125	81	0.044	0.1919	0.0012	0.513	0.010	13.56	0.27	0.143	97	2758	10
A.30-1	170	127	-0.061	0.1936	0.0009	0.513	0.009	13.70	0.25	0.143	96	2773	7
A.31-1	49	82	-0.013	0.1925	0.0015	0.531	0.012	14.10	0.34	0.144	99	2764	13
Discordant													
A.4-1	371	403	0.267	0.1755	0.0008	0.423	0.007	10.24	0.17	0.104	87	2611	7
A.11-1	114	26	0.568	0.1819	0.0016	0.413	0.008	10.36	0.21	0.096	83	2671	14
Young outlier													
A.19-1	53	7	-0.351	0.1822	0.0016	0.514	0.011	12.90	0.30	0.162	100	2673	14
Possible old outlier (?inherited)													
A.20-1	105	65	-0.049	0.1955	0.0010	0.509	0.010	13.72	0.27	0.142	95	2789	9

Data are at 1 $\sigma$  precision. All Pb data are common-Pb corrected (based on  $^{204}\text{Pb}$  and Broken Hill Pb composition). Analysis date: 11/11/2000; session Z3623j.

## 9996 6016A: biotite monzogranite, Tower Hill mine

**1:250,000 sheet:** Leonora (SH5101)

**1:100,000 sheet:** Leonora (3140)

**MGA:** 336483mE 6801738mN

**Location:** The sample was taken from the west wall in the southern part of the Tower Hill open pit.

**Description:** This sample is from a white, moderately foliated, quartz-feldspar porphyritic fine- to medium-grained biotite monzogranite. The monzogranite forms part of a leucocratic biotite monzogranite pluton on the contact between foliated biotite granodiorite and ultramafic rocks, and forms the western wall of the Tower Hill open pit (Witt, 2001). The biotite monzogranite is massive to weakly foliated, except for several metres at the contact with the ultramafic supracrustal rocks where it is strongly foliated and altered.

The sample has a recrystallised to granoblastic texture with a moderate alteration overprint. The principal minerals are plagioclase and quartz which both occur as phenocrysts set in a finer-grained biotite quartzofeldspathic matrix. Plagioclase phenocrysts comprise fractured and kinked unzoned subhedral to anhedral grains, while quartz phenocrysts occur as recrystallised elongate grains. Biotite (~5–7%) is present as fine-grained discrete flakes. Accessory phases include zircon and Fe-oxides. Secondary minerals present are moderate sericite and carbonate, with minor chlorite and rutile. Minor quartz-sericite-carbonate-biotite veinlets are also present within the sample.

**Mount, pop:** Z3623C

### Description of zircons

Zircon from this sample consists mainly of roughly equant, subhedral to euhedral fragments and crystals, ranging in size from about 65  $\mu\text{m}$  to 180  $\mu\text{m}$ . The grains are clear, colourless to pale brown, and many contain a few small inclusions. Well-defined euhedral, concentric zoning is visible in virtually all grains as seen on CL images (Fig. 14); zoning is also visible in many grains as seen in the transmitted and reflected light photographs. Many of the grains contain structurally distinct cores.

### Concurrent standard data

The first QGNG analysis is an outlier in Pb/U and UO/U, possibly because of poor beam centering following a break in magnet cycling. It has been omitted from the calibration. The cz3 analysis that follows is normal in UO/U and consistent with later cz3 analyses in Pb/U, so sample analyses before the second QGNG were retained. Analysis QGNG.6-1 has extreme U (>1000 ppm) and has been omitted, even though it appears normal in other respects.

The floating point calibration exponent is 2.38. Although this is not precise enough to distinguish it from the default value of 2.0, data from concurrently analysed sample 9696 9055 indicates a similar value. A value of 2.3 has been used for data reduction. The  $^{206}\text{Pb}/^{238}\text{U}$  reproducibility for QGNG is 1.53% ( $1\sigma$ ,  $n = 30$  of 32). The  $^{207}\text{Pb}/^{206}\text{Pb}$  age for the same analyses is  $1850.1 \pm 4.3$  Ma (MSWD = 1.3), but using a standardised set of criteria for assessment of the data (see “Data compilation for the QGNG standard”) gives a  $^{207}\text{Pb}/^{206}\text{Pb}$  age of  $1852.0 \pm 3.5$  Ma (MSWD = 1.01).

Element abundance calibration was based on CZ3 ( $n = 4$ ).

### Sample data

Thirty one analyses were made on 31 grains (Fig. 15, Table 7). Primary beam instabilities noted during several analyses appear to have no affect on final data. There are six analyses that are >5% discordant (4-1, 9-1, 11-1, 12-1, 15-1, 21-1). These points are omitted from the age determination even though the discordance trend appears to be due entirely to recent Pb loss and



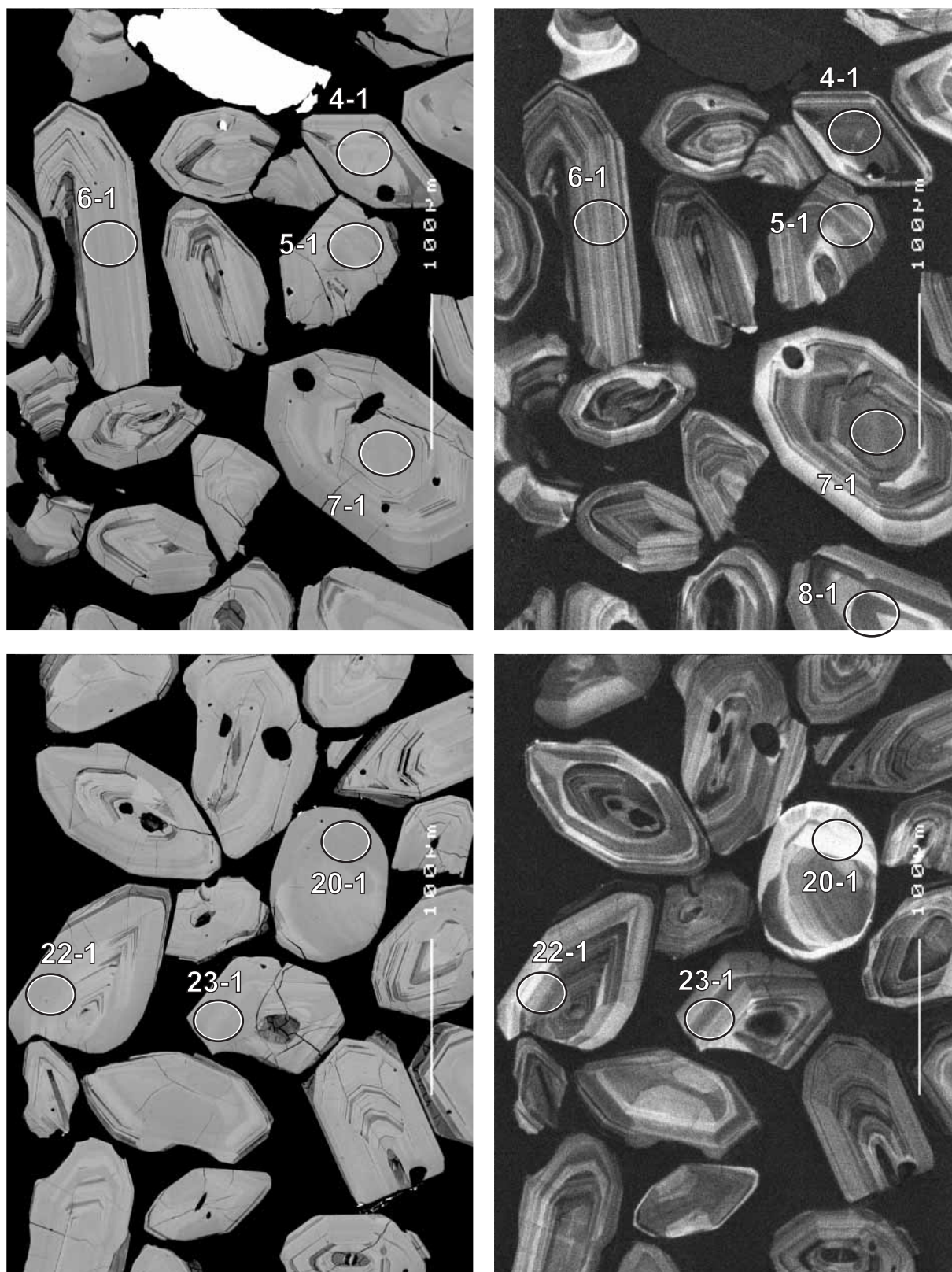


Figure 14. Representative SEM images (BSE on left, CL on right) for sample 9996 6016A: biotite monzogranite, Tower Hill. SHRIMP analysis spots are labelled. Scale bar is 100  $\mu$ m.

the weighted mean  $^{207}\text{Pb}/^{206}\text{Pb}$  for the entire data set is almost identical to that for the reduced data set. The 25 concordant points give a weighted mean  $^{207}\text{Pb}/^{206}\text{Pb}$  age of  $2752.6 \pm 5.4$  Ma (MSWD = 1.2). There is no evidence of inheritance in these data, but none of the analyses were conducted on visible cores, so the sample might still contain a record of inheritance.

### Geochronological interpretation

The  $^{207}\text{Pb}/^{206}\text{Pb}$  age of  $2753 \pm 6$  Ma is interpreted to be the magmatic age of the monzogranite.

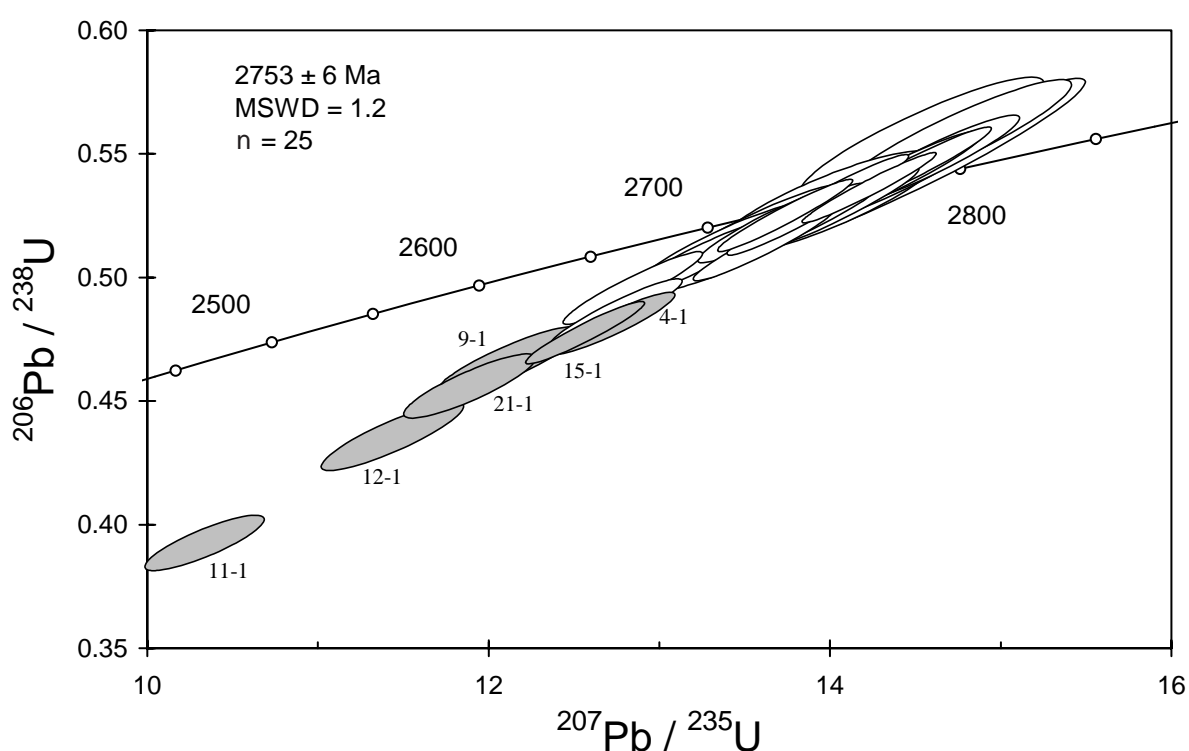


Figure 15: Concordia plot for zircon data from sample 9996 6016A: biotite monzogranite, Tower Hill mine. White filled symbols are used to define the age of the sample; discordant analyses are light grey.

Table 7. SHRIMP analytical results for zircon from sample 9996 6016A: biotite monzogranite, Tower Hill mine.

grain-spot	U (ppm)	Th (ppm)	4f206 (%)	$\frac{^{207}\text{Pb}}{^{206}\text{Pb}}$	$\pm$	$\frac{^{206}\text{Pb}}{^{238}\text{U}}$	$\pm$	$\frac{^{207}\text{Pb}}{^{235}\text{U}}$	$\pm$	$\frac{^{208}\text{Pb}}{^{232}\text{Th}}$	conc. (%)	$\frac{^{207}\text{Pb}}{^{206}\text{Pb}}$ Age (Ma)	$\pm$
Main group													
C.1-1	148	63	0.060	0.1922	0.0009	0.537	0.010	14.22	0.26	0.145	100	2761	7
C.2-1	49	23	-0.139	0.1926	0.0015	0.542	0.012	14.39	0.33	0.159	101	2765	13
C.3-1	29	12	-0.141	0.1895	0.0021	0.518	0.013	13.53	0.38	0.145	98	2738	18
C.5-1	78	52	0.412	0.1877	0.0013	0.495	0.010	12.83	0.27	0.079	95	2722	12
C.6-1	76	29	-0.003	0.1930	0.0012	0.529	0.011	14.07	0.30	0.147	99	2768	10
C.7-1	67	28	-0.007	0.1928	0.0013	0.530	0.011	14.09	0.30	0.146	99	2766	11
C.8-1	107	95	0.487	0.1902	0.0014	0.485	0.009	12.73	0.26	0.081	93	2744	12
C.10-1	117	55	-0.004	0.1895	0.0009	0.525	0.010	13.73	0.26	0.144	99	2738	8
C.13-1	34	12	-0.329	0.1891	0.0020	0.512	0.012	13.34	0.35	0.150	97	2735	18
C.14-1	89	46	0.237	0.1897	0.0014	0.521	0.010	13.63	0.28	0.140	99	2739	12
C.16-1	94	52	0.137	0.1921	0.0012	0.514	0.010	13.61	0.28	0.137	97	2760	10
C.17-1	117	47	0.012	0.1909	0.0010	0.524	0.010	13.78	0.27	0.147	99	2750	9
C.18-1	28	10	-0.431	0.1911	0.0031	0.531	0.014	13.98	0.43	0.155	100	2751	27
C.19-1	22	7	-0.224	0.1928	0.0024	0.548	0.022	14.56	0.62	0.170	102	2766	21
C.20-1	20	10	0.170	0.1892	0.0028	0.557	0.016	14.53	0.47	0.140	104	2735	24
C.22-1	66	27	0.233	0.1888	0.0014	0.507	0.011	13.19	0.29	0.138	97	2731	12
C.23-1	65	35	0.168	0.1909	0.0018	0.511	0.011	13.46	0.31	0.105	97	2750	16
C.24-1	51	19	-0.255	0.1931	0.0016	0.548	0.012	14.59	0.35	0.157	102	2768	14
C.25-1	94	41	-0.083	0.1903	0.0011	0.535	0.010	14.03	0.28	0.151	101	2745	9
C.26-1	92	34	0.195	0.1913	0.0013	0.529	0.010	13.96	0.29	0.145	99	2753	11
C.27-1	48	20	0.045	0.1929	0.0017	0.541	0.012	14.39	0.35	0.149	101	2767	14
C.28-1	66	23	0.120	0.1921	0.0015	0.528	0.011	13.99	0.31	0.143	99	2760	12
C.29-1	97	42	0.085	0.1918	0.0014	0.524	0.010	13.85	0.29	0.141	98	2758	12
C.30-1	25	13	0.006	0.1918	0.0024	0.557	0.016	14.73	0.45	0.145	104	2757	21
C.31-1	91	35	-0.046	0.1928	0.0011	0.545	0.011	14.49	0.30	0.156	101	2766	9
Discordant													
C.4-1	181	167	2.014	0.1916	0.0014	0.481	0.008	12.71	0.24	0.099	92	2756	12
C.9-1	68	52	1.420	0.1885	0.0021	0.465	0.010	12.09	0.28	0.062	90	2729	19
C.11-1	103	49	2.256	0.1909	0.0023	0.391	0.007	10.29	0.23	0.107	77	2750	20
C.12-1	57	31	1.151	0.1903	0.0022	0.435	0.009	11.41	0.28	0.082	85	2745	19
C.15-1	182	101	0.415	0.1907	0.0011	0.477	0.008	12.54	0.23	0.113	92	2748	10
C.21-1	106	112	1.424	0.1890	0.0020	0.455	0.009	11.86	0.26	0.062	88	2733	18

Data are at 1 $\sigma$  precision. All Pb data are common-Pb corrected (based on  $^{204}\text{Pb}$  and Broken Hill Pb composition). Analysis date: 11/11/2000; session 3623j.



## 9996 7007A: banded biotite granitic gneiss, Surprise Rocks

**1:250,000 sheet:** Minigwal (SH5107)

**1:100,000 sheet:** Lightfoot (3539)

**MGA:** 515568mE 6737539mN

**Location:** The sample was taken from a large pavement located on the south side of Surprise Rocks.

**Description:** This sample is from a grey, banded to locally migmatitic, fine- to medium-grained seriate biotite quartz-feldspathic granitic gneiss. The granitic gneiss has been intruded by a cream-pink, fine-grained, equigranular to seriate biotite monzogranite dyke, of which sample 9996 7007B is representative.

The unit is characterised by a granoblastic texture. Principal minerals are plagioclase (30–40%), quartz (30–40%), K-feldspar (20%) and biotite (7–8%). Plagioclase is recrystallised, displays no zoning, and is weakly altered to sericite and minor epidote. K-feldspar is dominantly microcline, interstitial to plagioclase and quartz, and locally perthitic. Quartz is recrystallised and granoblastic, and elongate in places. Myrmekite is also locally developed. Biotite and minor muscovite occur as aligned flakes and aggregates. Accessory minerals include apatite, Fe-oxides and zircon. Secondary phases include minor white mica, epidote and chlorite.

**Mount, pop:** Z3624A

### Description of zircons

Two size populations of zircon are present, with the larger grains ranging from approximately 200  $\mu\text{m}$  to 400  $\mu\text{m}$  in length, whereas the smaller grains are typically 70  $\mu\text{m}$  to 200  $\mu\text{m}$ . Both groups of zircon include white to pale brown whole grains (euhedral to subhedral crystals) with subordinate fragments. The grains are predominantly elongate (aspect ratio 2:1 to 3:1) and prismatic with well-defined crystal faces. Some inclusions and cracks are present, but are not pervasive. Most grains have well defined zoning, interpreted as a product of igneous crystallisation, seen in both transmitted and reflected light photographs and in the CL images, although a few grains are homogeneous (Fig. 16). Some grains contain structurally discontinuous zones, mainly in their core regions, interpreted as potential xenocrystic zircon. A few grains show complex recrystallisation features on the CL images.

### Concurrent standard data

One spot (15-1) is an outlier in both  $^{206}\text{Pb}/^{238}\text{U}$  and  $^{207}\text{Pb}/^{206}\text{Pb}$  and was omitted from the calibration, leaving  $n = 28$ . The floating point exponent determined internally by SQUID was 2.11, between the default 2.0 and an apparent slope  $>2.2$  for the concurrent samples. A slope of 2.1 was used, resulting in a Pb/U scatter of 0.96% ( $1\sigma$ ). The weighted mean  $^{207}\text{Pb}/^{206}\text{Pb}$  age for the same data is  $1848.5 \pm 2.7\text{Ma}$  ( $\text{MSWD} = 0.75$ ). Re-assessment of the data using a standardised set of criteria for assessment of the  $^{207}\text{Pb}/^{206}\text{Pb}$  (see “Data compilation for the QGNG standard”) does not change these results.

Element abundance calibration was based on CZ3 ( $n = 5$ ).

### Sample data

Twenty eight analyses were made on 22 grains (Table 8). The smaller grains were mounted in a separate strip and were found to be consistently high-U and/or high- $^{204}\text{Pb}$ ; only three of these (20-1, 21-1 and 22-1) were analysed. All data are within 5% of concordia, but spread from  $\sim 2770\text{ Ma}$  to  $\sim 2670\text{ Ma}$  (Fig. 17, 18). There is a cluster of seven analyses with  $\text{U} > 340\text{ppm}$  that suggests a magmatic age for the granite precursor of  $2760\text{--}2765\text{ Ma}$ . The overall data scatter probably reflects a combination of early and (minor) recent Pb loss. The  $^{208}\text{Pb}/^{232}\text{Th}$  data show

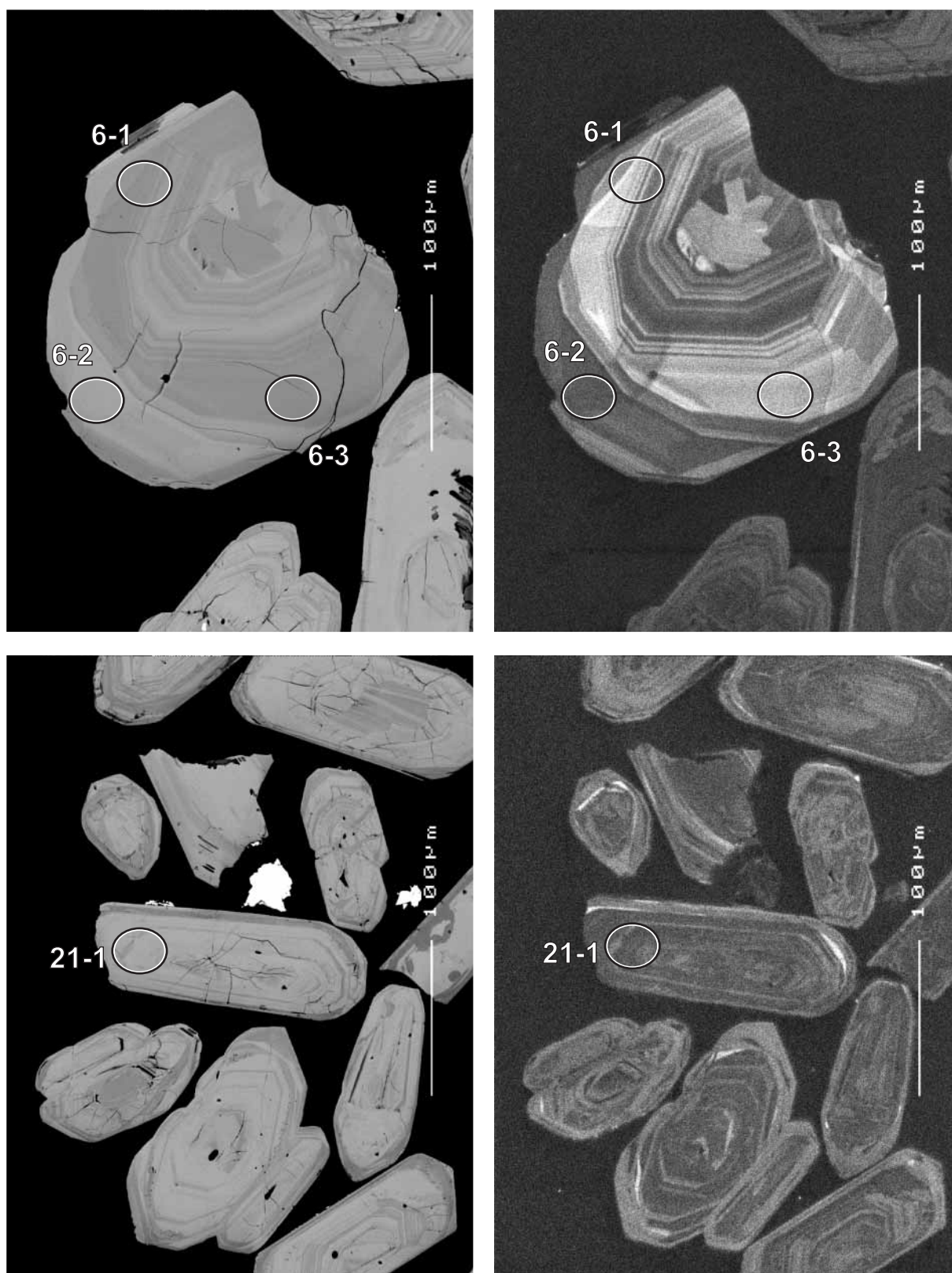


Figure 16. Representative SEM images (BSE on left, CL on right) for sample 9996 7007A: banded granitic gneiss, Surprise Rocks. SHRIMP analysis spots are labelled. Scale bar is 100  $\mu\text{m}$ .

significant disturbance amongst the main (?)magmatic group. The only structurally discontinuous (?xenocrystic) core analysed (5-1) does not have an age older than the interpreted magmatic age.

### Geochronological interpretation

Given the intrusive relationship between these this sample and monzogranite dyke 9996 7007B, it is considered that ~2765 Ma represents the magmatic age of the gneiss protolith, and the spread of data for this sample represents Pb loss either during the gneiss-forming event or at the time of monzogranite intrusion, though these two might be coincident. (The age of dyke intrusion is  $2645 \pm 6$  Ma).

*Table 8. SHRIMP analytical results for zircon from sample 9996 7007A: banded biotite granitic gneiss, Surprise Rocks.*

grain-spot	U (ppm)	Th (ppm)	4f206 (%)	$\frac{^{207}\text{Pb}}{^{206}\text{Pb}}$	$\pm$	$\frac{^{206}\text{Pb}}{^{238}\text{U}}$	$\pm$	$\frac{^{207}\text{Pb}}{^{235}\text{U}}$	$\pm$	$\frac{^{208}\text{Pb}}{^{232}\text{Th}}$	conc. (%)	$\frac{^{207}\text{Pb}}{^{206}\text{Pb}}$ Age (Ma)	$\pm$
Possibly magmatic													
A1.1-2	348	237	0.050	0.1916	0.0004	0.524	0.006	13.83	0.16	0.143	99	2756	4
A1.2-1	432	43	0.164	0.1920	0.0004	0.525	0.005	13.89	0.14	0.174	99	2759	3
A1.9-1	447	8	-0.009	0.1920	0.0004	0.525	0.005	13.88	0.14	0.149	99	2759	3
A1.14-1	426	117	0.001	0.1914	0.0004	0.523	0.005	13.80	0.14	0.143	98	2754	3
A1.17-1	417	12	0.098	0.1929	0.0004	0.517	0.005	13.74	0.14	0.205	97	2767	3
A2.20-1	431	25	0.013	0.1926	0.0004	0.517	0.006	13.74	0.15	0.142	97	2765	3
A2.21-1	439	143	0.079	0.1935	0.0005	0.517	0.005	13.80	0.15	0.142	97	2772	5
Early Pb loss													
A1.1-1	502	38	0.325	0.1810	0.0005	0.487	0.005	12.16	0.13	0.141	96	2662	5
A1.3-1	132	130	0.012	0.1856	0.0007	0.517	0.006	13.24	0.16	0.140	99	2703	6
A1.4-1	34	18	0.007	0.1835	0.0017	0.518	0.008	13.11	0.24	0.141	100	2685	15
A1.5-1	78	67	0.059	0.1858	0.0010	0.522	0.007	13.37	0.18	0.141	100	2706	9
A1.6-1	42	23	0.040	0.1910	0.0025	0.532	0.008	14.02	0.28	0.149	100	2751	21
A1.6-2	134	43	0.094	0.1915	0.0007	0.525	0.006	13.88	0.17	0.144	99	2755	6
A1.6-3	36	24	0.051	0.1912	0.0015	0.537	0.008	14.17	0.25	0.146	101	2753	13
A1.7-1	403	140	0.043	0.1817	0.0004	0.496	0.005	12.42	0.13	0.136	97	2668	4
A1.8-1	38	23	-0.043	0.1916	0.0017	0.553	0.008	14.60	0.26	0.154	103	2756	14
A1.8-2	75	38	0.081	0.1923	0.0011	0.503	0.006	13.33	0.19	0.144	95	2762	9
A1.10-1	67	61	-0.028	0.1885	0.0009	0.531	0.007	13.79	0.19	0.147	101	2729	8
A1.11-1	646	304	0.120	0.1855	0.0005	0.498	0.005	12.73	0.13	0.125	96	2703	5
A1.12-1	158	223	0.218	0.1875	0.0007	0.513	0.006	13.26	0.16	0.142	98	2720	6
A1.13-1	107	141	0.154	0.1850	0.0009	0.509	0.006	12.98	0.17	0.140	98	2698	8
A1.14-2	579	79	0.349	0.1897	0.0008	0.499	0.005	13.06	0.14	0.148	95	2740	7
A1.15-1	289	364	0.032	0.1865	0.0004	0.516	0.005	13.27	0.14	0.140	99	2712	4
A1.15-2	105	95	0.075	0.1860	0.0008	0.524	0.006	13.43	0.17	0.144	100	2707	7
A1.16-1	488	289	0.050	0.1822	0.0004	0.493	0.005	12.39	0.13	0.137	97	2673	3
A1.18-1	394	48	0.073	0.1900	0.0005	0.503	0.005	13.19	0.14	0.135	96	2742	4
A1.19-1	381	96	0.008	0.1824	0.0004	0.498	0.005	12.53	0.13	0.135	97	2675	4
A2.22-1	396	191	0.067	0.1821	0.0004	0.490	0.005	12.30	0.13	0.122	96	2673	4

Data are at  $1\sigma$  precision. All Pb data are common-Pb corrected (based on  $^{204}\text{Pb}$  and Broken Hill Pb composition). Analysis date: 29/09/2000; session Z3624i.

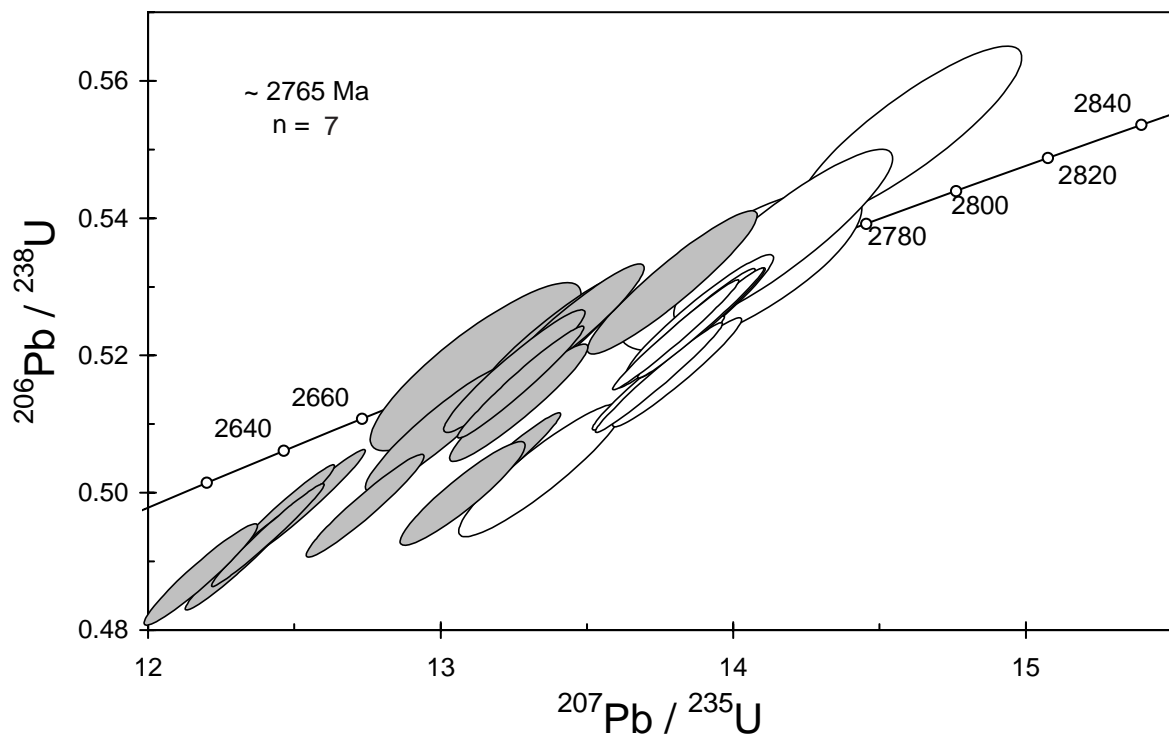


Figure 17. Concordia plot for zircon data from sample 9996 7007A: banded biotite granitic gneiss, Surprise Rocks. White filled symbols are used to define the age of the sample; analyses on grains considered to have experienced Pb loss are grey.

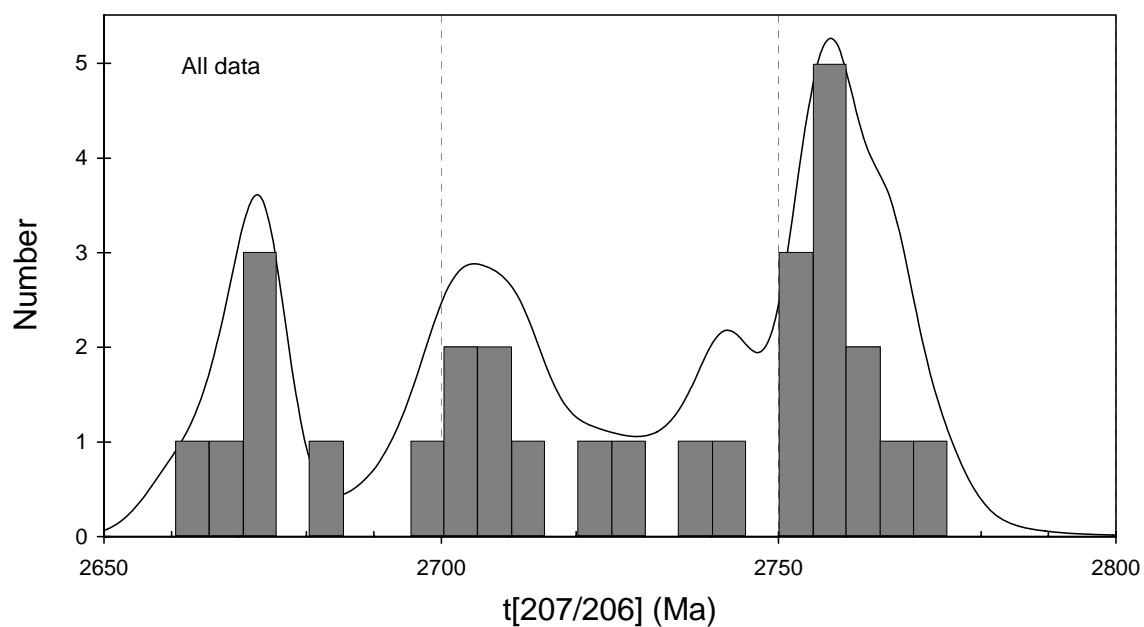


Figure 18. Gaussian-summation plot for zircon data from sample 9996 7007A: banded biotite granitic gneiss, Surprise Rocks.

## 9996 7007B: biotite monzogranite dyke, Surprise Rocks

<b>1:250,000 sheet:</b>	Minigwal (SH5107)
<b>1:100,000 sheet:</b>	Lightfoot (3539)
<b>MGA:</b>	515568mE                      6737539mN
<b>Location:</b>	The sample was taken from a large pavement located on the south side of Surprise Rocks.
<b>Description:</b>	<p>This sample is from a cream-pink, fine-grained, equigranular to seriate biotite monzogranite dyke that has intruded a grey banded to locally migmatitic, fine- to medium-grained, seriate biotite quartz-feldspathic granitic gneiss, of which sample 9996 7007A is representative. The dyke contains some xenoliths of the country rock.</p> <p>The principal minerals are quartz (40%), K-feldspar (30–35%), plagioclase (20–25%) and biotite (7–8%) with a granular to locally granoblastic texture. Quartz displays sutured grain boundaries and is locally recrystallised. K-feldspar occurs as microcline interstitial to plagioclase and quartz. Plagioclase is locally recrystallised, displays simple twinning and zoning, and is weakly altered to sericite and epidote. Biotite flakes are partly chloritised. Myrmekite is locally developed. Accessory phases include apatite, zircon and Fe-oxides. Secondary minerals include minor white mica, chlorite, epidote and hematite.</p>
<b>Mount:</b>	Z3624B

### Description of zircons

Zircon is present in a variety of morphological forms, ranging from thin, elongate (aspect ratio up to 5:1, length ranging from about 50  $\mu\text{m}$  to 280  $\mu\text{m}$ ), prismatic grains to more stubby, equant grains (80  $\mu\text{m}$  to 200  $\mu\text{m}$  in length, aspect ratio about 3:2), to smaller (50  $\mu\text{m}$  to 100  $\mu\text{m}$ ) sub-rounded grains. Both whole crystals and fragments are present. Most grains are white to pale brown-grey. A few small inclusions are present in many grains. Almost all grains show well-defined systematic zoning in photographs and CL images (Fig. 19), interpreted as a product of igneous crystallisation. A few grains are more homogeneous and do not have any visible zoning. Several grains show distinct core-rim relationships and some have complex irregular zoning, typical of recrystallisation.

### Concurrent standard data

One spot (15-1) is an outlier in both  $^{206}\text{Pb}/^{238}\text{U}$  and  $^{207}\text{Pb}/^{206}\text{Pb}$  and was omitted from the calibration, leaving  $n = 28$ . The floating point exponent determined internally by SQUID was 2.11, between the default 2.0 and an apparent slope  $>2.2$  for the concurrent samples. A slope of 2.1 was used, resulting in a Pb/U scatter of 0.96% ( $1\sigma$ ). The weighted mean  $^{207}\text{Pb}/^{206}\text{Pb}$  age for the same data is  $1848.5 \pm 2.7\text{Ma}$  (MSWD = 0.75). Re-assessment of the data using a standardised set of criteria for assessment of the  $^{207}\text{Pb}/^{206}\text{Pb}$  (see “Data compilation for the QGNG standard”) does not change these results.

Element abundance calibration was based on CZ3 ( $n = 5$ ).

### Sample data

Twenty seven analyses were performed on separate grains (Table 9; Fig. 20). Several grains are clearly older than the rest (1-1, 5-1, 13-1, 20-1, 22-1); these are taken to be inherited, though only one of these analyses is from a visible core (20-1). They give ages of  $\sim 2700$ , 2760 and 2900 Ma. Some of these grains could be inherited from the surrounding granitic gneiss.

There is a dominant data cluster at  $\sim 2650$  Ma, but this is much more scattered than expected for a single age population (Fig. 20). One discordant analysis (2-1) is disregarded. Given the obvious existence of xenocrysts amongst the other data, the main group is interpreted as a mixture of



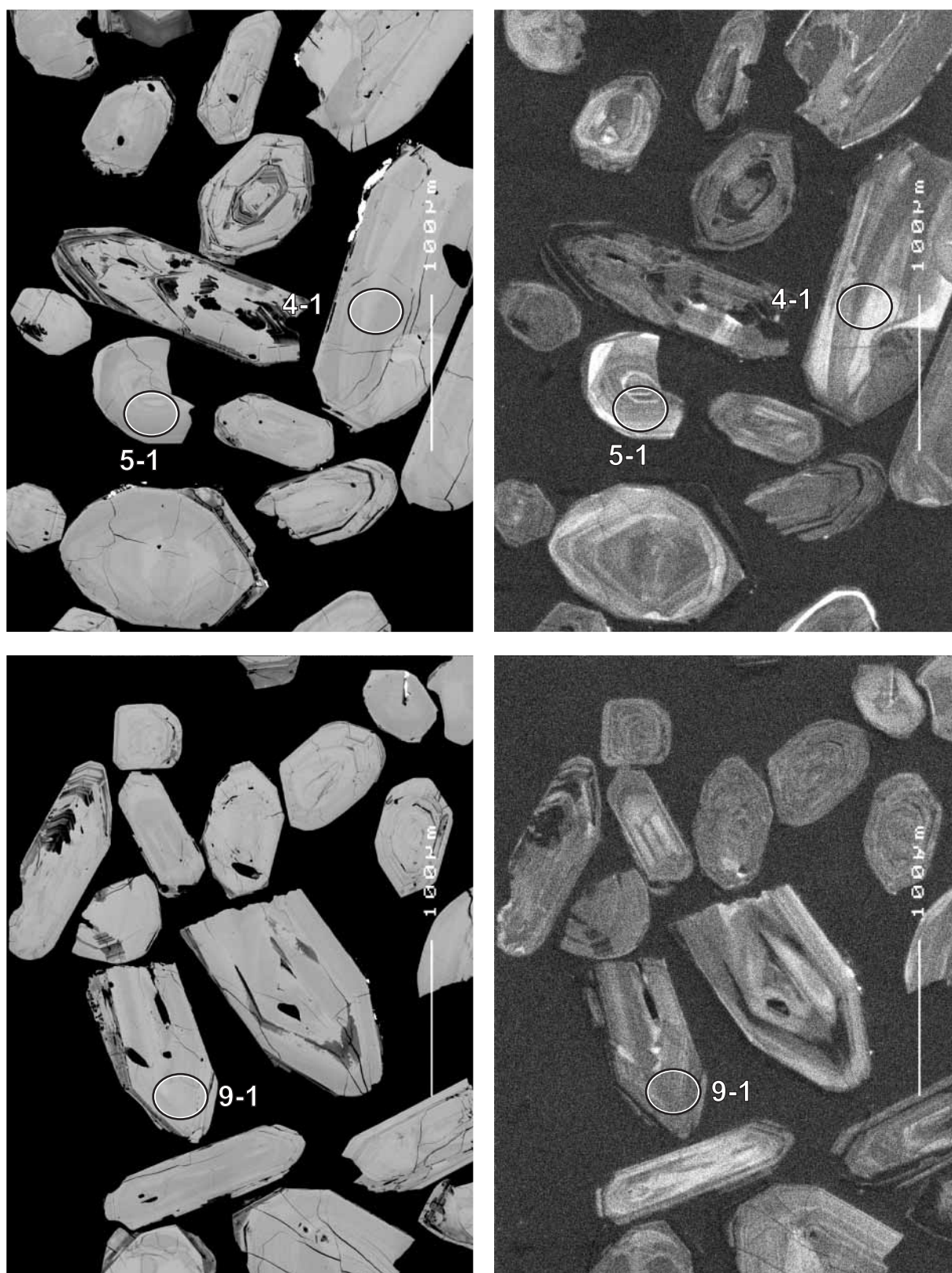


Figure 19. Representative SEM images (BSE on left, CL on right) for sample 9996-7007B: biotite monzogranite dyke, Surprise Rocks. SHRIMP analysis spots are labelled. Scale bar is 100 µm.

magmatic and inherited dates. Therefore dates were culled from the high-age side to produce a more self-consistent data set, although not all culled data come from apparent “cores”. A group of 15 has a  $^{207}\text{Pb}/^{206}\text{Pb}$  age of  $2645.0 \pm 4.8$  Ma (MSWD = 1.9). Further deletions would be rather subjective; the main possibilities are deleting one high-U (low age) or another high-age spot, which could change the average by 1 or 2 Ma. Some of the main data group have disturbed  $^{208}\text{Pb}/^{232}\text{Th}$ .

### Geochronological interpretation

The age of monzogranite dyke intrusion is  $2645 \pm 6$  Ma (precision expanded slightly to allow for uncertainty in the structure of the chosen main population).

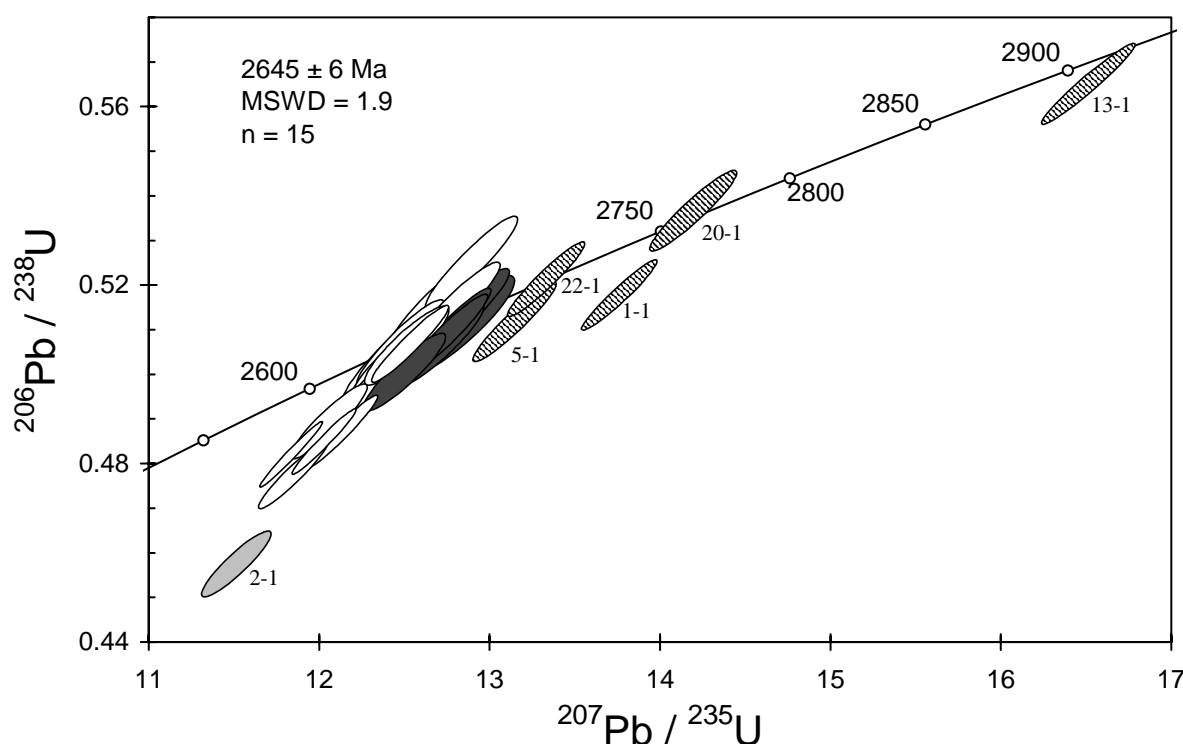


Figure 20. Concordia plot for zircon data from sample 9996-7007B: biotite monzogranite dyke, Surprise Rocks. White filled symbols are used to define the age of the sample; inherited grains have diagonal shading; old outliers (interpreted as inherited grains) are dark grey.

Table 9. SHRIMP analytical results for zircon from sample 9996-7007B: biotite monzogranite dyke, Surprise Rocks.

grain-spot	U (ppm)	Th (ppm)	4f206 (%)	$\frac{^{207}\text{Pb}}{^{206}\text{Pb}}$	$\pm$	$\frac{^{206}\text{Pb}}{^{238}\text{U}}$	$\pm$	$\frac{^{207}\text{Pb}}{^{235}\text{U}}$	$\pm$	$\frac{^{208}\text{Pb}}{^{232}\text{Th}}$	conc. (%)	$\frac{^{207}\text{Pb}}{^{206}\text{Pb}}$ Age (Ma)	$\pm$
Main Group													
B.3-1	121	119	1.026	0.1791	0.0010	0.506	0.006	12.49	0.16	0.140	100	2644	10
B.6-1	445	258	0.066	0.1780	0.0004	0.481	0.005	11.81	0.12	0.134	96	2634	3
B.7-1	77	78	0.111	0.1784	0.0009	0.506	0.006	12.45	0.17	0.138	100	2638	8
B.9-1	244	252	0.609	0.1799	0.0007	0.477	0.005	11.82	0.14	0.139	95	2652	6
B.10-1	145	89	-0.025	0.1793	0.0006	0.506	0.006	12.51	0.15	0.138	100	2646	6
B.12-1	65	71	0.059	0.1780	0.0009	0.524	0.007	12.87	0.18	0.143	103	2634	8
B.14-1	139	93	0.535	0.1786	0.0008	0.489	0.006	12.03	0.15	0.044	97	2640	8
B.15-1	437	229	0.339	0.1798	0.0004	0.484	0.005	12.00	0.13	0.123	96	2651	4
B.16-1	262	673	0.060	0.1806	0.0006	0.486	0.005	12.10	0.14	0.134	96	2658	5
B.17-1	92	59	0.459	0.1798	0.0011	0.500	0.006	12.38	0.17	0.144	99	2651	10
B.19-1	85	129	0.511	0.1792	0.0011	0.502	0.006	12.42	0.17	0.109	99	2646	10
B.21-1	73	77	0.231	0.1783	0.0010	0.515	0.007	12.65	0.19	0.139	102	2637	10
B.23-1	66	72	0.080	0.1797	0.0010	0.506	0.007	12.53	0.18	0.137	100	2650	9
B.24-1	62	63	-0.078	0.1786	0.0011	0.503	0.007	12.39	0.18	0.139	100	2640	10
B.26-1	101	116	0.275	0.1800	0.0009	0.515	0.006	12.79	0.17	0.114	101	2653	8
Inherited													
B.1-1	457	370	0.563	0.1927	0.0006	0.517	0.005	13.74	0.15	0.144	97	2765	5
B.5-1	127	73	0.121	0.1863	0.0007	0.511	0.006	13.13	0.16	0.129	98	2709	7
B.13-1	245	256	0.311	0.2120	0.0006	0.565	0.006	16.51	0.18	0.103	99	2921	5
B.20-1	147	50	-0.063	0.1918	0.0008	0.536	0.006	14.18	0.17	0.147	100	2757	7
B.22-1	272	139	0.536	0.1854	0.0006	0.521	0.006	13.31	0.15	0.128	100	2702	6
Possibly inherited and heavily reset													
B.4-1	124	105	-0.028	0.1816	0.0007	0.508	0.006	12.73	0.16	0.142	99	2667	7
B.8-1	109	119	0.043	0.1815	0.0008	0.510	0.006	12.75	0.16	0.104	100	2666	7
B.11-1	103	207	0.211	0.1820	0.0009	0.506	0.006	12.69	0.17	0.078	99	2671	8
B.18-1	116	144	0.578	0.1811	0.0010	0.500	0.006	12.48	0.16	0.127	98	2663	9
B.25-1	60	52	-0.046	0.1812	0.0010	0.513	0.007	12.81	0.19	0.143	100	2664	9
B.27-1	48	24	0.250	0.1820	0.0013	0.510	0.007	12.81	0.21	0.132	100	2671	12
Discordant													
B.2-1	214	168	1.130	0.1826	0.0009	0.456	0.005	11.48	0.14	0.120	91	2676	8

Data are at 1 $\sigma$  precision. All Pb data are common-Pb corrected (based on  $^{204}\text{Pb}$  and Broken Hill Pb composition). Analysis date: 29/09/2000; session Z3624i.



## 9996 9014: Alicia Granite

**1:250,000 sheet:** Leonora (SH5101)

**1:100,000 sheet:** Weebo (3141)

**MGA:** 320016mE 6859974mN

**Location:** The sample was taken from a moderate-sized boulder, just east of the highway along the fibre-optic line, approximately 1.9 km north of the turn-off to the old Teutonic Bore mine.

**Description:** This sample is a white medium-grained seriate-textured titanite-hornblende granodiorite phase of the Alicia Granite. The unit contains uncommon, thin microgranitic veins and is unfoliated.

The unit has a granular to locally granoblastic texture. Principal minerals are plagioclase (35–50%), minor K-feldspar (<10%), quartz (30–40%), and hornblende (5–7%). Plagioclase is present as subhedral laths, most of which have well-developed broad oscillatory zoning and prominent rims, although unzoned laths are also present. Quartz occurs as variably undulose interstitial grains to irregular grains intergrown with feldspar. Hornblende is present as anhedral and interstitial to subhedral, 2–4 mm grains, locally with relict pyroxene cores. Accessory phases include relatively common titanite (<2%, to 1–2 mm), as well as zircon, apatite and Fe-oxides. Secondary minerals comprise minor to moderate white mica, epidote, clinozoisite, and lesser chlorite.

**Mount, pop:** Z3672A

### Description of zircons

This sample contains abundant euhedral to subhedral zircon crystals and fragments with well-defined crystal faces and prismatic terminations. They are predominantly stubby and equant, with aspect ratios of 1:1 to 2:1. Most grains range from about 80  $\mu\text{m}$  to 200  $\mu\text{m}$  in length, with a few larger (up to 250  $\mu\text{m}$ ) grains present. The grains are colourless and clear; some contain a few inclusions. The grains have strong CL, with well-defined euhedral and concentric zoning visible in most grains (Fig. 21). Zoning is also visible in many grains in transmitted light photographs. Some grains clearly show core-rim discontinuities which are best defined in the CL images.

### Concurrent standard data

The floating point calibration exponent for this QGNG data set is 2.1. This is not significantly higher than the default value of 2.0, but the data for sample 9996 9014 also indicate a higher value (~2.3); a value of 2.1 was used for data reduction.

There is one outlier in  $^{206}\text{Pb}/^{238}\text{U}$  (16-3) and this has been omitted from the calibration, leaving 26 analyses with a  $1\sigma$  scatter in  $^{206}\text{Pb}/^{238}\text{U}$  of 1.26%. The same data have a weighted mean  $^{207}\text{Pb}/^{206}\text{Pb}$  age of  $1849 \pm 4$  Ma (rounded off by SQUID; MSWD = 1.3). There is one young outlier amongst these (25-2); omitting this leaves 25 analyses with a  $^{207}\text{Pb}/^{206}\text{Pb}$  age of  $1849.0 \pm 3.4$  Ma. (MSWD = 1.06). Using a standardised set of criteria for assessment of the data (see “Data compilation for the QGNG standard”) gives a  $^{207}\text{Pb}/^{206}\text{Pb}$  age of  $1849.7 \pm 3.5$  Ma (MSWD = 1.01).

Element abundance calibration was based on CZ3 ( $n = 2$ ).

### Sample data

Thirty four analyses were undertaken on 31 grains (Table 10). The data distribution is very simple, with only one significantly discordant analysis (19-1) and little, if any, scatter in  $^{207}\text{Pb}/^{206}\text{Pb}$  (Fig. 22). There is no age distinction between cores and rims. Omitting only the discordant

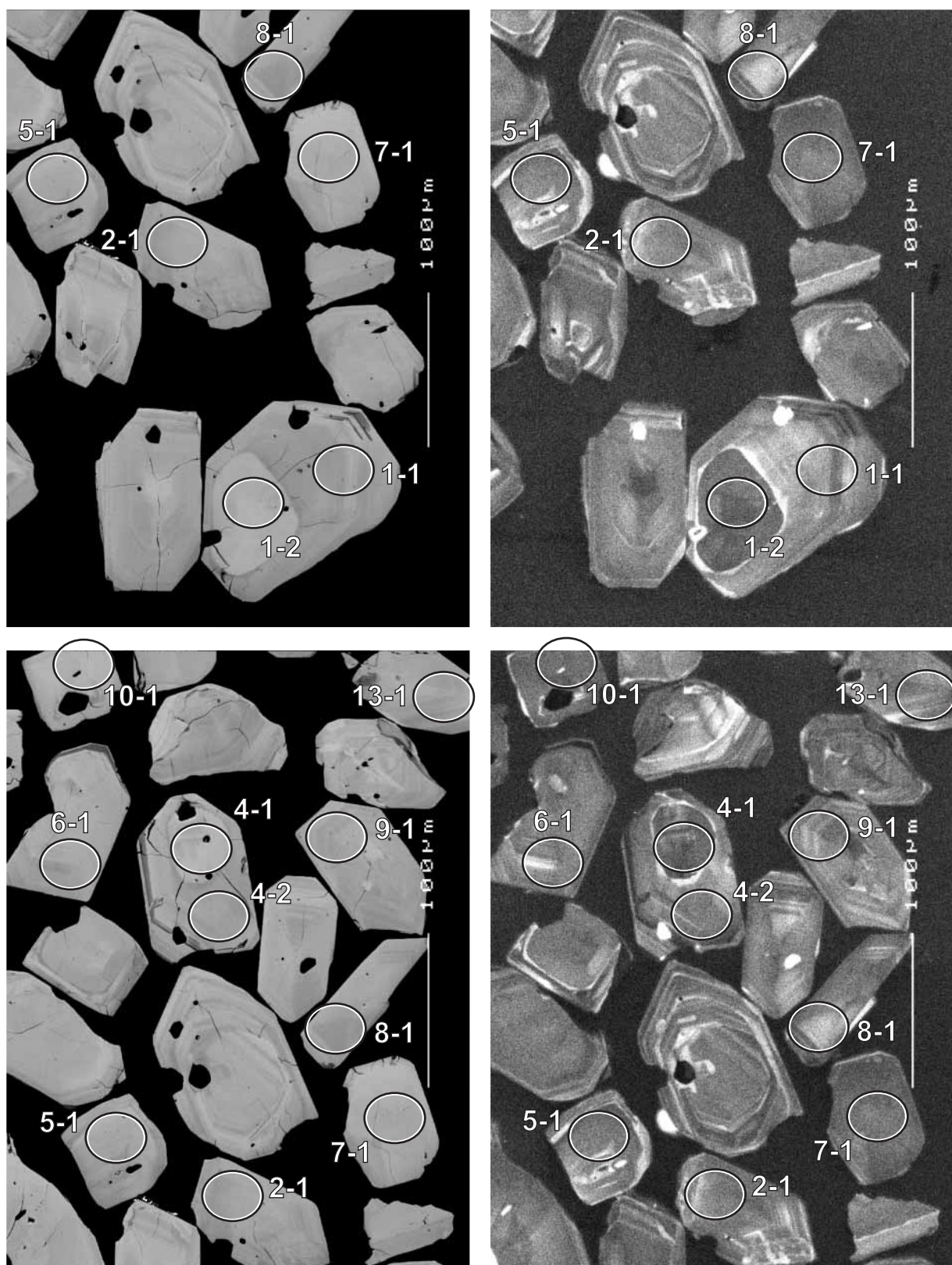


Figure 21. Representative SEM images (BSE on left, CL on right) for sample 9996 9014: Alicia Granite. SHRIMP analysis spots are labelled. Scale bar is 100  $\mu\text{m}$ .

analysis leaves 33 with weighted mean  $^{207}\text{Pb}/^{206}\text{Pb}$  age of  $2692.7 \pm 2.5$  Ma (MSWD = 1.10). With the further deletion of a possible young outlier (4-1) this would change to  $2693 \pm 2.5$  Ma (MSWD = 0.86).

### Geochronological interpretation

The  $^{207}\text{Pb}/^{206}\text{Pb}$  age of  $2693 \pm 3$  Ma is considered to be the crystallisation age of the granite.

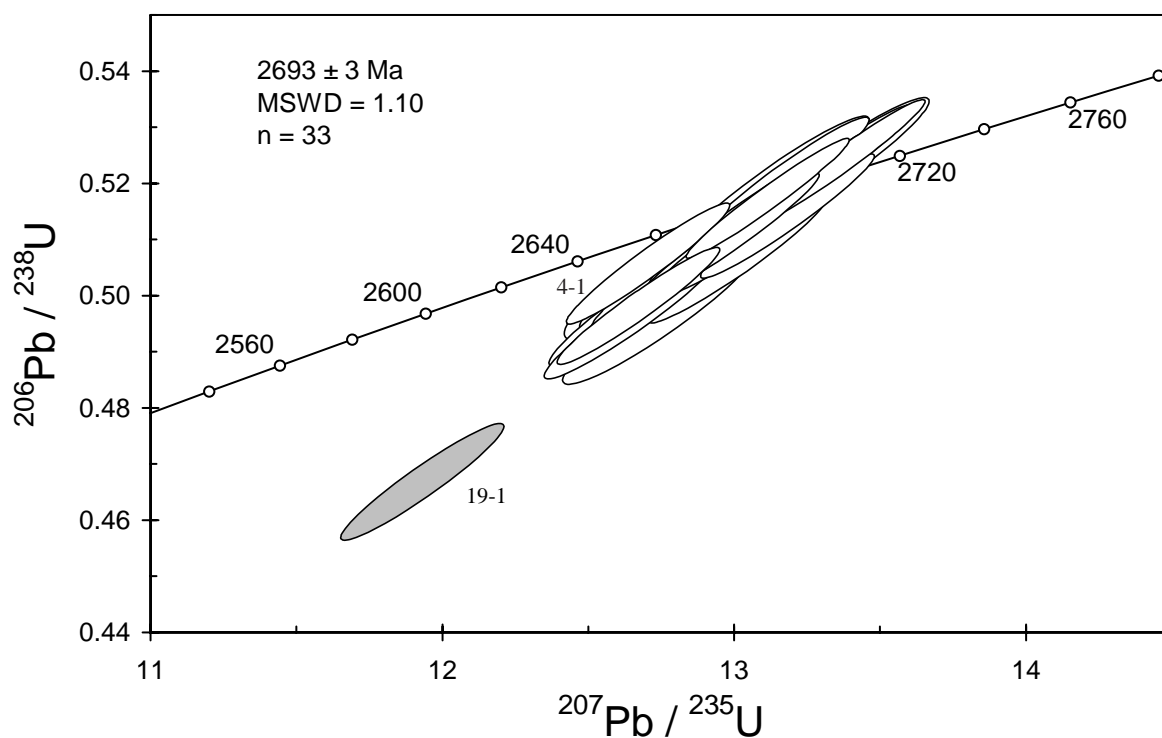


Figure 22. Concordia plot for zircon data from sample 9996 9014: Alicia Granite. White filled symbols are used to define the age of the sample; discordant analysis is light grey.

Table 10. SHRIMP analytical results for zircon from sample 9996 9014: Alicia Granite.

grain- spot	U (ppm)	Th (ppm)	4f206 (%)	<sup>207</sup> Pb/ <sup>206</sup> Pb	±	<sup>206</sup> Pb/ <sup>238</sup> U	±	<sup>207</sup> Pb/ <sup>235</sup> U	±	<sup>208</sup> Pb/ <sup>232</sup> Th	conc. (%)	<sup>207</sup> Pb/ <sup>206</sup> Pb Age (Ma)	±
Main group													
A.1-1	113	65	-0.060	0.1848	0.0009	0.496	0.008	12.65	0.20	0.138	96	2696	8
A.1-2	225	225	0.000	0.1844	0.0007	0.498	0.007	12.67	0.18	0.138	97	2693	7
A.2-1	100	55	-0.026	0.1833	0.0009	0.520	0.008	13.14	0.22	0.142	101	2683	8
A.3-1	119	68	0.000	0.1849	0.0009	0.507	0.008	12.92	0.20	0.140	98	2697	8
A.4-1	203	197	0.135	0.1822	0.0007	0.506	0.007	12.70	0.19	0.117	99	2673	7
A.4-2	108	58	0.034	0.1834	0.0009	0.505	0.008	12.78	0.21	0.139	98	2683	8
A.5-1	126	81	-0.059	0.1842	0.0009	0.499	0.008	12.67	0.20	0.140	97	2691	8
A.6-1	117	66	0.136	0.1844	0.0010	0.505	0.008	12.83	0.21	0.135	98	2693	9
A.7-1	146	87	-0.044	0.1852	0.0008	0.512	0.008	13.06	0.20	0.142	99	2700	7
A.8-1	125	84	0.021	0.1849	0.0009	0.509	0.008	12.99	0.21	0.138	98	2698	8
A.9-1	103	44	0.005	0.1849	0.0010	0.523	0.008	13.34	0.22	0.135	101	2697	9
A.10-1	238	226	0.010	0.1849	0.0006	0.524	0.007	13.36	0.19	0.144	101	2698	6
A.11-1	167	126	0.017	0.1842	0.0007	0.510	0.007	12.96	0.19	0.135	99	2691	6
A.12-1	121	50	0.161	0.1836	0.0009	0.508	0.008	12.87	0.20	0.135	99	2685	8
A.13-1	116	121	-0.008	0.1841	0.0009	0.513	0.008	13.02	0.21	0.077	99	2691	8
A.14-1	147	102	0.005	0.1847	0.0008	0.523	0.008	13.31	0.20	0.144	101	2696	7
A.15-1	89	45	-0.117	0.1862	0.0011	0.496	0.008	12.73	0.22	0.138	96	2709	10
A.15-2	263	273	0.031	0.1838	0.0006	0.517	0.007	13.11	0.19	0.141	100	2687	5
A.16-1	182	137	0.076	0.1843	0.0007	0.509	0.007	12.94	0.19	0.138	99	2692	7
A.17-1	138	86	-0.085	0.1854	0.0008	0.514	0.008	13.15	0.20	0.143	99	2702	7
A.18-1	124	71	-0.016	0.1846	0.0008	0.510	0.008	12.98	0.20	0.139	99	2695	8
A.20-1	141	78	-0.017	0.1838	0.0007	0.513	0.007	13.00	0.20	0.141	99	2688	7
A.21-1	95	75	0.068	0.1847	0.0009	0.504	0.008	12.84	0.21	0.135	98	2695	8
A.22-1	121	78	0.004	0.1862	0.0009	0.506	0.008	13.00	0.20	0.141	98	2709	8
A.23-1	131	79	0.089	0.1839	0.0008	0.505	0.007	12.80	0.20	0.113	98	2689	8
A.24-1	130	83	0.106	0.1839	0.0008	0.514	0.008	13.02	0.20	0.138	99	2688	7
A.25-1	146	105	0.126	0.1839	0.0008	0.511	0.007	12.96	0.20	0.136	99	2688	7
A.26-1	96	55	-0.024	0.1839	0.0009	0.519	0.008	13.15	0.21	0.142	100	2688	8
A.27-1	83	55	-0.100	0.1835	0.0014	0.504	0.008	12.75	0.22	0.121	98	2685	13
A.28-1	157	123	-0.012	0.1848	0.0007	0.520	0.007	13.26	0.20	0.141	100	2697	6
A.29-1	182	132	0.026	0.1845	0.0007	0.511	0.007	13.00	0.19	0.138	99	2694	6
A.30-1	134	82	0.008	0.1834	0.0008	0.521	0.008	13.16	0.20	0.143	101	2684	7
A.31-1	148	103	-0.040	0.1859	0.0007	0.514	0.007	13.18	0.20	0.142	99	2706	7
Discordant													
A.19-1	121	69	0.008	0.1854	0.0009	0.466	0.007	11.92	0.19	0.132	91	2702	8

Data are at 1 $\sigma$  precision. All Pb data are common-Pb corrected (based on <sup>204</sup>Pb and Broken Hill Pb composition).  
Analysis date: 06/04/2001; session Z3672j.

## 200096 7002B: amphibole-biotite tonalite, Mick Adam mine

<b>1:250,000 sheet:</b>	Kalgoorlie (SH5109)
<b>1:100,000 sheet:</b>	Kalgoorlie (3136)
<b>MGA:</b>	311388mE                      6609159mN
<b>Location:</b>	The sample was taken from Goldfields Ltd diamond drillhole CHRC447D, depth interval 106.0–107.0 m. The collar site is located immediately northeast of the Mick Adam open pit.
<b>Description:</b>	<p>This sample is from a grey fine-grained, amphibole-biotite tonalite. In the vicinity of the Mick Adam mine, the amphibole-biotite tonalite is a ~100 m-thick body intrusive into the surrounding mafic-ultramafic sequence. The unit rapidly thickens to the northwest and forms part of the 2 km wide Kintore Tonalite. The tonalite is altered and cut by quartz veinlets; the selected sample was free of obvious veins.</p> <p>The unit has a granular to granoblastic texture. Principal minerals are plagioclase (50–55%), quartz (35%), biotite (8–10%), amphibole (3–5%) and K-feldspar (&lt;2%). Plagioclase is zoned (normal, oscillatory and irregular) with internal zones often marked by thin sericitic mantles. Most quartz grains are recrystallised. Green amphibole is present as subhedral to anhedral grains of hornblende and metamorphic actinolite, and brown biotite occurs as irregular flakes and aggregates. Accessory phases include minor epidote, leucoxene/titanite, apatite and Fe-oxides and rare zircon. Secondary minerals include minor white mica, chlorite and carbonate.</p>
<b>Mount, pop:</b>	Z3672D

### Description of zircons

This sample contains a large number of predominantly euhedral zircon crystals and fragments having well formed crystal faces and sharp prismatic terminations. The grains are colourless and clear, with only a few inclusions in some grains. Most are elongate (aspect ratios are generally greater than 2:1, up to 4:1) and vary from about 100  $\mu\text{m}$  to 300  $\mu\text{m}$  in length. The CL of the zircon grains is strong, with most having well-defined euhedral concentric zoning (Fig. 23). Some grains have structurally discordant cores that are truncated and overgrown by younger zircon.

### Concurrent standard data

The floating point exponent for QGNG is 2.27 – apparently high, though not significantly different from the default 2.0. The data for sample 200096 7002B also suggests a high slope (2.05). A value of 2.1 was used for data reduction. No data were excluded from the Pb/U calibration, with 29 analyses giving a  $1\sigma$  scatter of 1.37%. The weighted mean  $^{207}\text{Pb}/^{206}\text{Pb}$  age for all 29 is  $1847.8 \pm 4.1$  Ma (MSWD = 1.2), but using a standardised set of criteria for assessment of the data (see “Data compilation for the QGNG standard”) gives a  $^{207}\text{Pb}/^{206}\text{Pb}$  age of  $1848.6 \pm 3.6$  Ma (MSWD = 1.07).

Element abundance calibration was based on CZ3 (n = 2).

### Sample data

Thirty eight analyses were made on 37 grains (Table 11, Fig. 24). Omitting seven discordant analyses (1-1, 2-1, 4-1, 10-1, 18-1, 19-1, 30-1) and one unusual young outlier (13-1) leaves a well-grouped cluster with a  $^{207}\text{Pb}/^{206}\text{Pb}$  date ~2690 Ma (Fig. 25) but with considerable excess scatter (MSWD > 4). Probability plots suggest that the older part of this group is the main data cluster, though there is no distinct separation (Fig. 26). The younger values might reflect early Pb loss, perhaps related to a hydrothermal event, but there is nothing in the appearance of the



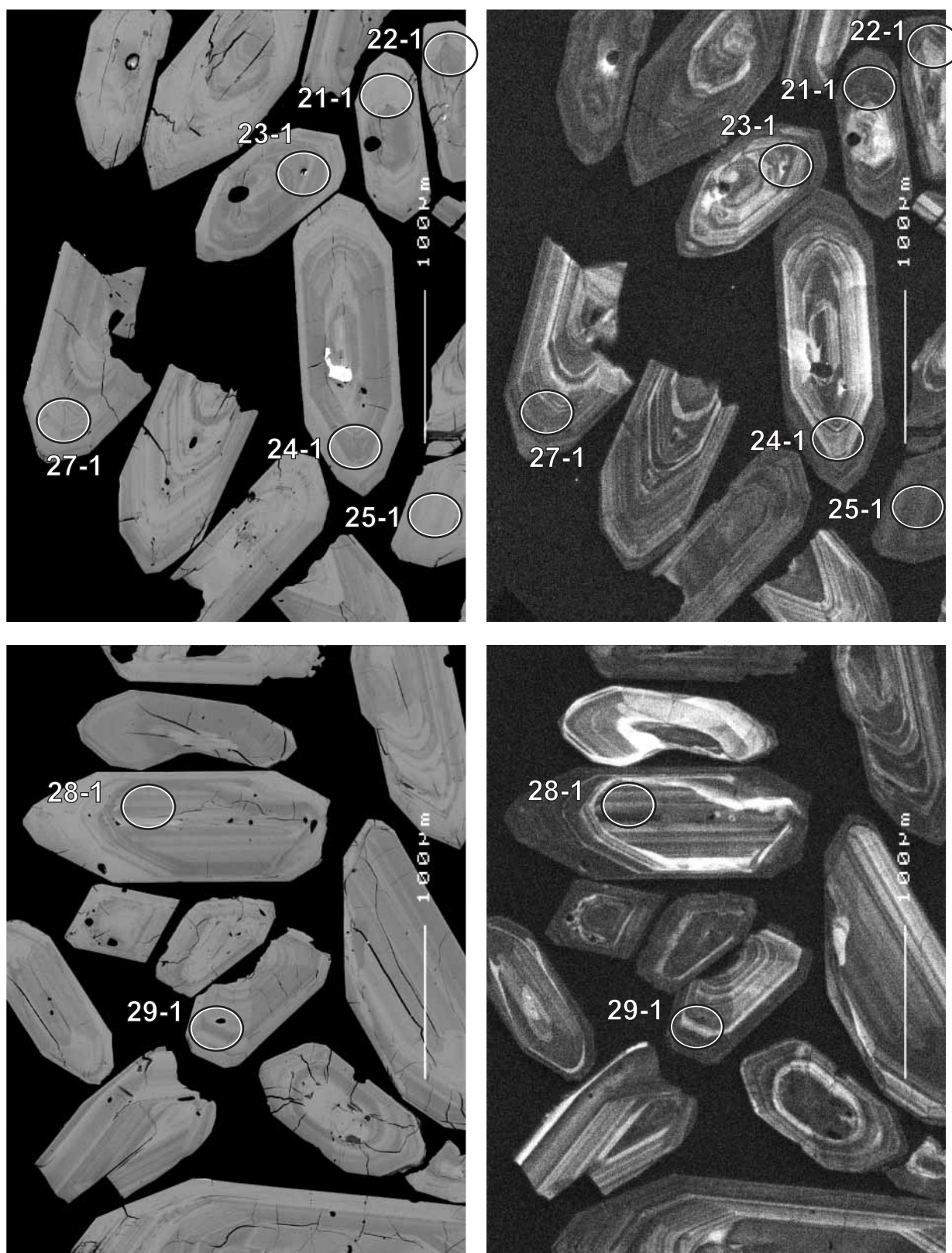


Figure 23. Representative SEM images (BSE on left, CL on right) for sample 200096 7002B: amphibole-biotite tonalite, Mick Adam mine. SHRIMP analysis spots are labelled. Scale bar is 100 µm.



grains or the data that directly indicates this. Data have been trimmed from the low-age side of the data cluster, though the extent of culling is highly subjective. Cutting to a main population of 25 analyses would give a weighted mean  $^{207}\text{Pb}/^{206}\text{Pb}$  age of  $2695.1 \pm 2.8$  Ma (MSWD = 1.6), while continuing to 21 analyses gives  $2697.2 \pm 2.3$  Ma (MSWD = 0.89). The preferred age is a conservative compromise:  $2696 \pm 4$  Ma.

None of the analyses of ?visible cores, or core-rim overlaps (28-1, 30-1, 32-1, 34-1, 36-1, 37-2) produced ages older than other grains or rims.

### Geochronological interpretation

The  $^{207}\text{Pb}/^{206}\text{Pb}$  age of  $2696 \pm 4$  Ma is considered to be the intrusive age of the tonalite. This is older than anticipated for intrusives in this greenstone belt, though it does not directly contradict existing data. The minor cluster of data at ~2665 Ma fits more comfortably with expectations, but if this is the magmatic age of the tonalite then the zircons in the main data cluster would necessarily be xenocrysts and their good preservation would be unusual, given that they appear to be a single age population, and some are high-U.

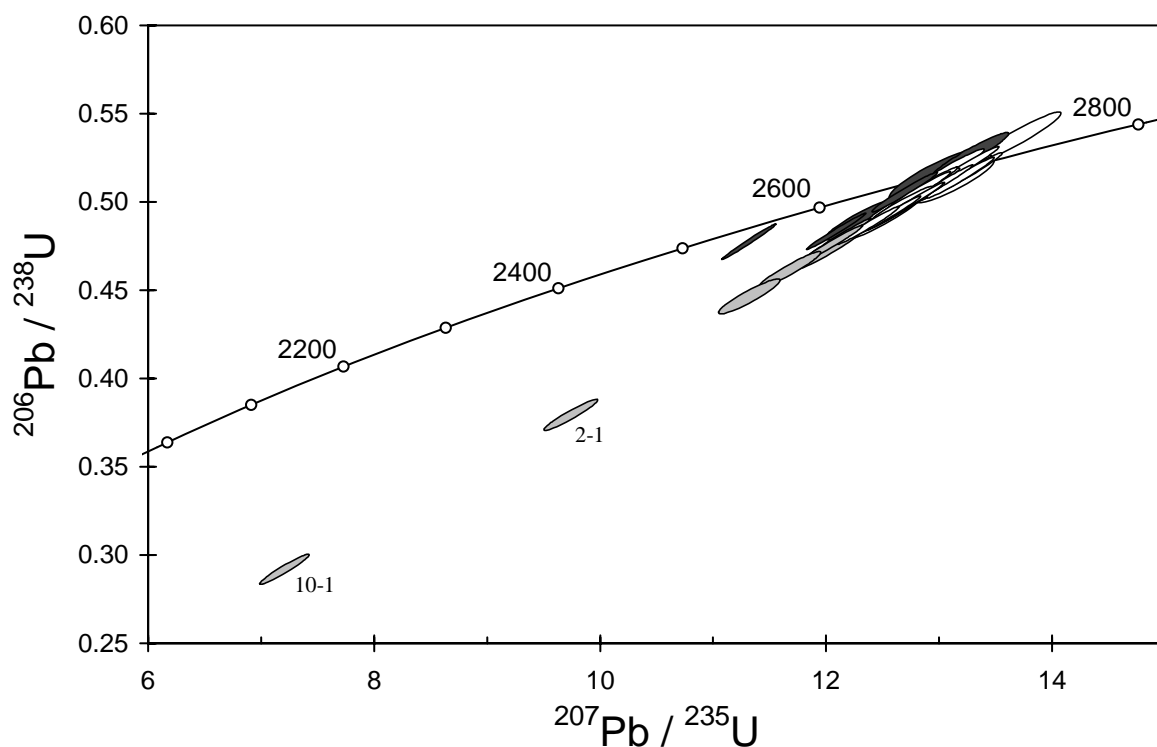


Figure 24. Concordia plot for zircon data from sample 200096 7002B: amphibole-biotite tonalite, Mick Adam mine. White filled symbols are used to define the age of the sample; discordant analyses are light grey; younger outliers are dark grey.

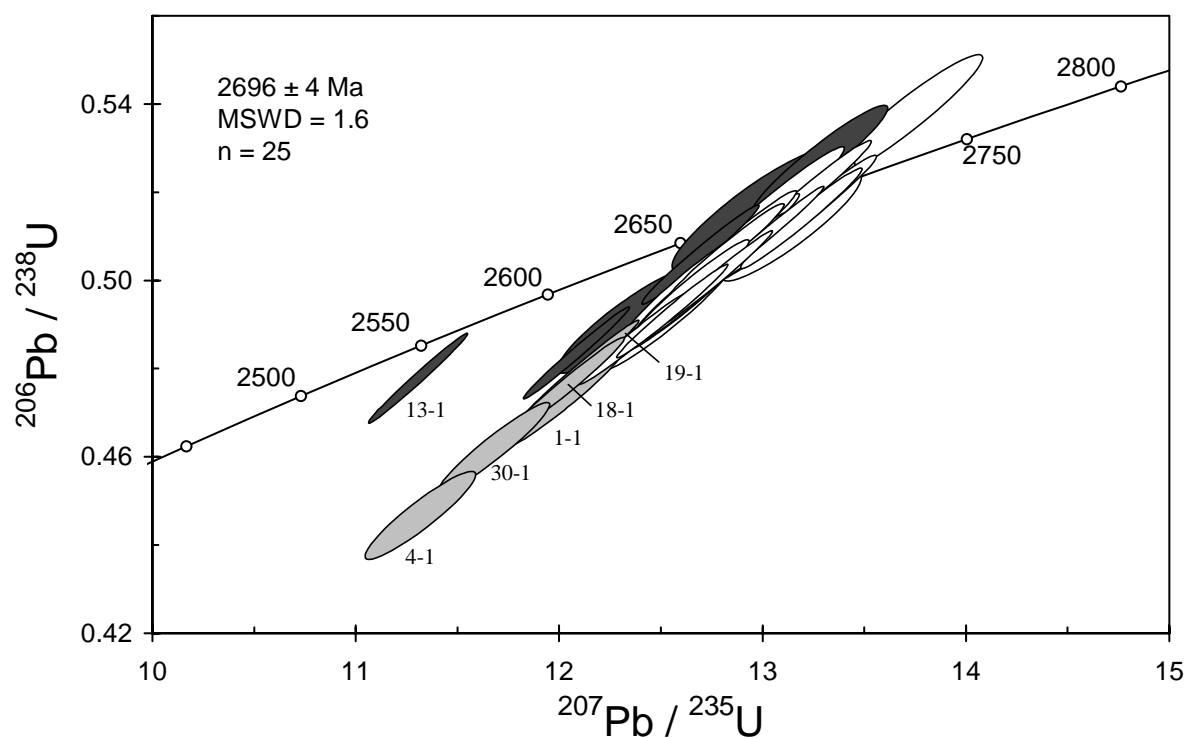


Figure 25. Enlargement of main group of zircon analyses for sample 200096 7002B: amphibole-biotite tonalite, Mick Adam mine. Symbol shading as in Figure 24.

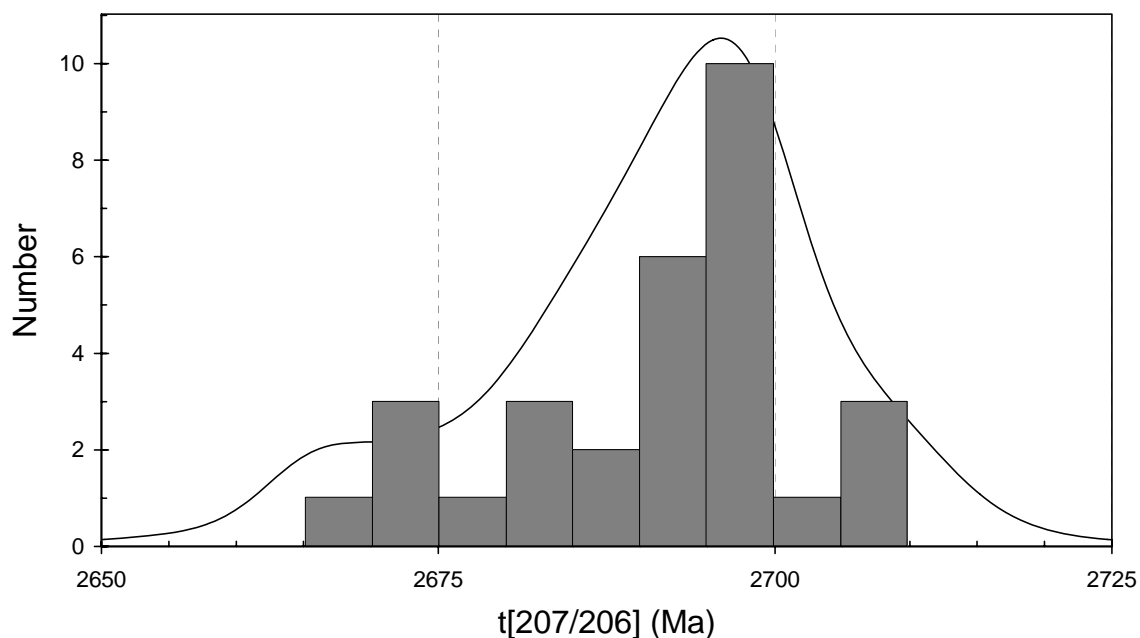


Figure 26. Gaussian-summation plot for zircon data from sample 200096 7002B: amphibole-biotite tonalite, Mick Adam mine.

Table 11. SHRIMP analytical results for zircon from sample 200096 7002B: amphibole-biotite tonalite, Mick Adam mine.

grain-spot	U (ppm)	Th (ppm)	4f206 (%)	$\frac{^{207}\text{Pb}}{^{206}\text{Pb}}$	$\pm$	$\frac{^{206}\text{Pb}}{^{238}\text{U}}$	$\pm$	$\frac{^{207}\text{Pb}}{^{235}\text{U}}$	$\pm$	$\frac{^{208}\text{Pb}}{^{232}\text{Th}}$	conc. (%)	$\frac{^{207}\text{Pb}}{^{206}\text{Pb}}$ Age (Ma)	$\pm$
Main group													
D.5-1	120	58	0.067	0.1849	0.0009	0.491	0.008	12.52	0.21	0.130	95	2698	8
D.7-1	431	211	0.030	0.1842	0.0006	0.498	0.007	12.66	0.19	0.131	97	2691	6
D.8-1	284	142	0.015	0.1848	0.0005	0.504	0.007	12.85	0.19	0.136	98	2696	5
D.9-1	345	252	0.039	0.1844	0.0005	0.487	0.007	12.37	0.18	0.135	95	2693	5
D.14-1	295	109	0.007	0.1839	0.0006	0.508	0.007	12.89	0.19	0.137	99	2688	6
D.15-1	235	102	0.050	0.1843	0.0007	0.498	0.007	12.66	0.19	0.116	97	2692	6
D.16-1	129	71	0.013	0.1848	0.0011	0.510	0.008	13.01	0.22	0.144	99	2697	10
D.17-1	512	400	0.037	0.1851	0.0004	0.510	0.007	13.02	0.19	0.138	99	2699	4
D.20-1	485	305	0.013	0.1848	0.0004	0.493	0.007	12.56	0.18	0.132	96	2697	4
D.21-1	465	287	0.014	0.1851	0.0004	0.500	0.007	12.77	0.19	0.141	97	2699	4
D.23-1	132	69	0.046	0.1861	0.0014	0.512	0.008	13.14	0.23	0.145	98	2708	12
D.24-1	330	199	0.035	0.1844	0.0006	0.504	0.008	12.82	0.20	0.134	98	2693	5
D.25-1	273	82	0.022	0.1845	0.0006	0.520	0.008	13.24	0.20	0.142	100	2694	5
D.26-1	276	183	-0.002	0.1845	0.0005	0.504	0.007	12.83	0.19	0.141	98	2694	5
D.27-1	232	118	0.040	0.1861	0.0006	0.517	0.008	13.26	0.20	0.139	99	2708	5
D.31-1	135	64	0.012	0.1852	0.0008	0.511	0.008	13.05	0.21	0.142	99	2700	7
D.34-1	257	153	0.020	0.1849	0.0006	0.496	0.007	12.66	0.19	0.140	96	2698	5
D.35-1	252	133	0.034	0.1862	0.0006	0.514	0.008	13.20	0.20	0.143	99	2709	5
D.36-1	105	59	0.018	0.1851	0.0009	0.514	0.008	13.13	0.22	0.147	99	2699	8
D.37-1	182	96	0.036	0.1849	0.0007	0.495	0.008	12.61	0.20	0.132	96	2697	6
D.37-2	77	31	0.067	0.1850	0.0011	0.538	0.009	13.71	0.25	0.148	103	2698	10
Marginal young outliers													
D.3-1	554	350	0.020	0.1814	0.0004	0.483	0.007	12.08	0.17	0.123	95	2666	4
D.6-1	292	179	0.037	0.1834	0.0006	0.509	0.007	12.88	0.19	0.129	99	2684	5
D.11-1	400	195	0.063	0.1836	0.0006	0.506	0.007	12.82	0.19	0.137	98	2686	5
D.12-1	250	161	0.028	0.1834	0.0006	0.500	0.007	12.64	0.19	0.136	97	2684	5
D.22-1	135	84	0.769	0.1821	0.0013	0.490	0.008	12.31	0.21	0.138	96	2672	12
D.28-1	117	56	0.139	0.1827	0.0010	0.527	0.008	13.28	0.22	0.140	102	2677	9
D.29-1	313	151	-0.008	0.1821	0.0005	0.506	0.007	12.70	0.19	0.137	99	2672	5
D.32-1	56	22	0.274	0.1821	0.0016	0.516	0.009	12.95	0.26	0.139	100	2673	14
D.33-1	155	67	0.053	0.1832	0.0007	0.518	0.008	13.09	0.21	0.143	100	2682	7
Discordant													
D.1-1	219	173	0.007	0.1846	0.0006	0.473	0.007	12.03	0.19	0.112	93	2694	6
D.2-1	144	253	0.042	0.1863	0.0009	0.378	0.006	9.72	0.16	0.035	76	2710	8
D.4-1	242	116	0.837	0.1840	0.0011	0.446	0.007	11.32	0.18	0.159	88	2689	10
D.10-1	274	236	0.703	0.1794	0.0010	0.290	0.006	7.16	0.15	0.068	62	2647	9
D.18-1	317	202	0.012	0.1835	0.0005	0.476	0.007	12.05	0.18	0.121	94	2685	5
D.19-1	658	733	0.189	0.1831	0.0004	0.480	0.007	12.10	0.19	0.119	94	2681	4
D.30-1	269	199	0.110	0.1835	0.0009	0.462	0.007	11.68	0.18	0.109	91	2684	8
Anomalous young outlier													
D.13-1	621	482	0.015	0.1717	0.0003	0.477	0.007	11.31	0.16	0.140	98	2575	3

Data are at 1 $\sigma$  precision. All Pb data are common-Pb corrected (based on  $^{204}\text{Pb}$  and Broken Hill Pb composition). Analysis date: 19/03/2001; session Z3672i.

## 200096 7004: Williamstown peridotite

<b>1:250,000 sheet:</b>	Kurnalpi (SH5110)
<b>1:100,000 sheet:</b>	Kanowna (3236)
<b>MGA:</b>	357754.04E                      6590939.3N
<b>Location:</b>	The sample was taken from Kalgoorlie Consolidated Gold Mines diamond drillhole BSD11, depth interval 117.10–136.00 m. The collar site is located 3 km south-southeast of the ‘Super Pit’ and 2.5 km west of Lakewood.
<b>Description:</b>	<p>This sample is from an altered, coarse-grained granophyric quartz pyroxene gabbro which forms a sub-unit within the Williamstown peridotite. The Williamstown peridotite is a 150-300 m thick, differentiated sill that intruded between the Devon Consuls Basalt and Paringa Basalt and above the Kapai Slate (Bateman et al., 2001).</p> <p>The unit has a granular to granophyric texture. Principal minerals are plagioclase (50%), amphibole (40–45%), and quartz (5–10%) with minor skeletal leucoxene and trace magnetite. Igneous textures have been extensively modified through metamorphism and alteration. Plagioclase occurs as laths, often with fine-grained amphibole and quartz inclusions. Plagioclase is also locally coarsely intergrown with quartz, forming a granophyric texture. Amphibole occurs as variably-grained aggregates, clearly pseudomorphing igneous pyroxene which has broken down to amphibole and quartz during metamorphism. Secondary minerals comprise moderate chlorite, epidote, carbonate and white mica.</p>
<b>Mount, pop:</b>	Z3672B

### Description of zircons

The zircon yield from this sample was very poor, with only 20 small fragments and whole crystals recovered. These are ~60 µm to 130 µm in length with the few discernible aspect ratios varying from ~2:1 to 4:1. The grains are colourless and clear, and contain rare inclusions. Euhedral and concentric zoning is visible in most grains (Fig. 27). Potential core-rim relationships are present in a few grains, but the small size precludes testing for any age differences.

### Concurrent standard data

The floating point exponent for QGNG is 2.27 – apparently high but not significantly different from the default 2.0. The data for sample 200096 7002B, analysed in this session, also suggests a high slope (2.05). A value of 2.1 was used for data reduction. No data were excluded from the Pb/U calibration, 29 analyses giving a 1 $\sigma$  scatter of 1.37%. The weighted mean  $^{207}\text{Pb}/^{206}\text{Pb}$  age for all 29 is  $1847.8 \pm 4.1$  Ma (MSWD = 1.2), but using a standardised set of criteria for assessment of the data (see “Data compilation for the QGNG standard”) gives a  $^{207}\text{Pb}/^{206}\text{Pb}$  age of  $1848.6 \pm 3.6$  Ma (MSWD = 1.07).

Element abundance calibration was based on CZ3 (n = 2).

### Sample data

Only 14 grains were found to have exposed sections suitable for analysis. In one case (9-2) a second analyses was fitted onto the grain. In seven cases, a second measurement was recorded without moving the spot. The second-measurement data (labels subscripted ‘b’ in Table 12) have  $^{207}\text{Pb}/^{206}\text{Pb}$  of similar quality to the original analyses, but Pb/U is not calibrated. In assessing data, the second measurements have been assumed to have the same concordance/discordance as the corresponding first measurements. Only the first measurements are shown in the concordia plot (Fig. 28).

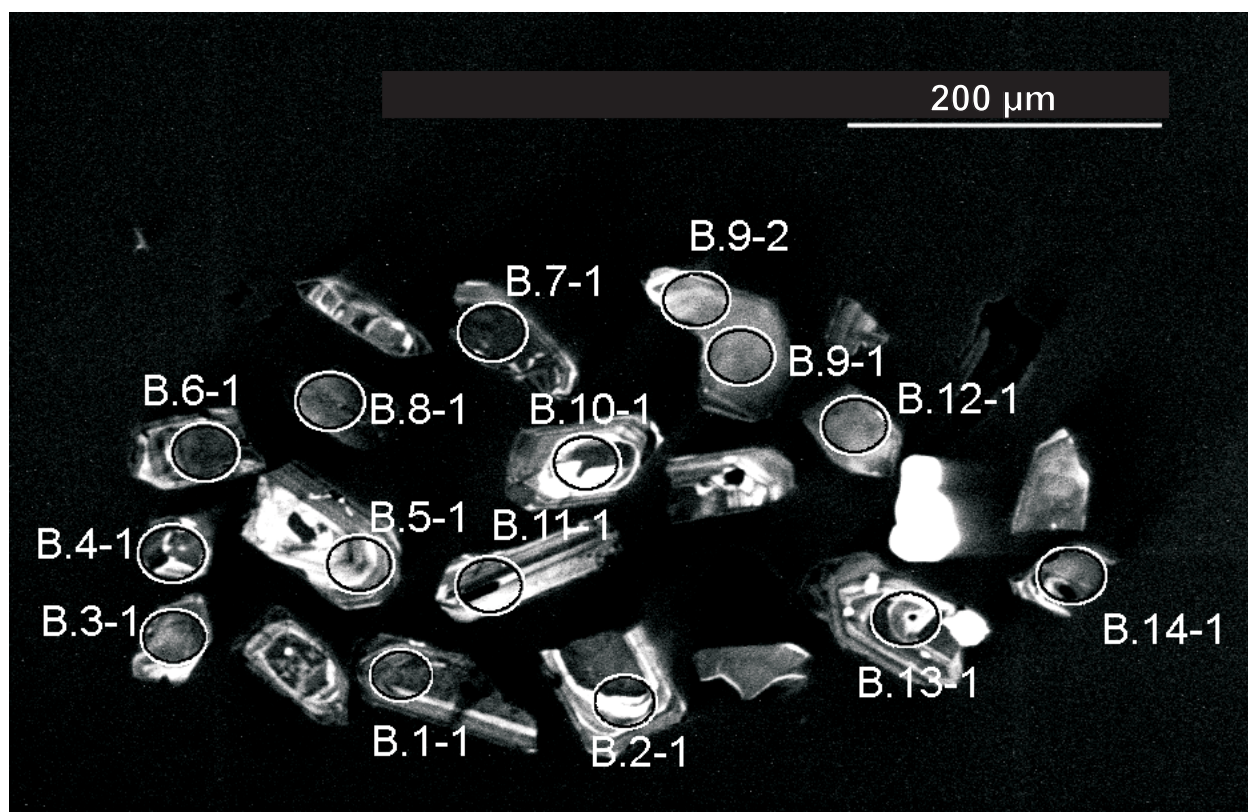


Figure 27. Representative SEM CL image for sample 200096 7004: Williamstown peridotite. SHRIMP analysis spots are labelled. Scale bar is 200  $\mu\text{m}$ . This is the original working image; the sample was not re-imaged for this report.

The data scatter suggests both early and recent Pb loss. Data from seven spots are >5% discordant and there is one distinct young outlier (11-1) amongst the concordant data. The remaining 10 analyses from six grains give a weighted mean  $^{207}\text{Pb}/^{206}\text{Pb}$  age of  $2695.8 \pm 4.3$  Ma (MSWD = 0.59).

### Geochronological interpretation

The lack of any old outliers amongst the data suggests that the grains are not inherited, or if they were, their U-Pb systems were thermally reset when they were incorporated into the melt. In either case, the  $^{207}\text{Pb}/^{206}\text{Pb}$  date of  $2696 \pm 5$  Ma is likely to represent the intrusive age of the dyke. However, it is also possible that all the zircons were inherited.

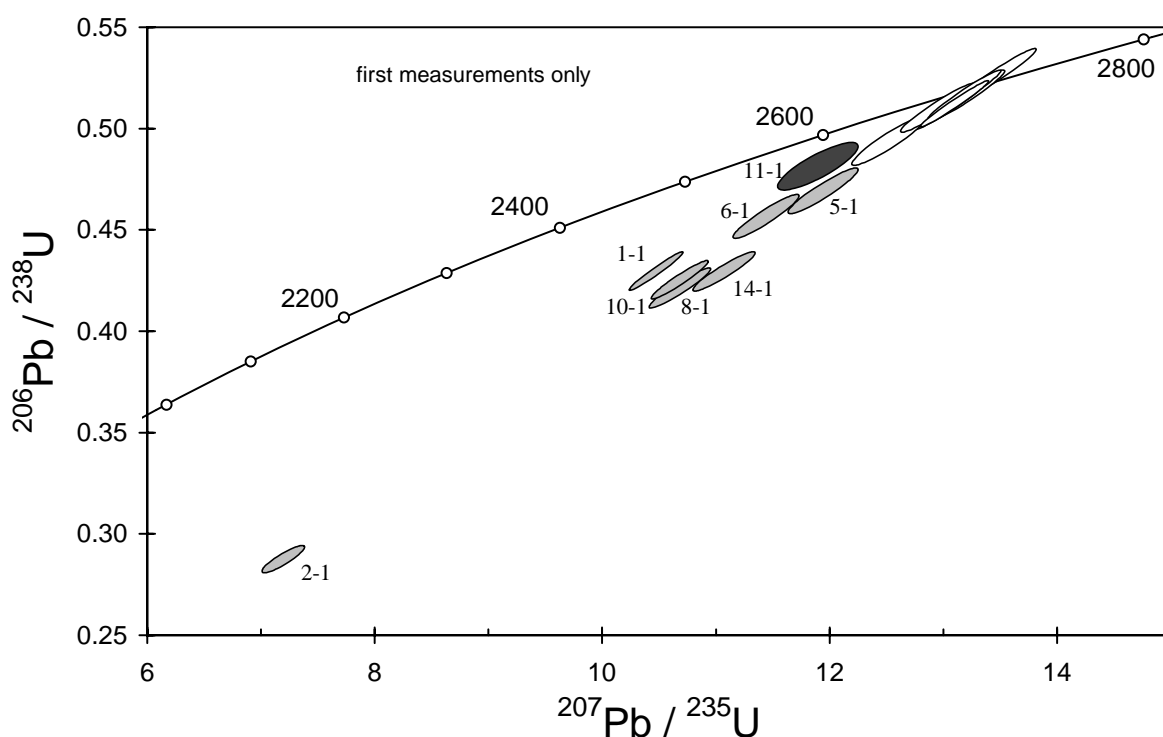


Figure 28. Concordia plot for sample 200096 7004: Williamstown peridotite. White filled symbols are used to define the age of the sample; discordant analyses are light grey; younger outlier is dark grey.



Table 12. SHRIMP analytical results for sample 200096 7004: Williamstown peridotite.

grain-spot	U (ppm)	Th (ppm)	4f206 (%)	$\frac{^{207}\text{Pb}}{^{206}\text{Pb}}$	$\pm$	$\frac{^{206}\text{Pb}}{^{238}\text{U}}$	$\pm$	$\frac{^{207}\text{Pb}}{^{235}\text{U}}$	$\pm$	$\frac{^{208}\text{Pb}}{^{232}\text{Th}}$	conc. (%)	$\frac{^{207}\text{Pb}}{^{206}\text{Pb}}$ Age (Ma)	$\pm$
Main group													
B.3-1	134	72	0.053	0.1837	0.0009	0.511	0.008	12.94	0.21	0.141	99	2687	8
B.3-1b			0.029	0.1846	0.0008							2694	7
B.4-1	140	90	0.144	0.1835	0.0011	0.494	0.008	12.51	0.21	0.142	96	2685	10
B.4-1b			0.096	0.1821	0.0013							2672	12
B.7-1	266	208	0.018	0.1852	0.0006	0.513	0.008	13.09	0.20	0.139	99	2700	5
B.9-1	132	84	0.044	0.1852	0.0008	0.517	0.008	13.21	0.22	0.142	100	2700	8
B.9-1b			0.045	0.1852	0.0008							2700	7
B.9-2	119	48	-0.005	0.1849	0.0008	0.512	0.008	13.06	0.22	0.136	99	2697	7
B.12-1	148	98	0.082	0.1852	0.0008	0.528	0.008	13.49	0.22	0.145	101	2700	7
B.13-1	177	132	-0.014	0.1848	0.0007	0.517	0.008	13.19	0.21	0.140	100	2696	6
Discordant													
B.1-1	276	176	0.095	0.1764	0.0006	0.430	0.006	10.45	0.16	0.085	88	2620	6
B.1-1b			0.217	0.1785	0.0008							2639	8
B.2-1	147	841	0.674	0.1817	0.0014	0.286	0.004	7.16	0.12	0.013	61	2669	13
B.2-1b			0.426	0.1809	0.0019							2661	17
B.5-1	110	128	0.158	0.1844	0.0012	0.469	0.008	11.93	0.21	0.080	92	2693	10
B.5-1b			0.164	0.1833	0.0013							2683	11
B.6-1	336	348	0.201	0.1814	0.0011	0.457	0.007	11.43	0.19	0.099	91	2666	10
B.8-1	129	193	0.113	0.1837	0.0010	0.421	0.007	10.67	0.18	0.048	84	2686	9
B.8-1b			0.043	0.1838	0.0008							2688	7
B.10-1	212	310	0.178	0.1820	0.0009	0.425	0.006	10.67	0.17	0.040	85	2671	8
B.14-1	181	118	0.484	0.1867	0.0011	0.429	0.007	11.05	0.18	0.124	85	2714	9
Young outlier													
B.11-1	99	164	0.155	0.1789	0.0019	0.482	0.008	11.88	0.23	0.070	96	2643	18

Data are at 1 $\sigma$  precision. All Pb data are common-Pb corrected (based on  $^{204}\text{Pb}$  and Broken Hill Pb composition).

Label postscript 'b' indicates second measurement on spot; Pb/U not calibrated.

Analysis date:19/03/2001; session Z3672i.

## 200096 7006D: feldspar-amphibole porphyry clast in volcanoclastic conglomerate, Parkeston

**1:250,000 sheet:** Kurnalpi (SH5110)

**1:100,000 sheet:** Kanowna (3236)

**MGA:** 358797mE 6600487mN

**Location:** The sample was taken from Kalgoorlie Consolidated Gold Mines diamond drillhole MAD2, depth interval 318.8–319.3 m. The collar site is located about 2.5 km northeast of Parkeston and 2 km southeast of Yarri Road.

**Description:** This sample is from a single large (>40 cm diameter) clast of altered feldspar-amphibole porphyry within a volcanoclastic and epiclastic conglomerate unit of the Black Flag Beds. The feldspar-amphibole porphyry clast represents the major type of clast in the conglomerate unit.

The sample has a recrystallised granoblastic texture. It is a moderately altered rock comprising altered phenocrysts (to 3 mm) of amphibole (>50%; represented by aggregates of actinolite, chlorite, biotite, quartz and Fe-oxides) and feldspar (25–20%; represented by secondary albite, quartz, leucoxene, epidote and carbonate) in a groundmass of recrystallised quartz, feldspar (dominantly albite), epidote, actinolite, chlorite, leucoxene and Fe-oxides. Minor aggregates of epidote are also present. Accessory phases include trace zircon. Alteration minerals include minor carbonate, epidote, chlorite and biotite.

**Mount, pop:** Z3730A

### Description of zircons

Relatively few zircon grains were recovered from this sample (about 25). They are subhedral to anhedral and have rounded crystal faces (no sharp prismatic terminations are preserved). Most grains are equant and stubby (~65 µm), but a few are more elongate (aspect ratio 3:1, up to 130 µm long). The grains are colourless and clear, and contain rare inclusions. CL is moderate to strong, with systematic zoning patterns visible in many grains (Fig. 29). No distinct core/rim relationships were observed.

### Concurrent standard data

One analysis, unintentionally limited to 5 scans, was deleted. The apparent floating point exponent for the remaining 35 is ~2.5 and the two samples analysed concurrently also suggest values well above the default 2.0. An exponent of 2.25 was used for data reduction, resulting in a 1σ scatter in  $^{206}\text{Pb}/^{238}\text{U}$  data for QGNG of 1.01%. The weighted mean  $^{207}\text{Pb}/^{206}\text{Pb}$  age from these data is  $1848.9 \pm 2.6$  Ma (MSWD = 1.19), but using a standardised set of criteria for assessment of the data (see “Data compilation for the QGNG standard”) gives a  $^{207}\text{Pb}/^{206}\text{Pb}$  age of  $1849.3 \pm 2.3$  Ma (MSWD = 1.02).

Element abundance calibration was based on CZ3 (n = 1).

### Sample data

Twenty four analyses were obtained from the 23 grains that were suitable for analysis (Table 13). The data show both early and recent Pb loss, though none are strongly discordant (Fig. 30). Omitting two discordant analyses (1-1, 2-1), one with high common Pb (10-1) and five distinct young outliers (3-1, 6-1, 7-1, 15-1, 20-1) leaves 16 that cluster on concordia and give a weighted mean  $^{207}\text{Pb}/^{206}\text{Pb}$  age of  $2661.2 \pm 2.6$  Ma (MSWD = 0.89).

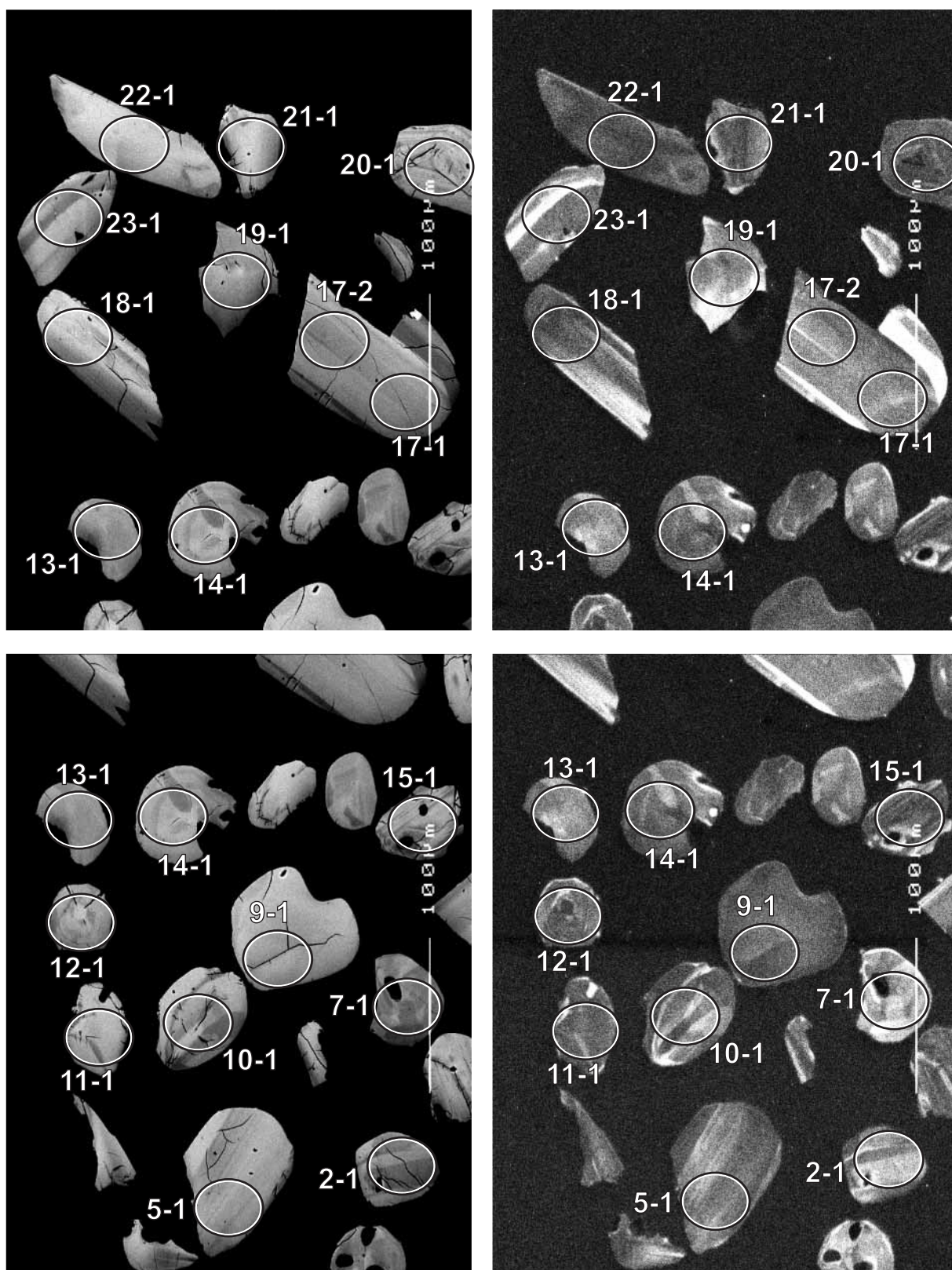


Figure 29. Representative SEM images (BSE on left, CL on right) for sample 200096 7006D: feldspar-amphibole porphyry clast in volcanoclastic conglomerate, Parkeston. SHRIMP analysis spots are labelled. Scale bar is 100  $\mu\text{m}$ .

## Geochronological interpretation

The  $^{207}\text{Pb}/^{206}\text{Pb}$  age of  $2661 \pm 3$  Ma is probably the magmatic age of the parent porphyry. It is a maximum depositional age for the clast-supported conglomerate.

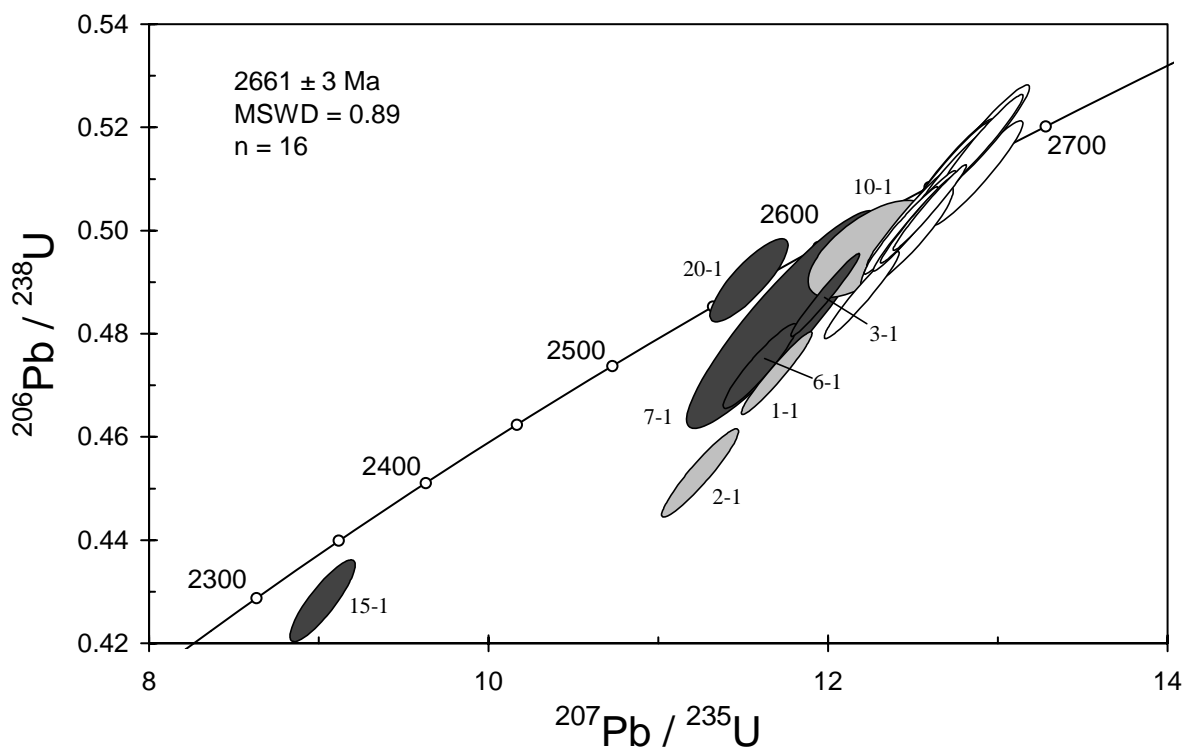


Figure 30. Concordia plot for zircon data from sample 200096 7006D: feldspar-amphibole porphyry clast in volcanoclastic conglomerate, Parkeston. White filled symbols are used to define the age of the sample; discordant and/or high common Pb analyses are light grey; younger outliers are dark grey.

Table 13. SHRIMP analytical results for zircon from sample 200096 7006D: feldspar-amphibole porphyry clast in volcanoclastic conglomerate, Parkeston.

grain-spot	U (ppm)	Th (ppm)	4f206 (%)	$\frac{^{207}\text{Pb}}{^{206}\text{Pb}}$	$\pm$	$\frac{^{206}\text{Pb}}{^{238}\text{U}}$	$\pm$	$\frac{^{207}\text{Pb}}{^{235}\text{U}}$	$\pm$	$\frac{^{208}\text{Pb}}{^{232}\text{Th}}$	conc. (%)	$\frac{^{207}\text{Pb}}{^{206}\text{Pb}}$ Age (Ma)	$\pm$
Main group													
A.4-1	98	167	0.145	0.1813	0.0011	0.499	0.007	12.46	0.18	0.137	98	2665	10
A.5-1	164	319	0.019	0.1807	0.0006	0.511	0.006	12.72	0.16	0.139	100	2659	6
A.8-1	310	707	0.013	0.1807	0.0006	0.503	0.006	12.53	0.15	0.138	99	2659	5
A.9-1	216	501	0.023	0.1814	0.0005	0.505	0.007	12.63	0.18	0.137	99	2666	5
A.11-1	227	406	0.008	0.1816	0.0006	0.487	0.006	12.20	0.15	0.134	96	2667	5
A.12-1	312	289	0.029	0.1809	0.0004	0.502	0.006	12.52	0.14	0.141	99	2661	4
A.13-1	105	141	0.062	0.1827	0.0008	0.511	0.007	12.88	0.18	0.142	99	2678	7
A.14-1	202	346	-0.019	0.1810	0.0006	0.517	0.006	12.91	0.16	0.140	101	2662	5
A.16-1	232	434	0.050	0.1801	0.0005	0.502	0.006	12.47	0.16	0.137	99	2654	5
A.17-1	122	168	0.072	0.1808	0.0007	0.518	0.007	12.93	0.17	0.141	101	2661	7
A.17-2	89	116	0.057	0.1808	0.0009	0.515	0.007	12.84	0.19	0.140	101	2660	8
A.18-1	275	633	0.034	0.1803	0.0005	0.500	0.006	12.43	0.14	0.137	98	2656	4
A.19-1	134	197	0.027	0.1803	0.0007	0.512	0.006	12.72	0.17	0.142	100	2655	6
A.21-1	389	955	0.023	0.1812	0.0004	0.504	0.006	12.60	0.14	0.137	99	2664	4
A.22-1	297	568	0.013	0.1809	0.0005	0.500	0.006	12.48	0.14	0.137	98	2661	4
A.23-1	114	212	0.039	0.1803	0.0007	0.512	0.007	12.72	0.17	0.141	100	2655	7
Discordant or high common Pb													
A.1-1	286	841	0.116	0.1797	0.0006	0.472	0.005	11.69	0.14	0.130	94	2650	5
A.2-1	130	168	0.119	0.1802	0.0008	0.452	0.006	11.24	0.15	0.140	91	2655	8
A.10-1	120	195	3.360	0.1787	0.0026	0.496	0.006	12.23	0.23	0.147	98	2641	24
Young outliers													
A.3-1	367	777	0.037	0.1784	0.0004	0.487	0.005	11.98	0.14	0.134	97	2638	4
A.6-1	219	421	0.347	0.1777	0.0008	0.473	0.005	11.60	0.14	0.132	95	2632	7
A.7-1	100	103	0.130	0.1763	0.0022	0.482	0.014	11.73	0.37	0.131	97	2618	21
A.15-1	416	1576	0.749	0.1530	0.0010	0.427	0.005	9.01	0.13	0.116	96	2379	12
A.20-1	390	242	1.034	0.1706	0.0012	0.490	0.005	11.53	0.15	0.148	100	2564	12

Data are at 1 $\sigma$  precision. All Pb data are common-Pb corrected (based on  $^{204}\text{Pb}$  and Broken Hill Pb composition). Analysis date: 18/06/2001; session Z3730i.



## 200096 7007: feldspar-amphibole-phyric quartz diorite dyke, Tarmoola mine

<b>1:250,000 sheet:</b>	Leonora (SH5101)
<b>1:100,000 sheet:</b>	Leonora (3140)
<b>MGA:</b>	320524mE                      6827254mN
<b>Location:</b>	The sample was taken from survey station 562 in the 'Canyon' area of the Tarmoola open pit.
<b>Description:</b>	<p>This sample is from a grey, altered, fine- to medium-grained feldspar-amphibole-phyric quartz diorite dyke. The quartz diorite dyke intruded a biotite granodiorite pluton, the Tarmoola Granodiorite. Both units are cut by quartz veins and associated hydrothermal alteration; the chosen sample is free from obvious quartz veins.</p> <p>The unit is moderately altered and recrystallised. The sample comprises altered phenocrysts (&lt;2.5 mm) of amphibole (&gt;30%; represented by aggregates of chlorite, carbonate, white mica, quartz and Fe-oxides) and feldspar (10–20%; represented by secondary albite and minor white mica, carbonate, quartz and Fe-oxides) in a fine-grained groundmass of recrystallised quartz, feldspar, carbonate and white mica, minor chlorite, leucoxene, pyrite and Fe-oxides and trace zircon.</p>
<b>Mount, pop:</b>	Z3672C

### Description of zircons

A moderate number of zircon fragments and crystals was recovered from this sample. Most grains are colourless and clear, subhedral to euhedral, with slight rounding of crystal faces. The grains vary from equant (aspect ratio 1:1) to more elongate (aspect ratio 4:1), with lengths ranging from about 85  $\mu\text{m}$  to 165  $\mu\text{m}$ , although a few grains are larger (>300  $\mu\text{m}$ ). A few inclusions are present in many grains. Both the transmitted and reflected light photographs and the CL images show well-defined euhedral zoning in most of the grains (Fig. 31). There are some clear structural discontinuities between core regions and rim zones in several grains as seen in the CL images. A few rare grains have extremely bright CL.

### Concurrent standard data

The floating point calibration exponent for this QGNG data set is 2.1. This is not significantly higher than the default value of 2.0, but the data for sample 9996 9014 (analysed concurrently) indicate a higher value (~2.3); a value of 2.1 was used for data reduction.

There is one outlier in  $^{206}\text{Pb}/^{238}\text{U}$  (16-3) and this has been omitted from the calibration, leaving 26 analyses with a  $1\sigma$  scatter in  $^{206}\text{Pb}/^{238}\text{U}$  of 1.26%. The same data have a weighted mean  $^{207}\text{Pb}/^{206}\text{Pb}$  age of  $1849 \pm 4$  Ma (rounded off by SQUID; MSWD = 1.3). There is one young outlier amongst these (25-2); omitting this leaves 25 analyses with a  $^{207}\text{Pb}/^{206}\text{Pb}$  age of  $1849.0 \pm 3.4$  Ma (MSWD = 1.06), but using a standardised set of criteria for assessment of the data (see "Data compilation for the QGNG standard") gives a  $^{207}\text{Pb}/^{206}\text{Pb}$  age of  $1849.7 \pm 3.5$  Ma (MSWD = 1.01).

Element abundance calibration was based on CZ3 (n = 2).

### Sample data

Fourty five analyses on 43 grains show considerable discordance, with more than half the data being >5% discordant (Table 14, Fig. 32). Many also have high common Pb. However, the Pb loss is dominantly recent, and there is only moderate dispersion in  $^{207}\text{Pb}/^{206}\text{Pb}$ , apart from one apparently inherited grain at ~2850 Ma (31-1). This analysis does not come from a distinct core



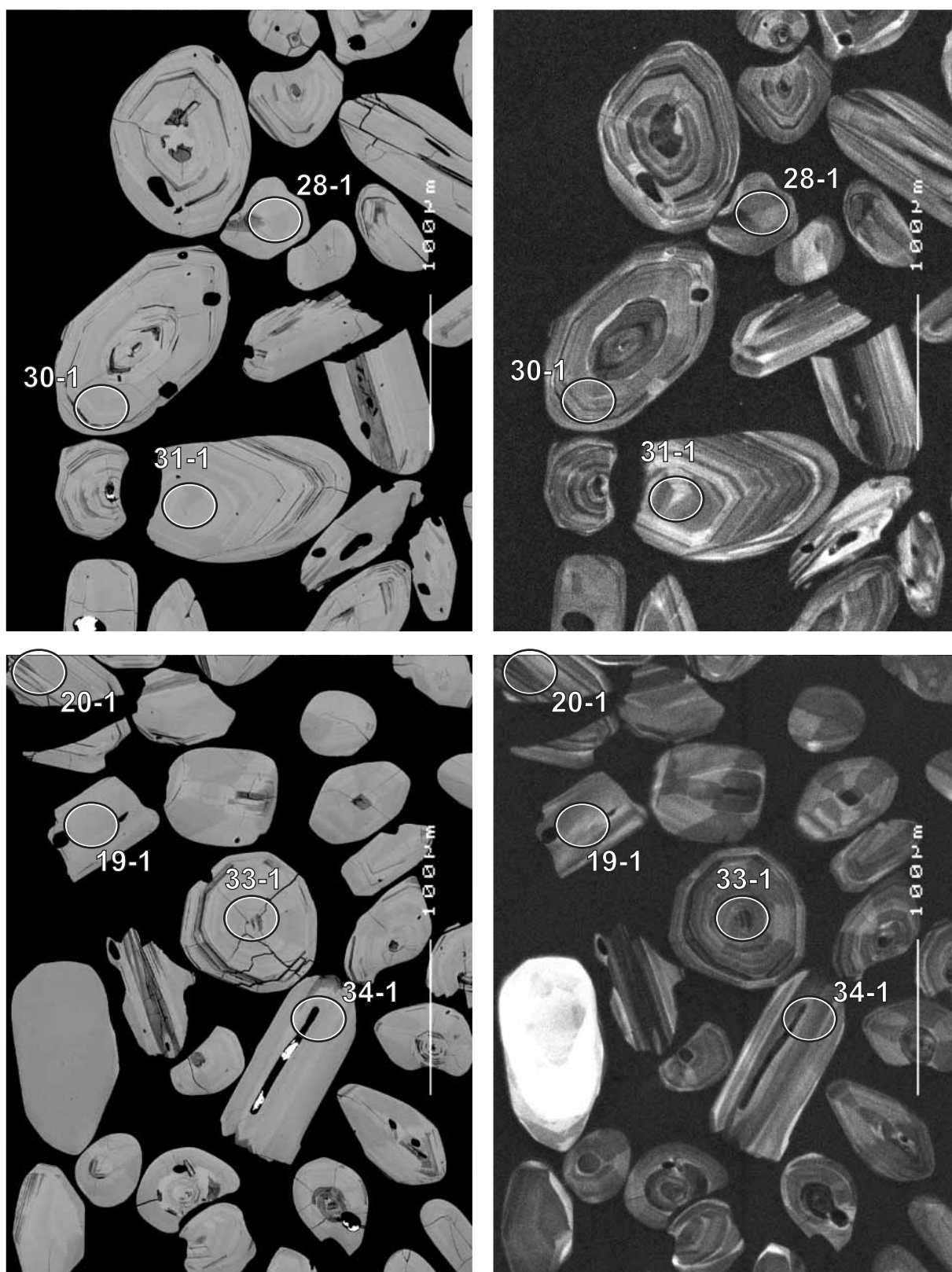


Figure 31. Representative SEM images (BSE on left, CL on right) for sample 200096 7007: feldspar-amphibole-phyric quartz diorite dyke, Tarmoola mine. SHRIMP analysis spots are labelled. Scale bar is 100  $\mu\text{m}$ .

and there are no other apparent core-rim age contrasts, despite targeting both cores and rims.

Omitting the discordant analyses and inherited grain leaves a group of 19 with a weighted mean  $^{207}\text{Pb}/^{206}\text{Pb}$  age of  $2667.1 \pm 7.5$  Ma (MSWD = 2.0). There are two possible young outliers in this group (3-1, 13-1); omitting them increases the mean age to  $2669 \pm 7$  Ma (MSWD = 1.7; Fig. 33). The discordance trend is unusually linear, indicating that the radiogenic Pb loss was dominantly recent. Adding the six low-common Pb data with 6–10% discordance to the reduced set of concordant data would actually improve the weighted mean  $^{207}\text{Pb}/^{206}\text{Pb}$  age to  $2666.8 \pm 5.2$  Ma (MSWD = 1.4). Because the age is subject to data selection, we use a preferred age of 2667 Ma with an uncertainty of 8 Ma that includes essentially all the possible groupings.

### Geochronological interpretation

The  $^{207}\text{Pb}/^{206}\text{Pb}$  age of  $2667 \pm 8$  Ma is likely to be the intrusive age of the dyke.

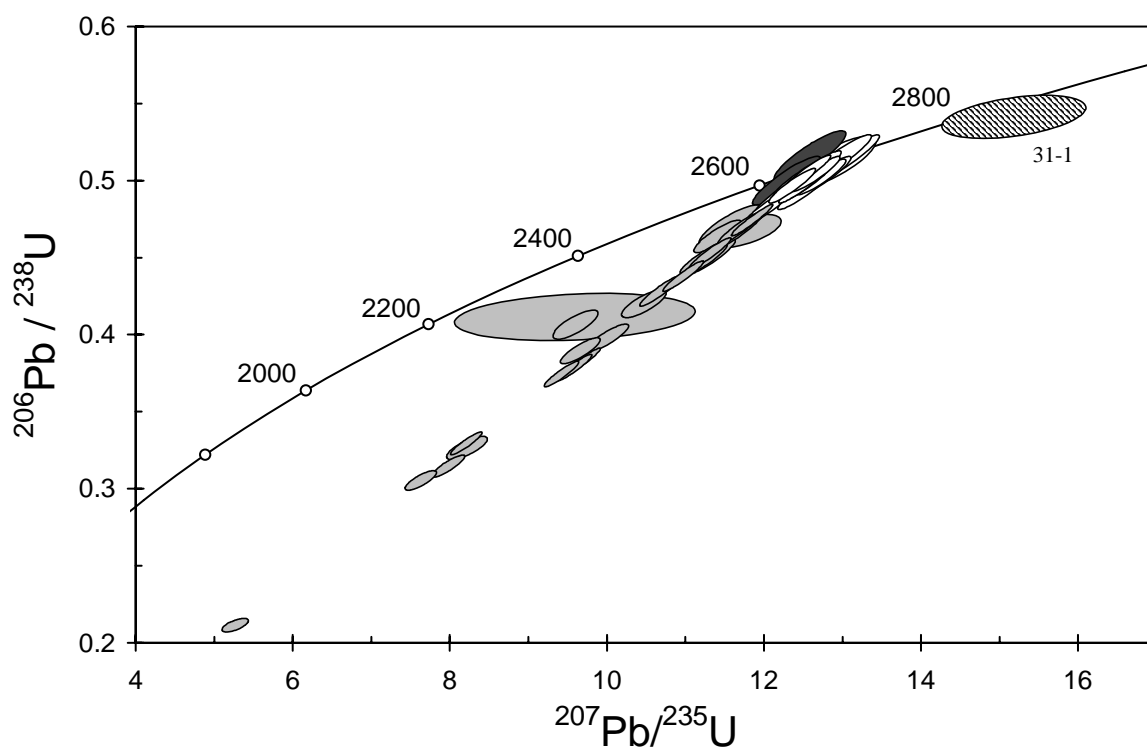


Figure 32. Concordia plot for zircon data from sample 200096 7007: feldspar-amphibole-phyric quartz diorite dyke, Tarmoola mine. White filled symbols are the main group of data used to define the age of the sample, but see text for details; inherited grain has diagonal shading; discordant and/or high common Pb analyses are light grey; younger outliers are dark grey.

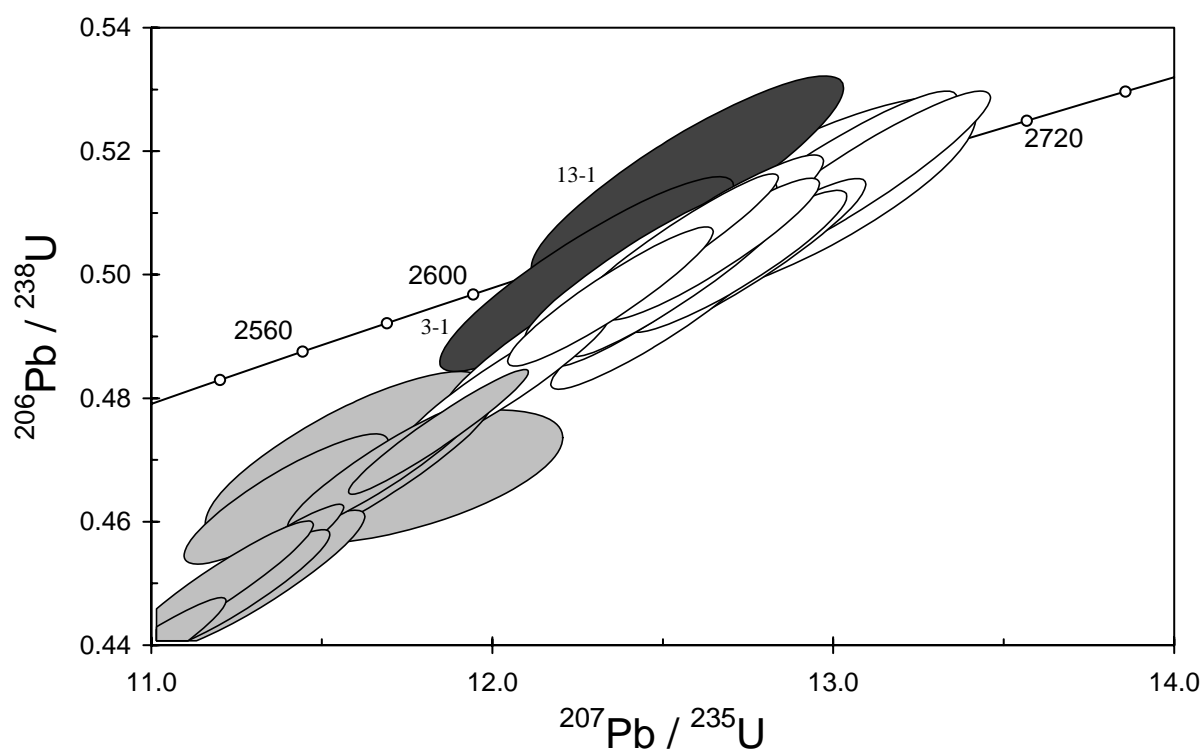


Figure 33. Enlargement of main group of zircon analyses for sample 200096 7007: feldspar-amphibole-phyric quartz diorite dyke, Tarmoola mine. Symbol shading as in Figure 32.

Table 14. SHRIMP analytical results for zircon from sample 200096 7007: feldspar-amphibole-phyrlic quartz diorite dyke, Tarmoola mine.

grain-spot	U (ppm)	Th (ppm)	4f206 (%)	$^{207}\text{Pb}/^{206}\text{Pb}$	$\pm$	$^{206}\text{Pb}/^{238}\text{U}$	$\pm$	$^{207}\text{Pb}/^{235}\text{U}$	$\pm$	$^{208}\text{Pb}/^{232}\text{Th}$	conc. (%)	$^{207}\text{Pb}/^{206}\text{Pb}$ Age (Ma)	$\pm$
Main group													
C.4-1	128	121	0.284	0.1803	0.0011	0.496	0.008	12.34	0.20	0.138	98	2656	10
C.6-1	27	63	0.515	0.1825	0.0030	0.512	0.011	12.88	0.35	0.140	100	2676	27
C.7-1	66	63	0.117	0.1806	0.0013	0.507	0.008	12.62	0.23	0.136	99	2658	12
C.11-1	72	60	-0.035	0.1834	0.0011	0.498	0.008	12.59	0.22	0.135	97	2684	10
C.14-1	43	18	-0.030	0.1824	0.0014	0.515	0.010	12.96	0.26	0.143	100	2675	13
C.16-1	55	49	-0.103	0.1838	0.0013	0.502	0.009	12.73	0.24	0.138	98	2687	12
C.19-1	45	41	-0.455	0.1838	0.0014	0.515	0.010	13.06	0.26	0.144	100	2688	12
C.23-1	79	68	0.152	0.1837	0.0011	0.493	0.008	12.48	0.21	0.128	96	2686	10
C.25-1	90	90	-0.003	0.1823	0.0010	0.497	0.008	12.49	0.21	0.132	97	2674	9
C.26-1	57	43	-0.055	0.1804	0.0012	0.490	0.008	12.19	0.23	0.130	97	2656	11
C.30-1	83	60	0.040	0.1808	0.0011	0.482	0.008	12.03	0.21	0.126	95	2661	10
C.32-1	106	105	0.580	0.1819	0.0011	0.504	0.008	12.64	0.21	0.139	99	2670	10
C.34-1	77	79	0.153	0.1796	0.0011	0.501	0.008	12.41	0.21	0.142	99	2650	10
C.35-1	99	42	0.459	0.1836	0.0012	0.502	0.008	12.71	0.21	0.137	98	2686	11
C.36-1	104	83	0.095	0.1800	0.0009	0.505	0.008	12.53	0.20	0.134	99	2653	8
C.40-1	90	86	0.210	0.1803	0.0011	0.503	0.008	12.51	0.21	0.139	99	2656	10
C.43-1	85	83	-0.031	0.1824	0.0009	0.498	0.008	12.54	0.21	0.136	97	2675	8
Possible young outliers													
C.3-1	31	10	0.188	0.1779	0.0018	0.500	0.011	12.27	0.29	0.131	99	2634	17
C.13-1	112	73	0.111	0.1767	0.0020	0.516	0.011	12.56	0.30	0.137	102	2622	19
5%–10% discordant and low common Pb													
C.1-1	68	51	0.245	0.1821	0.0014	0.450	0.008	11.30	0.21	0.119	90	2672	13
C.21-1	81	67	0.105	0.1812	0.0011	0.468	0.007	11.68	0.20	0.127	93	2664	10
C.27-1	157	210	0.081	0.1810	0.0007	0.474	0.007	11.83	0.18	0.124	94	2662	7
C.33-1	96	81	0.033	0.1806	0.0010	0.449	0.007	11.19	0.18	0.113	90	2658	9
C.37-1	139	94	0.045	0.1810	0.0009	0.452	0.007	11.29	0.17	0.123	90	2662	8
C.38-1	136	75	0.126	0.1807	0.0010	0.468	0.007	11.67	0.18	0.126	93	2659	10
>10% discordant or high common Pb													
C.2-1	291	189	2.655	0.1712	0.0021	0.405	0.006	9.57	0.19	0.104	85	2570	21
C.5-1	102	46	0.928	0.1823	0.0016	0.397	0.006	9.97	0.18	0.079	81	2674	15
C.5-2	217	227	1.584	0.1812	0.0019	0.303	0.004	7.58	0.13	0.055	64	2664	17
C.8-1	118	99	0.068	0.1815	0.0009	0.437	0.007	10.94	0.17	0.115	88	2667	8
C.9-1	155	162	0.676	0.1840	0.0015	0.313	0.005	7.94	0.14	0.072	65	2689	13
C.10-1	109	125	2.736	0.1822	0.0039	0.467	0.007	11.73	0.31	0.133	92	2673	36
C.12-1	119	117	1.333	0.1782	0.0015	0.463	0.007	11.38	0.20	0.124	93	2636	14
C.15-1	142	48	0.196	0.1832	0.0010	0.378	0.006	9.55	0.15	0.091	77	2683	9
C.17-1	121	129	25.267	0.1690	0.0175	0.410	0.010	9.56	1.02	0.092	87	2548	174
C.18-1	122	154	2.592	0.1782	0.0025	0.470	0.009	11.56	0.27	0.127	94	2636	23
C.20-1	205	440	3.655	0.1810	0.0030	0.208	0.003	5.20	0.11	0.045	46	2662	27
C.22-1	119	129	0.161	0.1808	0.0011	0.328	0.005	8.17	0.13	0.074	69	2660	10
C.24-1	167	257	0.041	0.1834	0.0009	0.381	0.006	9.63	0.17	0.027	77	2684	8
C.28-1	140	184	0.370	0.1824	0.0010	0.373	0.005	9.38	0.15	0.095	76	2675	9
C.29-1	105	112	0.228	0.1809	0.0010	0.427	0.007	10.66	0.18	0.109	86	2661	9
C.39-1	128	108	0.456	0.1819	0.0011	0.448	0.007	11.24	0.18	0.126	89	2670	10
C.39-2	105	89	1.632	0.1827	0.0025	0.325	0.005	8.18	0.17	0.086	68	2678	22
C.41-1	146	130	1.152	0.1798	0.0017	0.388	0.006	9.63	0.17	0.105	80	2651	15
C.42-1	144	155	1.294	0.1808	0.0021	0.419	0.006	10.44	0.19	0.110	85	2660	19
Inherited													
C.31-1	66	33	-0.051	0.2032	0.0074	0.542	0.009	15.18	0.61	0.143	98	2852	59

Data are at 1 $\sigma$  precision. All Pb data are common-Pb corrected (based on  $^{204}\text{Pb}$  and Broken Hill Pb composition). Analysis date: 06/04/2001; session Z3672j.

## 200096 7011D: feldspar porphyry, Centurian mine

<b>1:250,000 sheet:</b>	Kalgoorlie (SH5109)
<b>1:100,000 sheet:</b>	Kalgoorlie (3136)
<b>MGA:</b>	347276mE                      6587355mN
<b>Location:</b>	The sample was taken from Croesus diamond drillhole CD29, depth interval 162.0–171.0 m. The diamond drillhole is located in the area now occupied by the Centurian open pit.
<b>Description:</b>	<p>This sample is from an altered feldspar porphyry, locally referred to as the Centurian porphyry. The Centurian porphyry intrudes volcanoclastic and epiclastic breccia, conglomerate and sandstone and carbonaceous shale units of the Black Flag Beds. The feldspar porphyry is intensely altered and cut by numerous quartz veinlets; the selected sample was free of obvious veins.</p> <p>The sample has a granular to granoblastic texture. The principal minerals are albite (&gt;50%), quartz (25%), carbonate (&lt;10%), white mica (&lt;10%) and biotite (5%). Abundant (50–60%) feldspar phenocrysts (&lt;4 mm) are represented by secondary albite and minor white mica, quartz and hematite. Minor (&lt;10%) intensely altered ferromagnesian phenocrysts (&lt;2.5 mm) are represented by aggregates of secondary carbonate, biotite, chlorite and Fe-oxides; the oxides form a 'ghost' outline of the original phenocryst shape. The recrystallised groundmass is fine-grained, and comprises quartz, feldspar, white mica, biotite, chlorite, pyrite and Fe-oxides. Accessory phases include trace apatite and zircon. Fine hematite dusting gives the rock a red colour.</p>
<b>Mount, pop:</b>	Z3730D

### Description of zircons

Zircon from this sample consists of euhedral to subhedral whole grains and fragments with well-defined crystal faces and prismatic terminations. Only very slight rounding of some grains is noted. They are colourless to pale brown and most are clear, with only a few rare inclusions. The grains range in size from about 70  $\mu\text{m}$  to 190  $\mu\text{m}$  and have aspect ratios of 1:1 to 3:1. Zoning is clearly visible in the grains in transmitted and reflected light. CL is strong, and almost all grains display clear concentric euhedral zoning patterns (Fig. 34). A few rare grains contain possible xenocrystic cores, as evidenced by structurally discordant patterns in their central regions.

### Concurrent standard data

One analysis, unintentionally limited to 5 scans, was deleted. The apparent floating point exponent for the remaining 35 is  $\sim 2.5$  and the two samples analysed concurrently also suggest values well above the default 2.0. An exponent of 2.25 was used for data reduction, resulting in a  $1\sigma$  scatter in  $^{206}\text{Pb}/^{238}\text{U}$  data for QGNG of 1.01%. The weighted mean  $^{207}\text{Pb}/^{206}\text{Pb}$  age from these data is  $1848.9 \pm 2.6$  Ma (MSWD = 1.19), but using a standardised set of criteria for assessment of the data (see "Data compilation for the QGNG standard") gives a  $^{207}\text{Pb}/^{206}\text{Pb}$  age of  $1849.3 \pm 2.3$  Ma (MSWD = 1.02).

Element abundance calibration was based on CZ3 (n = 1).

### Sample data

Thirty five analyses were obtained from separate grains (Table 15). There is evidence in the data for both early and recent Pb loss, though no data are strongly discordant (Fig. 35). One analysis with extreme common Pb (1-1) and one discordant point (12-1) were not considered for age determinations. Omitting a further five analyses that are distinct young outliers (3-1, 8-1, 20-1, 24-1, 35-1) leaves a concordant cluster of 28 that has a weighted mean  $^{207}\text{Pb}/^{206}\text{Pb}$  age of  $2666.4 \pm 2.1$  Ma but still has excess scatter (MSWD = 2.5). Omitting two closer outliers (11-1,



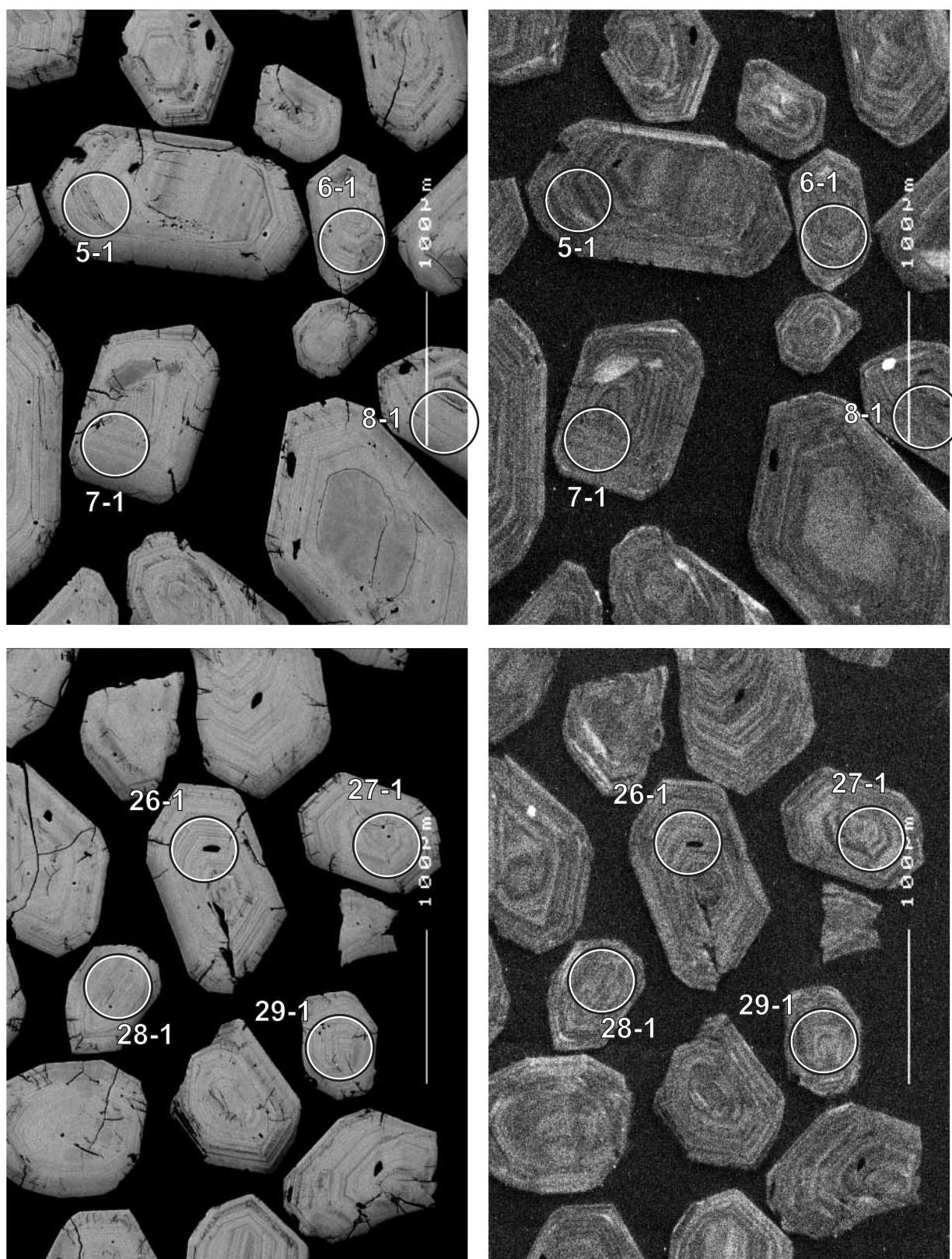


Figure 34. Representative SEM images (BSE on left, CL on right) for sample 200096 7011D: feldspar porphyry, Centurian mine. SHRIMP analysis spots are labelled. Scale bar is 100  $\mu\text{m}$ .

33-1) gives  $2667.3 \pm 1.9$  (MSWD = 1.8). Several other deletions of marginal outliers are possible, but difficult to justify. These could change the average age by up to ~1 Ma, so we use a conservative uncertainty of 3 Ma with the 2667 Ma age.

### Geochronological interpretation

The  $2667 \pm 3$  Ma  $^{207}\text{Pb}/^{206}\text{Pb}$  age is considered to be the intrusive age of the porphyry.

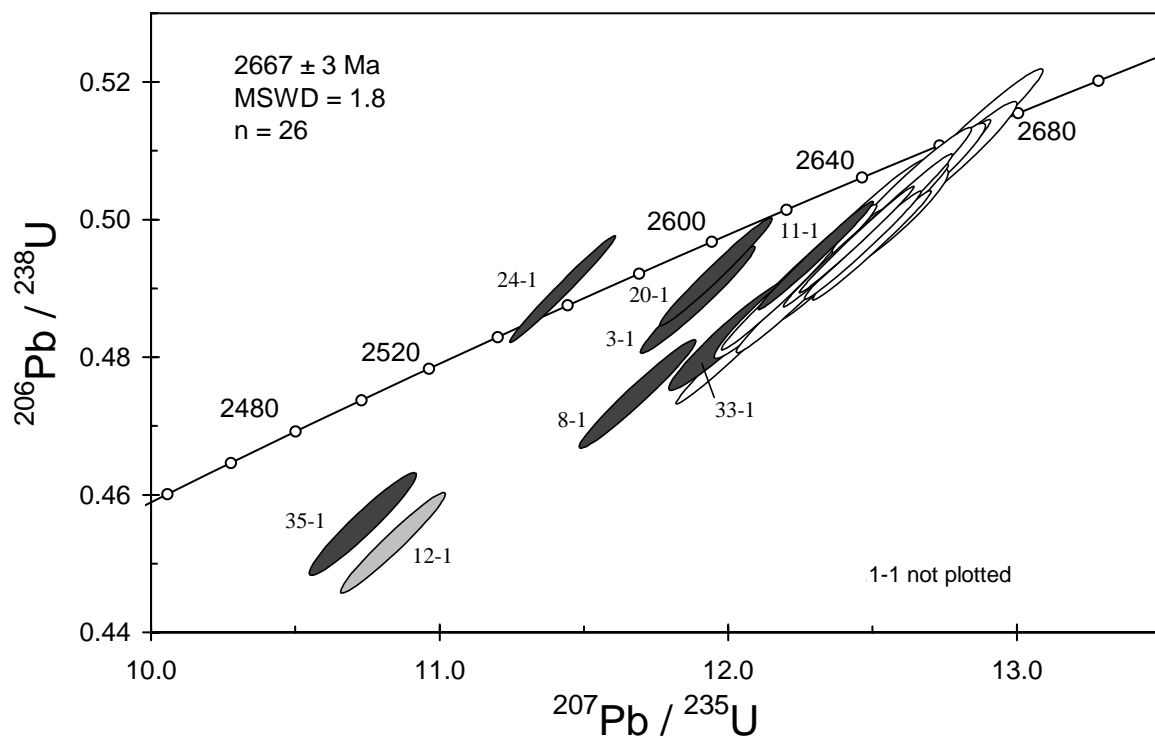


Figure 35. Concordia plot for zircon data from sample 200096 7011D: feldspar porphyry, Centurian mine. White filled symbols are used to define the age of the sample; discordant analysis is light grey; younger outliers are dark grey.

Table 15. SHRIMP analytical results for zircon from sample 200096 7011D: feldspar porphyry, Centurian mine.

grain-spot	U (ppm)	Th (ppm)	4f206 (%)	$\frac{^{207}\text{Pb}}{^{206}\text{Pb}}$		$\frac{^{206}\text{Pb}}{^{238}\text{U}}$		$\frac{^{207}\text{Pb}}{^{235}\text{U}}$		$\frac{^{208}\text{Pb}}{^{232}\text{Th}}$		conc. (%)	$\frac{^{207}\text{Pb}}{^{206}\text{Pb}}$ Age (Ma)	
				$\pm$	$\pm$	$\pm$	$\pm$	$\pm$	$\pm$					
Main group														
D.2-1	500	295	0.050	0.1816	0.0004	0.488	0.005	12.23	0.13	0.134	96	2667	3	
D.4-1	284	157	0.060	0.1815	0.0005	0.497	0.006	12.44	0.14	0.137	98	2666	4	
D.5-1	644	591	0.289	0.1821	0.0008	0.499	0.005	12.54	0.14	0.140	98	2673	7	
D.6-1	688	725	0.044	0.1822	0.0003	0.496	0.005	12.46	0.13	0.139	97	2673	3	
D.7-1	295	139	0.084	0.1818	0.0005	0.513	0.006	12.87	0.15	0.139	100	2669	5	
D.9-1	505	371	0.170	0.1807	0.0004	0.494	0.005	12.31	0.14	0.136	97	2659	4	
D.10-1	453	305	0.265	0.1808	0.0005	0.487	0.005	12.15	0.14	0.134	96	2660	5	
D.13-1	288	183	0.207	0.1817	0.0008	0.498	0.006	12.49	0.15	0.135	98	2668	7	
D.14-1	312	178	0.012	0.1806	0.0005	0.493	0.006	12.28	0.14	0.133	97	2658	4	
D.15-1	499	343	0.015	0.1821	0.0004	0.500	0.005	12.55	0.14	0.137	98	2672	3	
D.16-1	582	461	0.035	0.1806	0.0003	0.489	0.005	12.17	0.13	0.135	96	2659	3	
D.17-1	569	421	0.011	0.1815	0.0003	0.500	0.006	12.51	0.14	0.136	98	2667	3	
D.18-1	910	968	0.021	0.1816	0.0002	0.497	0.005	12.44	0.13	0.138	98	2667	2	
D.19-1	529	392	0.148	0.1817	0.0006	0.506	0.005	12.67	0.14	0.139	99	2669	6	
D.21-1	349	191	0.011	0.1822	0.0006	0.509	0.006	12.78	0.15	0.139	99	2673	5	
D.22-1	321	193	0.100	0.1807	0.0005	0.500	0.006	12.47	0.14	0.136	98	2659	4	
D.23-1	663	626	0.067	0.1818	0.0003	0.501	0.005	12.57	0.14	0.141	98	2669	3	
D.25-1	397	240	-0.026	0.1818	0.0004	0.506	0.006	12.69	0.14	0.137	99	2670	4	
D.26-1	875	962	0.041	0.1815	0.0003	0.495	0.005	12.38	0.13	0.138	97	2667	2	
D.27-1	546	528	0.009	0.1826	0.0003	0.496	0.005	12.49	0.14	0.137	97	2677	3	
D.28-1	361	280	0.046	0.1814	0.0004	0.494	0.005	12.35	0.14	0.137	97	2665	4	
D.29-1	639	605	0.266	0.1813	0.0005	0.505	0.005	12.63	0.14	0.141	99	2665	4	
D.30-1	456	325	-0.008	0.1817	0.0004	0.498	0.005	12.48	0.14	0.137	98	2669	3	
D.31-1	454	319	0.000	0.1814	0.0004	0.493	0.005	12.34	0.14	0.133	97	2665	4	
D.32-1	699	559	0.094	0.1812	0.0004	0.481	0.006	12.03	0.15	0.133	95	2664	3	
D.34-1	747	674	0.217	0.1820	0.0003	0.493	0.005	12.38	0.14	0.136	97	2671	3	
Discordant or extreme common Pb														
D.1-1	298	178	20.739	0.1951	0.0409	0.562	0.023	15.12	3.23	0.197	103	2786	343	
D.12-1	522	413	0.481	0.1736	0.0005	0.452	0.005	10.83	0.12	0.127	93	2593	5	
Young outliers														
D.3-1	594	613	0.450	0.1767	0.0005	0.488	0.005	11.89	0.13	0.134	98	2622	4	
D.8-1	353	204	0.103	0.1786	0.0005	0.474	0.005	11.68	0.13	0.127	95	2640	4	
D.11-1	717	704	0.060	0.1803	0.0003	0.495	0.005	12.30	0.13	0.135	98	2656	3	
D.20-1	710	767	0.228	0.1761	0.0004	0.492	0.005	11.95	0.13	0.135	99	2616	3	
D.24-1	860	924	0.126	0.1691	0.0003	0.490	0.005	11.42	0.12	0.134	101	2549	3	
D.33-1	335	216	0.263	0.1802	0.0006	0.483	0.005	12.00	0.14	0.132	96	2655	5	
D.35-1	380	289	0.554	0.1709	0.0006	0.455	0.005	10.72	0.12	0.126	94	2567	6	

Data are at 1σ precision. All Pb data are common-Pb corrected (based on  $^{204}\text{Pb}$  and Broken Hill Pb composition). Analysis date: 18/06/2001; session Z3730i.

## 200096 7013: meta-feldspathic greywacke, Navajo mine

<b>1:250,000 sheet:</b>	Kalgoorlie (SH5109)	
<b>1:100,000 sheet:</b>	Kalgoorlie (3136)	
<b>MGA:</b>	346550mE	6588541mN
<b>Location:</b>	The sample was taken from Croesus diamond drillhole ND14, depth interval 84.0–88.0 m. The collar site is within the Navajo prospect, about 1.5 km northwest of the Centurian open pit.	
<b>Description:</b>	<p>This sample is from an altered, graded, medium to coarse, poorly sorted meta-feldspathic greywacke, locally referred to as the Navajo sandstone. The metagreywacke unit is interpreted to form part of the basal sequence of the Kurrawang Conglomerate. The metagreywacke is moderately altered and cut by quartz veinlets and fractures; the sample was free of obvious veins.</p> <p>This is a pervasively altered medium- to coarse-grained albite-quartz-white mica-carbonate-chlorite metagreywacke, with accessory Fe-oxides and leucoxene and trace zircon. The thin section shows abundant clasts of albitised feldspar (50%), quartz (25%) and altered lithic fragments (&lt;5%; represented by sericite-carbonate-chlorite aggregates outlined by Fe-oxides) in a quartzo-feldspathic matrix with white mica, carbonate and minor chlorite, leucoxene and oxides. White mica flakes (5–10%) are disseminated or in small aggregates and form a weak foliation. The low roundness and sphericity of the clasts indicate a relatively immature medium- to coarse-grained greywacke as the protolith.</p>	
<b>Mount, pop:</b>	Z3730B	

### Description of zircons

This sample contains predominantly subhedral to euhedral colourless and clear zircon grains (fragments and whole crystals) which have a large variation in size from about 40  $\mu\text{m}$  to 270  $\mu\text{m}$ . The grains range from equant to elongate (aspect ratio to 3:1). There is a slight to moderate rounding of some crystal faces, although prismatic terminations are preserved in many grains. Small inclusions are present in many grains. Well-defined zoning is present in most grains, as seen in the CL images (Fig. 36) and in the transmitted and reflected light photos. Most grains display concentric euhedral zoning patterns, with several containing structurally discontinuous cores. A few grains have more complex and irregular zoning patterns, particularly in the central regions.

### Analytical details

Data were collected in two analytical sessions, in conjunction with zircons from granitic samples. Data for this sample were collected over five scans while those for QGNG and the granitic samples were seven scans. Prior to data reduction, a duplicate file including data for QGNG and this sample was truncated to 5 scans. Data reduction was independent of data reduction using the 7-scan data.

### Concurrent standard data

In both analytical sessions the apparent floating point calibration exponent was significantly above 2.0 for both QGNG and samples. A value of 2.25 was used for all data.

In the first session, 35 analyses of QGNG had a  $1\sigma$  scatter in  $^{206}\text{Pb}/^{238}\text{U}$  of 0.85%. The corresponding  $^{207}\text{Pb}/^{206}\text{Pb}$  age is  $1848.3 \pm 2.8$  Ma (MSWD = 0.99). The second session was interrupted by a cooling water failure, and towards the end of the session the primary beam became increasingly unstable. Data continuity across the interruption is good, but there is unacceptable scatter in  $^{206}\text{Pb}/^{238}\text{U}$  data for QGNG in the last seven hours. This last portion of the



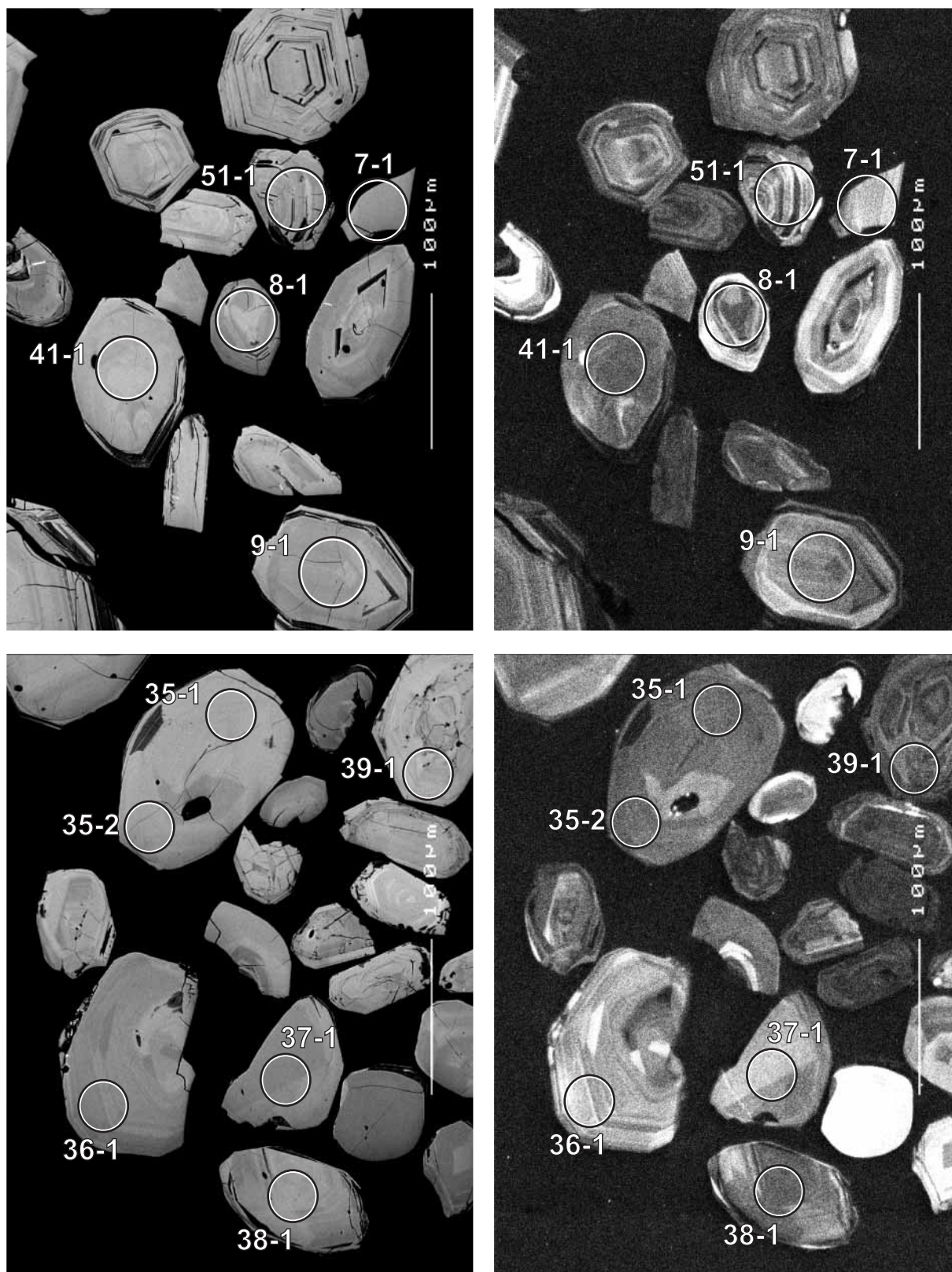


Figure 36. Representative SEM images (BSE on left, CL on right) for sample 200096 7013: meta-feldspathic greywacke, Navajo mine. SHRIMP analysis spots are labelled. Scale bar is 100  $\mu\text{m}$ .



data set was deleted, resulting in the loss of six QGNG analyses, but only two of this sample. The remaining 24 QGNG analyses have a  $1\sigma$  scatter in  $^{206}\text{Pb}/^{238}\text{U}$  of 1.10% and a  $^{207}\text{Pb}/^{206}\text{Pb}$  age of  $1848.0 \pm 3.5$  Ma (MSWD = 0.69).

Element abundance calibration was based on CZ3 (n = 1 and 4, for the two sessions).

### Sample data

A total of 53 analyses were obtained from 49 grains (Table 16). The data form a dominant cluster at ~ 2655 Ma (Fig. 37, 38), with two distinctly older results (33-1, 38-1), considerable discordance in some analyses and elevated common Pb in others. The main concordant cluster of 39 analyses has appreciably more scatter than is attributable to analytical precision, as expected for a detrital sample.

The minimum age of the zircon population could be defined in two ways, neither of which is absolute:

The youngest single near-concordant analysis is 16-1, at  $2632 \pm 4$  Ma ( $1\sigma$ ), a date that falls below the probability trend of other data (Fig. 39). However, this is a high-U grain, with a significant (though small) common Pb content, and the age is not considered highly reliable.

The youngest self-consistent group can be defined by progressively rejecting older data from the main group of 39 analyses. Using a 2672 Ma cutoff (and omitting 16-1) leaves 29 analyses with a weighted mean  $^{207}\text{Pb}/^{206}\text{Pb}$  age of  $2657 \pm 4$  Ma (MSWD = 1.4).

### Geochronological interpretation

The maximum age for the sandstone is considered to be  $2657 \pm 4$  Ma. A single grain suggests a maximum closer to 2632 Ma, but this is not regarded as a reliable limit. The provenance for detrital zircons is dominantly 2.64 – 2.70 Ga but includes components at least as old as ~2.8 Ga.

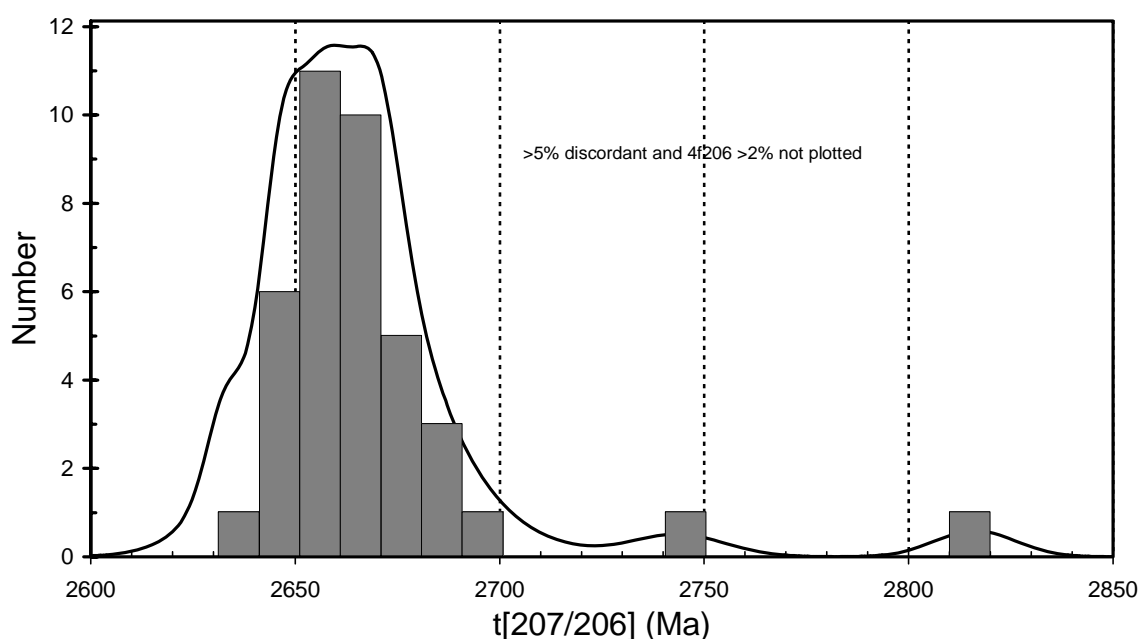


Figure 37. Gaussian-summation plot for zircon age data from sample 200096 7013: meta-feldspathic greywacke, Navajo mine.

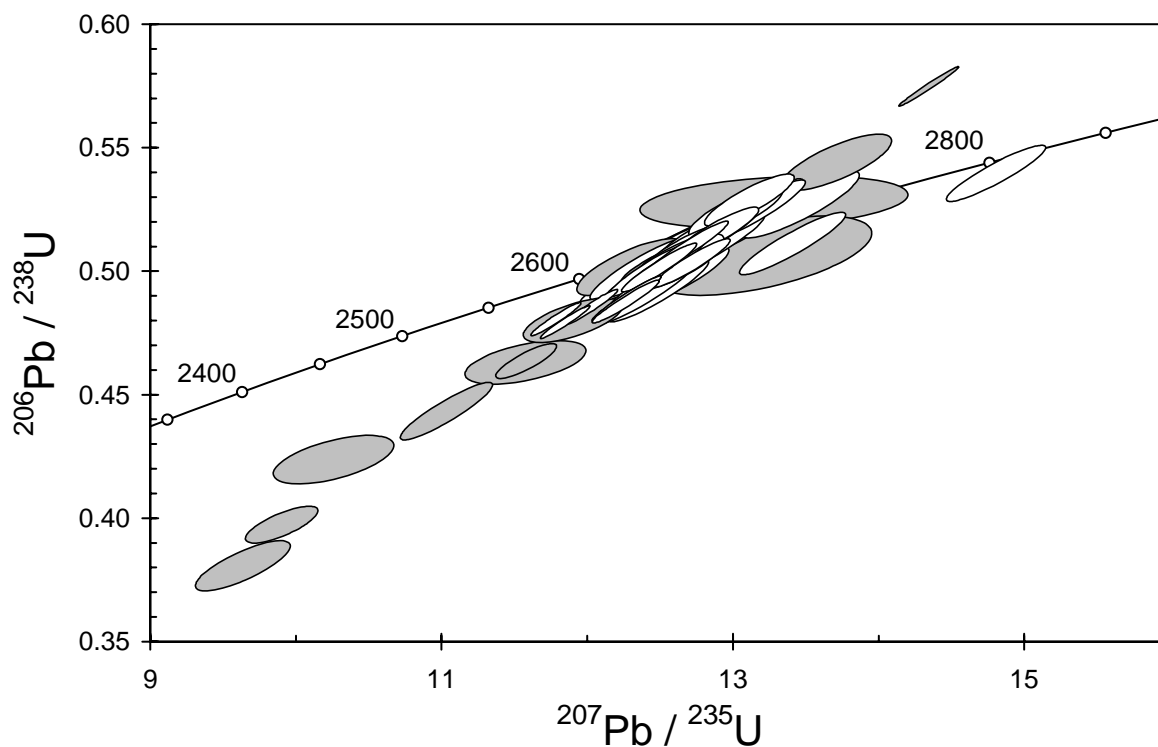


Figure 38. Concordia plot for zircon data from sample 200096 7013: meta-feldspathic greywacke, Navajo mine. White filled symbols are used to assess the maximum age of the sample; discordant and/or high common Pb analyses are light grey.

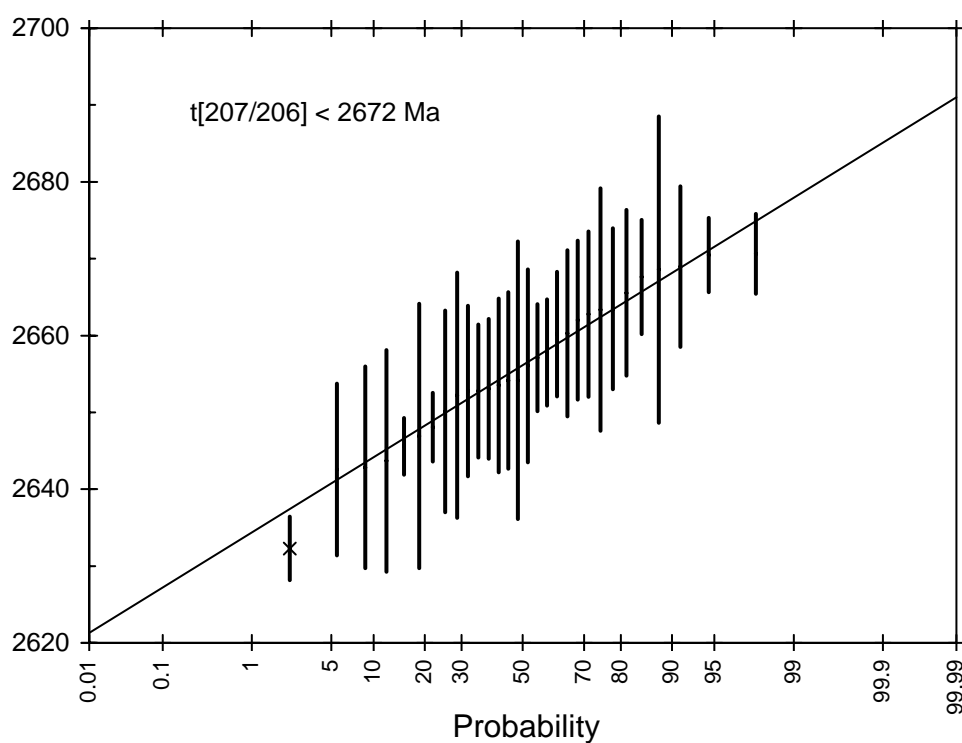


Figure 39. Probability diagram for zircon age data from sample 200096 7013: meta-feldspathic greywacke, Navajo mine. Error bars are  $1\sigma$ .

Table 16. SHRIMP analytical results for zircon from sample 200096 7013: meta-feldspathic greywacke, Navajo mine.

grain-spot	U (ppm)	Th (ppm)	4f206 (%)	<sup>207</sup> Pb/ <sup>206</sup> Pb		<sup>206</sup> Pb/ <sup>238</sup> U		<sup>207</sup> Pb/ <sup>235</sup> U		<sup>208</sup> Pb/ <sup>232</sup> Th	conc. (%)	<sup>207</sup> Pb/ <sup>206</sup> Pb Age (Ma)	
					±		±		±			±	
Main group													
B.1-1	55	49	0.012	0.1803	0.0014	0.516	0.008	12.84	0.23	0.142	101	2656	13
B.3-1	103	38	0.287	0.1811	0.0012	0.516	0.007	12.87	0.19	0.137	101	2663	11
B.4-1	74	82	-0.050	0.1810	0.0011	0.513	0.008	12.81	0.21	0.139	100	2662	10
B.5-1	76	47	-0.047	0.1818	0.0011	0.525	0.008	13.16	0.22	0.143	102	2669	10
B.6-1	114	123	1.490	0.1799	0.0017	0.524	0.007	13.01	0.21	0.145	102	2652	16
B.7-1	65	34	-0.011	0.1814	0.0012	0.525	0.008	13.14	0.22	0.146	102	2666	11
B.10-1	443	514	0.157	0.1795	0.0005	0.485	0.005	12.01	0.12	0.133	96	2648	4
B.13-1	35	25	0.240	0.1817	0.0022	0.519	0.010	13.01	0.30	0.143	101	2669	20
B.15-1	70	86	0.041	0.1812	0.0011	0.515	0.008	12.85	0.21	0.139	100	2663	10
B.16-1	787	524	0.338	0.1778	0.0004	0.480	0.004	11.77	0.11	0.144	96	2632	4
B.17-1	116	79	-0.010	0.1831	0.0009	0.503	0.007	12.70	0.18	0.135	98	2681	8
B.20-1	802	381	0.241	0.1792	0.0004	0.479	0.004	11.83	0.11	0.152	95	2646	4
B.21-1	120	114	1.737	0.1811	0.0017	0.505	0.006	12.62	0.20	0.138	99	2663	16
B.22-1	107	71	0.872	0.1797	0.0014	0.529	0.007	13.11	0.20	0.146	103	2650	13
B.23-1	86	85	0.105	0.1801	0.0012	0.507	0.007	12.60	0.20	0.136	100	2654	11
B.26-1	39	39	0.069	0.1794	0.0019	0.503	0.011	12.43	0.30	0.138	99	2647	17
B.27-1	80	65	0.193	0.1789	0.0014	0.501	0.009	12.35	0.23	0.134	99	2643	13
B.28-1	597	529	0.453	0.1819	0.0006	0.489	0.006	12.26	0.15	0.137	96	2671	5
B.29-1	91	83	0.513	0.1837	0.0016	0.498	0.008	12.61	0.23	0.142	97	2687	15
B.32-1	82	86	-0.013	0.1829	0.0012	0.491	0.008	12.38	0.22	0.136	96	2680	11
B.33-1	95	47	0.204	0.1902	0.0013	0.511	0.008	13.40	0.24	0.138	97	2744	12
B.34-2	73	56	0.082	0.1789	0.0012	0.507	0.009	12.49	0.23	0.132	100	2643	11
B.34-3	47	29	-0.049	0.1790	0.0016	0.499	0.010	12.33	0.27	0.136	99	2644	14
B.34-4	159	118	0.220	0.1800	0.0010	0.500	0.007	12.41	0.19	0.141	99	2653	9
B.35-1	203	71	0.044	0.1805	0.0008	0.510	0.007	12.68	0.18	0.139	100	2657	7
B.35-2	174	62	0.219	0.1808	0.0009	0.502	0.007	12.52	0.18	0.138	99	2660	8
B.36-1	87	42	1.341	0.1801	0.0020	0.510	0.008	12.68	0.25	0.144	100	2654	18
B.37-1	82	69	-0.122	0.1840	0.0013	0.492	0.008	12.48	0.23	0.139	96	2690	12
B.38-1	178	63	0.915	0.1988	0.0012	0.540	0.008	14.80	0.23	0.159	99	2816	10
B.39-1	409	120	0.058	0.1819	0.0005	0.489	0.006	12.26	0.16	0.128	96	2670	5
B.41-1	204	114	-0.029	0.1816	0.0008	0.496	0.007	12.42	0.18	0.137	97	2668	7
B.42-1	82	71	0.056	0.1808	0.0012	0.507	0.008	12.63	0.23	0.139	99	2660	11
B.43-1	83	45	-0.099	0.1801	0.0012	0.524	0.009	13.01	0.24	0.143	102	2654	11
B.44-1	91	63	-0.085	0.1827	0.0012	0.511	0.008	12.87	0.22	0.141	99	2678	10
B.45-1	144	138	0.024	0.1800	0.0009	0.499	0.007	12.39	0.19	0.139	98	2653	9
B.46-1	97	104	0.352	0.1800	0.0012	0.514	0.008	12.76	0.22	0.142	101	2653	11
B.47-1	637	195	0.028	0.1823	0.0006	0.487	0.006	12.25	0.15	0.165	96	2674	6
B.48-1	73	79	0.979	0.1849	0.0019	0.527	0.009	13.45	0.27	0.142	101	2698	17
B.50-1	267	319	0.270	0.1805	0.0008	0.501	0.007	12.48	0.17	0.136	99	2658	7
Discordant and/or high common Pb													
B.8-1	144	103	3.835	0.1796	0.0026	0.480	0.006	11.89	0.23	0.126	95	2650	24
B.9-1	120	96	1.886	0.1809	0.0020	0.396	0.005	9.88	0.17	0.108	81	2661	18
B.11-1	157	141	6.263	0.1813	0.0036	0.463	0.006	11.56	0.27	0.140	92	2664	33
B.12-1	459	216	1.498	0.1811	0.0012	0.463	0.005	11.56	0.14	0.143	92	2663	11
B.14-1	33	4	5.741	0.1891	0.0058	0.506	0.011	13.19	0.49	0.185	97	2734	51
B.18-1	116	44	2.152	0.1826	0.0021	0.544	0.008	13.71	0.25	0.156	105	2676	19
B.19-1	1036	278	0.020	0.1807	0.0003	0.575	0.005	14.34	0.14	0.139	110	2659	3
B.24-1	239	83	5.972	0.1822	0.0080	0.528	0.007	13.27	0.61	0.182	102	2673	73
B.25-1	92	80	2.205	0.1813	0.0021	0.502	0.007	12.55	0.23	0.138	98	2665	20
B.30-1	72	126	0.090	0.1805	0.0014	0.442	0.008	11.01	0.21	0.076	89	2658	13
B.31-1	124	128	3.384	0.1776	0.0022	0.502	0.008	12.28	0.24	0.145	100	2631	21
B.34-1	67	74	1.094	0.1838	0.0025	0.379	0.007	9.61	0.22	0.071	77	2688	23
B.40-1	122	77	2.570	0.1803	0.0023	0.502	0.008	12.48	0.25	0.142	99	2656	21
B.49-1	121	77	9.396	0.1757	0.0038	0.423	0.007	10.24	0.27	0.114	87	2613	36

Data are at 1 $\sigma$  precision. All Pb data are common-Pb corrected (based on  $^{204}\text{Pb}$  and Broken Hill Pb composition). Analyses dates: 18/06/2001 and 22/06/2001; sessions Z3730i and Z3730j, respectively.

## 200096 9003: Maori Queen Tonalite

**1:250,000 sheet:** Edjudina (SH5106)

**1:100,000 sheet:** Lake Carey (3339)

**MGA:** 404282mE 6779460mN

**Location:** The sample was taken from a mine dump at the Maori Queen battery.

**Description:** This sample is from a black and white, medium- to coarse-grained, seriate-textured, hornblende-biotite tonalite. The tonalite was sampled from a mine dump but is representative of a group of mineralogically and geochemically similar tonalitic rocks interpreted to form part of the Maori Queen Tonalite. The tonalite is cut by quartz veins and a weak foliation that is best developed marginal to veins; the selected sample was free of obvious veins.

The unit has a granular to locally granoblastic texture. Principal minerals are feldspar (65–70%, dominated by plagioclase but including K-feldspar), quartz (20–25%), biotite (2–4%), and hornblende (5–6%). Hornblende is present as subhedral, 3–5 mm grains and biotite occurs as subordinate fine flakes and aggregates. Quartz is largely interstitial, finer grained and variably undulose. Accessory phases include zircon, apatite and Fe-oxides. Secondary minerals comprise minor to moderate white mica, epidote, clinozoisite, and lesser carbonate.

**Mount, pop:** Z3679D

### Description of zircons

This sample contains euhedral to subhedral, colourless and clear zircon crystals and fragments. Grains with equant morphology range in size from about 80  $\mu\text{m}$  to 120  $\mu\text{m}$ , whereas elongate grains (aspect ratio up to 4:1) vary from about 115  $\mu\text{m}$  to 200  $\mu\text{m}$  in length. The grains generally have well-formed crystal faces. A strong CL signature was recorded for the grains (Fig. 40). Many grains have simple concentric or parallel zoning patterns but a number of grains display complex and irregular zoning patterns in their central core regions; these are overgrown by more systematic and concentric zoned zircon rims.

### Concurrent standard data

The U/Pb calibration for this session was unusually variable. It drifted rapidly early in the session before becoming more stable for the remainder of the first 24 hours, then dropped back to original values at the start of the second 24 hours and thereafter remained very constant. During the first 24 hours the spot-to-spot variation in  $\text{Zr}_2\text{O}^+$  beam strength was also unusually large. Although the mid-session change in characteristics corresponds to a changeover of operators and mid-session checks, we have been unable to identify a cause for the performance in the first 24 hours. Although the U/Pb variability is obvious, there is no discernible time-related irregularity in  $^{207}\text{Pb}/^{206}\text{Pb}$ .

The first few hours of data, when the U/Pb calibration drifted rapidly, have been deleted and the remainder split into two data batches corresponding to periods of relatively stable U/Pb calibration. The floating-point exponent appears to be higher than the default 2.0 (as commonly noted in this project) but it is not defined well enough to justify replacing the default value. The  $1\sigma$  U/Pb reproducibility for QGNG is 1.29% for the first data batch ( $n = 17$ ) and 0.91% for the second ( $n = 18$ ).

The weighted mean  $^{207}\text{Pb}/^{206}\text{Pb}$  age for all QGNG data is  $1847.1 \pm 3.4$  Ma ( $n = 35$ ; MSWD = 2.3). Omitting four  $2\sigma$  outliers changes this to  $1848.3 \pm 2.6$  Ma (MSWD = 1.2). Using a standardised set of criteria for assessment of the data (see “Data compilation for the QGNG standard”) gives a  $^{207}\text{Pb}/^{206}\text{Pb}$  age of  $1849.9 \pm 2.5$  Ma (MSWD = 1.02).

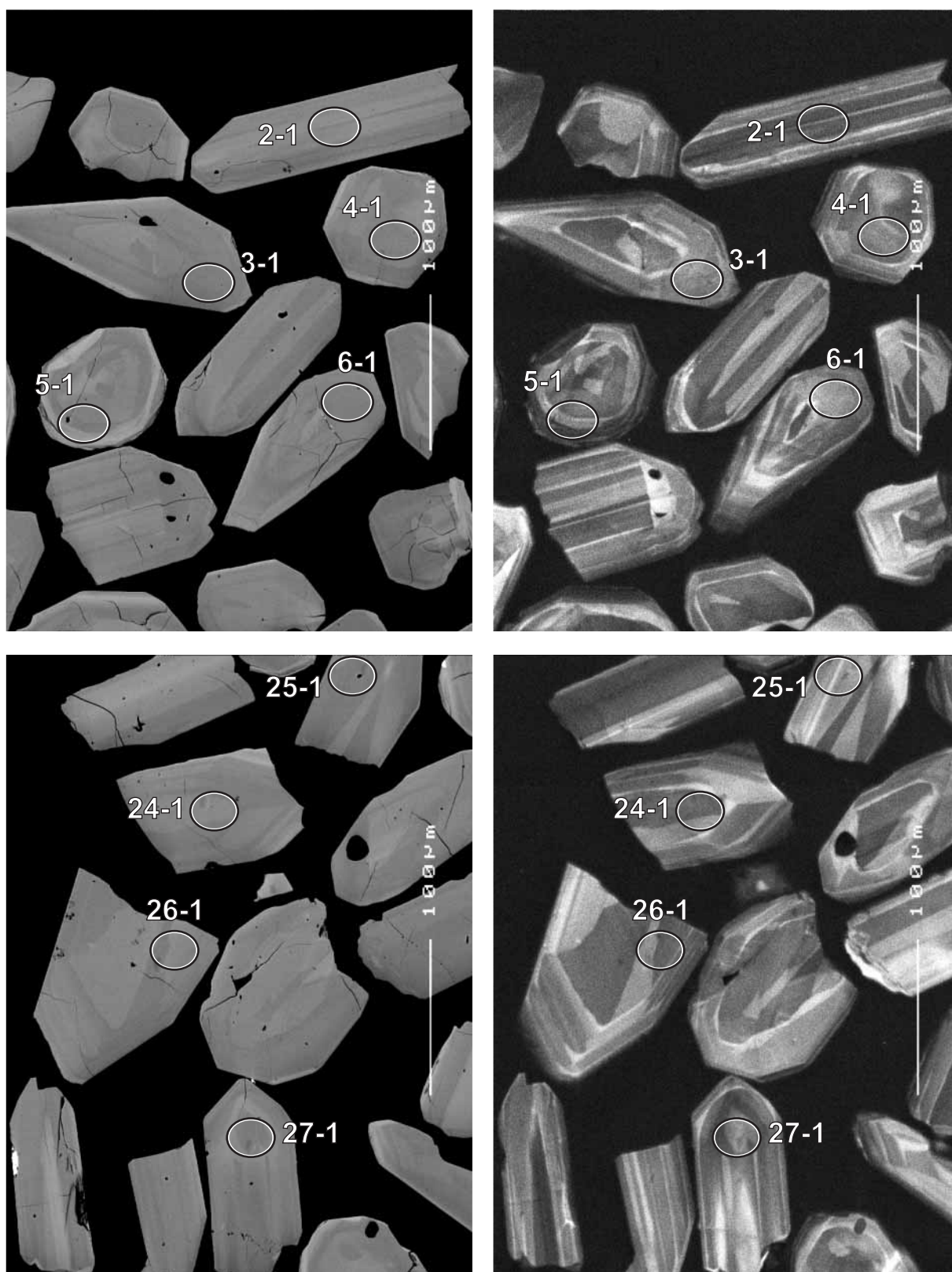


Figure 40. Representative SEM images (BSE on left, CL on right) for sample 200096 9003: Maori Queen Tonalite. SHRIMP analysis spots are labelled. Scale bar is 100  $\mu\text{m}$ .



Element abundance calibration was based on CZ3 (n = 1 for the first batch and n = 2 for the second).

## Sample data

Thirty seven analyses on individual grains were collected, but the first three were deleted (as for the concurrent QGNG data) (Table 17). Data from the two processing batches have been combined, and are here treated as a single data set.

The data distribution is very simple (Fig. 41). Three analyses are moderately discordant (10-1, 14-1, 20-1) and are not used in the age determination. The remaining 31 analyses fall in a single cluster, with a weighted mean  $^{207}\text{Pb}/^{206}\text{Pb}$  age of  $2703.3 \pm 4.3$  Ma (MSWD = 1.40). The analyses on central regions of grains give no indication of zircon inheritance.

## Geochronological interpretation

The  $2703 \pm 5$  Ma  $^{207}\text{Pb}/^{206}\text{Pb}$  date is considered to be the crystallisation age of the tonalite.

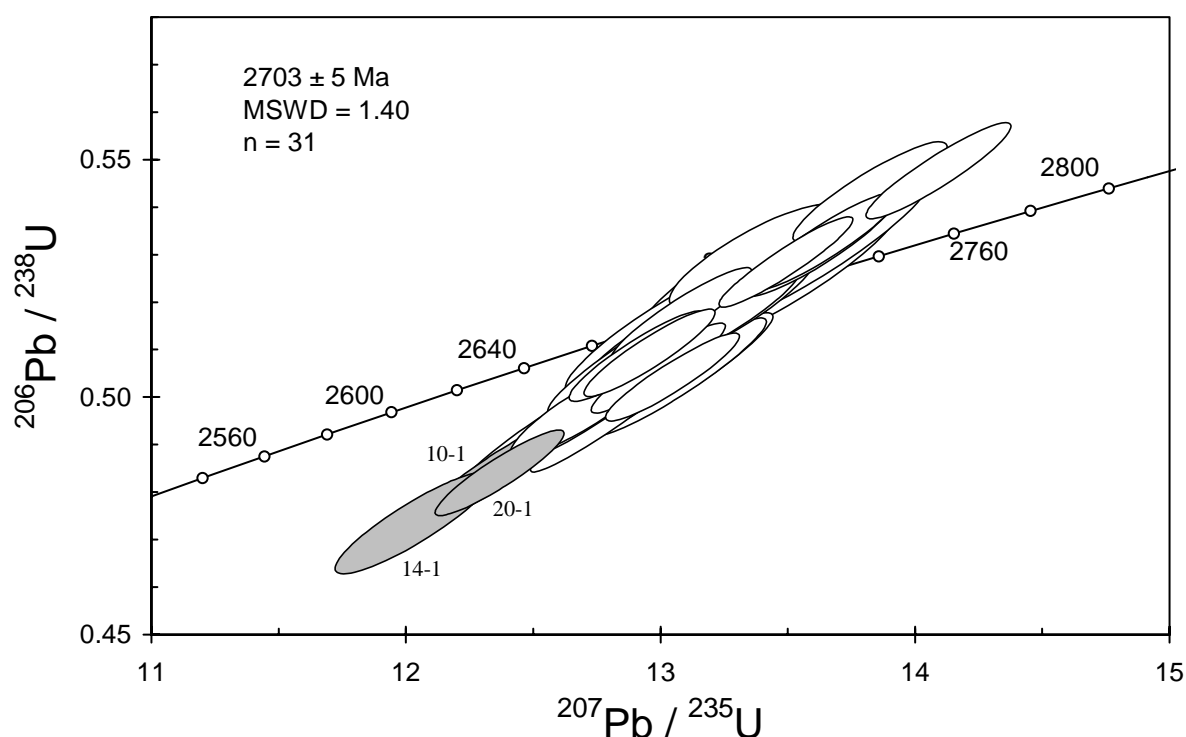


Figure 41. Concordia plot for zircon data from sample 200096 9003: Maori Queen Tonalite. White filled symbols are used to define the age of the sample; discordant analyses are light grey.

Table 17. SHRIMP analytical results for zircon from sample 200096 9003: Maori Queen Tonalite.

grain-spot	U (ppm)	Th (ppm)	4f206 (%)	<sup>207</sup> Pb		<sup>206</sup> Pb		<sup>207</sup> Pb		<sup>208</sup> Pb	conc. (%)	<sup>207</sup> Pb/ <sup>206</sup> Pb	
				<sup>206</sup> Pb	±	<sup>238</sup> U	±	<sup>235</sup> U	±			<sup>232</sup> Th	Age (Ma)
Main group													
D.4-1	68	26	0.041	0.1845	0.0010	0.513	0.008	13.05	0.22	0.137	99	2694	9
D.5-1	73	36	0.196	0.1851	0.0020	0.512	0.008	13.07	0.26	0.137	99	2699	18
D.6-1	43	22	0.068	0.1867	0.0014	0.526	0.009	13.54	0.26	0.144	100	2713	12
D.7-1	94	75	-0.099	0.1873	0.0008	0.495	0.007	12.78	0.20	0.140	95	2719	7
D.8-1	47	30	-0.035	0.1850	0.0011	0.491	0.008	12.53	0.22	0.136	95	2698	10
D.9-1	31	13	0.054	0.1836	0.0016	0.514	0.009	13.01	0.26	0.138	100	2685	15
D.11-1	43	19	-0.042	0.1880	0.0012	0.505	0.009	13.08	0.24	0.139	97	2725	10
D.12-1	41	22	-0.078	0.1862	0.0013	0.499	0.008	12.81	0.23	0.130	96	2709	11
D.13-1	39	18	0.209	0.1833	0.0017	0.527	0.010	13.31	0.27	0.138	102	2683	15
D.15-1	84	55	0.094	0.1857	0.0009	0.515	0.008	13.18	0.21	0.145	99	2704	8
D.16-1	54	39	0.068	0.1838	0.0010	0.508	0.008	12.88	0.22	0.139	99	2687	9
D.17-1	50	32	-0.181	0.1881	0.0012	0.504	0.008	13.07	0.23	0.140	97	2725	10
D.18-1	66	51	-0.003	0.1850	0.0009	0.514	0.008	13.12	0.22	0.141	99	2698	8
D.19-1	51	27	0.031	0.1851	0.0011	0.511	0.008	13.04	0.23	0.140	99	2699	10
D.21-1	39	19	0.010	0.1858	0.0013	0.518	0.007	13.28	0.21	0.143	100	2705	12
D.22-1	48	33	0.108	0.1852	0.0013	0.497	0.007	12.69	0.19	0.133	96	2700	11
D.23-1	51	19	-0.032	0.1835	0.0010	0.517	0.007	13.08	0.18	0.143	100	2684	9
D.24-1	61	44	0.063	0.1850	0.0010	0.516	0.008	13.18	0.21	0.142	99	2699	9
D.25-1	34	19	-0.212	0.1865	0.0014	0.499	0.007	12.82	0.21	0.141	96	2711	13
D.26-1	49	32	0.070	0.1866	0.0012	0.531	0.009	13.66	0.25	0.143	101	2712	10
D.27-1	63	35	0.033	0.1841	0.0010	0.508	0.006	12.90	0.18	0.136	98	2690	9
D.28-1	71	34	0.000	0.1845	0.0010	0.509	0.006	12.95	0.17	0.141	98	2694	9
D.29-1	55	31	0.028	0.1858	0.0011	0.532	0.007	13.62	0.20	0.147	102	2705	10
D.30-1	45	32	-0.105	0.1857	0.0013	0.517	0.007	13.24	0.20	0.143	99	2704	11
D.31-1	64	50	-0.078	0.1877	0.0009	0.504	0.006	13.04	0.17	0.143	97	2722	8
D.32-1	76	46	-0.027	0.1852	0.0008	0.528	0.006	13.49	0.17	0.145	101	2700	7
D.33-1	67	53	-0.018	0.1862	0.0009	0.506	0.006	12.99	0.18	0.141	97	2709	8
D.34-1	46	26	0.139	0.1830	0.0016	0.530	0.007	13.36	0.22	0.143	102	2680	14
D.35-1	57	25	-0.002	0.1845	0.0012	0.543	0.007	13.82	0.20	0.152	104	2694	11
D.36-1	55	21	0.014	0.1857	0.0010	0.533	0.007	13.64	0.19	0.143	102	2705	9
D.37-1	69	51	-0.072	0.1866	0.0009	0.548	0.007	14.09	0.19	0.151	104	2712	8
Discordant													
D.10-1	65	52	0.105	0.1851	0.0011	0.484	0.008	12.36	0.21	0.132	94	2699	10
D.14-1	75	58	0.436	0.1844	0.0014	0.473	0.007	12.02	0.21	0.134	93	2693	13
D.20-1	72	33	-0.020	0.1854	0.0010	0.484	0.006	12.36	0.17	0.134	94	2701	9

Data are at 1 $\sigma$  precision. All Pb data are common-Pb corrected (based on  $^{204}\text{Pb}$  and Broken Hill Pb composition). Analysis date: 02/07/2001; session Z3679j.

## 200096 9004: Danjo Monzogranite

<b>1:250,000 sheet:</b>	Edjudina (SH5106)
<b>1:100,000 sheet:</b>	Lake Carey (3339)
<b>MGA:</b>	403627mE                      6781015mN
<b>Location:</b>	The sample was taken from a large boulder located on the western side of a track and 1.5 km north of Maori Queen Bore.
<b>Description:</b>	<p>This sample is from a white to white-pink, medium- to coarse-grained seriate titanite-hornblende-biotite granodiorite to monzogranite of the Danjo Monzogranite. The Danjo monzogranite is moderately foliated defined by aligned biotite, hornblende, and elongate quartz grains. The sample site is close to the granitoid contact with greenstone. A number of small pits and workings occur within the unit near the sample locality. The sample was free of obvious veins.</p> <p>The sample has a granular to granoblastic texture. The principal minerals are plagioclase (30–40%), quartz (35–40%), biotite (5–7%), hornblende (2–3%), and K-feldspar (10–20%). Plagioclase forms subhedral laths, often with homogeneous cores mantled by zoned rims. Quartz is present as recrystallised to moderately-strongly undulose grains. K-feldspar is largely anhedral and interstitial and commonly associated with myrmekite. Biotite occurs as large irregular to elongate flakes and aggregates to 5–8 mm, hornblende as larger skeletal and smaller irregular grains. Accessories include minor titanite (&lt;1%) and rarer allanite, as well as zircon, apatite and Fe-oxides. Secondary minerals include moderate white mica, epidote and clinozoisite, and lesser carbonate.</p>
<b>Mount, pop:</b>	Z3679C

### Description of zircons

Abundant colourless and clear zircon crystals and fragments were recovered from this sample. The grains are relatively small (50  $\mu\text{m}$  to 130  $\mu\text{m}$  in size) and vary from equant to elongate (most have an aspect ratio of 2:1 to 3:1, but a few grains are up to 5:1). Most grains have well-formed crystal faces, although minor rounding is noted in some grains. Both round and elongate inclusions are present in some grains. CL is moderate to strong (Fig. 42). Some grains have well-defined euhedral and concentric zoning, whereas other grains are more homogeneous. A minority of the grains have complex and irregular zoning patterns. A few grains have structurally distinct cores.

### Concurrent standard data

The U/Pb calibration for this session was unusually variable. It drifted rapidly early in the session before becoming more stable for the remainder of the first 24 hours, then dropped back to original values at the start of the second 24 hours and thereafter remained very constant. During the first 24 hours the spot-to-spot variation in  $\text{Zr}_2\text{O}^+$  beam strength was also unusually large. Although the mid-session change in characteristics corresponds to a changeover of operators and mid-session checks, we have been unable to identify a cause for the performance in the first 24 hours. Although the U/Pb variability is obvious, there is no discernible time-related irregularity in  $^{207}\text{Pb}/^{206}\text{Pb}$ .

The first few hours of data, when the U/Pb calibration drifted rapidly, have been deleted and the remainder split into two data batches corresponding to periods of relatively stable U/Pb calibration. The floating-point exponent appears to be higher than the default 2.0 (as commonly noted in this project) but it is not defined well enough to justify replacing the default value. The  $1\sigma$  U/Pb reproducibility for QGNG is 1.29% for the first data batch ( $n = 17$ ) and 0.91% for the second ( $n = 18$ ).

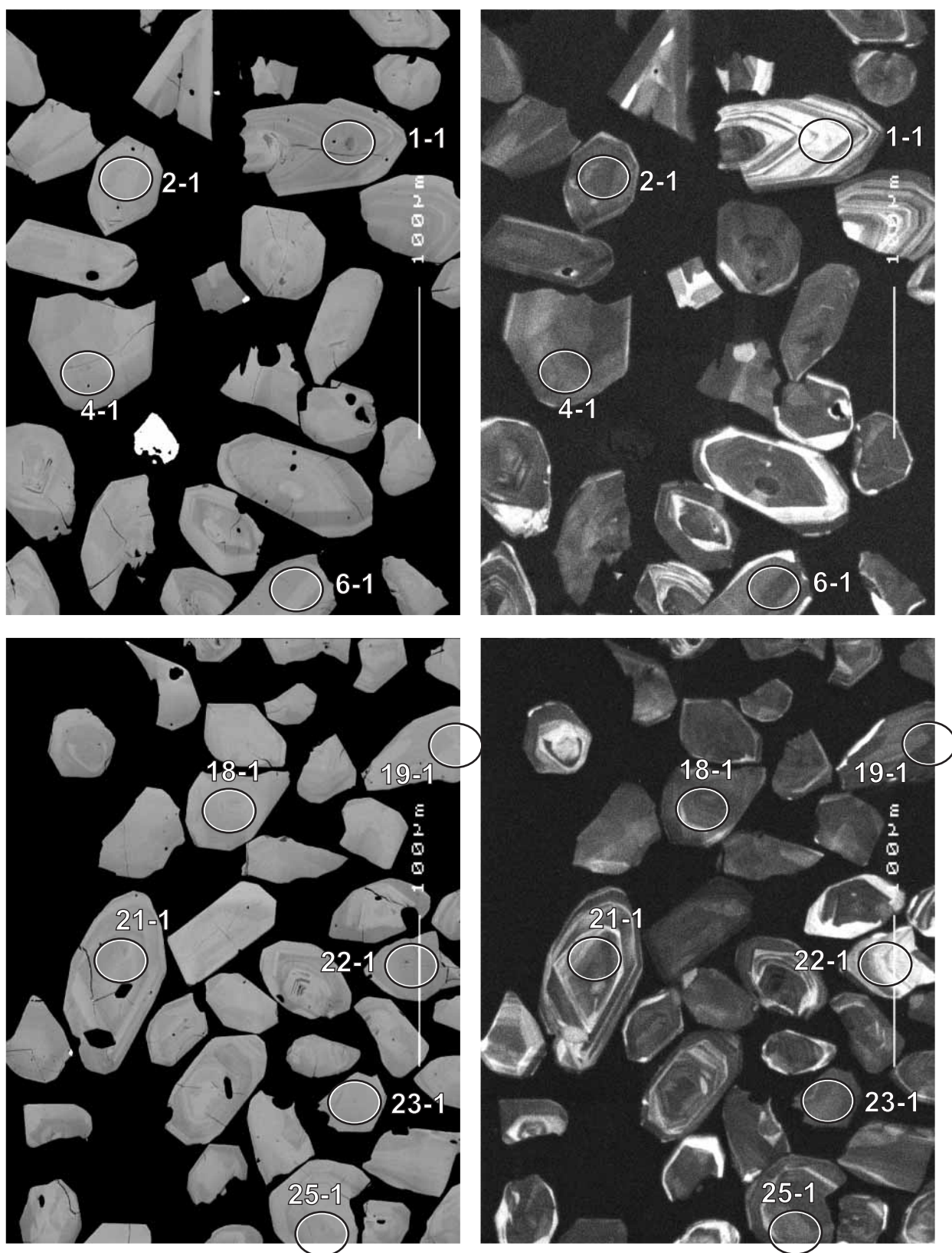


Figure 42. Representative SEM images (BSE on left, CL on right) for sample 200096 9004: Danjo Monzogranite. SHRIMP analysis spots are labelled. Scale bar is 100  $\mu\text{m}$ .

The weighted mean  $^{207}\text{Pb}/^{206}\text{Pb}$  age for all QGNG data is  $1847.1 \pm 3.4$  Ma ( $n = 35$ ; MSWD = 2.3). Omitting four  $2\sigma$  outliers changes this to  $1848.3 \pm 2.6$  Ma (MSWD = 1.2). Using a standardised set of criteria for assessment of the data (see “Data compilation for the QGNG standard”) gives a  $^{207}\text{Pb}/^{206}\text{Pb}$  age of  $1849.9 \pm 2.5$  Ma (MSWD = 1.02).

Element abundance calibration was based on CZ3 ( $n = 1$  for the first batch and  $n = 2$  for the second).

## Sample data

Thirty five analyses on 35 grains were retained (Table 18), after deletion of the first few hours of data (as for the concurrent QGNG data). Data from the two processing batches have been combined, and are here treated as a single data set.

The data distribution is relatively simple (Fig. 43). Eight analyses are discordant (4-1, 5-1, 6-1, 9-1, 19-1, 22-1, 34-1, 37-1) and are not used in the age determination although they all have  $^{207}\text{Pb}/^{206}\text{Pb}$  dates consistent with the main group. The remaining 27 analyses fall in a discrete cluster, with a weighted mean  $^{207}\text{Pb}/^{206}\text{Pb}$  age of  $2702.6 \pm 3.9$  Ma (MSWD = 1.7). Omitting the one statistical outlier (17-1) changes this to  $2703.5 \pm 3.5$  Ma (MSWD = 1.30). The few analyses on central regions of grains suggest there is no zircon inheritance, but some distinctive, possibly older cores were not analysed.

## Geochronological interpretation

The  $2703 \pm 4$  Ma  $^{207}\text{Pb}/^{206}\text{Pb}$  date is considered to be the crystallisation age of the monzogranite.

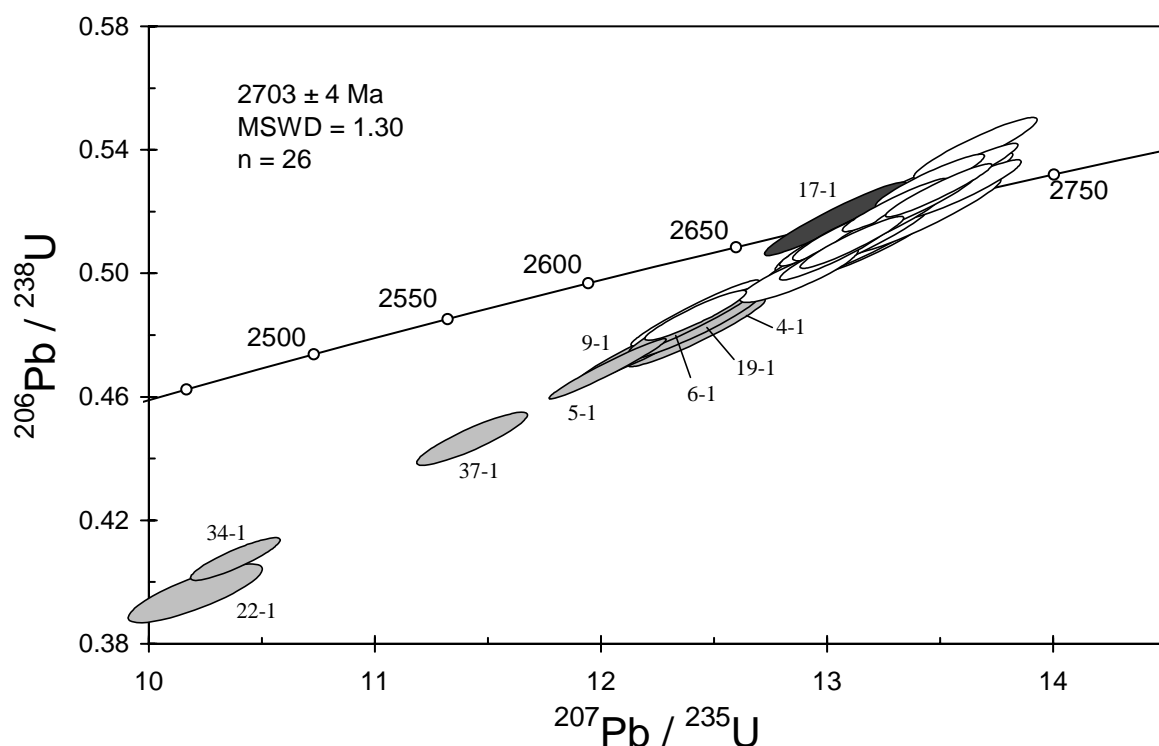


Figure 43. Concordia plot for zircon data from sample 200096 9004: Danjo Monzogranite. White filled symbols are used to define the age of the sample; discordant analyses are light grey; younger outlier is dark grey.



Table 18. SHRIMP analytical results for zircon from sample 200096 9004: Danjo Monzogranite.

grain-spot	U (ppm)	Th (ppm)	4f206 (%)	$\frac{^{207}\text{Pb}}{^{206}\text{Pb}}$	$\pm$	$\frac{^{206}\text{Pb}}{^{238}\text{U}}$	$\pm$	$\frac{^{207}\text{Pb}}{^{235}\text{U}}$	$\pm$	$\frac{^{208}\text{Pb}}{^{232}\text{Th}}$	conc. (%)	$\frac{^{207}\text{Pb}}{^{206}\text{Pb}}$ Age (Ma)	$\pm$
Main group													
C.7-1	55	17	-0.081	0.1870	0.0013	0.508	0.008	13.11	0.23	0.142	98	2716	11
C.8-1	100	50	0.081	0.1848	0.0008	0.487	0.007	12.41	0.19	0.131	95	2697	7
C.10-1	96	27	0.032	0.1868	0.0010	0.510	0.008	13.13	0.21	0.133	98	2714	9
C.11-1	61	18	-0.035	0.1854	0.0011	0.513	0.008	13.10	0.22	0.141	99	2702	10
C.12-1	63	19	-0.045	0.1878	0.0010	0.519	0.008	13.43	0.22	0.147	99	2723	9
C.13-1	107	45	-0.042	0.1861	0.0008	0.498	0.007	12.79	0.19	0.137	96	2708	7
C.14-1	65	38	0.230	0.1846	0.0014	0.525	0.009	13.36	0.25	0.134	101	2695	13
C.15-1	119	55	0.057	0.1859	0.0008	0.508	0.007	13.03	0.20	0.136	98	2706	7
C.16-1	123	57	0.069	0.1848	0.0007	0.514	0.007	13.08	0.20	0.136	99	2696	6
C.18-1	104	35	0.005	0.1849	0.0008	0.514	0.008	13.11	0.20	0.142	99	2698	7
C.20-1	80	30	-0.043	0.1857	0.0009	0.527	0.008	13.50	0.22	0.147	101	2705	8
C.21-1	70	30	0.008	0.1831	0.0009	0.541	0.007	13.66	0.18	0.147	104	2682	8
C.23-1	78	22	-0.077	0.1853	0.0008	0.523	0.006	13.37	0.17	0.145	100	2701	7
C.24-1	124	56	-0.027	0.1861	0.0007	0.523	0.006	13.42	0.15	0.143	100	2708	6
C.25-1	63	21	0.080	0.1852	0.0010	0.514	0.006	13.12	0.18	0.141	99	2700	9
C.26-1	100	47	0.008	0.1849	0.0008	0.533	0.006	13.60	0.17	0.143	102	2698	7
C.27-1	137	65	0.067	0.1864	0.0007	0.510	0.006	13.11	0.15	0.141	98	2711	6
C.28-1	119	46	0.230	0.1851	0.0008	0.486	0.005	12.41	0.15	0.145	95	2699	7
C.29-1	96	48	-0.057	0.1862	0.0008	0.516	0.006	13.25	0.16	0.145	99	2709	7
C.30-1	120	40	0.041	0.1847	0.0007	0.522	0.006	13.30	0.16	0.139	100	2696	6
C.31-1	94	48	-0.015	0.1865	0.0008	0.506	0.006	13.03	0.16	0.142	97	2712	7
C.32-1	121	64	0.026	0.1841	0.0008	0.530	0.006	13.46	0.16	0.144	102	2690	7
C.33-1	73	25	-0.076	0.1869	0.0009	0.527	0.006	13.59	0.18	0.149	101	2715	8
C.35-1	29	13	-0.166	0.1869	0.0016	0.509	0.008	13.11	0.24	0.146	98	2715	14
C.36-1	137	50	0.049	0.1857	0.0006	0.527	0.006	13.49	0.15	0.145	101	2705	6
C.38-1	93	46	0.049	0.1869	0.0012	0.499	0.006	12.87	0.18	0.151	96	2715	11
Young outlier													
C.17-1	116	66	0.034	0.1826	0.0009	0.518	0.008	13.03	0.21	0.146	101	2676	8
Discordant													
C.4-1	84	40	0.006	0.1873	0.0010	0.481	0.007	12.42	0.20	0.088	93	2719	8
C.5-1	178	87	0.059	0.1860	0.0006	0.469	0.007	12.02	0.17	0.130	92	2707	5
C.6-1	103	56	0.020	0.1857	0.0008	0.484	0.007	12.40	0.19	0.121	94	2704	7
C.9-1	137	55	0.371	0.1860	0.0009	0.475	0.007	12.18	0.20	0.142	93	2707	8
C.19-1	91	27	0.221	0.1863	0.0011	0.483	0.007	12.40	0.20	0.145	94	2710	9
C.22-1	27	19	0.270	0.1869	0.0021	0.395	0.006	10.18	0.20	0.056	79	2715	18
C.34-1	116	45	0.430	0.1849	0.0011	0.406	0.005	10.36	0.13	0.145	81	2698	9
C.37-1	63	21	0.207	0.1858	0.0012	0.446	0.006	11.42	0.16	0.149	88	2705	11

Data are at 1 $\sigma$  precision. All Pb data are common-Pb corrected (based on  $^{204}\text{Pb}$  and Broken Hill Pb composition). Analysis date: 02/07/2001; session Z3679j.

## 200096 9005: biotite monzogranite dyke, Marloo Well

<b>1:250,000 sheet:</b>	Edjudina (SH5106)
<b>1:100,000 sheet:</b>	Lake Carey (3339)
<b>MGA:</b>	409477mE                      6752705mN
<b>Location:</b>	The sample was taken from a small boulder, on the western edge of a large area of good outcrop, located about 4.5 km west-northeast of Marloo Well.
<b>Description:</b>	<p>This sample is from a grey, medium-grained biotite monzogranite dyke that intrudes the Pindinnis Granite (sample 200096 9006). The sampled dyke is ~5 m wide, striking east-west at a high angle to the foliation present within the host granite. The foliation is not as strongly expressed in the dyke as in the coarser-grained host.</p> <p>The unit has a granular to granoblastic, seriate to porphyritic texture, with 50–60% crystals of plagioclase, quartz, biotite and K-feldspar in a finer grained groundmass of similar mineralogy. Principal minerals are plagioclase (40–50%), quartz (25–30%), K-feldspar (10–20%), and biotite (5–6%). Plagioclase is often zoned, mostly with broad oscillatory zoning. Quartz is variably recrystallised to moderately undulose. Biotite occurs as ragged elongate grains and aggregates. Accessory minerals include zircon and apatite. Secondary minerals include moderate white mica and epidote and minor clinozoisite and carbonate.</p>
<b>Mount, pop:</b>	Z3679B

### Description of zircons

This sample contains mainly euhedral to subhedral, colourless and clear zircon fragments and whole crystals. Both equant (about 50 µm to 150 µm in diameter) and elongate (about 65 µm to 300 µm in length) grains are present, most of which preserve well-formed crystal faces, although slight rounding is noted for many grains. The grains have strong to moderate CL (Fig. 44). Concentric, euhedral zoning is present in many grains, with some containing structurally discontinuous core regions. A few grains display complex irregular zoning typical of resorption and/or recrystallisation.

### Concurrent standard data

The average floating point exponent (all QGNG data) is 2.32, the high value deriving largely from analyses with low  $UO^+/U^+$ . With three of these analyses (6-1, 6-2 and 7-2) removed, the value is 2.20. The sample data indicate values slightly higher than this (2.22 and 2.45); a value of 2.20 was used for data reduction. The three low  $UO^+/U^+$  analyses were omitted from the calibration, using a cutoff ratio of 6.2. No samples have  $UO^+/U^+$  lower than this cutoff. Two analyses (13-1 and 14-1) have anomalously low  $^{207}Pb/^{206}Pb$  (significant reverse discordance) and were also omitted from the calibration. The  $1\sigma$  scatter in the Pb/U calibration is 1.47% ( $n = 31$ , MSWD = 5.25). The weighted mean  $^{207}Pb/^{206}Pb$  age for the calibration set is  $1845.2 \pm 3.5$  Ma (MSWD = 1.20), but using a standardised set of criteria for assessment of the data (see “Data compilation for the QGNG standard”) gives a  $^{207}Pb/^{206}Pb$  age of  $1847.1 \pm 3.2$  Ma (MSWD = 1.00).

Element abundance calibration was based on CZ3 ( $n = 2$ ).

### Sample data

Thirty four analyses were performed on individual grains (Table 19). Three data points are discordant (19-1, 21-1, 32-1) and are not used in age assessment (Fig. 45). One analysis (24-1) has unusually high U and is a distinct young outlier; it is also omitted. Three others have significant common Pb ( $4f206 = 1\text{--}2\%$ ; analyses 6-1, 13-1, 17-1) but they are otherwise part of the main data group and they have been retained (their exclusion would increase the weighted mean age

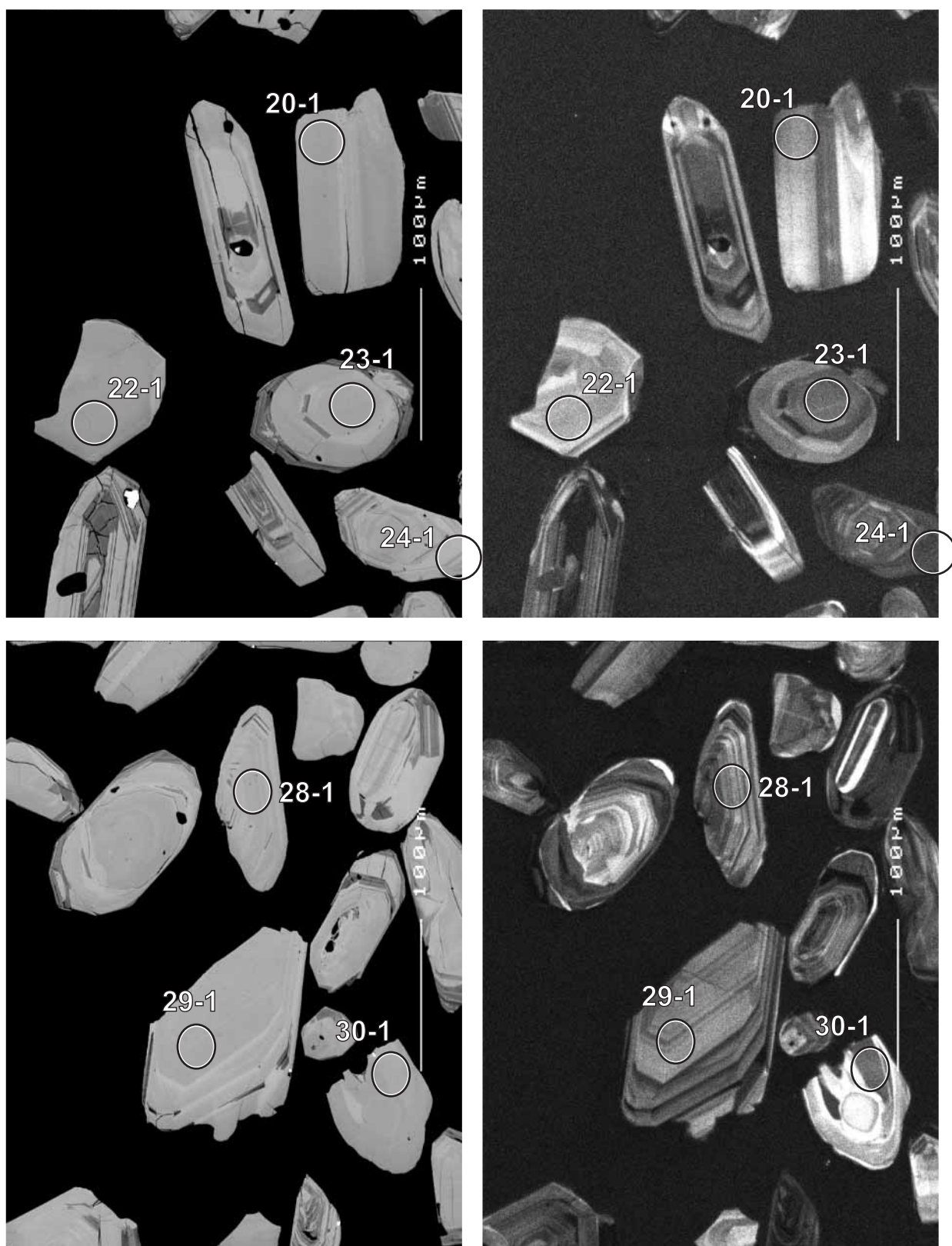


Figure 44. Representative SEM images (BSE on left, CL on right) for sample 200096 9005: biotite monzogranite dyke, Marloo Well. SHRIMP analysis spots are labelled. Scale bar is 100  $\mu\text{m}$ .

by 1 Ma).

These data are similar in every respect to those for the Pindinnis Granite, which this dyke cuts. As with the Pindinnis Granite, there is a small proportion of apparently older grains (8-1, 16-1, 22-1, 33-1; Fig. 46) that are visually indistinguishable from the main population. Omitting four of these leaves a group of 25 with weighted mean  $^{207}\text{Pb}/^{206}\text{Pb}$  age of  $2667 \pm 4$  Ma (MSWD = 0.90). Two analyses on possible cores did not produce older ages.

### Geochronological interpretation

There are two possible interpretations of these data. Either the zircons are inherited from the Pindinnis Granite (in which case they give no information on the age of the dyke) or the dyke was derived from the same magmatic source as the granite (in which case the dyke intruded very soon after granite crystallisation).

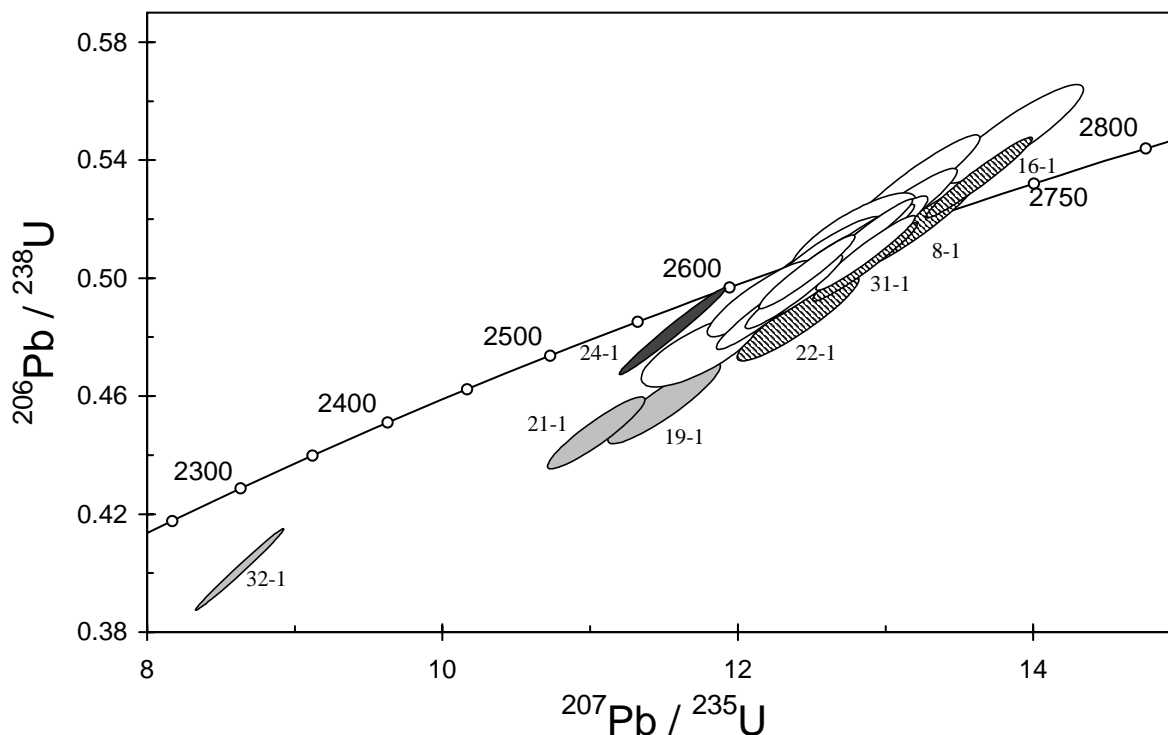


Figure 45. Concordia plot for zircon data from sample 200096 9005: biotite monzogranite dyke, Marloo Well. White filled symbols are used to define the age of the sample; older outliers (?inherited grains) have diagonal shading; discordant analyses are light grey; younger outlier is dark grey.

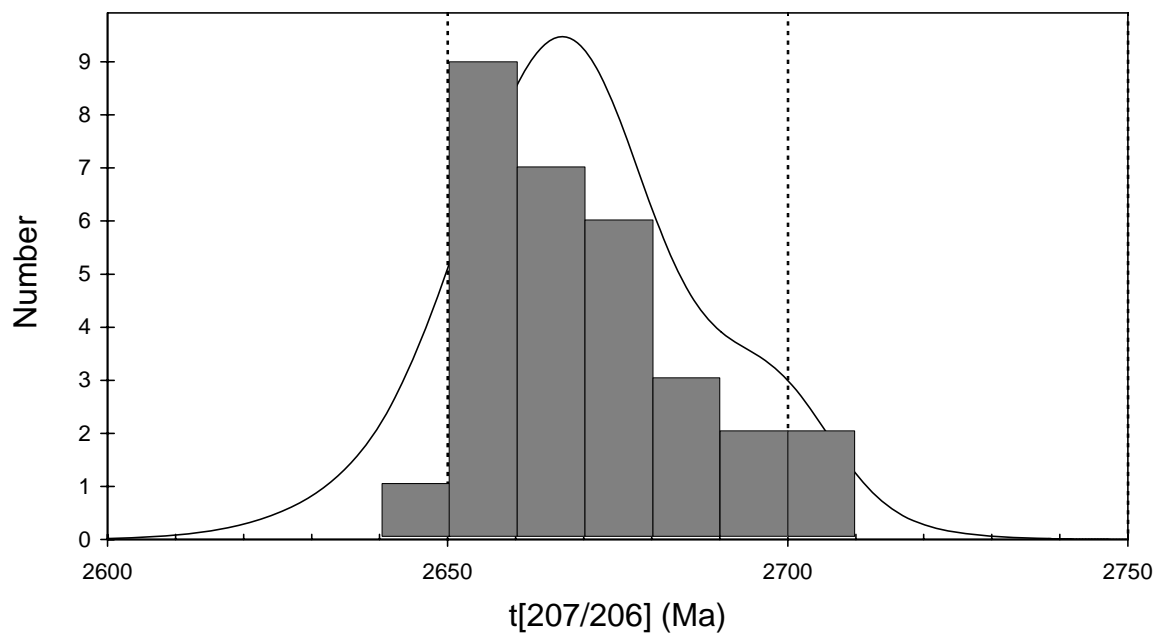


Figure 46. Gaussian-summation plot for zircon age data from sample 200096 9005: biotite monzogranite dyke, Marloo Well.



Table 19. SHRIMP analytical results for sample 200096 9005: biotite monzogranite dyke, Marloo Well.

grain-spot	U (ppm)	Th (ppm)	4f206 (%)	$\frac{^{207}\text{Pb}}{^{206}\text{Pb}}$		$\frac{^{206}\text{Pb}}{^{238}\text{U}}$		$\frac{^{207}\text{Pb}}{^{235}\text{U}}$		$\frac{^{208}\text{Pb}}{^{232}\text{Th}}$		conc. (%)	$\frac{^{207}\text{Pb}}{^{206}\text{Pb}}$ Age (Ma)	
				$\pm$	$\pm$	$\pm$	$\pm$	$\pm$	$\pm$	$\pm$				
Main group														
B.1-1	64	54	0.139	0.1819	0.0011	0.497	0.009	12.47	0.25	0.135	97	2670	10	
B.2-1	64	19	0.052	0.1805	0.0012	0.501	0.010	12.46	0.25	0.134	98	2658	11	
B.3-1	159	58	0.286	0.1802	0.0009	0.502	0.008	12.46	0.22	0.126	99	2654	8	
B.4-1	30	1	-0.029	0.1814	0.0017	0.509	0.012	12.73	0.32	0.222	99	2666	15	
B.5-1	61	8	0.153	0.1801	0.0018	0.502	0.012	12.47	0.33	0.109	99	2654	17	
B.6-1	76	14	1.695	0.1804	0.0018	0.507	0.009	12.60	0.26	0.137	99	2656	17	
B.7-1	88	42	0.050	0.1822	0.0009	0.511	0.009	12.83	0.24	0.141	100	2673	8	
B.9-1	97	18	0.063	0.1814	0.0008	0.513	0.009	12.84	0.23	0.133	100	2666	7	
B.10-1	92	32	0.416	0.1811	0.0011	0.488	0.008	12.18	0.22	0.138	96	2663	10	
B.11-1	60	25	-0.062	0.1813	0.0010	0.509	0.009	12.71	0.25	0.140	99	2664	9	
B.12-1	69	17	-0.046	0.1802	0.0023	0.515	0.009	12.78	0.28	0.146	101	2654	21	
B.13-1	87	46	1.136	0.1789	0.0016	0.492	0.009	12.14	0.24	0.134	98	2642	15	
B.14-1	103	34	0.294	0.1823	0.0013	0.514	0.009	12.92	0.24	0.115	100	2674	12	
B.15-1	110	22	-0.071	0.1822	0.0008	0.506	0.012	12.70	0.32	0.142	99	2673	7	
B.17-1	123	48	1.898	0.1794	0.0026	0.474	0.008	11.73	0.26	0.121	95	2648	24	
B.18-1	130	13	0.009	0.1836	0.0009	0.508	0.008	12.86	0.22	0.136	99	2686	8	
B.20-1	63	47	-0.073	0.1831	0.0012	0.494	0.010	12.48	0.25	0.138	97	2681	11	
B.23-1	87	19	0.103	0.1806	0.0010	0.510	0.012	12.70	0.31	0.135	100	2659	9	
B.25-1	83	38	0.210	0.1805	0.0010	0.500	0.009	12.45	0.24	0.136	98	2658	10	
B.26-1	50	29	0.130	0.1834	0.0018	0.549	0.011	13.88	0.31	0.140	105	2684	16	
B.27-1	97	54	0.024	0.1824	0.0009	0.499	0.009	12.56	0.23	0.140	98	2675	8	
B.28-1	55	28	0.181	0.1803	0.0015	0.518	0.014	12.87	0.35	0.133	101	2656	13	
B.29-1	46	8	0.182	0.1800	0.0014	0.532	0.011	13.21	0.29	0.139	104	2653	13	
B.30-1	54	49	0.064	0.1819	0.0013	0.521	0.010	13.07	0.28	0.142	101	2670	12	
B.31-1	133	61	0.552	0.1815	0.0010	0.495	0.008	12.38	0.22	0.138	97	2666	9	
B.34-1	55	19	0.072	0.1816	0.0013	0.499	0.010	12.50	0.26	0.132	98	2667	12	
Possible old outliers														
B.8-1	86	40	0.074	0.1853	0.0010	0.518	0.009	13.22	0.25	0.142	100	2701	9	
B.16-1	106	37	-0.038	0.1852	0.0008	0.534	0.009	13.64	0.24	0.148	102	2700	7	
B.22-1	47	13	0.289	0.1852	0.0017	0.486	0.010	12.40	0.28	0.135	95	2700	15	
B.33-1	104	84	0.011	0.1847	0.0009	0.505	0.009	12.86	0.24	0.139	98	2695	8	
Discordant														
B.19-1	50	37	0.363	0.1825	0.0017	0.456	0.009	11.49	0.25	0.139	91	2676	16	
B.21-1	75	25	0.698	0.1792	0.0014	0.446	0.008	11.02	0.22	0.145	90	2645	13	
B.32-1	799	226	0.102	0.1560	0.0005	0.399	0.009	8.59	0.20	0.117	90	2413	5	
Young outlier														
B.24-1	639	92	0.087	0.1740	0.0006	0.481	0.010	11.55	0.24	0.129	98	2597	6	

Data are at 1σ precision. All Pb data are common-Pb corrected (based on  $^{204}\text{Pb}$  and Broken Hill Pb composition). Analysis date: 05/06/2001; session Z3679i.

## 200096 9006: Pindinnis Granite

- 1:250,000 sheet:** Edjudina (SH5106)
- 1:100,000 sheet:** Lake Carey (3339)
- MGA:** 409672mE 6752610mN
- Location:** The sample was taken from a small pavement, 150 m southeast of sample 200096 9005, in an area of good outcrop, located about 4.5 km north-northeast of Marloo Well.
- Description:** This sample is from a foliated grey-white, medium-fine to medium-coarse grained, seriate-textured, allanite-biotite granodiorite of the Pindinnis Granite. The outcrop has a strong south-dipping sub-horizontal mineral stretching lineation and a mild to moderate steep north-south foliation, defined by elongate quartz and aligned biotite. The Pindinnis Granite has been intruded by thin (<5 m) dykes of equigranular biotite monzogranite (e.g., sample 200096 9005).
- The unit is characterised by a granoblastic texture. Principal minerals are plagioclase (50–55%), quartz (25–30%), K-feldspar (10–20%), and biotite (6–8%). Plagioclase is commonly zoned (both fine oscillatory and irregular zoning). Quartz is variably recrystallised with very common sub-grain development. Original quartz grains were elongate and strongly aligned. K-feldspar is largely interstitial. Biotite occurs as aligned anhedral to irregular grains and aggregates. Relatively common (to 1%) allanite, up to ~2 mm, is also present. Other accessory minerals include minor subhedral titanite, zircon, apatite and Fe-oxides. Secondary phases include moderate white mica and epidote and minor chlorite and rutile.
- Mount, pop:** Z3679A

### Description of zircons

A variety of zircon fragments and whole crystals was recovered from this sample, ranging from equant sub-rounded grains, about 50 µm to 100 µm in diameter, to euhedral and subhedral elongate grains (aspect ratio 2:1 to 5:1, length from 80 µm to 160 µm), as well as a few larger grains (up to 300 µm). Many of the elongate grains display well-formed crystal faces and sharp prismatic terminations, but some are slightly rounded. The grains are colourless to pale brown and clear, although small, mainly ovoid inclusions are present in some grains. Zoning and core/rim relationships are visible in both transmitted and reflected light photographs and in the CL images (Fig. 47). Many grains display systematic concentric zoning, sometimes with structurally discontinuous core regions.

### Concurrent standard data

The average floating point exponent (all QGNG data) is 2.32, the high value deriving largely from analyses with low  $UO^+/U^+$ . With three of these analyses (6-1, 6-2 and 7-2) removed, the value is 2.20. The sample data indicate values slightly higher than this (2.22 and 2.45); a value of 2.20 was used for data reduction. The three low  $UO^+/U^+$  analyses were omitted from the calibration, using a cutoff ratio of 6.2. No samples have  $UO^+/U^+$  lower than this cutoff. Two analyses (13-1 and 14-1) have anomalously low  $^{207}Pb/^{206}Pb$  (significant reverse discordance) and were also omitted from the calibration. The  $1\sigma$  scatter in the Pb/U calibration is 1.47% ( $n = 31$ ,  $MSWD = 5.25$ ). The weighted mean  $^{207}Pb/^{206}Pb$  age for the calibration set is  $1845.2 \pm 3.5$  Ma ( $MSWD = 1.20$ ), but using a standardised set of criteria for assessment of the data (see “Data compilation for the QGNG standard”) gives a  $^{207}Pb/^{206}Pb$  age of  $1847.1 \pm 3.2$  Ma ( $MSWD = 1.00$ ).

Element abundance calibration was based on CZ3 ( $n = 2$ ).

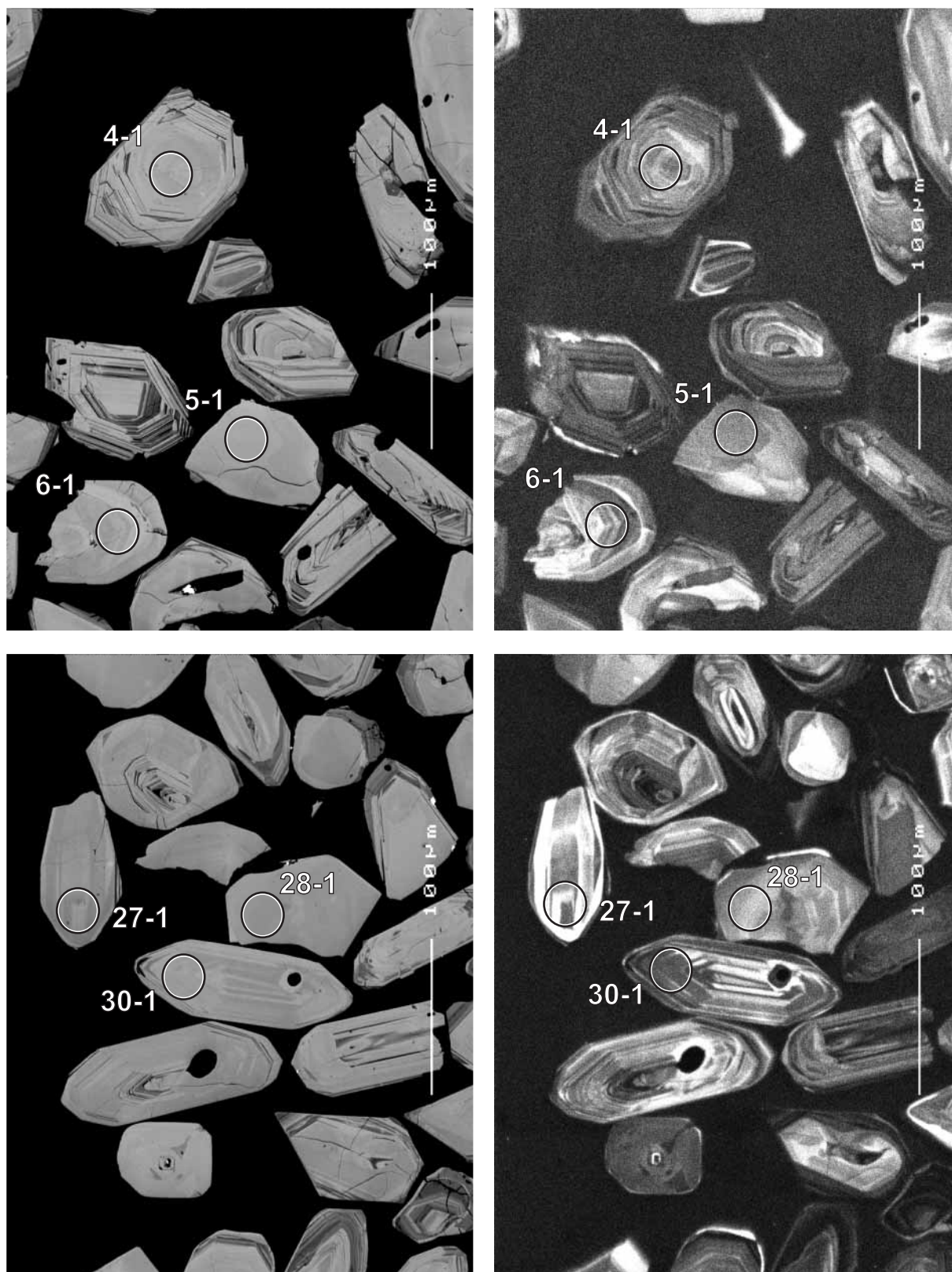


Figure 47. Representative SEM images (BSE on left, CL on right) for sample 200096 9006: Pindinnis Granite. SHRIMP analysis spots are labelled. Scale bar is 100  $\mu\text{m}$ .

## Sample data

Thirty three grains were individually analysed and the results are presented in Table 20. Six analyses are discordant (6-1, 16-1, 22-1, 25-1, 29-1, 32-1) and have not been used in the age determination (Fig. 48). One of these (32-1) is highly anomalous and might be a contaminant, though no potential source samples can be identified in mineral processing records. The grain is not anomalous in appearance and the spot was placed in an area of seemingly well-preserved magmatic zoning. The remaining data form a coherent cluster, but with considerable excess scatter in  $^{207}\text{Pb}/^{206}\text{Pb}$  (MSWD = 4.9). The  $^{207}\text{Pb}/^{206}\text{Pb}$  dates include an outlying group of 5 higher values (1-1, 2-1, 4-1, 7-1, 8-1; Fig. 49), which is difficult to explain except as a residual older real age; either a preserved inherited component slightly older than the main group, or inherited grains that were almost entirely reset during the main thermal event. The possibility that the younger portion of the distribution is due to early Pb loss, with the older grains preserving the 'true' age, is considered less likely, partly because of the internal consistency of this main group. Three of the older spots (2-1, 4-1 and 7-1) are on central parts of grains, which were generally avoided later in the session, and 4-1 could be a discrete core. However, several other spots in the centres of grains, some of which are distinctive in CL (e.g. 14-1, 15-1 and 16-1) gave dates within the main group.

Omitting the six discordant data and five old outliers leaves a group of 22 with weighted mean  $^{207}\text{Pb}/^{206}\text{Pb}$  age of  $2664.0 \pm 5.0$  Ma (MSWD = 1.16).

The data distribution is very similar to that for the crosscutting vein 200096 9005.

## Geochronological interpretation

The age of  $2664 \pm 5$  Ma is considered to be the age of granite formation. If the data for the crosscutting dyke 200096 9005 record the intrusive age of the dyke, deformation of the granite followed almost immediately (within a couple of million years) after crystallisation.

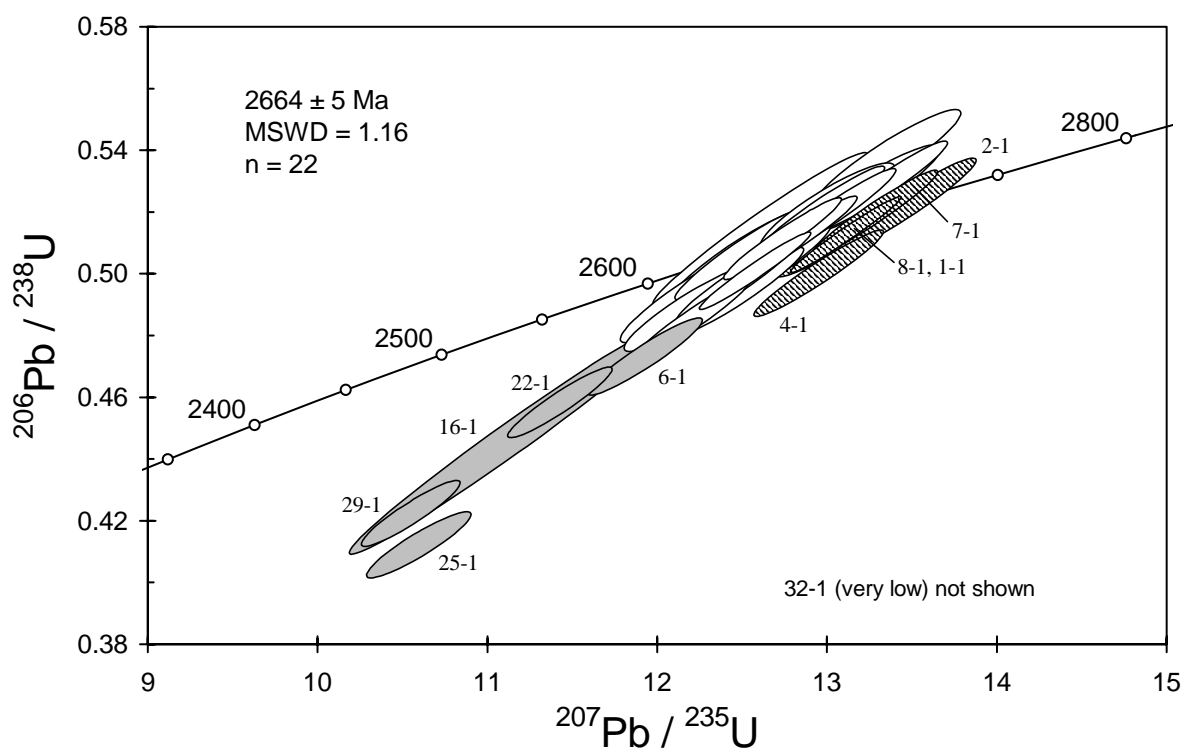


Figure 48. Concordia plot for zircon data from sample 200096 9006: Pindinnis Granite. White filled symbols are used to define the age of the sample; older outliers (?inherited grains) have diagonal shading; discordant analyses are light grey.

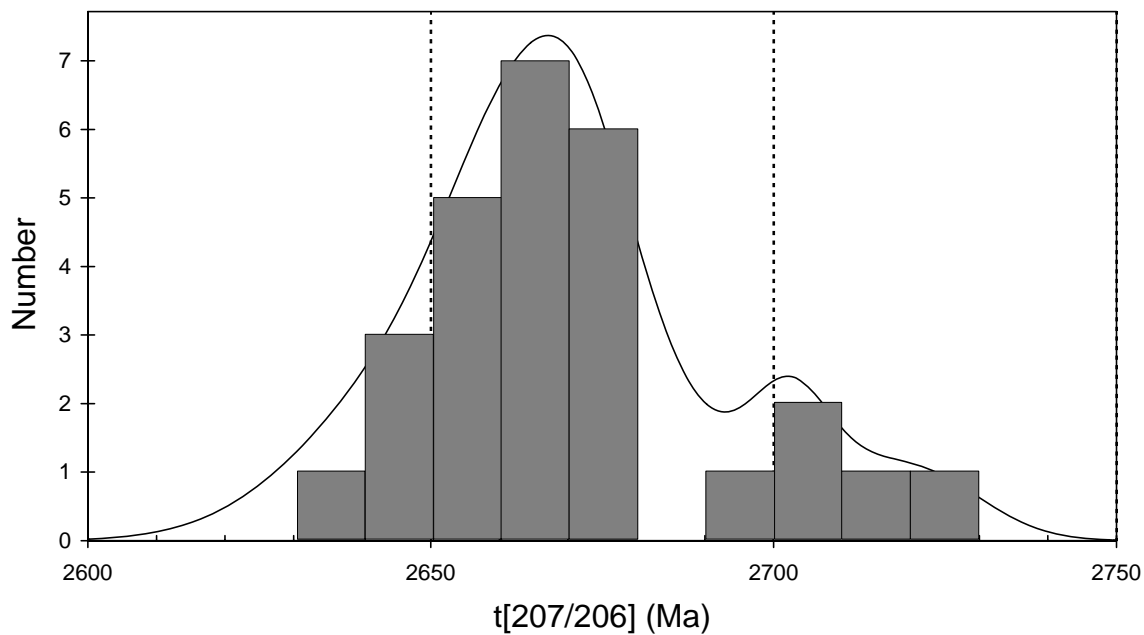


Figure 49. Gaussian-summation plot for sample 200096 9006: Pindinnis Granite.



Table 20. SHRIMP analytical results for zircon from sample 200096 9006: Pindinnis Granite.

grain-spot	U (ppm)	Th (ppm)	4f206 (%)	$\frac{^{207}\text{Pb}}{^{206}\text{Pb}}$		$\frac{^{206}\text{Pb}}{^{238}\text{U}}$		$\frac{^{207}\text{Pb}}{^{235}\text{U}}$		$\frac{^{208}\text{Pb}}{^{232}\text{Th}}$	conc. (%)	$\frac{^{207}\text{Pb}}{^{206}\text{Pb}}$ Age (Ma)	
				$\pm$		$\pm$		$\pm$				$\pm$	
Main group													
A.3-1	140	102	-0.009	0.1821	0.0007	0.501	0.008	12.57	0.22	0.137	98	2672	7
A.5-1	91	62	0.052	0.1813	0.0010	0.509	0.009	12.72	0.24	0.142	99	2665	9
A.9-1	63	41	-0.014	0.1807	0.0016	0.522	0.009	13.00	0.26	0.148	102	2659	15
A.10-1	47	27	0.191	0.1789	0.0012	0.506	0.010	12.49	0.26	0.137	100	2643	11
A.11-1	74	19	0.091	0.1824	0.0010	0.485	0.009	12.20	0.23	0.122	95	2675	9
A.12-1	39	12	0.071	0.1778	0.0014	0.514	0.017	12.61	0.42	0.135	102	2632	13
A.13-1	70	44	0.011	0.1805	0.0010	0.521	0.010	12.96	0.25	0.144	102	2658	9
A.14-1	49	13	0.002	0.1809	0.0012	0.506	0.011	12.63	0.30	0.137	99	2661	11
A.15-1	74	43	0.238	0.1818	0.0011	0.497	0.009	12.46	0.24	0.142	97	2669	10
A.17-1	95	52	0.031	0.1806	0.0009	0.511	0.009	12.73	0.23	0.140	100	2659	8
A.18-1	65	23	0.163	0.1808	0.0014	0.488	0.009	12.18	0.25	0.120	96	2660	13
A.19-1	99	63	0.087	0.1817	0.0010	0.512	0.009	12.82	0.24	0.138	100	2669	9
A.20-1	85	2	0.092	0.1823	0.0015	0.528	0.009	13.27	0.26	0.118	102	2674	14
A.21-1	85	62	0.032	0.1822	0.0015	0.503	0.009	12.63	0.26	0.137	98	2673	14
A.23-1	47	21	-0.039	0.1810	0.0016	0.510	0.010	12.72	0.28	0.141	100	2662	14
A.24-1	58	35	0.136	0.1802	0.0015	0.538	0.011	13.36	0.29	0.142	104	2655	13
A.26-1	48	27	0.139	0.1790	0.0014	0.505	0.010	12.47	0.27	0.136	100	2643	13
A.27-1	48	49	0.098	0.1805	0.0013	0.536	0.011	13.33	0.29	0.149	104	2657	12
A.28-1	47	27	0.243	0.1794	0.0015	0.493	0.010	12.19	0.27	0.131	98	2647	14
A.30-1	96	99	0.132	0.1828	0.0010	0.529	0.009	13.34	0.25	0.146	102	2679	9
A.31-1	49	28	-0.145	0.1827	0.0013	0.506	0.010	12.74	0.28	0.141	99	2678	12
A.33-1	88	57	0.037	0.1817	0.0010	0.520	0.009	13.03	0.25	0.144	101	2669	9
Old outliers													
A.1-1	200	18	0.001	0.1855	0.0006	0.513	0.008	13.11	0.21	0.149	99	2703	5
A.2-1	64	38	0.005	0.1870	0.0011	0.523	0.010	13.47	0.27	0.143	100	2716	10
A.4-1	82	54	-0.055	0.1878	0.0010	0.500	0.009	12.95	0.25	0.139	96	2723	9
A.7-1	93	32	-0.011	0.1853	0.0009	0.520	0.009	13.28	0.25	0.139	100	2701	8
A.8-1	44	23	-0.142	0.1849	0.0013	0.515	0.011	13.13	0.29	0.145	99	2697	12
Discordant													
A.6-1	95	96	0.435	0.1829	0.0011	0.473	0.008	11.92	0.22	0.047	93	2680	10
A.16-1	57	21	0.152	0.1810	0.0017	0.446	0.025	11.13	0.63	0.116	89	2662	16
A.22-1	135	31	0.664	0.1809	0.0011	0.458	0.008	11.42	0.20	0.153	91	2661	10
A.25-1	90	56	0.832	0.1868	0.0014	0.411	0.007	10.59	0.20	0.142	82	2714	13
A.29-1	144	68	0.728	0.1814	0.0012	0.421	0.007	10.54	0.19	0.144	85	2665	11
A.32-1	505	331	0.112	0.0506	0.0010	0.039	0.001	0.27	0.01	0.012	111	221	47

Data are at 1 $\sigma$  precision. All Pb data are common-Pb corrected (based on  $^{204}\text{Pb}$  and Broken Hill Pb composition). Analysis date: 05/06/2001; session Z3679i.

## 200096 9007: Ellington Granite

<b>1:250,000 sheet:</b>	Kurnalpi (SH5110)
<b>1:100,000 sheet:</b>	Kanowna (3236)
<b>MGA:</b>	364143mE                      6579319mN
<b>Location:</b>	The sample, supplied by Roger Bateman (Kalgoorlie Consolidated Gold Mines), was taken from Kalgoorlie Consolidated Gold Mines diamond drillhole SHD13, depth interval 188–205m. The collar site is located approximately 4 km southeast of Hannan South mine, and 3 km east of Presleys Tank.
<b>Description:</b>	This sample is from a fine- to medium-grained, holocrystalline to feldspar-phyric hornblende-bearing quartz diorite from the Ellington Granite. The Ellington Granite is an intrusive body that intruded into the lower portions of the Black Flag Beds. The body is elongate north-south and oblique to stratigraphic contacts, and adjacent to an important north-south shear zone along its western margin. The core of the body is trondhjemitic, with a discontinuous dioritic rim.
<b>Mount, pop:</b>	Z3730C

### Description of zircons

Virtually all zircon grains recovered from this sample are anhedral, equant, sub-angular fragments. The zircon is colourless and clear and contains some small inclusions. Grain size is relatively uniform from about 50  $\mu\text{m}$  to 90  $\mu\text{m}$ . Most grains have systematic and regular zoning patterns (Fig. 50).

### Concurrent standard data

This analytical session was interrupted by a cooling water failure, and towards the end of the session the primary beam became increasingly unstable. Data continuity across the interruption is good, but there is unacceptable scatter in  $^{206}\text{Pb}/^{238}\text{U}$  data for QGNG in the last seven hours. This last portion of the data set was deleted, resulting in the loss of six QGNG analyses and eight of this sample (although the data for these sample grains was compatible with the main body of data that was retained). One analysis of QGNG that was inadvertently limited to five scans was also deleted. The remaining 23 QGNG analyses have a  $1\sigma$  scatter in  $^{206}\text{Pb}/^{238}\text{U}$  of 1.09% and a  $^{207}\text{Pb}/^{206}\text{Pb}$  age of  $1849.0 \pm 3.0$  Ma (MSWD = 0.71). Re-assessment of the data using a standardised set of criteria for assessment of the data (see “Data compilation for the QGNG standard”) does not change these results.

Element abundance calibration was based on CZ3 (n = 4).

### Sample data

Twenty eight analyses on individual grains are presented (Table 21, Fig. 51). Only one analysis is >5% discordant (26-1); it is omitted from age considerations. The remaining 27 have a weighted mean  $^{207}\text{Pb}/^{206}\text{Pb}$  age of  $2662 \pm 3$  Ma. There is appreciable scatter in the data (MSWD = 1.5) but there are no clear grounds for excluding any particular data.

### Geochronological interpretation

The  $^{207}\text{Pb}/^{206}\text{Pb}$  age of  $2662 \pm 3$  Ma is considered to be the intrusive age of the granite.

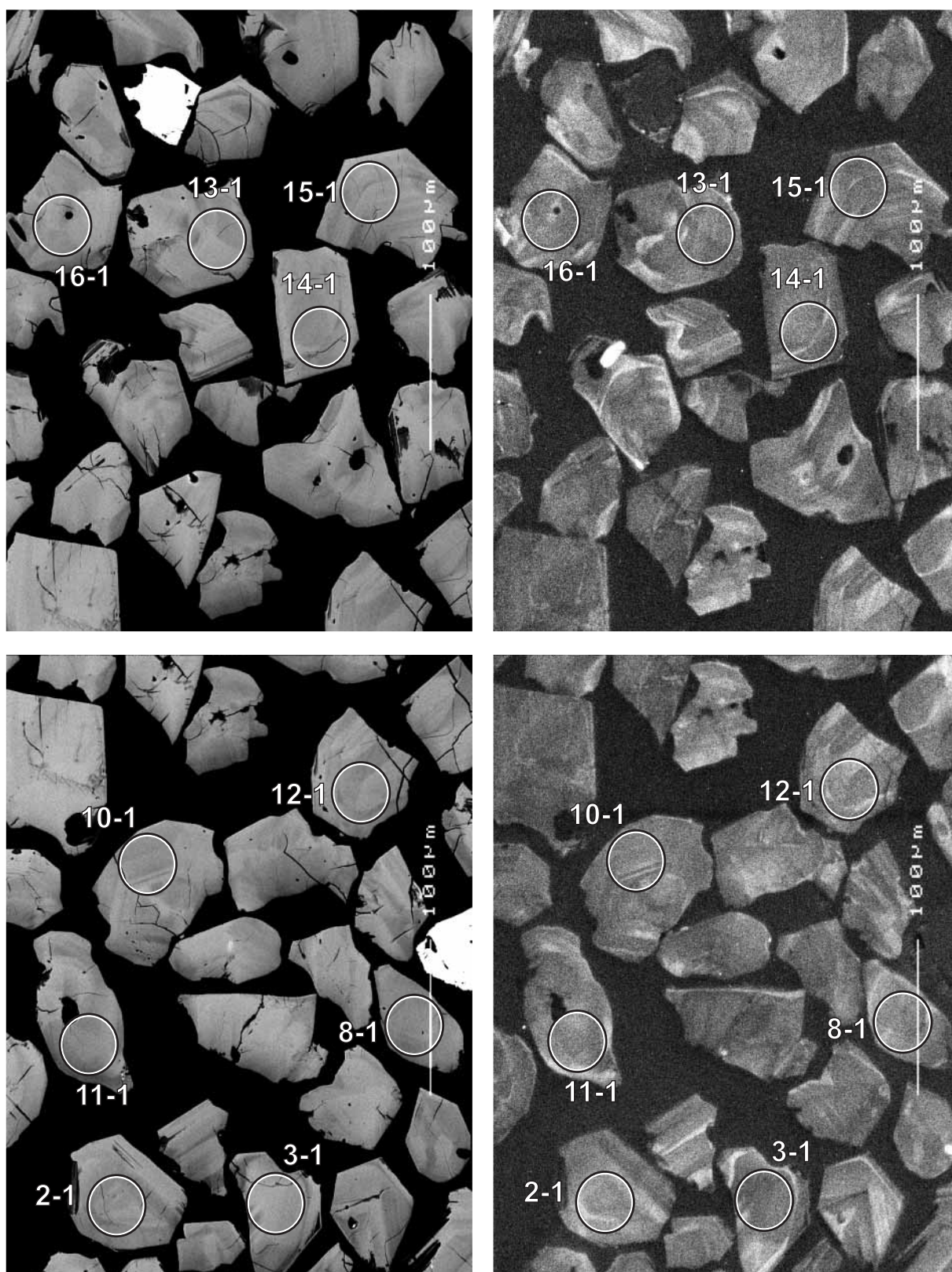


Figure 50. Representative SEM images (BSE on left, CL on right) for sample 200096 9007: Ellington Granite. SHRIMP analysis spots are labelled. Scale bar is 100  $\mu\text{m}$ .

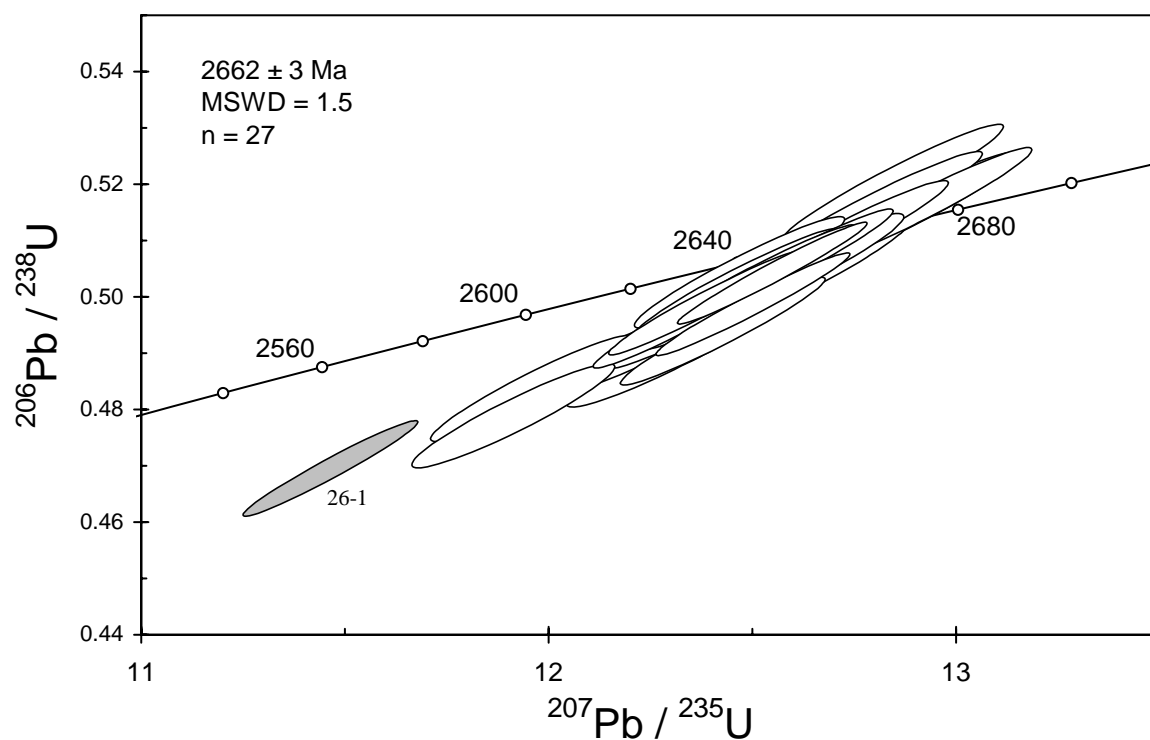


Figure 51. Concordia plot for zircon data from sample 200096 9007: Ellington Granite. White filled symbols are used to define the age of the sample; discordant analysis is light grey.

Table 21. SHRIMP analytical results for sample 200096 9007: Ellington Granite.

grain-spot	U (ppm)	Th (ppm)	4f206 (%)	<sup>207</sup> Pb/ <sup>206</sup> Pb		<sup>206</sup> Pb/ <sup>238</sup> U		<sup>207</sup> Pb/ <sup>235</sup> U		<sup>208</sup> Pb/ <sup>232</sup> Th	conc. (%)	<sup>207</sup> Pb/ <sup>206</sup> Pb Age (Ma)	
					±		±		±				±
Main group													
C.1-1	184	327	0.149	0.1808	0.0009	0.478	0.006	11.92	0.16	0.121	95	2660	8
C.2-1	132	151	0.027	0.1804	0.0008	0.486	0.007	12.08	0.17	0.126	96	2657	7
C.3-1	217	182	0.014	0.1805	0.0006	0.503	0.006	12.51	0.16	0.136	99	2658	5
C.4-1	133	152	0.019	0.1815	0.0008	0.515	0.007	12.88	0.19	0.140	100	2667	7
C.5-1	151	172	0.044	0.1820	0.0007	0.503	0.007	12.62	0.18	0.140	98	2671	7
C.6-1	167	187	0.054	0.1802	0.0007	0.502	0.007	12.47	0.17	0.139	99	2654	6
C.7-1	162	231	0.039	0.1812	0.0007	0.497	0.007	12.40	0.17	0.137	98	2664	6
C.8-1	153	197	0.032	0.1810	0.0007	0.503	0.007	12.54	0.18	0.138	99	2662	7
C.9-1	294	468	0.004	0.1821	0.0005	0.498	0.006	12.51	0.16	0.135	98	2672	5
C.10-1	159	158	-0.036	0.1809	0.0007	0.510	0.007	12.72	0.18	0.140	100	2661	6
C.11-1	152	168	0.055	0.1793	0.0007	0.520	0.007	12.85	0.18	0.142	102	2646	7
C.12-1	147	190	0.020	0.1807	0.0008	0.501	0.007	12.49	0.18	0.135	98	2660	7
C.13-1	230	359	0.052	0.1803	0.0006	0.498	0.006	12.39	0.16	0.137	98	2656	5
C.14-1	169	210	0.038	0.1802	0.0007	0.515	0.007	12.80	0.18	0.136	101	2655	6
C.15-1	176	207	0.009	0.1817	0.0007	0.516	0.007	12.93	0.17	0.141	101	2668	6
C.16-1	164	245	0.074	0.1796	0.0007	0.504	0.007	12.47	0.17	0.130	99	2649	7
C.17-1	94	100	0.069	0.1814	0.0009	0.492	0.007	12.31	0.19	0.135	97	2665	9
C.18-1	130	143	0.068	0.1813	0.0008	0.511	0.007	12.77	0.18	0.140	100	2664	7
C.19-1	352	527	0.002	0.1808	0.0005	0.504	0.006	12.55	0.15	0.138	99	2660	4
C.20-1	232	302	0.303	0.1813	0.0008	0.505	0.006	12.62	0.17	0.134	99	2665	8
C.21-1	244	340	0.044	0.1824	0.0008	0.490	0.007	12.31	0.17	0.137	96	2675	8
C.22-1	166	247	-0.049	0.1811	0.0007	0.500	0.007	12.48	0.17	0.139	98	2663	6
C.23-1	150	206	-0.011	0.1812	0.0007	0.493	0.007	12.31	0.17	0.137	97	2664	7
C.24-1	170	326	0.249	0.1797	0.0008	0.483	0.006	11.96	0.16	0.105	96	2650	7
C.25-1	186	314	-0.019	0.1828	0.0006	0.493	0.006	12.43	0.17	0.137	97	2678	6
C.27-1	196	283	-0.008	0.1808	0.0006	0.505	0.006	12.60	0.17	0.138	99	2660	6
C.28-1	224	213	0.049	0.1807	0.0006	0.496	0.006	12.36	0.16	0.136	98	2659	5
Discordant													
C.26-1	339	486	0.097	0.1775	0.0005	0.469	0.006	11.47	0.14	0.128	94	2630	5

Data are at 1 $\sigma$  precision. All Pb data are common-Pb corrected (based on  $^{204}\text{Pb}$  and Broken Hill Pb composition).  
Analysis date: 22/06/2001; session Z3730j.



## 200196 9007A: Monument Monzogranite

<b>1:250,000 sheet:</b>	Laverton (SH5102)
<b>1:100,000 sheet:</b>	Minerie (3240)
<b>MGA:</b>	377272mE                      6824735mN
<b>Location:</b>	The sample was taken from a pavement located ~150 m northeast of a track and ~2.5 km north of Minara Well.
<b>Description:</b>	This sample is from a white medium-grained, sparsely to moderately (hornblende-) quartz-K-feldspar porphyritic titanite-hornblende-biotite monzogranite of the Monument Monzogranite. The monzogranite contains a mild to moderate foliation defined by elongate quartz grains and alignment of biotite. The monzogranite contains sparsely distributed small amphibolite (?greenstone) enclaves to 10 cm and titanite-biotite-hornblende granodiorite to quartz diorite ovoid to irregular and elongate enclaves to 2 m. On regional aeromagnetic images the Monument Monzogranite is characterised by magnetic zonation from a strongly magnetised rim to less magnetised core.
<b>Mount, pop:</b>	Z3734C

### Description of zircons

This sample contains predominantly large zircon grains, ranging in size from 100  $\mu\text{m}$  to 280  $\mu\text{m}$ , with aspect ratios of 2:1 to 3:1, although a few smaller, more equant grains are present. Almost all grains are euhedral to subhedral whole crystals with few inclusions. A minor proportion are fragments. The grains are pale grey and translucent. They display very clear euhedral and concentric zoning in both the photographs and the CL images, with most showing continuous core to rim growth (Fig. 52). However, a few grains have structurally discontinuous cores, overgrown by euhedral rims. A few grains have very bright CL (e.g., grains 13, 33).

### Concurrent standard data

One QGNG analysis has anomalously low  $^{206}\text{Pb}/^{238}\text{U}$  and  $^{207}\text{Pb}/^{206}\text{Pb}$ , and is not considered as part of the calibration dataset. The average floating point exponent for the remaining 18 analyses is 2.24. The concurrent sample data also indicate a calibration slope higher than 2.0; a value of 2.20 was used for data reduction. The  $1\sigma$  scatter in the Pb/U calibration is 0.62% (MSWD = 9.3). There is a rather large scatter in  $^{207}\text{Pb}/^{206}\text{Pb}$  for these data (MSWD = 1.8). Omitting one  $3\sigma$  young outlier gives a weighted mean  $^{207}\text{Pb}/^{206}\text{Pb}$  age of  $1848.7 \pm 3.7$  Ma, with MSWD = 1.3. A further deletion of one  $2\sigma$  outlier gives  $1850.2 \pm 2.7$  (MSWD = 0.78). Using a standardised set of criteria for assessment of the data (see "Data compilation for the QGNG standard") gives a  $^{207}\text{Pb}/^{206}\text{Pb}$  age of  $1849.1 \pm 3.8$  Ma (MSWD = 1.30; but also see footnote on Table 3).

Element abundance calibration was based on CZ3 (n = 2).

### Sample data

Thirty one analyses were obtained from 31 grains (Table 22). One analysis is >5% discordant (6-1) and is not considered in age determinations. The remaining data mostly fall in a single cluster (Fig. 53), but there is a distinct group of three at ~2700 Ma (4-1, 13-1, 26-1). These data are all from low-U, CL-bright grains. These three grains are considered to be xenocrysts, possibly from a metamorphosed source. Additional data from two other low-U, CL-bright grains (23-1, 33-1) fall in the main data cluster, and may have been reset, however they are excluded from the main group for age calculation. With the additional exclusion of one  $4\sigma$  young outlier (37-1), the main data group gives a weighted mean  $^{207}\text{Pb}/^{206}\text{Pb}$  age of  $2659.1 \pm 1.9$  Ma (MSWD = 1.11, n = 24). There are no core/rim distinctions apparent in the ages.

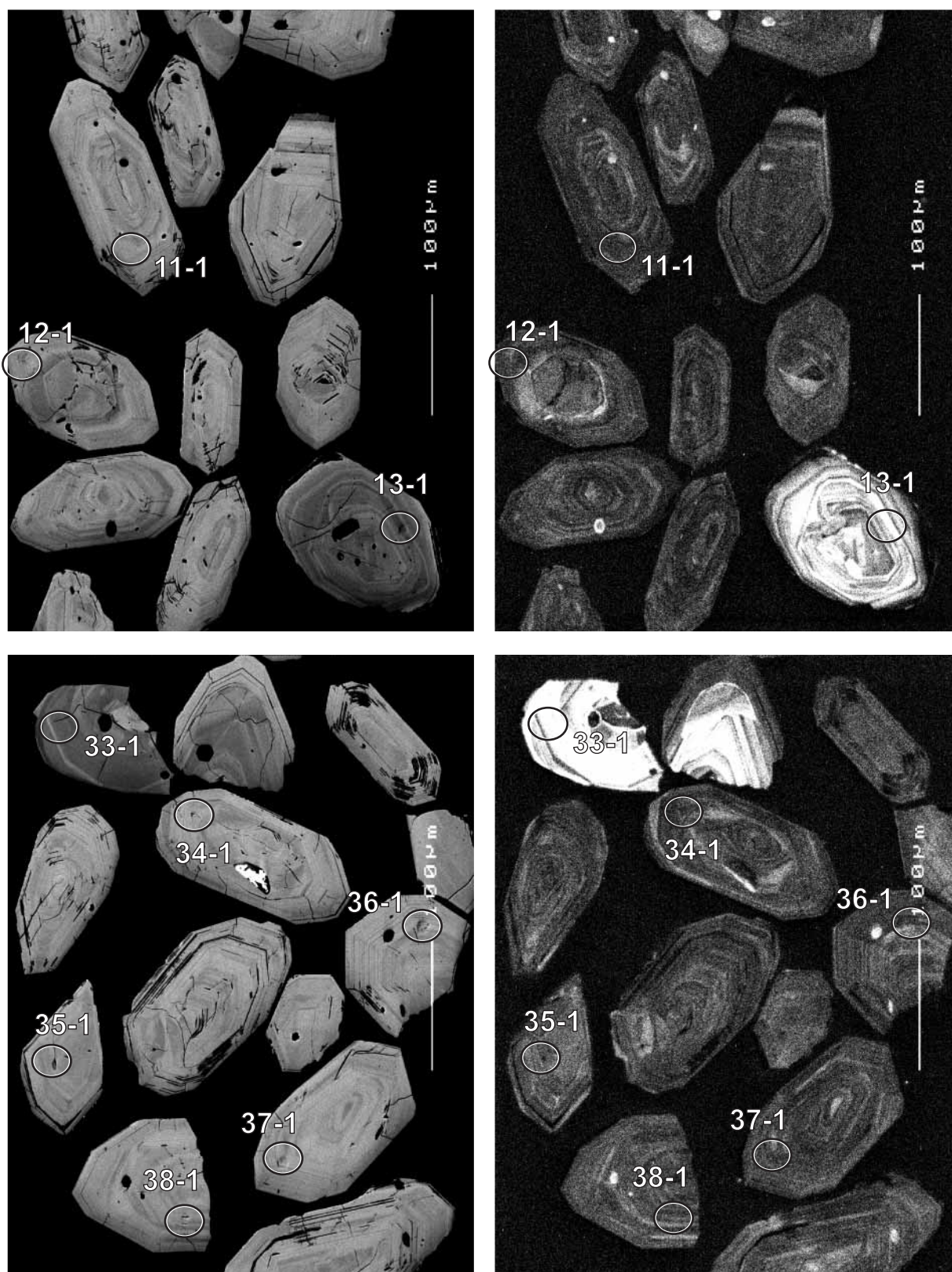


Figure 52. Representative SEM images (BSE on left, CL on right) for sample 200196 9007A: Monument Monzogranite. SHRIMP analysis spots are labelled. Scale bar is 100  $\mu\text{m}$ .

## Geochronological interpretation

The age of  $2659 \pm 2$  Ma is interpreted to be the age of the granite.

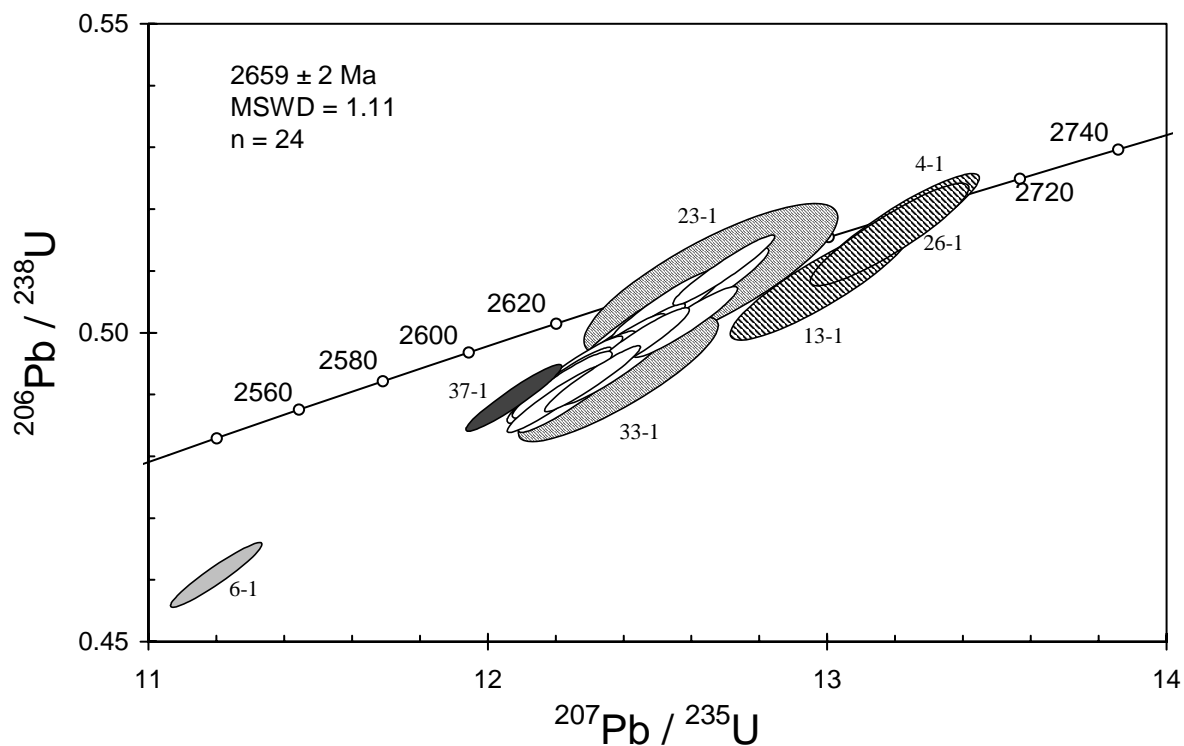


Figure 53. Concordia plot for zircon data from sample 200196 9007A: Monument Monzogranite. White filled symbols are used to define the age of the sample; discordant analysis is light grey, inherited and possibly inherited analyses have diagonal shading; younger outlier is dark grey.

Table 22. SHRIMP analytical results for sample 200196 9007A: Monument Monzogranite.

grain-spot	U (ppm)	Th (ppm)	4f206 (%)	<sup>207</sup> Pb/ <sup>206</sup> Pb		<sup>206</sup> Pb/ <sup>238</sup> U		<sup>207</sup> Pb/ <sup>235</sup> U		<sup>208</sup> Pb/ <sup>232</sup> Th	conc. (%)	<sup>207</sup> Pb/ <sup>206</sup> Pb	
				±		±		±		Age (Ma)		±	
Main group													
C.1-1	302	180	0.053	0.1812	0.0004	0.492	0.004	12.30	0.09	0.137	97	2664	4
C.2-1	183	95	0.139	0.1809	0.0006	0.508	0.004	12.66	0.11	0.140	99	2662	5
C.5-1	269	157	0.008	0.1805	0.0004	0.510	0.004	12.69	0.10	0.141	100	2657	4
C.8-1	197	93	0.147	0.1800	0.0005	0.501	0.005	12.45	0.12	0.133	99	2653	5
C.9-1	236	119	0.043	0.1819	0.0005	0.502	0.004	12.58	0.10	0.145	98	2670	5
C.10-1	209	82	0.052	0.1805	0.0005	0.497	0.004	12.37	0.10	0.134	98	2657	5
C.12-1	208	151	0.249	0.1801	0.0005	0.494	0.004	12.27	0.10	0.136	98	2654	5
C.14-1	202	119	0.106	0.1816	0.0005	0.494	0.004	12.36	0.10	0.139	97	2667	5
C.15-1	249	130	0.065	0.1799	0.0005	0.494	0.004	12.24	0.10	0.135	98	2652	4
C.16-1	115	97	0.038	0.1805	0.0007	0.497	0.004	12.38	0.12	0.137	98	2658	6
C.19-1	173	58	0.202	0.1811	0.0006	0.493	0.004	12.32	0.11	0.140	97	2663	6
C.20-1	203	95	0.117	0.1804	0.0005	0.492	0.004	12.24	0.10	0.134	97	2657	5
C.21-1	220	114	0.011	0.1804	0.0006	0.491	0.004	12.20	0.10	0.135	97	2656	5
C.22-1	159	70	0.111	0.1810	0.0008	0.498	0.004	12.41	0.12	0.139	98	2662	7
C.24-1	290	137	0.157	0.1803	0.0006	0.491	0.004	12.21	0.10	0.131	97	2655	5
C.25-1	134	27	0.139	0.1813	0.0006	0.500	0.004	12.50	0.12	0.137	98	2664	6
C.27-1	197	99	0.015	0.1805	0.0005	0.503	0.004	12.53	0.10	0.139	99	2657	5
C.29-1	272	165	0.000	0.1811	0.0005	0.498	0.004	12.44	0.10	0.142	98	2663	5
C.30-1	196	118	-0.002	0.1806	0.0005	0.499	0.004	12.42	0.10	0.140	98	2659	4
C.34-1	203	99	0.030	0.1800	0.0005	0.504	0.004	12.51	0.10	0.138	99	2653	4
C.35-1	132	78	0.091	0.1804	0.0007	0.494	0.004	12.28	0.11	0.139	97	2656	6
C.36-1	282	216	0.141	0.1808	0.0004	0.489	0.004	12.19	0.10	0.136	96	2661	4
C.38-1	178	131	0.026	0.1814	0.0005	0.489	0.004	12.24	0.10	0.141	96	2665	5
C.40-1	255	118	0.048	0.1801	0.0004	0.492	0.004	12.21	0.10	0.133	97	2654	4
Low-U, CL-bright													
C.4-1	59	24	-0.022	0.1852	0.0009	0.517	0.006	13.21	0.16	0.140	100	2700	8
C.13-1	48	21	0.138	0.1853	0.0012	0.508	0.006	12.98	0.18	0.141	98	2701	10
C.23-1	23	9	0.363	0.1804	0.0020	0.509	0.008	12.65	0.25	0.132	100	2657	19
C.26-1	65	37	0.078	0.1854	0.0009	0.516	0.006	13.19	0.16	0.138	99	2702	8
C.33-1	36	19	0.096	0.1824	0.0015	0.492	0.007	12.38	0.20	0.134	96	2675	13
Young outlier													
C.37-1	307	186	0.177	0.1789	0.0005	0.489	0.004	12.07	0.09	0.143	97	2643	4
Discordant													
C.6-1	240	119	0.009	0.1763	0.0005	0.460	0.003	11.19	0.09	0.123	93	2618	4

Data are at 1 $\sigma$  precision. All Pb data are common-Pb corrected (based on  $^{204}\text{Pb}$  and Broken Hill Pb composition). Analyses missing from the number sequence were aborted when high common Pb (seen as high  $^{204}\text{Pb}$  counts) was recognised.

Analysis date: 13/08/2001; session Z3734j.



## 200196 9019A: biotite granodiorite, Ironstone Point

<b>1:250,000 sheet:</b>	Laverton (SH5102)
<b>1:100,000 sheet:</b>	Burtville (3440)
<b>MGA:</b>	493149mE                      6801680mN
<b>Location:</b>	The sample was taken from a large boulder on the northeast side of a bouldery hill, just south of the track, about 9 km east of the Coglia-Merolia Road, and approximately 9 km south of Ironstone Point.
<b>Description:</b>	<p>This sample is from a grey fine- to medium-grained equigranular biotite granodiorite. The sampled unit forms one of a number of bands that vary in thickness from &lt;1 cm to &gt;80 cm within a banded granitoid complex; other bands comprise pegmatite, felsic granitoid, medium- to coarse-grained granodiorite, and thin biotite-rich layers and schlieren. The sampled layer is interpreted to have been a thin dyke in coarser-grained granodiorite. The banded granitoid complex is moderately foliated, defined by aligned minerals and elongate quartz grains. The unit is cut by a swarm of late syenogranite dykes, of which sample 200196 9019B is representative.</p> <p>The unit is characterised by a granoblastic texture. Principal minerals are plagioclase (50–60%), quartz (20–30%), biotite (10%), and lesser (mostly interstitial) K-feldspar (&lt;10%). Accessory minerals include Fe oxides, zircon and (acicular and more equant) apatite. Secondary phases include minor white mica, and lesser chlorite and carbonate.</p>
<b>Mount, pop:</b>	Z3734B

### Description of zircons

Most zircon grains recovered from this sample are colourless, clear, euhedral to subhedral whole grains with only slightly rounded crystal faces. Equant to elongate grains (aspect ratios to >5:1) are present, ranging from about 65  $\mu\text{m}$  to 240  $\mu\text{m}$  in length. A large proportion of the grains have distinct structurally discontinuous core zones which are overgrown by thin rims, as seen in CL images (Fig. 54) and transmitted and reflected light photographs. A small number of grains appear homogeneous in the photographs but exhibit well-defined zoning in the CL images. Irregular zoning patterns are present in only a few grains.

### Concurrent standard data

The average floating point exponent (all QGNG data) is 2.25, dropping to 2.20 after removal of one highly anomalous point (8-1). The concurrent sample data also indicate calibration slopes higher than 2.0 (~2.2 and ~2.4); a value of 2.20 was used for data reduction. The  $1\sigma$  scatter in the Pb/U calibration is 0.98% ( $n = 35$  of 36, MSWD = 4.75). However, there is unacceptable scatter in  $^{207}\text{Pb}/^{206}\text{Pb}$  for these data (MSWD = 2.1). Omitting 5 young outliers gives a  $^{207}\text{Pb}/^{206}\text{Pb}$  age of  $1845.7 \pm 3.1$  Ma. This reduced dataset still has considerable scatter in  $^{207}\text{Pb}/^{206}\text{Pb}$  (MSWD = 1.4) which is probably not attributable to operating conditions, given that one of the concurrent samples (data below) has MSWD < 1.0. The only other  $2\sigma$  outlier has high  $^{207}\text{Pb}/^{206}\text{Pb}$ . Omitting this gives a weighted mean  $^{207}\text{Pb}/^{206}\text{Pb}$  age of  $1845.1 \pm 2.9$  Ma (MSWD = 1.20), but using a standardised set of criteria for assessment of the data (see “Data compilation for the QGNG standard”) gives a  $^{207}\text{Pb}/^{206}\text{Pb}$  age of  $1850.0 \pm 3.0$  Ma (MSWD = 1.01).

Element abundance calibration was based on CZ3 ( $n = 2$ ).

### Sample data

Thirty four analyses were made on separate grains (Table 23, Fig. 55). Of these, three are >5% discordant (13-1, 17-1, 31-1) and are not considered in age assessments. The  $^{207}\text{Pb}/^{206}\text{Pb}$  for these three are consistent with the bulk of the data, indicating that Pb loss was dominantly



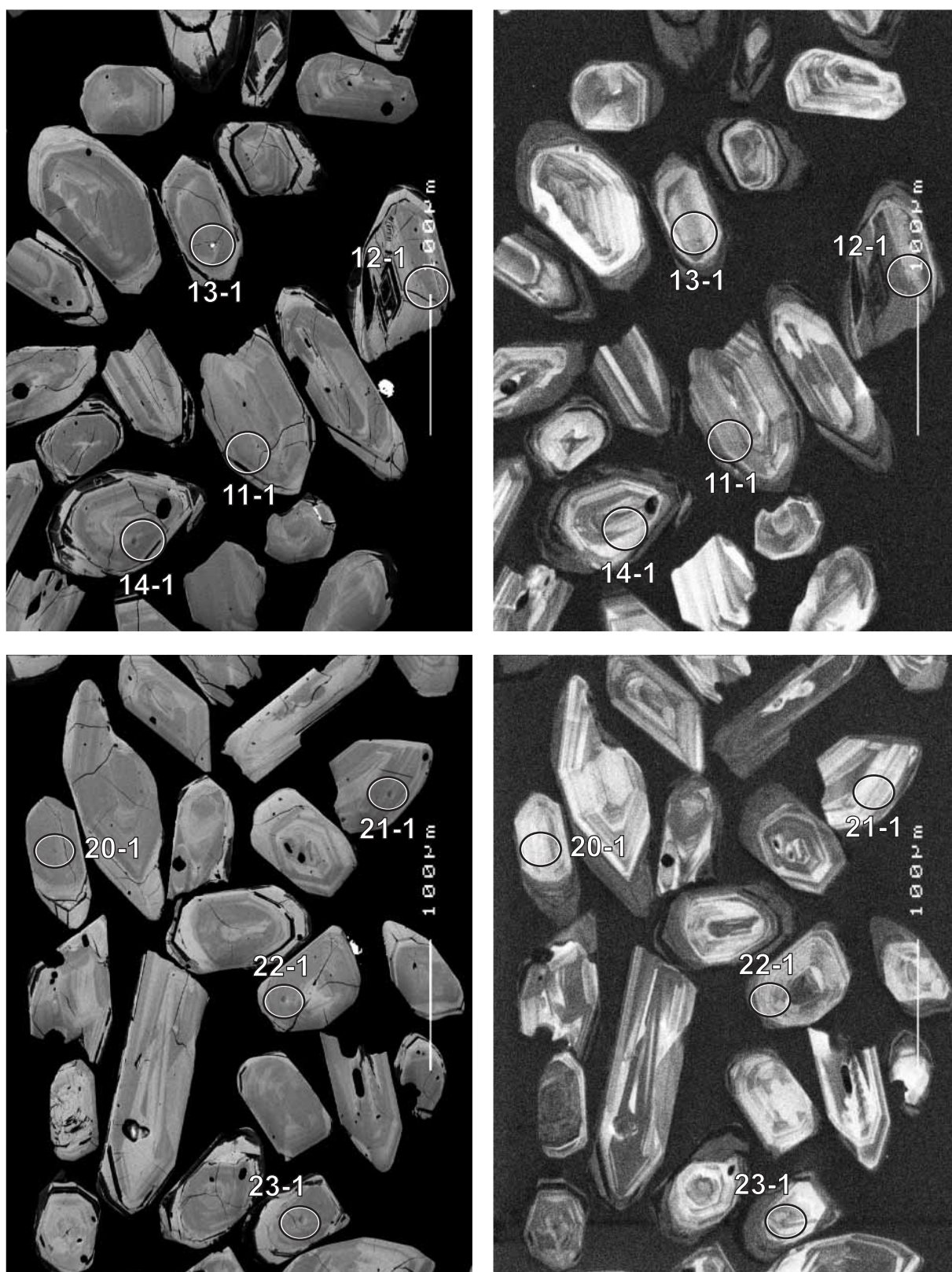


Figure 54. Representative SEM images (BSE on left, CL on right) for sample 200196 9019A: biotite granodiorite, Ironstone Point. SHRIMP analysis spots are labelled. Scale bar is 100  $\mu\text{m}$ .

recent. Of the identified cores, only one (12-1) is clearly older than the rest and is taken to be a xenocryst. All other visually identified cores (10-1, 14-1, 19-1, 20-1, 32-1, 33-1) plot with the remainder of the data. Omitting the xenocryst and discordant data leaves 30 analyses with a weighted average  $^{207}\text{Pb}/^{206}\text{Pb}$  age of  $2663.8 \pm 5.4$  Ma (MSWD = 2.5). One of the identified rims (18-1) is a  $2\sigma$  young outlier, but the other (26-1) is not. Omitting three young (14-1, 18-1, 25-1) and one old (2-1)  $2\sigma$  outliers gives  $2667.8 \pm 3.6$  Ma ( $n = 26$ , MSWD = 1.09).

### Geochronological interpretation

The age of  $2668 \pm 4$  Ma is considered most likely to be the age of the granitic protolith of the gneiss.

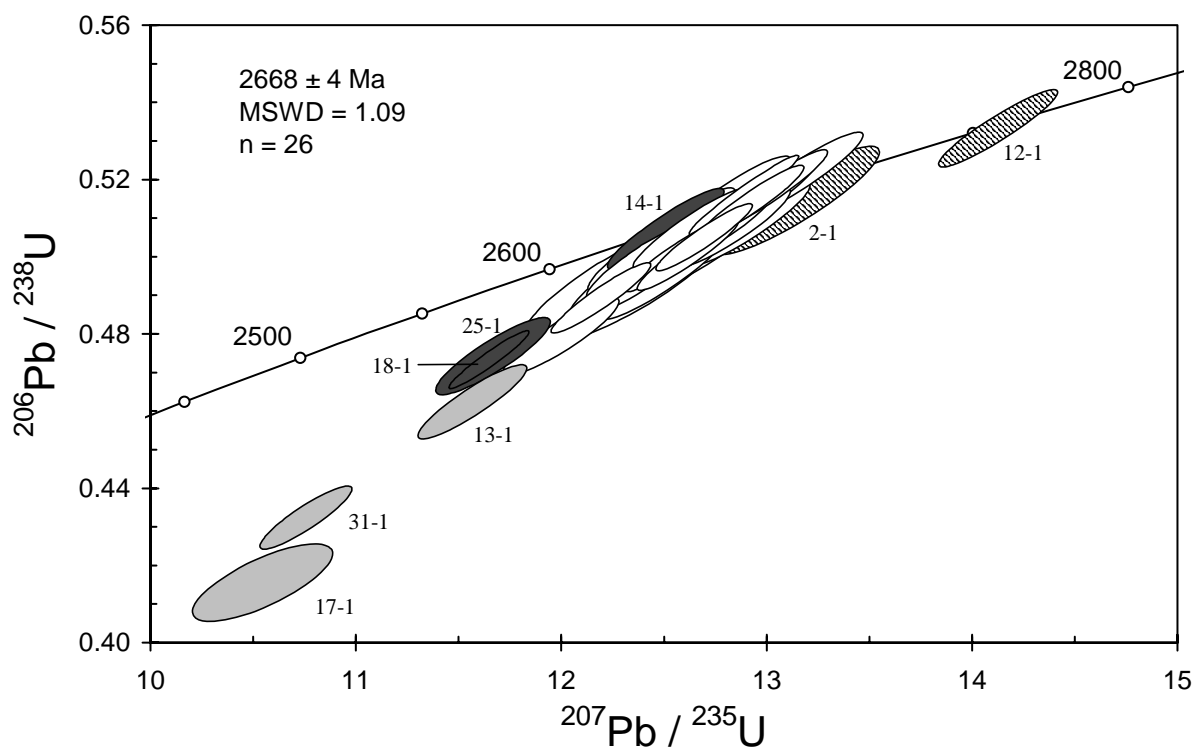


Figure 55. Concordia plot for zircon data from sample 200196 9019A: biotite granodiorite, Ironstone Point. White filled symbols are used to define the age of the sample; inherited grain and older outlier (?inherited grain) have diagonal shading; discordant analyses are light grey; younger outliers are dark grey.

Table 23. SHRIMP analytical results for sample 201096 9019A: biotite granodiorite, Ironstone Point.

grain-spot	U (ppm)	Th (ppm)	4f206 (%)	<sup>207</sup> Pb/ <sup>206</sup> Pb		<sup>206</sup> Pb/ <sup>238</sup> U		<sup>207</sup> Pb/ <sup>235</sup> U		<sup>208</sup> Pb/ <sup>232</sup> Th	conc. (%)	<sup>207</sup> Pb/ <sup>206</sup> Pb Age	
				±		±		±				(Ma)	±
Main group													
B.1-1	74	36	0.029	0.1817	0.0016	0.502	0.007	12.58	0.20	0.141	98	2668	15
B.3-1	41	48	0.177	0.1796	0.0013	0.502	0.008	12.44	0.21	0.137	99	2649	12
B.4-1	112	89	0.163	0.1819	0.0008	0.500	0.006	12.54	0.16	0.132	98	2671	8
B.5-1	50	30	-0.019	0.1830	0.0011	0.495	0.007	12.49	0.20	0.138	97	2681	10
B.6-1	108	43	0.117	0.1806	0.0008	0.489	0.006	12.18	0.16	0.137	97	2658	8
B.7-1	54	41	0.145	0.1812	0.0013	0.495	0.007	12.37	0.20	0.134	97	2664	11
B.8-1	32	20	0.048	0.1812	0.0017	0.496	0.009	12.39	0.24	0.139	97	2664	16
B.9-1	15	9	0.324	0.1809	0.0026	0.493	0.011	12.30	0.33	0.129	97	2661	24
B.10-1	55	34	-0.042	0.1830	0.0010	0.521	0.007	13.16	0.20	0.143	101	2680	9
B.11-1	64	71	0.112	0.1801	0.0011	0.499	0.007	12.39	0.19	0.139	98	2654	11
B.15-1	56	39	0.027	0.1813	0.0012	0.505	0.007	12.62	0.20	0.138	99	2665	11
B.16-1	69	67	0.025	0.1803	0.0009	0.507	0.007	12.61	0.18	0.138	100	2656	8
B.19-1	40	38	-0.016	0.1803	0.0011	0.514	0.008	12.79	0.21	0.140	101	2656	11
B.20-1	52	35	0.032	0.1815	0.0010	0.507	0.007	12.70	0.19	0.139	99	2667	9
B.21-1	48	33	-0.195	0.1839	0.0012	0.508	0.007	12.89	0.20	0.144	99	2689	11
B.22-1	66	36	0.207	0.1818	0.0014	0.508	0.007	12.73	0.20	0.136	99	2669	12
B.23-1	55	50	0.204	0.1815	0.0012	0.479	0.007	11.99	0.19	0.137	95	2666	11
B.24-1	54	53	0.106	0.1823	0.0011	0.515	0.007	12.94	0.20	0.142	100	2673	10
B.26-1	63	51	0.010	0.1831	0.0012	0.508	0.007	12.81	0.20	0.136	99	2681	11
B.27-1	33	25	-0.238	0.1827	0.0016	0.502	0.008	12.65	0.23	0.141	98	2677	15
B.28-1	39	35	0.047	0.1794	0.0011	0.507	0.008	12.53	0.20	0.136	100	2647	10
B.29-1	135	78	0.148	0.1822	0.0008	0.505	0.006	12.69	0.16	0.145	99	2673	7
B.30-1	61	54	-0.005	0.1823	0.0009	0.518	0.007	13.00	0.19	0.139	101	2674	8
B.32-1	83	119	0.039	0.1821	0.0008	0.514	0.006	12.91	0.17	0.143	100	2673	7
B.33-1	127	121	-0.027	0.1810	0.0006	0.516	0.007	12.88	0.18	0.144	101	2662	6
B.34-1	88	98	0.108	0.1827	0.0008	0.500	0.006	12.60	0.16	0.142	98	2677	7
Xenocryst													
B.12-1	89	39	0.038	0.1920	0.0009	0.534	0.007	14.12	0.19	0.149	100	2759	8
Old outlier													
B.2-1	26	17	0.080	0.1851	0.0017	0.515	0.009	13.14	0.27	0.142	99	2699	15
Young Outliers													
B.14-1	61	81	0.223	0.1787	0.0010	0.507	0.007	12.50	0.19	0.138	100	2640	10
B.18-1	334	81	0.236	0.1783	0.0006	0.473	0.005	11.63	0.13	0.129	95	2638	5
B.25-1	52	34	0.308	0.1783	0.0013	0.474	0.007	11.65	0.18	0.122	95	2637	12
Discordant													
B.13-1	55	37	0.293	0.1814	0.0012	0.462	0.006	11.55	0.18	0.134	92	2666	11
B.17-1	34	22	1.677	0.1842	0.0026	0.414	0.007	10.53	0.23	0.144	83	2691	23
B.31-1	77	110	0.350	0.1804	0.0011	0.432	0.005	10.74	0.15	0.083	87	2657	10

Data are at 1 $\sigma$  precision. All Pb data are common-Pb corrected (based on  $^{204}\text{Pb}$  and Broken Hill Pb composition). Analysis date: 08/08/2001; session Z3734i.

## 200196 9019B: allanite-fluorite-biotite syenogranite dyke, Ironstone Point

**1:250,000 sheet:** Laverton (SH5102)

**1:100,000 sheet:** Burtville (3440)

**MGA:** 493149mE 6801680mN

**Location:** The sample was taken from a ridge of outcrop on the northeast side of a bouldery hill, just south of the track, about 9 km east of the Coglia-Merolia Road, and approximately 9 km south of Ironstone Point.

**Description:** This sample is from a pink to brick-red, medium-grained, sparsely to very sparsely feldspar porphyritic to equigranular allanite-fluorite-biotite syenogranite dyke. The dyke is one of numerous dykes and small pods forming a dyke swarm that intruded a grey, banded granitoid complex, including a banded biotite granodiorite of which sample 200196 9019A is representative. The presence of fluorite and allanite clearly identify the syenogranite as belonging to the Low-Ca group of Champion & Sheraton (1997).

The unit has a granular to granular-granoblastic texture. Principal minerals are K-feldspar (30–35%), plagioclase (25%), quartz (30%), and biotite (5–6%). K-feldspar is locally perthitic, with common tartan twinning. Quartz is weakly to moderately undulose. The unit contains relatively common fluorite, associated with chloritised biotite, and common subhedral allanite (1–2%) grains to 1 mm. Other accessory phases include relatively common zircon and Fe-oxides, and apatite. Biotite occurs as fine flakes and aggregates. Secondary phases include minor to moderate white mica and chlorite, and minor rutile and carbonate.

**Mount, pop:** Z3734A

### Description of zircons

Zircon from this sample consists of both angular anhedral fragments and euhedral to subhedral whole grains and fragments with rounded edges and terminations. All grains are colourless and translucent, with few inclusions. Grains mostly range in size from 75  $\mu\text{m}$  to 185  $\mu\text{m}$  and have aspect ratios of 1:1 to 3:1, with a few larger grains present (up to 270  $\mu\text{m}$  long). Rare thin rims are present on some grains, and structurally discontinuous cores are visible in some of the CL images (Fig. 56). Most grains display weak CL, although a few grains (e.g. grain 4) have a strong response. Concentric and/or linear zoning patterns are visible in the CL images and transmitted light photographs for many grains.

### Concurrent standard data

The average floating point exponent (all QGNG data) is 2.25, dropping to 2.20 after removal of one highly anomalous point (8-1). The concurrent sample data also indicate calibration slopes higher than 2.0 (~2.2 and ~2.4); a value of 2.20 was used for data reduction. The  $1\sigma$  scatter in the Pb/U calibration is 0.98% ( $n = 35$  of 36, MSWD = 4.75). However, there is unacceptable scatter in  $^{207}\text{Pb}/^{206}\text{Pb}$  for these data (MSWD = 2.1). Omitting 5 young outliers gives a  $^{207}\text{Pb}/^{206}\text{Pb}$  age of  $1845.7 \pm 3.1$  Ma. This reduced dataset still has considerable scatter in  $^{207}\text{Pb}/^{206}\text{Pb}$  (MSWD = 1.4) which is probably not attributable to operating conditions, given that one of the concurrent samples (data below) has MSWD < 1.0. The only other  $2\sigma$  outlier has high  $^{207}\text{Pb}/^{206}\text{Pb}$ . Omitting this gives a weighted mean  $^{207}\text{Pb}/^{206}\text{Pb}$  age of  $1845.1 \pm 2.9$  Ma (MSWD = 1.20). Using a standardised set of criteria for assessment of the data (see “Data compilation for the QGNG standard”) gives a  $^{207}\text{Pb}/^{206}\text{Pb}$  age of  $1850.0 \pm 3.0$  Ma (MSWD = 1.01).

Element abundance calibration was based on CZ3 ( $n = 2$ ).



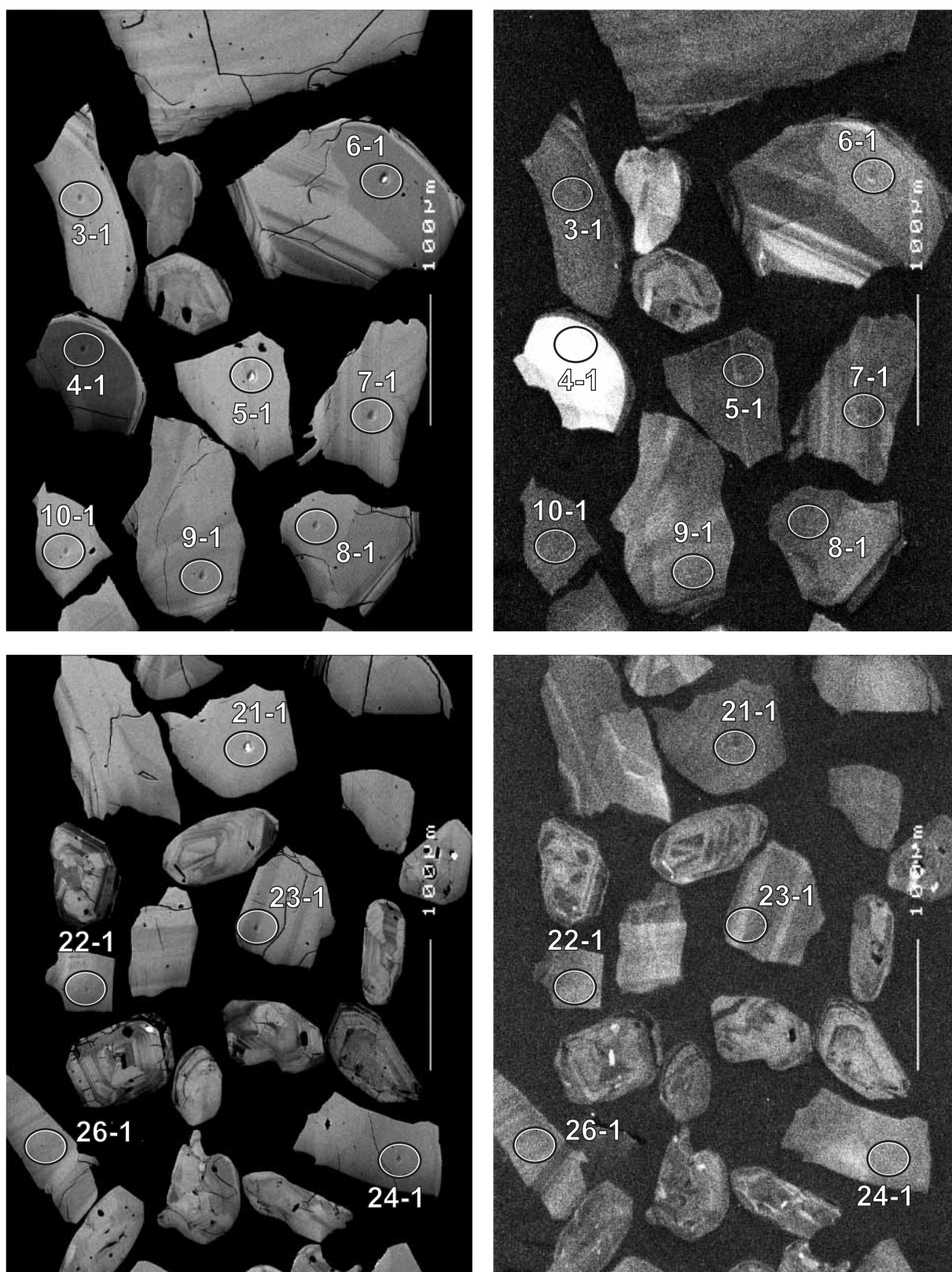


Figure 56. Representative SEM images (BSE on left, CL on right) for sample 200196 9019B: allanite-fluorite-biotite syenogranite dyke, Ironstone Point. SHRIMP analysis spots are labelled. Scale bar is 100  $\mu\text{m}$ .



## Sample data

Two analyses (20-1 and 27-1) were deleted from the data file because of data interruptions during analysis. The remaining 32 analyses from separate grains give data that are all with 5% of concordance and fall in a single cluster in a concordia plot (Table 24, Fig. 57). The corresponding  $^{207}\text{Pb}/^{206}\text{Pb}$  age is  $2638.3 \pm 1.9$  Ma (MSWD = 0.89).

## Geochronological interpretation

The  $2638 \pm 2$  Ma age is considered to be the age of intrusion of the dyke.

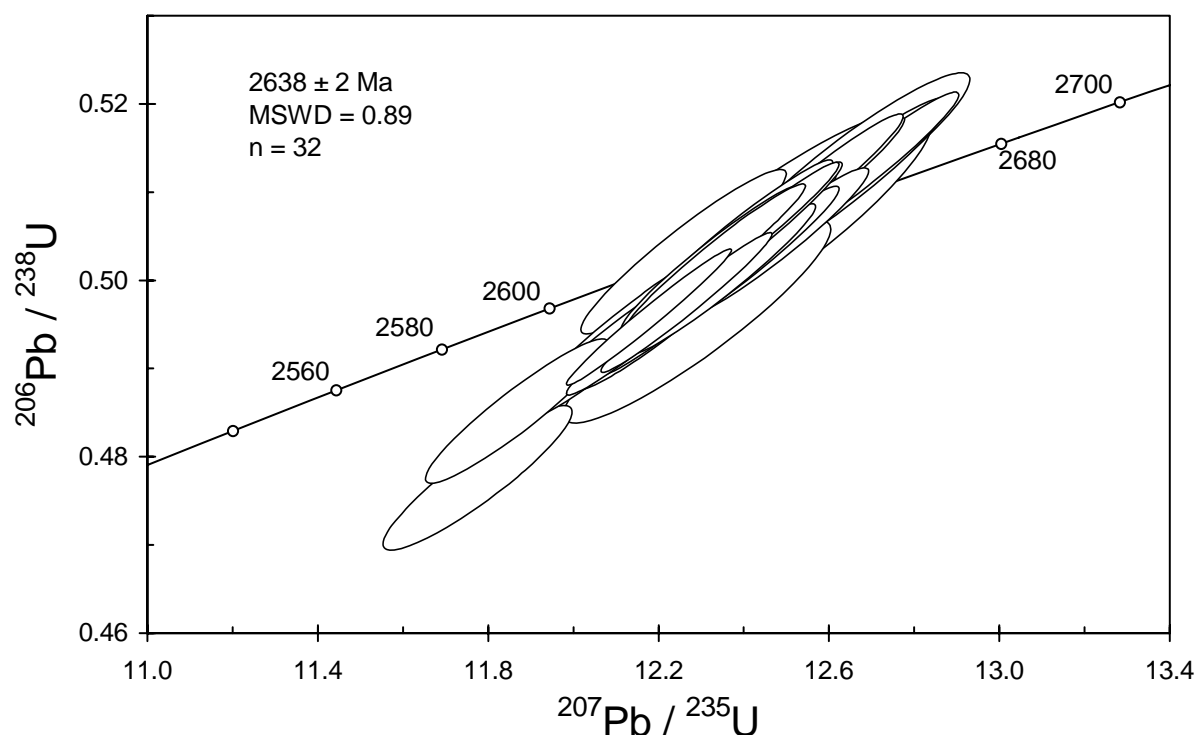


Figure 57. Concordia plot for zircon data from sample 200196 9019B: allanite-fluorite-biotite syenogranite dyke, Ironstone Point. All data are used to define the age of the sample.

Table 24. SHRIMP analytical results for sample 200196 9019B: allanite-fluorite-biotite syenogranite dyke, Ironstone Point.

grain-spot	U (ppm)	Th (ppm)	4f206 (%)	$\frac{^{207}\text{Pb}}{^{206}\text{Pb}}$		$\frac{^{206}\text{Pb}}{^{238}\text{U}}$		$\frac{^{207}\text{Pb}}{^{235}\text{U}}$		$\frac{^{208}\text{Pb}}{^{232}\text{Th}}$		conc. (%)	$\frac{^{207}\text{Pb}}{^{206}\text{Pb}}$ Age (Ma)	
				$\pm$	$\pm$	$\pm$	$\pm$	$\pm$	$\pm$	$\pm$	$\pm$			
Main group														
A.1-1	148	67	-0.048	0.1781	0.0006	0.505	0.006	12.40	0.15	0.138	100	2636	6	
A.2-1	211	115	0.197	0.1793	0.0006	0.504	0.006	12.47	0.15	0.142	99	2647	6	
A.3-1	198	78	-0.007	0.1791	0.0005	0.502	0.006	12.40	0.14	0.138	99	2645	5	
A.4-1	23	15	0.009	0.1786	0.0017	0.505	0.010	12.44	0.26	0.137	100	2640	16	
A.5-1	304	313	0.029	0.1785	0.0005	0.495	0.005	12.18	0.13	0.135	98	2639	4	
A.6-1	113	127	0.122	0.1766	0.0008	0.503	0.006	12.25	0.16	0.136	100	2621	7	
A.7-1	175	106	0.054	0.1787	0.0006	0.497	0.006	12.25	0.15	0.137	99	2641	5	
A.8-1	185	162	-0.005	0.1788	0.0006	0.497	0.006	12.26	0.14	0.136	99	2641	5	
A.9-1	143	56	0.065	0.1787	0.0006	0.506	0.007	12.46	0.18	0.138	100	2640	6	
A.10-1	268	159	-0.009	0.1782	0.0005	0.505	0.005	12.41	0.14	0.138	100	2636	4	
A.11-1	177	135	0.027	0.1781	0.0006	0.496	0.006	12.18	0.15	0.136	98	2636	6	
A.12-1	226	108	0.019	0.1783	0.0005	0.505	0.006	12.41	0.14	0.138	100	2637	5	
A.13-1	183	129	0.521	0.1774	0.0007	0.485	0.005	11.86	0.14	0.142	97	2628	7	
A.14-1	186	244	0.042	0.1785	0.0006	0.504	0.006	12.39	0.15	0.138	100	2639	5	
A.15-1	348	153	-0.006	0.1788	0.0004	0.497	0.005	12.26	0.13	0.137	99	2642	4	
A.16-1	229	93	0.052	0.1778	0.0005	0.503	0.006	12.32	0.14	0.139	100	2633	5	
A.17-1	39	29	-0.063	0.1799	0.0012	0.495	0.008	12.29	0.21	0.137	98	2652	11	
A.18-1	171	92	-0.016	0.1791	0.0006	0.500	0.006	12.35	0.14	0.137	99	2644	5	
A.19-1	152	125	0.611	0.1788	0.0009	0.477	0.005	11.77	0.15	0.149	95	2642	9	
A.21-1	230	105	0.005	0.1779	0.0005	0.503	0.005	12.33	0.14	0.138	100	2633	4	
A.22-1	144	54	0.101	0.1778	0.0006	0.495	0.006	12.13	0.15	0.134	98	2632	6	
A.23-1	149	102	0.015	0.1791	0.0007	0.504	0.006	12.45	0.15	0.139	99	2645	6	
A.24-1	132	55	-0.028	0.1786	0.0007	0.496	0.006	12.22	0.15	0.139	98	2640	6	
A.25-1	162	82	0.068	0.1780	0.0006	0.492	0.006	12.08	0.14	0.140	98	2635	6	
A.28-1	79	80	-0.079	0.1792	0.0008	0.511	0.006	12.63	0.17	0.141	101	2645	7	
A.29-1	155	90	-0.007	0.1793	0.0006	0.513	0.006	12.68	0.15	0.142	101	2647	5	
A.30-1	171	120	0.075	0.1778	0.0005	0.505	0.006	12.39	0.14	0.139	100	2633	5	
A.31-1	179	87	-0.035	0.1784	0.0005	0.510	0.006	12.55	0.14	0.141	101	2638	5	
A.32-1	50	38	0.083	0.1788	0.0010	0.513	0.007	12.65	0.19	0.140	101	2642	9	
A.33-1	419	543	0.010	0.1781	0.0003	0.496	0.005	12.17	0.13	0.135	98	2635	3	
A.34-1	186	130	0.016	0.1786	0.0005	0.510	0.006	12.56	0.15	0.139	101	2640	5	

Data are at 1 $\sigma$  precision. All Pb data are common-Pb corrected (based on  $^{204}\text{Pb}$  and Broken Hill Pb composition). Analysis date: 08/08/2001; session Z3734i.

## 200196 9020: Isolated Hill Granodiorite

<b>1:250,000 sheet:</b>	Rason (SH5103)
<b>1:100,000 sheet:</b>	Mount Toppin (3540)
<b>MGA:</b>	574458mE                      6818505mN
<b>Location:</b>	The sample was taken from a low pavement, approximately 200 m east of the track, and approximately 1 km south-southeast of Isolated Hill.
<b>Description:</b>	<p>This sample is from a grey to grey-pink, medium-grained, moderately to strongly (quartz) feldspar porphyritic, titanite-hornblende-biotite granodiorite of the Isolated Hill Granodiorite. The granodiorite is characterised by a moderate to strong foliation and a strong sub-horizontal stretching lineation. The deformation has also affected pegmatite (2 generations) and granite dykes intrusive into the granodiorite.</p> <p>The principal minerals are plagioclase (35–40%), quartz (25–30%), biotite (7–8%), hornblende (&lt;5%) and K-feldspar (15–20%), in a granoblastic texture. Feldspar forms mostly aligned and stretched phenocrysts up to 2–5 cm, including both plagioclase and perthitic K-feldspar. Quartz is variably recrystallised to strongly undulose. Biotite and hornblende comprise 10–12% of the rock with biotite dominant; titanite is relatively common, up to 2%, forming subhedral grains to 2–3 mm. Other accessory phases include Fe-oxides, zircon, apatite and rare allanite. Secondary minerals include minor white mica, epidote, chlorite and uncommon carbonate.</p>
<b>Mount, pop:</b>	Z3734E

### Description of zircons

Euhedral to subhedral zircon grains and fragments were recovered from this sample. Most have only slightly rounded crystal faces and minor inclusions. They are predominantly 70 µm to 200 µm in size with aspect ratios from 2:1 to 3:1, although a small number of equant grains and rare longer, thinner grains are present. The grains are colourless and clear and virtually all show well-defined zoning patterns on CL images (Fig. 58). About half the grains display truncated zoning patterns with crosscutting overgrowths. These rims are of variable thickness both between grains and within individual grains.

### Concurrent standard data

The average floating point exponent for QGNG, after rejection of one analysis with anomalously low  $^{207}\text{Pb}/^{206}\text{Pb}$  and  $^{206}\text{Pb}/^{238}\text{U}$ , is 2.3 and the concurrent sample data suggest calibration slopes higher than 2.3. A value of 2.30 was used for data reduction. The  $1\sigma$  scatter in the Pb/U calibration is 1.22% ( $n = 33$ , MSWD = 4.6). The scatter in  $^{207}\text{Pb}/^{206}\text{Pb}$  for these data is rather large (MSWD = 1.4). Omitting three young  $2\sigma$  outliers gives a weighted mean  $^{207}\text{Pb}/^{206}\text{Pb}$  age of  $1848.5 \pm 2.7$  Ma (MSWD = 0.89), but using a standardised set of criteria for assessment of the data (see “Data compilation for the QGNG standard”) gives a  $^{207}\text{Pb}/^{206}\text{Pb}$  age of  $1847.9 \pm 2.7$  Ma (MSWD = 1.09).

Element abundance calibration was based on CZ3 ( $n = 2$ ).

### Sample data

Twenty nine analyses were obtained from individual grains (Table 25). Most analyses were on systematically zoned regions of the grains. No distinct cores were analysed. The majority of data cluster on U–Pb concordia, but there is also a significant number of discordant data that indicate both early and recent Pb loss (Fig. 59). Data >5% discordant are not considered in the age assessment. The concordant cluster exhibits scatter in  $^{207}\text{Pb}/^{206}\text{Pb}$  that is considerably beyond that attributable to analytical precision, even after exclusion of the obvious outlier 2-1 (Fig. 60).

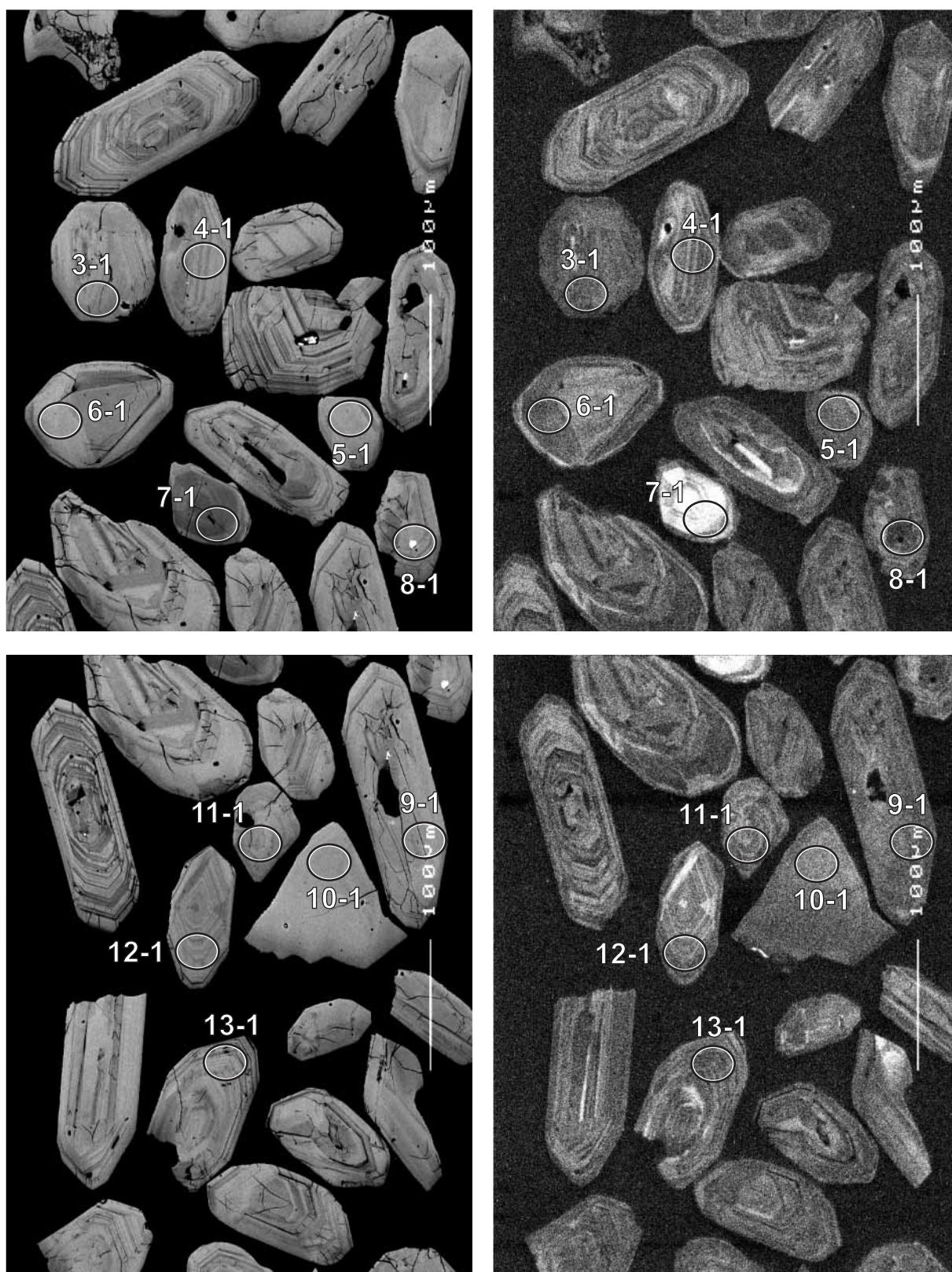


Figure 58. Representative SEM images (BSE on left, CL on right) for sample 200196 9020: Isolated Hill Granodiorite. SHRIMP analysis spots are labelled. Scale bar is 100  $\mu\text{m}$ .

In light of the evidence from the discordant data for early Pb loss, data have been culled from the low-age side of the main cluster to give a reasonably self-consistent population of 14 analyses that gives a weighted mean  $^{207}\text{Pb}/^{206}\text{Pb}$  age of  $2681.3 \pm 3.6$  Ma (MSWD = 1.6). One high-Th analysis (8-1) amongst this group has highly discordant Pb/Th:Pb/U and possibly should be rejected, but this would have no effect on the  $^{207}\text{Pb}/^{206}\text{Pb}$  date.

### Geochronological interpretation

The  $^{207}\text{Pb}/^{206}\text{Pb}$  age of  $2681 \pm 4$  Ma is considered to be the intrusive age of the granodiorite.

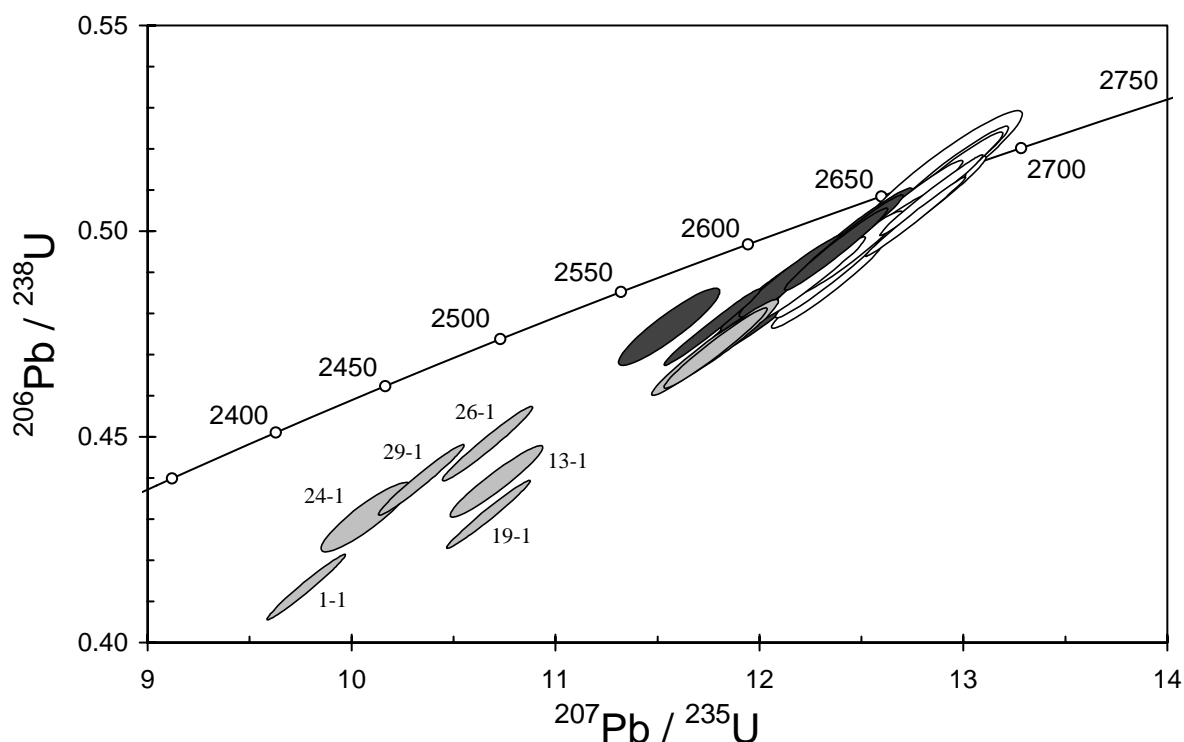


Figure 59. Concordia plot for zircon data from sample 200196 9020: Isolated Hill Granodiorite. White filled symbols are used to define the age of the sample; younger outliers are dark grey; discordant analyses are light grey.



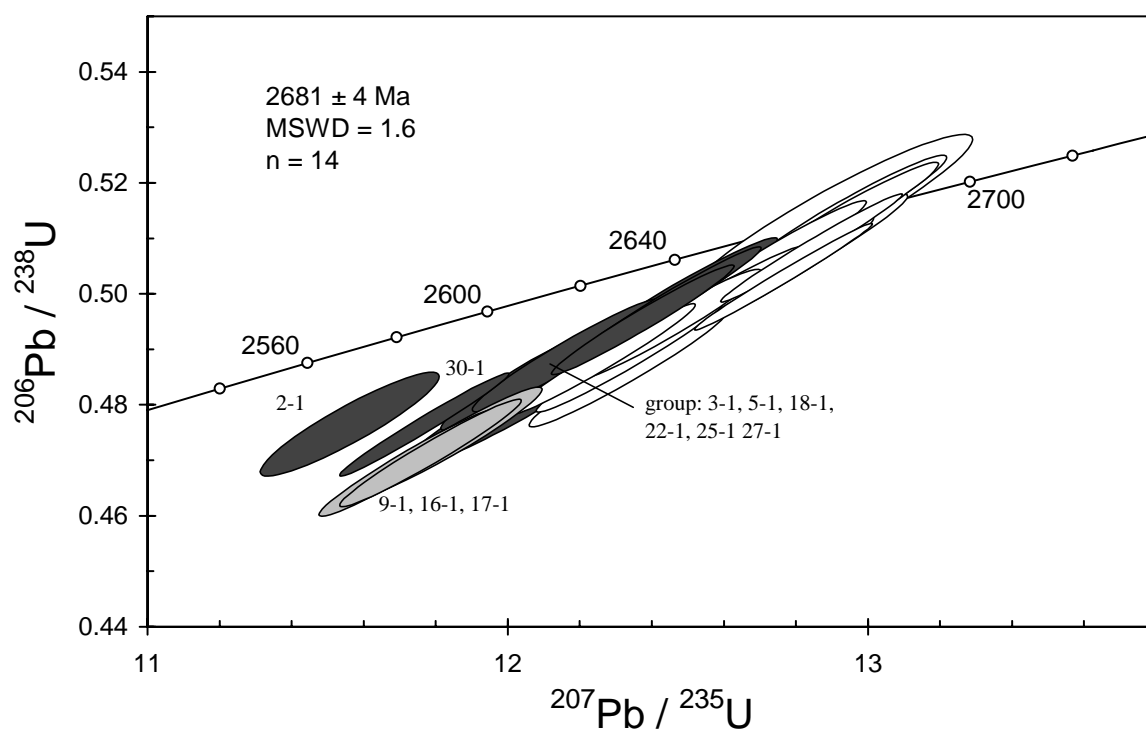


Figure 60. Enlargement of main group of zircon analyses for sample 200196 9020: Isolated Hill Granodiorite. Symbol shading as in Figure 59.

Table 25. SHRIMP analytical results for sample 200196 9020: Isolated Hill Granodiorite.

grain-spot	U (ppm)	Th (ppm)	4f206 (%)	$\frac{^{207}\text{Pb}}{^{206}\text{Pb}}$		$\frac{^{206}\text{Pb}}{^{238}\text{U}}$		$\frac{^{207}\text{Pb}}{^{235}\text{U}}$		$\frac{^{208}\text{Pb}}{^{232}\text{Th}}$	conc. (%)	$\frac{^{207}\text{Pb}}{^{206}\text{Pb}}$ Age	
				$\pm$	$\pm$	$\pm$	$\pm$	(Ma)	$\pm$				
Main group													
E.4-1	222	171	0.059	0.1831	0.0006	0.488	0.007	12.34	0.17	0.137	96	2682	5
E.6-1	251	36	0.004	0.1822	0.0005	0.488	0.007	12.26	0.17	0.137	96	2673	5
E.7-1	46	49	0.143	0.1819	0.0013	0.514	0.010	12.90	0.26	0.144	100	2670	11
E.8-1	645	1354	0.087	0.1833	0.0004	0.508	0.007	12.84	0.17	0.276	99	2683	3
E.10-1	161	29	-0.004	0.1835	0.0007	0.507	0.007	12.82	0.19	0.140	98	2685	6
E.11-1	165	150	0.052	0.1839	0.0007	0.486	0.007	12.33	0.18	0.136	95	2688	6
E.12-1	164	118	-0.016	0.1822	0.0007	0.498	0.007	12.51	0.18	0.138	97	2673	6
E.14-1	648	376	-0.001	0.1840	0.0003	0.503	0.006	12.76	0.16	0.141	98	2690	3
E.15-1	297	315	-0.011	0.1836	0.0006	0.503	0.007	12.73	0.18	0.141	98	2685	5
E.20-1	180	40	0.049	0.1826	0.0007	0.513	0.007	12.91	0.19	0.136	100	2677	6
E.21-1	299	158	0.221	0.1825	0.0007	0.494	0.007	12.44	0.17	0.140	97	2676	6
E.23-1	263	59	0.099	0.1828	0.0006	0.498	0.007	12.56	0.18	0.138	97	2678	5
E.28-1	262	51	0.077	0.1823	0.0006	0.506	0.007	12.73	0.18	0.133	99	2674	5
E.31-1	156	44	0.109	0.1824	0.0007	0.514	0.007	12.92	0.19	0.140	100	2675	7
Young outliers													
E.2-1	458	171	0.134	0.1759	0.0010	0.476	0.006	11.55	0.17	0.129	96	2615	10
E.3-1	180	62	0.090	0.1811	0.0006	0.499	0.007	12.47	0.18	0.141	98	2663	6
E.5-1	289	38	0.042	0.1811	0.0005	0.498	0.007	12.44	0.17	0.140	98	2663	5
E.18-1	218	249	0.253	0.1805	0.0007	0.489	0.007	12.16	0.18	0.136	97	2657	7
E.22-1	190	48	0.502	0.1805	0.0008	0.485	0.007	12.07	0.18	0.183	96	2657	7
E.25-1	111	88	0.240	0.1815	0.0010	0.479	0.007	12.00	0.19	0.140	95	2667	9
E.27-1	312	110	0.071	0.1812	0.0005	0.495	0.007	12.37	0.17	0.136	97	2664	5
E.30-1	476	43	0.095	0.1792	0.0004	0.476	0.006	11.76	0.16	0.128	95	2645	4
Discordant													
E.1-1	697	378	0.311	0.1716	0.0004	0.412	0.005	9.75	0.13	0.114	86	2573	4
E.9-1	208	83	0.117	0.1812	0.0006	0.469	0.007	11.72	0.17	0.102	93	2664	6
E.13-1	371	412	1.401	0.1771	0.0008	0.438	0.006	10.69	0.15	0.118	89	2625	7
E.16-1	220	135	0.072	0.1814	0.0006	0.471	0.007	11.78	0.17	0.131	93	2666	5
E.17-1	207	40	0.361	0.1815	0.0007	0.473	0.007	11.83	0.17	0.141	94	2666	7
E.19-1	711	588	0.366	0.1797	0.0004	0.430	0.005	10.65	0.14	0.110	87	2650	4
E.24-1	423	472	0.282	0.1698	0.0011	0.429	0.006	10.05	0.15	0.121	90	2555	11
E.26-1	294	229	0.042	0.1727	0.0005	0.447	0.006	10.65	0.15	0.126	92	2584	5
E.29-1	437	185	0.189	0.1707	0.0005	0.439	0.006	10.32	0.14	0.119	91	2565	5

Data are at 1 $\sigma$  precision. All Pb data are common-Pb corrected (based on  $^{204}\text{Pb}$  and Broken Hill Pb composition). Analysis date: 25/08/2001; session Z3734k.

## 200196 9021: biotite monzogranite dyke, Isolated Hill

- 1:250,000 sheet:** Rason (SH5103)
- 1:100,000 sheet:** Mount Toppin (3640)
- MGA:** 574453mE 6818450mN
- Location:** The sample was taken from a small low pavement, 50 m south of sample 200196 9021, approximately 200 m east of the track, and approximately 1 km south-southeast of Isolated Hill.
- Description:** This sample is from a white, medium-grained, equigranular to seriate, biotite monzogranite dyke. The monzogranite dyke is one of numerous thin (<5 m) dykes that intruded into the Isolated Hill Granodiorite, of which sample 200196 9020 is representative. The dykes and the Isolated Hill Granodiorite are intruded by two phases of pegmatites. All phases are strongly deformed and lineated.
- The principal minerals are plagioclase (25–30%), K-feldspar (30–35%), quartz (30–40%), and biotite (<5%), with a granoblastic texture. Quartz is variably recrystallised to strongly undulose, while the K-feldspar shows minor perthite development and relatively common tartan twinning. Myrmekite is also relatively common. Biotite occurs as small flakes and aggregates. Accessory phases include opaque minerals, zircon, and apatite. Secondary minerals include white mica, chlorite, epidote and minor-rare carbonate.
- Mount, pop:** Z3734D

### Description of zircons

Zircon crystals and fragments from this sample have variable morphologies ranging from stubby and equant to euhedral-subhedral to angular and anhedral. The grains range from ~55  $\mu\text{m}$  to 220  $\mu\text{m}$  in size with aspect ratios to about 4:1. Some are colourless and clear whereas others are brownish and probably variably metamict. Cracks and inclusions are common. Zoning is visible in the photographs and CL images (Fig. 61). Many grains display systematic, parallel zoning, but others have more complex, irregular patterns. Several grains have distinct structurally discontinuous cores overgrown by younger rims. Some cores are rounded, indicating prior mechanical abrasion or resorption.

### Concurrent standard data

The average floating point exponent for QGNG, after rejection of one analysis with anomalously low  $^{207}\text{Pb}/^{206}\text{Pb}$  and  $^{206}\text{Pb}/^{238}\text{U}$ , is 2.3 and the concurrent sample data suggest calibration slopes higher than 2.3. A value of 2.30 was used for data reduction. The  $1\sigma$  scatter in the Pb/U calibration is 1.22% ( $n = 33$ , MSWD = 4.6). The scatter in  $^{207}\text{Pb}/^{206}\text{Pb}$  for these data is rather large (MSWD = 1.4). Omitting three young  $2\sigma$  outliers gives a weighted mean  $^{207}\text{Pb}/^{206}\text{Pb}$  age of  $1848.5 \pm 2.7$  Ma (MSWD = 0.89), but using a standardised set of criteria for assessment of the data (see “Data compilation for the QGNG standard”) gives a  $^{207}\text{Pb}/^{206}\text{Pb}$  age of  $1847.9 \pm 2.7$  Ma (MSWD = 1.09).

Element abundance calibration was based on CZ3 ( $n = 2$ ).

### Sample data

Thirty two analyses were obtained, each from a separate grain (Table 26, Fig. 62). The data scatter widely, both in apparent age and discordance, with one reversely discordant analysis (27-1) giving a  $^{207}\text{Pb}/^{206}\text{Pb}$  age (commonly interpreted as a minimum age of crystallisation) of ~3000 Ma. Given that this dyke intrudes the 2680 Ma Isolated Hill granodiorite, this is clearly a xenocrystic grain, as are the cores with ages ~2770 Ma (analyses 2-1, 18-1 and 24-1; grain 18 is almost entirely core, with a fine rim).

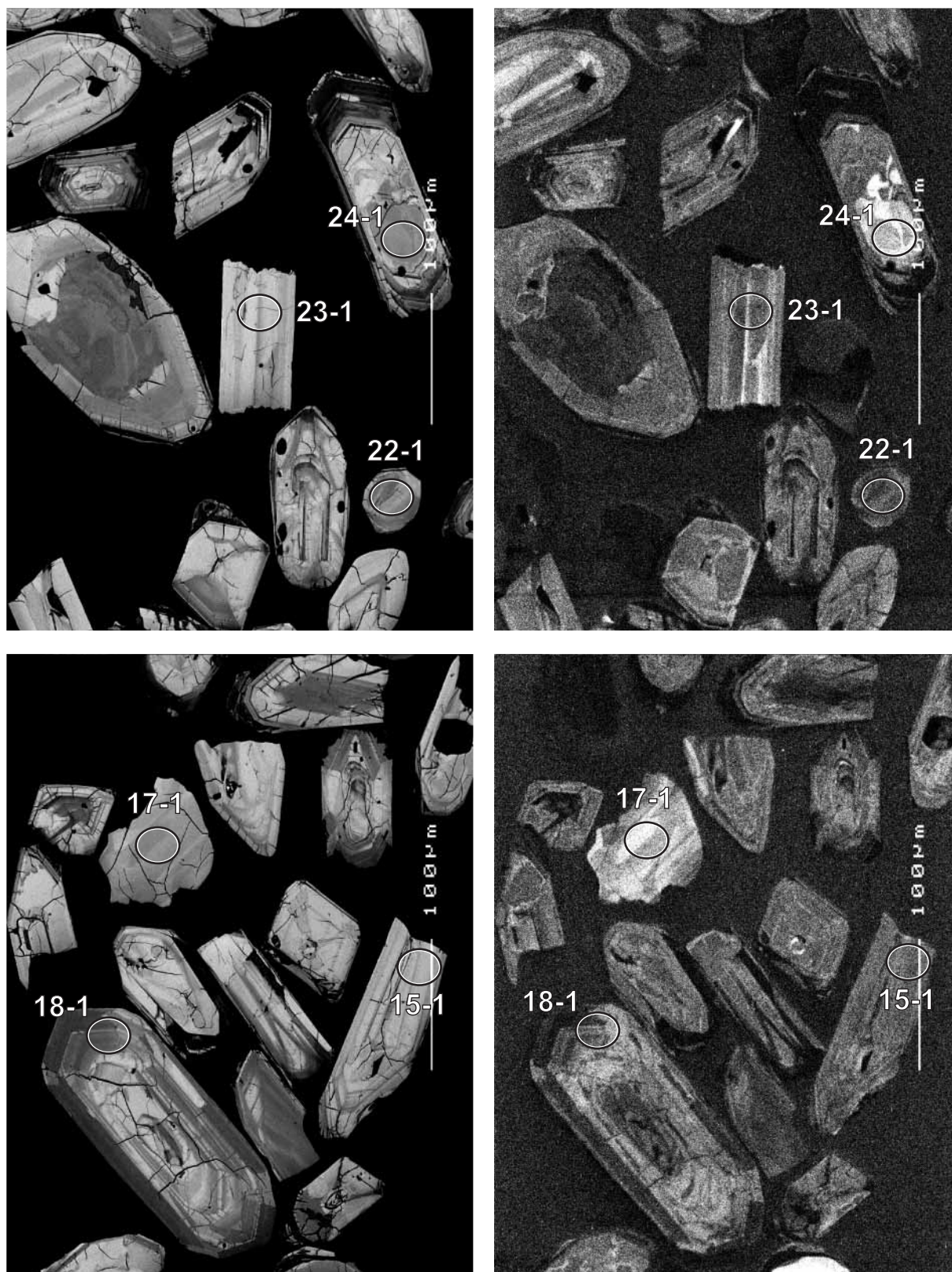


Figure 61. Representative SEM images (BSE on left, CL on right) for sample 900196 9021: biotite monzogranite dyke, Isolated Hill. SHRIMP analysis spots are labelled. Scale bar is 100 µm.

There is a cluster of five concordant analyses (1-1, 6-1, 13-1, 17-1 and 23-1) that gives a  $^{207}\text{Pb}/^{206}\text{Pb}$  age of  $2663 \pm 7$  Ma (MSWD = 0.83) which might record the intrusive age of the dyke (Fig. 63). One slightly older analysis (4-1), from a possible structural core, is presumed to record a xenocrystic (or possibly a mixed) age.

There is a strong discordance pattern in the data, with an alignment between  $\sim 2650$  Ma and  $\sim 1200$  Ma (Fig. 62). One distinctly younger point (26-1) is presumed to have suffered significant recent Pb loss and is not considered further. The discordance trend is unusual in that the data array is more scattered at the upper intercept than near the lower one. In fact, it could be argued that the data converge on  $\sim 1200$  Ma. Given the diversity in grain morphologies, this could be interpreted to indicate that all the zircons are Archaean xenocrysts within a  $\sim 1200$  Ma dyke.

### Geochronological interpretation

It is most likely that the dyke is either  $2663 \pm 7$  Ma or  $\sim 1200$  Ma. The data do not permit a choice between these two options.

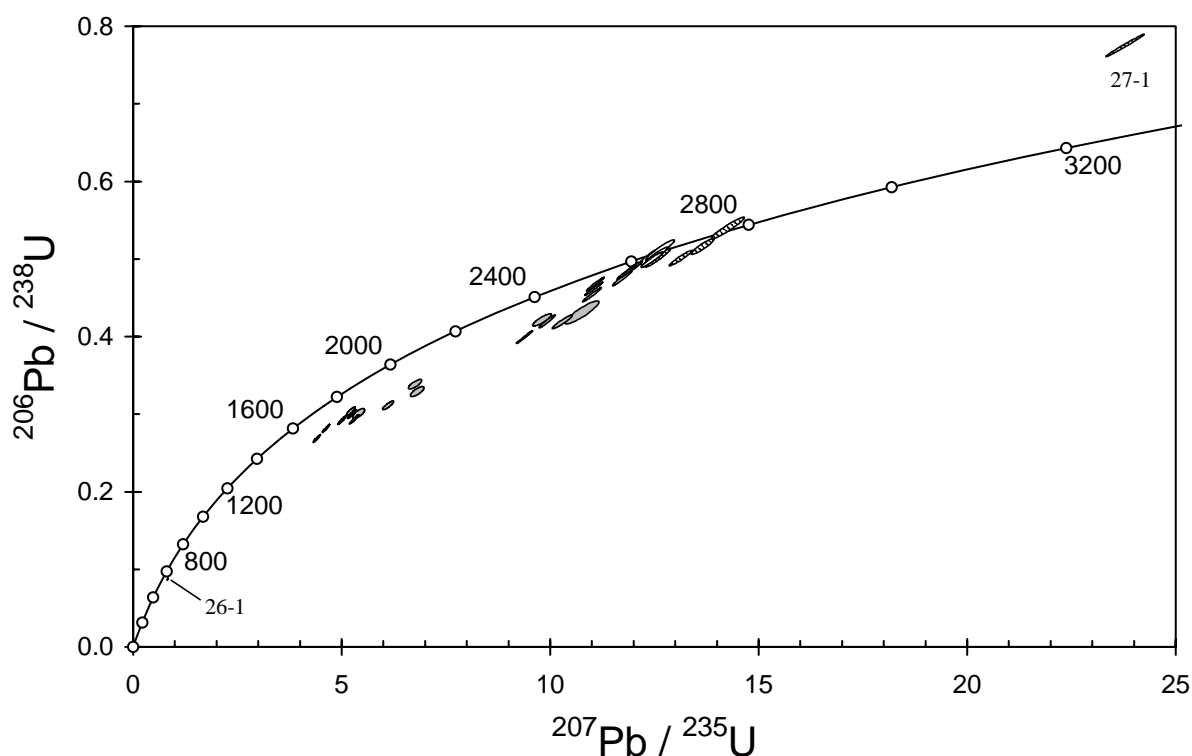


Figure 62. Concordia plot for zircon data from sample 900196 9021: biotite monzogranite dyke, Isolated Hill. White filled symbols are used to define the possible Archaean age of the sample; inherited grains have diagonal shading; discordant analyses are light grey; younger outliers are dark grey.



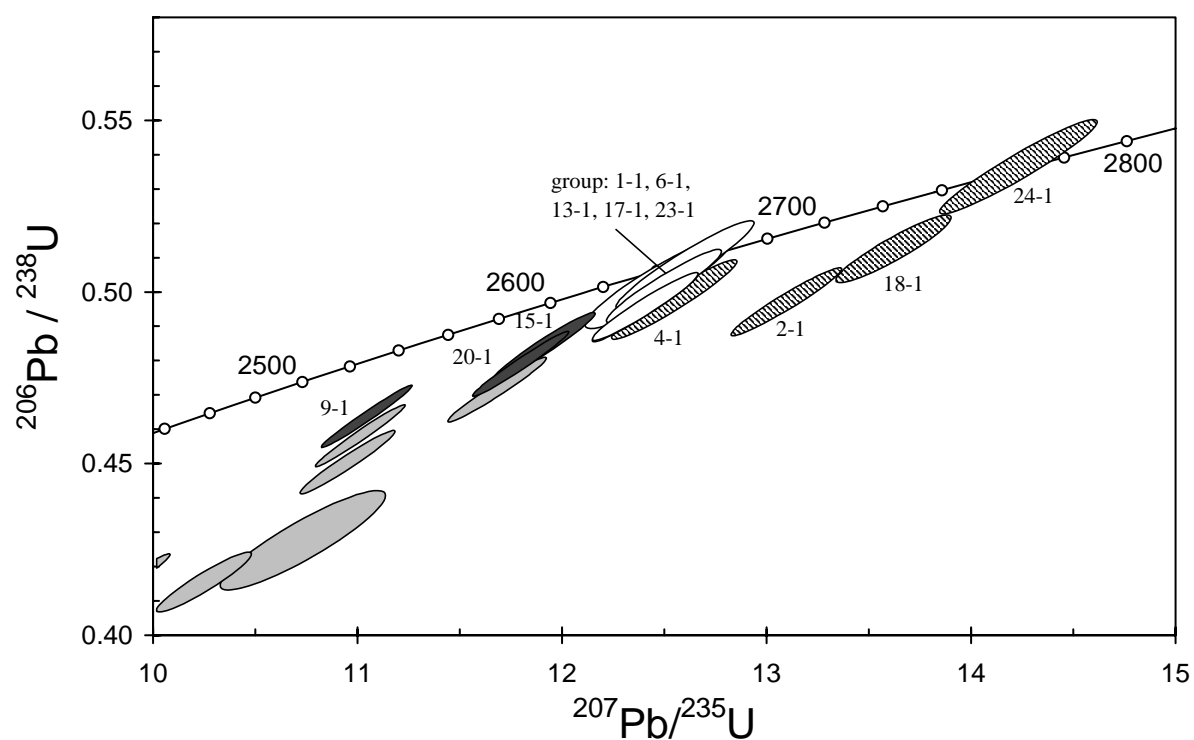


Figure 63. Enlargement of main group of zircon analyses for sample 900196 9021: biotite monzogranite dyke, Isolated Hill. Symbol shading as in Figure 62.

Table 26. SHRIMP analytical results for sample 900196 9021: biotite monzogranite dyke, Isolated Hill.

grain-spot	U (ppm)	Th (ppm)	4f206 (%)	<sup>207</sup> Pb/ <sup>206</sup> Pb		<sup>206</sup> Pb/ <sup>238</sup> U		<sup>207</sup> Pb/ <sup>235</sup> U		<sup>208</sup> Pb/ <sup>232</sup> Th	conc. (%)	<sup>207</sup> Pb/ <sup>206</sup> Pb Age	
				±	±	±	±	(Ma)	±				
Possible magmatic group													
D.1-1	202	103	0.738	0.1807	0.0009	0.502	0.007	12.50	0.19	0.145	99	2659	8
D.6-1	58	15	0.336	0.1799	0.0014	0.503	0.009	12.47	0.24	0.131	99	2652	12
D.13-1	324	197	0.004	0.1815	0.0007	0.496	0.007	12.40	0.17	0.135	97	2667	6
D.17-1	72	57	0.106	0.1799	0.0010	0.508	0.009	12.60	0.22	0.137	100	2652	10
D.23-1	310	845	0.454	0.1816	0.0006	0.495	0.007	12.40	0.17	0.140	97	2668	6
Inherited													
D.2-1	377	60	0.193	0.1911	0.0007	0.497	0.007	13.10	0.18	0.124	95	2752	6
D.4-1	107	43	0.029	0.1828	0.0009	0.498	0.008	12.55	0.20	0.138	97	2679	8
D.18-1	902	61	0.149	0.1927	0.0010	0.513	0.006	13.62	0.19	0.139	96	2765	9
D.24-1	69	30	0.048	0.1924	0.0010	0.537	0.009	14.24	0.26	0.146	100	2763	9
D.27-1	829	61	0.131	0.2230	0.0004	0.774	0.010	23.81	0.31	0.371	123	3002	3
Younger, concordant													
D.9-1	474	153	0.056	0.1727	0.0004	0.463	0.006	11.03	0.15	0.126	95	2584	4
D.15-1	291	162	0.387	0.1784	0.0006	0.484	0.007	11.90	0.17	0.135	96	2638	6
D.20-1	464	195	0.291	0.1786	0.0005	0.479	0.006	11.79	0.16	0.133	96	2640	5
Discordant													
D.3-1	512	398	0.927	0.1430	0.0011	0.306	0.004	6.03	0.09	0.084	76	2263	13
D.5-1	1247	206	0.085	0.1821	0.0020	0.427	0.010	10.72	0.27	0.135	86	2672	18
D.7-1	521	495	0.221	0.1507	0.0016	0.324	0.004	6.74	0.11	0.085	77	2354	19
D.8-1	334	45	0.152	0.1763	0.0006	0.450	0.006	10.94	0.15	0.121	91	2619	6
D.10-1	591	562	0.249	0.1307	0.0016	0.296	0.004	5.33	0.10	0.084	79	2108	22
D.11-1	514	407	0.247	0.1697	0.0012	0.417	0.005	9.75	0.15	0.117	88	2555	12
D.12-1	412	249	0.247	0.1725	0.0005	0.415	0.005	9.86	0.13	0.133	87	2582	5
D.14-1	787	419	0.340	0.1273	0.0005	0.294	0.004	5.16	0.07	0.081	81	2061	7
D.16-1	183	94	0.386	0.1790	0.0010	0.415	0.006	10.23	0.15	0.143	85	2644	9
D.19-1	731	1085	0.661	0.1249	0.0007	0.298	0.004	5.13	0.07	0.083	83	2028	10
D.21-1	758	524	0.557	0.1249	0.0006	0.287	0.004	4.93	0.07	0.067	80	2027	8
D.22-1	921	131	0.447	0.1193	0.0004	0.276	0.004	4.54	0.06	0.099	81	1946	6
D.25-1	545	536	0.078	0.1455	0.0016	0.333	0.004	6.69	0.11	0.096	81	2294	18
D.26-1	5932	1183	0.395	0.0651	0.0004	0.079	0.001	0.71	0.01	0.028	63	778	14
D.28-1	486	277	0.159	0.1743	0.0004	0.458	0.006	11.00	0.15	0.124	93	2600	4
D.29-1	347	118	0.276	0.1797	0.0006	0.471	0.006	11.68	0.16	0.139	94	2650	5
D.30-1	812	816	0.317	0.1190	0.0005	0.263	0.003	4.31	0.06	0.074	78	1941	7
D.31-1	443	316	0.408	0.1314	0.0005	0.288	0.004	5.21	0.07	0.081	77	2117	7
D.32-1	474	383	0.106	0.1712	0.0004	0.395	0.005	9.32	0.13	0.112	84	2569	4

Data are at 1 $\sigma$  precision. All Pb data are common-Pb corrected (based on  $^{204}\text{Pb}$  and Broken Hill Pb composition). Analysis date: 25/08/2001; session Z3734k.

## **Acknowledgements**

The Curtin University-Geoscience Australia collaborative research agreement was coordinated by Neal McNaughton. Special thanks go to John de Laeter and Barney Glover (Curtin University) and Chris Pigram and Russell Korsch (Geoscience Australia) for their assistance in establishing and maintaining the agreement.

We acknowledge the technical assistance of Peter Taylor in the collection of field samples. Sample preparation was undertaken by Tas Armstrong, Stephen Ridgway and Gerald Kuehlich, and the preparation, photography and SEM imaging of mineral mounts was undertaken by Chris Foudoulis at the mineral separation laboratories at Geoscience Australia.

SHRIMP analyses were undertaken by the Curtin authors with assistance from Matt Godfrey, April Pickard, Brock Salier, Natalie Kositcin and J-P. Pigois. SEM imaging for this report was performed by Janet Muhling.

Constructive comments by Lance Black and Jonathon Claoue-Long during internal review improved this report.

The SHRIMP II is maintained by Allen Kennedy (Curtin University) and operated by a consortium consisting of Curtin University of Technology, the Geological Survey of Western Australia and the University of Western Australia with the support of the Australian Research Council.

## References

- Bateman, R., Costa, S., Swe, T. and Lambert, D., 2001. Archaean mafic magmatism in the Kalgoorlie area of the Yilgarn Craton, Western Australia: a geochemical and Nd isotopic study of the petrogenetic and tectonic evolution of a greenstone belt. *Precambrian Research*, **108**, 75–112.
- Champion, D.C. and Sheraton, J.W., 1997. Geochemistry and Nd isotope systematics of Archaean granites of the Eastern Goldfields, Yilgarn Craton, Western Australia: implications for crustal growth. *Precambrian Research*, **83**, 109–132.
- Compston, W., Williams, I.S. and Meyer, C., 1984. U–Pb geochronology of zircons from lunar breccia 73217 using a sensitive high-resolution ion microprobe. *Journal of Geophysical Research*, **98**, B525–B534.
- Daly, S.J., Fanning, C.M. and Fairclough, M.C., 1998. Tectonic evolution and exploration potential of the Gawler Craton, South Australia. *AGSO Journal of Australian Geology and Geophysics*, **17**, 145–168.
- Ludwig, K.R., 2001. SQUID 1.00 Berkley Geochronology Centre, Special Publication **2**.
- Nelson, D.R., 1997. Compilation of SHRIMP U–Pb zircon geochronology data, 1996. Western Australia Geological Survey, Record **1997/2**.
- Pidgeon, R.T., Furfaro, D., Kennedy, A.K., Nemchin, A.A. and van Bronswijk, W., 1994. Calibration of zircon standards for the Curtin SHRIMP II. Abstracts of the 8<sup>th</sup> International Conference on Geochronology, Cosmochronology and Isotope Geology, Berkeley, USA. U.S. Geological Survey Circular, **1107**, 251.
- Smith, J.B., Barley, M.E., Groves, D.I., Krapez, B., McNaughton, N.J., Bickle, M.J. and Chapman, H.J., 1998. The Sholl Shear Zone, West Pilbara: evidence for a domain boundary structure from integrated tectonostratigraphic analyses, SHRIMP U–Pb dating and isotopic and geochemical data of granitoids. *Precambrian Research*, **88**, 143–171.
- Williams, I.S., 1998. U–Th–Pb Geochronology by Ion Microprobe. *In: Applications of microanalytical techniques to understanding mineralizing processes. Reviews in Economic Geology*, **7**, 1–35.
- Witt, W.K., 2001. Tower Hill gold deposit, Western Australia: an atypical, multiply deformed Archaean gold-quartz vein deposit. *Australian Journal of Earth Sciences*, **48**, 81–99.